Chemistry of Cyclometalated Gold(III) Complexes: Outfit for Mechanistic Investigations and Beyond

Dissertation

zur

Erlangung der naturwissenschaftlichen Doktorwürde

(Dr. sc. nat.)

vorgelegt der

Mathematisch-naturwissenschaftlichen Fakultät

der

Universität Zürich

von

Roopender Kumar

aus

Indien

Promotionskommission

Prof. Dr. Cristina Nevado (Vorsitz und Leitung der Dissertation)

Prof. Dr. Roland Sigel

Prof. Dr. Bernhard Spingler

Zürich, 2017

To my Mother and Motherland!

ACKNOWLEDGEMENTS

I have been very fortunate to be associated with some great teachers, dedicated scientists and wonderful colleagues throughout my studies which helped me in so many ways to shape my philosophy and enhance my confidence, enthusiasm and strengthened my motivation to do research in chemistry with high ethical research principles. Like every single Indian, I had heard time and time again one word "Vasudhavia Kutambakam" (the world is one family), a core philosophy of India which I never fully understood until I came to Europe for my education. So, my highest gratitude towards those amazing people who directly/indirectly have been involved in this journey, is something I was tempted to write some time ago. But I kept telling myself lets hold it for the end. And finally the dream day come and here I am writing these acknowledgements with all the deepness of my heart. Although during a PhD in chemistry, how many synthetic methods/catalysts/materials were developed or how many mechanisms were solved or how many papers one published etc… is often defines ones accomplishments (and I do not argue with that), for me, my greatest accomplishments are the relations I have developed and the lessons I have learned working with so many incredible people over this pleasant period of time. In this sense, it is by far the most important part of my thesis.

Many thanks to Professors Roland Sigel and Bernhard Spingler for their participation in the PhD committee and for their valuable feedback during the annual meetings. Perhaps, Roland is the liveliest Professor in the Department of Chemistry and easy to talk to: I appreciate his efforts to encourage students to be more interactive. Bernard taught me how to present X-Ray structures and the importance of little details while presenting scientific results.

I thank the Graduate School of Chemical and Molecular Sciences Zurich (CMSZH). This work would not have been possible without cutting age facilities provided by the Department of Chemistry of the UZH. Particularly, the wonderful NMR team with Professor Oliver Zerbe (one weekend I had some problem with 500 NMR, I called for help and within few minutes, Oliver was there which showed his enormous commitment to science), Nadia Bros, Simon Jurt and Thomas Fox (the most helpful person I have ever worked with). X-Ray crystallography has been instrumental for the success of this work and I am grateful to Professor Spingler and my friend Dr. Olivier Blacque. A big thank to Professor Anthony Linden: he is a wonderful crystallographer to whom I have bothered so much with poor quality crystals, but I learned a lot from him during many discussions. I am thankful to Dr. Laurent Bigler and coworkers for the analytical service (MS, Elemental analysis), especially, to Urs Stalder who is a great analyst and do his work with absolute perfection and joy. I thank Benjamin Probst, from Professor Roger Alberto group, for teaching me how to use Cyclic Voltammetry as well as the GC for hydrogen detection. Benji is an extremely helpful person and he used to have answers for all my questions related to his expertise. I am thankful to the people from Venkatesan group (Michael Bachmann, Alexander Szentkuti and Tobias Van Arx) for their valuable help in photophysical

properties measurements. I admire the efforts and help of Ferdinand Wild for TGA, DSC and Raman experiments. I would like to thank the technical team (Hanspeter Stalder and Serkan Sariyildiz) for their help, particularly, for making several setups (until we find the best one) to use carbon monoxide. My sincere thanks to the people associated with administration (Larissa Mostacciuolo, Chantal Henningsen-Conus, Nathalie Melunsky-Fichter, Beatrice Spichtig and Marianne Grima-Karpf) who really made everything (all the paper work and finances) simpler for me. I extend my thanks to the security people of the department of chemistry, particularly, my friend Wolfram Böhm (often he used to come at late evening to complain that "your colleague again left the door open", and I used to tell him about the great science I am doing ☺).

I feel highly indebted to my undergraduate teachers who introduced me to this world of chemistry. I will always remember the unique interactive teaching style of Dr. S. V. Eswaren and philosophical discussions he promote. I thank Dr. Harish Chandra for his inspiring mentoring and Dr. Mirdula Mittal for being such a wonderful educator. I will always be highly indebted to Professor Eckhard Otto for his excellent guidence, inspiration and great help. I am extremely thankful to my master thesis advisor Professor Hans-Ulrich Reissig for his constant supports and encouragements. It was Reissig group where I developed a keen interest for research in chemistry and I will always remember the fantastic time I spent in FU Berlin.

For the pleasing environment in the lab, for their friendship and for many interesting discussions during this thesis I would like to thank all the members of Cristina's group. I thoroughly enjoy while working alone on a research project but when I am in a team, it is awesome. Time to time, I have been very lucky to join two excellent scientists Jean-Philippe Kriger and Hélène Beucher. JP and I worked together on the mission "dehydrogenation of formic acid" which was successful, whereas Hélène was with me on the battle of "water gas shift reaction" and we are very close to the victory, unfortunately, I have to leave her alone in the battel field. It was a real pleasure and satisfaction to share my little understanding and ideas on gold(III) chemistry with Hélène Beucher, Felipe Verdugo and Michael Böhler. I am also grateful to Estibaliz Merino for her help over these years. Esti is the nicest and most helpful person one can meet in a lifetime. My thanks to our computational collaborator, Professor Enrique Gómez-Bengoa (an extremely humble person), whose efforts and help guided us in the right direction.

I want to thank the most organized, tidy, disciplined and humble person I have worked with during my PhD, who to me is like an elder brother and a good friend, Manuel Hofer. In Zurich, he has been my guide for food, to tell me which one is vegetarian and which one is not. Enormous chemical, philosophical and social discussions I had with Manuel were essential gradients to make my stay pleasant. I am thankful to Patricia García-Domínguez who is a great experimentalist, wonderful friend, and the most caring human being. I remember she was the one who forced me to take my first vacation

by asking every single day “when will you go home? I am going to book a flight for you”, without her, my time in the lab would not have been the same, thank you so much Patri. Another amiable colleague was Noelia Fuentes, my dance teacher, and a good friend. Thanks Noe for being so nice and I will always miss the “Delicious Tiramisu” prepared by you. I want to thank Wangquing Kong (the paper machine of our group) for the great time in the lab. I am sure he will do very well at Wuhan University. My desk-mate Luis Fernández-Sánchez, it was fun to fight with him for four years and I thank Luis for keep reminding me about Friday group seminar which otherwise I would have missed multiple times. I must thank my friend Andres García-Domínguez for countless discourses on various topics, having him in the lab and in parties was a great delight. I appreciate Andres for the fact that he is as weird as I am and he sort of understands my stupid scientific questions and proposals. My thanks to Adriana Lorente, who is a wonderful chemist and a good friend. She is one of the most positive persons I have worked with during my PhD. Meeting and talking with one of the hardest working scientists like Wei Shu and Zhaodong Li was a real joy. Wei is amazing, he knows a tons of things and I thoroughly enjoyed countless discussions with him. Perhaps, Zhaodong is the most humble and down to earth person I know, he also has been my kitchen mate (cooking around midnight and having scientific conversations with him was ecstacy) in the past three years, however he is not such a good cook and I like more his chemistry. Rumor has it that soon he will join the academic position (which he holds since 13 months) next year. It was great to meet Eswararo Doni (a smart scientist, a wonderful cook and an incredible person). I remember, once, I tried to show off to Eswar that after living in Zurich for four years I knew a lot about the city and its culture (which was not true at all). So I forcibly took him to the Zurich–Street parade and, in the first two minutes, someone snatch his gold chain necklace (this was my fault as I must have told him not to wear any necklace in such a crazy crowd, but the fact is that it was also my first time to the street-parade) and we both came back to the lab with long faces. I thank to the natural product subgroup (Martin Arthuis, Giulia Rusconi, Adriana Lorente, and Tamara Arto) of Cristina’s group. Martin was a very good scientist and a person who do little more things than he was responsible for, no matter whether he was in the lab or outside (for BBQ, he was the one who took care of fire, food and all other things, also time to time he used to send me the cheap tickets to India): thanks Martin. When I joined Nevado group, it was Manuel, Martin and Andrea who really helped me to adapt in the group. Giulia (Juli) and I started in the group almost at the same time and I thank her for many things but especially for her care in the early days of my PhD.

Thanks to the bromodomain subgroup (Andrea Unzue, Aymeric Dolbois, Melanie Zechner, Charel Prost, Fabrice Hassler, Isabel Córdoba Coto, Alvaro Salvador-González, Claudia Trefzer, Xuan Wang, Vlad Pascanu) of our group for introducing me to the epigenetic world. I thank another tidy chemist and a good colleague (Aymeric) for being so nice and for taking care of the lab in recent months. I really enjoyed the company of two brilliant master students Philipp Waser and Manuela Brütsch. It was fun to have Alexandre Genoux around, his childish behavior is something I am going

to miss. Cedric Hervieu and Jyoti Dhankar though they joined/associated the group at the end of my journey, I have got to know them well and they are highly motivated and talented chemist. I must thank Ilija Čorić who is exceptionally smart scientist, helpful person, ideal experimentalist, and a good friend. It was a real delight to know Ilija and several long discussions I had with him really helped me.

I would like to thank the Jessen group members (Samanta Capolicchio, Igor Pavlovic, Alexandre Hofer and Devyeshsinh Thakor) for their friendship. In terms of NMR time, Igor was like a "trusted bank" for me, if I forget to book the NMR time, I always knew, I can borrow it from him (especially at late nights or on weekends). My thanks to the people from Luedtke group (Olivia Schmidt, Therese Triemer, Jawad Alzeer, Alessandra Messikommer, Aron Johnson and Anna Bujalska) to create a friendly environment in the corridor. Olivia is the liveliest person I have met in Zurich, she also has been my fantastic mate in the NMR (as we both in parallel had some projects which demand variable temperature NMR studies and we used to share a mutual feeling/nightmare that "something might go wrong with the machine and we will be fired", although luckily, nothing wrong ever happened).

Life is as good as the people you are associated with. I feel highly blessed to have incredibly great friends Ravinder Pundir, Satish Sharma, and Pradeep Kumar. The most lovable friend whom I must thank is Jyoti Singh, her help and care during these years is incomparable. Undoubtedly, without the support and blessing of my exceptionally loving parents (Vimla Devi Singh (my mother) and Vinod Kumar Singh (my father)) I would not have made it that far. They have been the powerhouse of my life, my inspiration and the real source of motivation. My mother knows me more than I know myself and she is my real role model. I have immense amount of appreciation to my sisters (Pooja Singh and Radha Singh), my sister in-law (Babita Singh) and my brother (Shiv Kumar Singh) for their unconditional love and support. Since their birth, my nieces (Aarti Singh and Annu Singh) have been a big reason of my happiness, though I have made them wait a little bit too long but soon I will see them and play with them.

I think, I have acknowledged my teachers, my colleagues, my friends and my family. And now, I would like to express my sincerest gratitude to the person who really fit in all these categories, supervisor of this thesis Professor Cristina Nevado. In fact, I never had any problem to communicate anything to Cristina but it is ironic that I am having difficulty to thank her. I do not know how to even start, how to thank a person who has done everything possible in her power to make sure that I succeed. She is a great guide, a highly dedicated and fearless scientist and a very kind person. Looking back, I have huge amount of appreciation and respect to the amount of time she devoted on countless invaluable discussions I had with her, which helped me in many ways besides to perform this work and to be a better chemist. After handling so many things in parallel it had never happened that Cristina refuse to talk whenever I knocked her door, this showed her deep passion for science. She is the hardest

working individual I know. Thinking about the beginning of my PhD which was a bit unusual, I feel highly indebted to Cristina for trusting me and giving me the chance to read and come up with some innovative ideas, and for her support and encouragements for all the stupid/crazy ideas I proposed. In more recent years, Cristina continued to be a mentor, a guardian, a role model and a friend to me. It has been a great honor to be a part of Cristina's group. It is true, PhD defense marks my end in the Nevado group but I am sure it also marks the beginning of a lifelong friendship. It is sad to be leaving, yet, I am very much looking forward for the future and I will be constantly watching the success of the group in up coming years.

PREFACE

This PhD thesis is based on the results which were published or which are going to be published in international, peer-reviewed scientific journals. Except the conclusion and outlook part in Chapter 6, Chapters 1 to 5 correspond to the papers in an as much as possible unchanged form to the respective manuscripts. Consequently, compounds and references are numbered independently for each chapter.

The following publications and manuscripts are part of this PhD thesis:

1. **"Cyclometalated Au^{III} Complexes: Synthesis, Reactivity and Physicochemical Properties"**
   Roopender Kumar and Cristina Nevado. *Angew. Chem. Int. Ed.* **2017**, *56*, 1994-2015.

2. **"Luminescent (N^C^C) Gold(III) Complexes: Stabilized Gold(III) Fluorides"**
   Roopender Kumar, Anthony Linden, and Cristina Nevado. *Angew. Chem. Int. Ed.* **2015**, *54*, 14287-14290.

3. **"Evidence for Direct Transmetalation of Au^{III}-F with Boronic Acids"**
   Roopender Kumar, Anthony Linden, and Cristina Nevado. *J. Am. Chem. Soc.* **2016**, *138*, 13790-13793.

4. **"First Gold(III)-Formate: Evidence for β-Hydride Elimination"**

   Roopender Kumar, Jean-Philippe Krieger, Enrique Gómez-Bengoa, Tomas Fox, Anthony Linden, and Cristina Nevado. *Angew. Chem. Int. Ed.* **2017**, *accepted.*

5. **"Alkyne Hydrometallation by (N^C^C)-Gold(III) Complexes: A Detailed Mechanistic Investigation"**
   Roopender Kumar, Estibaliz Merino, Enrique Gómez -Bengoa, Laura Gómez Martín, Xavi Ribas, and Cristina Nevado. *Manuscript in preparation.*

ZUSAMMENFASSUNG

Fluoride der späten Übergangsmetalle spielen eine zentrale Rolle als Zwischenprodukte in Transformationen zur Bildung von C-C und C-X-Bindungen. Obwohl Pd^{II} and Pd^{IV}-fluoride bereits synthetisiert und untersucht wurden um ein besseres mechanistisches Verständnis dieser Transformationen zu erhalten, wurden Au^{III}-fluoride bisher nur beschränkt untersucht. In den letzten zehn Jahren wurden zahlreiche Au^{I}/Au^{III}-katalysierte Transformation entwickelt, um C-C-, C-X- und C-F-Bindungen zu bilden. Csp^2- and Csp^3-Gold(III)-fluoride sind als Zwischenprodukte in Au^{I}/Au^{III} Redox-Katalysezyklen vorgeschlagen worden, aber der experimentelle Nachweis dieser Spezies ist schwierig aufgrund der hohen Instabilität dieser Verbindungen. Somit blieb die Reaktivität von Au^{III}-F-Bindungen weitgehend unerforscht und das mechanistische Verständnis dieser Transformationen ist bei weitem nicht vollständig.

Das Hauptziel dieser Arbeit war die Synthese und Isolierung von stabilen Gold(III)-fluoriden, um ihre chemische Reaktivität zu untersuchen. Anschließend beabsichtigten wir die Mechanismen von goldkatalysierten Reaktionen aufzuklären, bei welchen Gold(III)-fluoride als produktive Zwischenprodukte vorgeschlagen werden.

Im zweiten Kapitel dieser Arbeit berichten wir die Synthese von monomeren (N^C^C)Au^{III}-F-Komplexen, die stabil und einfach zu handhaben sind. Schlüssel für den Erfolg der Synthese ist die Bildung von stabilen (N^C^C)Au^{III}-Cl über zwei aufeinanderfolgende C-H-Aktivierungen eines (N^C^C)-Liganden durch Au^{III}, gefolgt von einem einfachen Cl/F-Ligandenaustausch. Unter Vermeidung oxidativer Bedingungen oder der stöchiometrischen Verwendung von toxischen Hg-Salzen, wurde unsere Methode für die Herstellung mehrerer Csp^2-Au^{III}-fluoride verwendet. Diese Verbindungen bildeten eine hervorragende Plattform, um ihre Reaktivität zu untersuchen. Die Reaktion der Au^{III}-fluoride mit Alkinen ergab die entsprechenden (N^C^C)Au^{III}-Alkinylkomplexe durch C-H-Aktivierung. Diese Komplexe zeigen starke Lumineszenz im Vergleich zu ihren analogen (C^N^C)Au^{III}-Alkinylkomplexen.

Erweiterungen der Reaktivität von Au^{III}-fluoriden werden im dritten Kapitel beschrieben. Dort berichten wir unsere Ergebnisse zur Herstellung und Charakterisierung einer Reihe von (C^N)-stabilisierten Gold(III)-fluoriden in monomerer Form und einer eingehenden Untersuchung ihrer Reaktivität mit organischen Derivaten der Borsäure, wobei die enentsprechenden Transmetallierungs-produkte isoliert werden konnten.

Kapitel vier behandelt die Synthese der ersten (N^C^C)Au^{III}-formiate unter Verwendung von (N^C^C)Au^{III}-fluoriden. Das Studium der β-Hydrid-Eliminierung dieser Gold(III)-formiate liefert ein

reaktives Gold(III)-hydrid, das mit Alkinen reagiert um (*Z*)-Vinylgold(III)-Komplexe zu bilden. Schliesslich konnte auch eine katalytische Dehydrierung von Ameisensäure nachgewiesen werden.

Im fünften Kapitel dieser Arbeit werden mechanistische Untersuchungen zur Hydrometallierung von Alkinen durch (N^C^C)-Au^{III}-X-Komplexe (X = CHO, F) und der Bildung von (*Z*)-Vinylgold(III)-Spezies mittels Niedrigtemperatur-^{1}H-NMR, Cryo-MS und DFT-Berechnungen dargelegt.

SUMMARY

Late-transition metal fluorides play a pivotal role as intermediates in C-C and C-X bond forming transformations. Although Pd^{II} and Pd^{IV}-fluorides have been synthesized and fully studied in order to gain a better mechanistic understanding of such transformations, the study of Au^{III}-fluorides is very limited. In the past decade numerous Au^{I}/Au^{III} catalyzed transformations have been developed in order to construct C-C, C-X and C-F bonds. The formation of Csp^2 and Csp^3-gold(III)-fluorides as intermediates has been proposed in Au^{I}/Au^{III} redox catalytic cycles but the experimental evidence of these species remains scarce due to their high instability. Thus, the reactivity of Au^{III}-F bonds remains largely unexplored and mechanistic understanding of such transformations is far from being complete.

The main objective of this work was the synthesis and isolation of stable gold(III)-fluorides in order to study their chemical reactivity. Subsequently, we aimed to shed light on the mechanisms of gold catalysed reactions where gold(III)-fluorides are proposed as productive intermediates.

In the second chapter of this thesis, we report the synthesis of monomeric, easy to handle, bench-stable (N^C^C)Au^{III}-F complexes. Key for the success is the formation of stable (N^C^C)Au^{III}-Cl via two sequential C-H activation of an (N^C^C) ligand by Au^{III} followed by a facile Cl/F ligand-exchange reaction. Devoid of oxidative conditions or stoichiometric use of toxic Hg salts, our method was applied to the preparation of multiple Csp^2-Au^{III}-F complexes. These gold(III)-fluorides provided a great platform to study their reactivity. Offering alkynes to these gold fluorides resulted into the corresponding (N^C^C)Au^{III}-alkynyl complexes via C-H activation. These complexes show high luminescent properties compared to their analogous (C^N^C)Au^{III}-alkynyl complexes.

Extensions of Au^{III}-F reactivity are reported in the third chapter. There we present our results on the preparation and characterization of a series of (C^N)-stabilized gold(III)-fluorides in monomeric form and an in depth study on their reactivity with aryl boronic acids where corresponding transmetalation products could be isolated.

Chapter four deals with the utilization of (N^C^C)Au^{III}-F to synthesize the first (N^C^C)Au^{III}-formate. Study of this gold(III)-formate towards β-hydride elimination delivers a reactive gold(III)-hydride which reacted with alkynes to afford (*Z*)-vinyl gold(III) complexes. Ultimately, a catalytic dehydrogenation of formic acid could also be demonstrated.

In the fifth chapter of this thesis, mechanistic investigations by low temperature ^1H NMR, Cryo-MS and DFT calculations on the hydrometallation of alkynes by (N^C^C)Au^{III}-X complexes (X = CHO, F) to form (*Z*)-vinyl gold(III) species is presented.

TABLE OF CONTENTS

CHAPTER 1

INTRODUCTION

CHAPTER 1

Introduction

Roopender Kumar and Prof. Dr. Cristina Nevado

(*Angew. Chem. Int. Ed.* **2017**, *54*, 142-87-14290)

"twere absurd to think that nature in the earth bred gold perfect in the instant; something went before [..] Nature doth first beget the imperfect, then proceeds she to the perfect"

'The Alchemist' by Ben Jonson- 17th Century

All that is gold does not glitter,
Not all those who wander are lost;
The old that is strong does not wither,
Deep roots are not reached by the frost.
The Fellowship of the Ring, — J.R.R. Tolkien

Zero-valent gold, the most stable metal form in the periodic table, has managed to conceal the attention of alchemists first and chemists later because of its precious appearance and intrinsic inertness. Despite being known for centuries, the past two decades have witnessed a gold "reinassance" based on the applications of both Au^{I} and Au^{III} species in catalysis. Complexes of gold have emerged as powerful carbophilic Lewis Acids able to activate with upmost efficiency the π-system of alkenes, alkynes and allenes thus enabling a broad palette of transformations rooted on the strong relativistic effects that govern its coordination chemistry.[1-7] Interestingly, and in particular in the case of Au^{I} complexes, the argument for its superior catalytic activity as π-Lewis acids is based on its high redox stability that precludes potential deactivation pathways. However, transformations invoking Au^{I}/Au^{III} species have recently emerged: in the presence of suitable oxidants, catalytic cycles involving a change in the oxidation state of gold could be devised thus broadening the scope of gold catalysis, particularly in the context of oxidative cross-coupling reactions.[8-13] Further developments in this still young area have been hampered by the lack of mechanistic understanding of the individual steps along the proposed catalytic cycles due to the uncontrolled reactivity of high-valent gold intermediates and the challenges associated with the synthesis of these rather labile and rapidly evolving species.[14, 15] A strategy to overcome these limitations relies on the use of ligand templates able to stabilize Au^{III} in the form of cyclometalated complexes. These species have been known for many years although in most cases, investigations have focused on their preparation and ligand exchange reactivity. The photophysical properties of these compounds have also been the subject of intense research efforts following the development of cyclometalated Ir^{III} complexes as OLEDs.[16-18] Nonetheless, and despite attractive

properties such as its low toxicity and environmentally benign nature, the use of Au^{III} complexes as efficient emissive species has lied behind in comparison to other metals such as Pt^{II}, Ir^{III} or Ru^{II}. The non-radiative excited-state deactivation caused by the low lying d–d states that are energetically close to the potentially emissive intraligand (IL) or metal-to-ligand charge transfer (MLCT) states constitute a major problem for gold based systems. Furthermore, the electrophilicity of the Au^{III} center might lead to photodecomposition or other side reactions. Recently though, interest in understanding the basic photoluminescence (PL) properties of Au^{III} complexes has gained attention in the quest for novel small molecule phosphors.[19-22]

In this introduction, our aim has been to give an overview of the key design principles behind the different existing ligand templates and the representative methods to access the corresponding stabilized Au^{III} complexes. In addition, we have aimed at providing a basic understanding on the reactivity of these motifs as a guiding principle to generate derivatives on which to further acquire the desirable both chemical and photophysical properties. Finally, the role of some of these species as probes to unravel mechanistic insights of catalytic transformations has also been discussed.

To facilitate such an integrative discussion, we opted for a "structure-based" organization of the introduction with the coordinating atoms of the prototypical ligand templates as thread. First, tridentate ligands yielding biscyclometalated gold(III) species are presented divided into four main groups: dianionic 2,6- and 3,5-diarylsubstituted phenyl-pyridine ligands assemble neutral, highly stable (C^N^C) and (N^C^C) gold(III) complexes, the former having been profusely studied. Monoanionic (C^N^N) and (N^C^N) ligands, in contrast, afford far less stable cationic gold(III) species whose chemistry, in comparison, to the previous case, has been much less explored. In a second section, monocyclometalated gold(III) species are disclosed starting with classical 2-aryl pyridine ligands. (C^C), (P^C), (N^N), (N^O) and (N^P) ligand templates and the corresponding monocyclometalated gold(III) species have been summarized next. Within each of these sections, an attempt has been made to discuss the results in a chronological order, prioritizing more recent developments over those which have already been revisited in the existing literature.

1. Bis-cyclometalated Gold Complexes

1.1 [(C^N^C)Au^{III}] Complexes

Pincer (C^N^C) ligands represent the most widely explored template to stabilize Au^{III} species. Pioneering work by Che and co-workers back in 1998 set the ground for in depth follow-up studies on the synthesis, reactivity and physicochemical properties of highly versatile biscyclometalated [(C^N^C)Au^{III}] species containing two C-based anionic ligands in *trans* relative position.[23] Using 2,6-diarylpyridines as starting materials, the corresponding [(C^N^C)AuCl] complexes were prepared by transmetalation of $KAuCl_4$ with [(C^N^C)HgCl] in refluxing acetonitrile. One of the most remarkable features of this neutral compound class is their highly stable nature as well as the facile displacement of the chloro ligand in **1** with soft N, S and P nucleophiles as shown by the efficient synthesis of complexes **2-4** (Scheme 1).

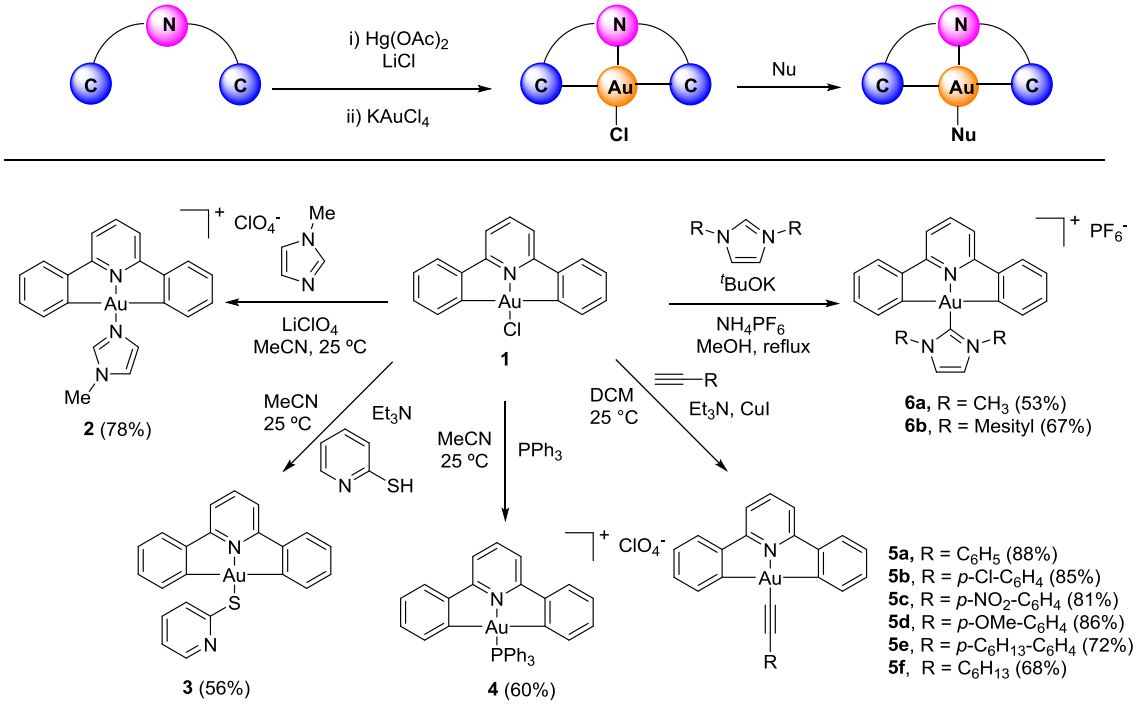

Scheme 1. [(C^N^C)Au^{III}] complexes. Synthesis and Reactivity.

1.1.1 [(C^N^C)Au(Alkynyl)] and [(C^N^C)Au(NHC)] Complexes

Complexes **1-4** were found to be low luminescent even under cryogenic conditions (77 K), a behavior that can be traced back to the low-energy d-d ligand field states that can quench the luminescence of the excited state by thermal equilibration or energy transfer in Au^{III} species. As a result, strategies have been sought to overcome these limitations, including the introduction of additional carbon-based strong σ-donor ligands *trans* to the N-donor (*i.e.* [(C^N^C)AuX], X = -C≡C-R, , NHC: *N*-heterocyclic carbene) to increase the electron density of the metal center and raise the non-emissive

d-d states, resulting in the enhancement of luminescence by increasing the chances of highly populated emissive states. In this context, Yam and co-workers reported the synthesis of Au^{III}-alkynyl complexes [(C^N^C)Au(C≡CR)] **5a-f**, by reaction of **1** with different terminal alkynes in the presence of trimethylamine and a catalytic amount of CuI (Scheme 1).[24, 25] [(C^N^C)Au(NHC)] complexes **6a-b** were prepared by reaction of **1** with the corresponding NHC precursors produced in situ by deprotonation of the imidazolium salts with potassium *tert*-butoxide in refluxing methanol.[26] Interestingly, some of these compounds have also found application as chemical probes in biology and their anti-proliferative activity has been evaluated *in vivo*.[27-30]

In degassed dichloromethane at room temperature, [(C^N^C)Au^{III}(alkynyl)] complexes **5a-f** are luminescent at 468-611 nm upon excitation at $\lambda \geq 360$ nm, with lifetimes in the sub-microsecond range. DFT and TDDFT computational studies suggest that the low-energy emission bands observed for these complexes can be assigned to a π-π* (C^N^C) intraligand (IL) transition in line with the moderate influence that the nature of the alkyne exerts on their emissive properties.[31] These complexes have continued to receive increasing attention as of their potential use in the context of light-emitting devices. In Figure 1, representative examples of improved members of this compound class have been depicted. The electronic nature of the alkyne but more importantly, the rigidity as well as electronic nature of the (C^N^C) ligand have been tuned to modulate their photophysical properties. Thus, alkynyl gold(III) complexes [(C^N^C)Au(C≡CR)] bearing *N*-donors on the *para* position of the arylalkyne unit (R = *p*-$N(C_6H_5)_2$-C_6H_4-, **7a-c**) have been successfully applied as phosphorescent dopants of OLEDs. When conjugation of the pyridine ring of the (C^N^C) ligand was extended (**7b**), external quantum efficiencies comparable to those reported for $Ir(ppy)_3$ based devices (EQE up to 11%) could be observed.[32],[33] Interestingly, complex **7c** has also been successfully applied in the fabrication of memory devices with high ON/OFF ratio, long retention time and good stability.[34] Higher order derivatives such as **7d** have been employed in the preparation of solution-processable OLEDs.[31d, 35] The presence of both electron-rich and electron-deficient units in the same molecule as well as the incorporation of methyl groups to increase rigidity and debilitate the π-conjugation between the donor and acceptor unit enhanced the photoluminescence quantum yields > 75% (in spin coated thin film) in complex **7e** .[36]

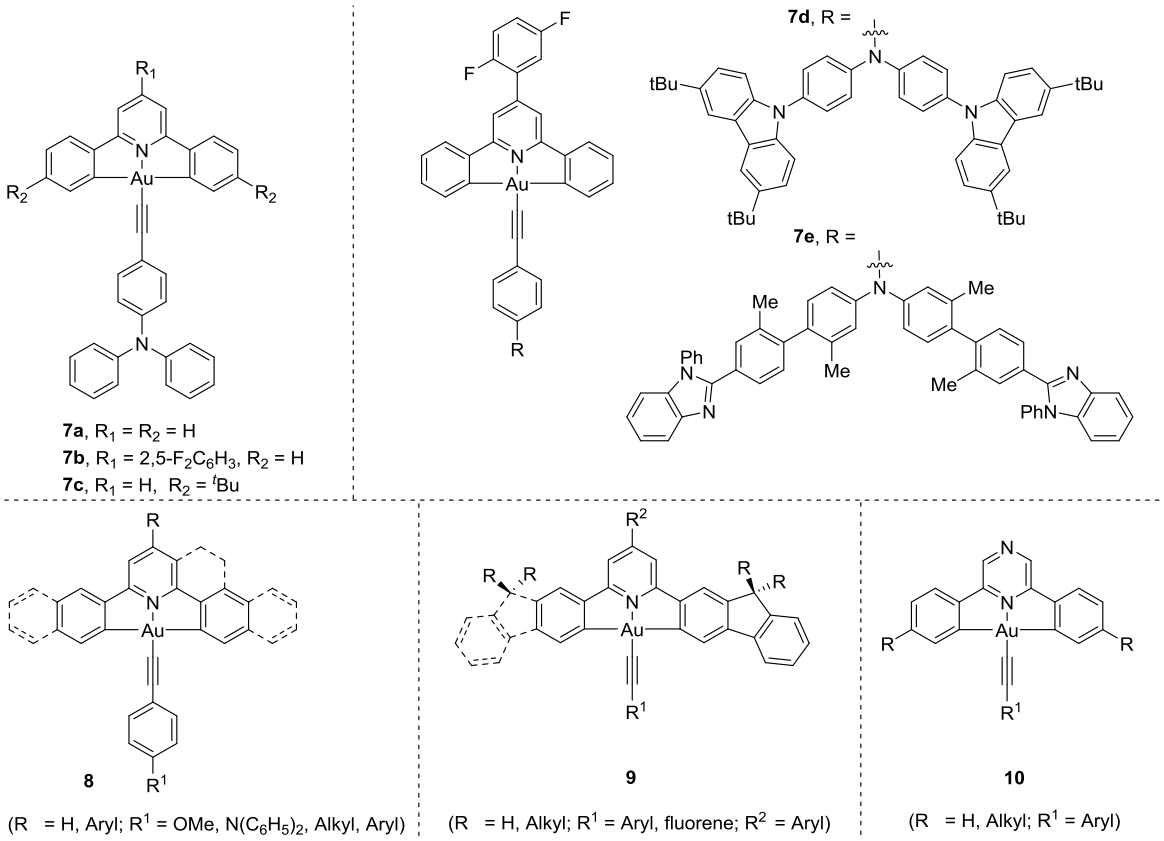

Figure. 1. Luminescent [(C^N^C)Au^{III}(alkynyl)] complexes.

To gain a better understanding on how the nature of the (C^N^C) ligand affects the luminescent properties, a detailed study on the physico- and electrochemical properties of substituted [(R-C^N^C)Au(C≡C_6H_4-R^1)] complexes **8** was undertaken by Yam and co-workers.[37] The incorporation of an aryl group to the central pyridine ring or the introduction of more conjugated 2-naphthyl moieties resulted in red shift in the emission maxima. In solid state, quantum yields up to 44% were observed for some of these compounds. Along the same lines, Che and co-workers demonstrated that the incorporation of fluorene motifs onto the phenyl ring of the (C^N^C) ligand (**9**) alter the lowest excited state from intraligand (IL) to ligand-centered π-π* charge transfer.[38,39] Thus complexes **9** present remarkably high quantum yields (up to 61%) and long-lived excited state lifetimes up to >400 μs. In 2015, 2,6-diphenylpyrazine (pz) based Au^{III} complexes **10** were reported by Bochmann and co-workers.[40] Interestingly, the luminescence of these species, both in solution and in the solid state, could be modulated by protonation, or addition of metal ions or Lewis acids to the pyrazine group so that no structural modifications of the ligand framework is needed. Modulation of the emissive properties is proposed to stem from the coexistence of high energy thermally activated delayed fluorescence and ^{3}IL (C^Npz^C)/LLCT (X to C^Npz^C;LLCT = ligand-to-ligand charge transfer, pz = pyrazine) transitions.

The photophysical properties of [(C^N^C)Au(NHC)] complexes have also been the subject of substantial research efforts. Dinuclear Au^{III}-NHC complexes **11** have been prepared and their photophysical properties studied in detail (Figure 2).[26]

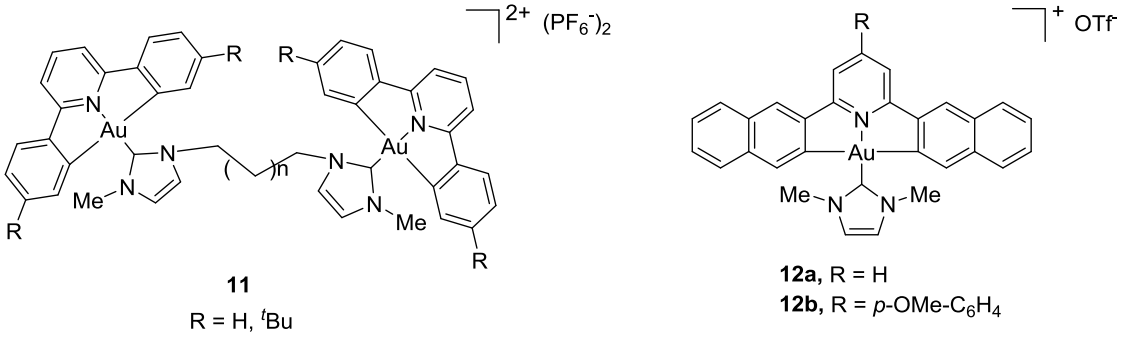

Figure.2. Luminescent [(C^N^C)Au^{III}(NHC)] complexes.

As expected, similar emissive properties in line with a π-π* intraligand (IL) transition could be determined for these compounds. As already seen for Au^{III}-alkynyl complexes, efforts to improve their photoluminescence properties have focused on chemical edition of the pincer (C^N^C) ligand. Thus, Che and co-workers showed that replacement of the benzene ring with a naphthyl group as well as addition of an aromatic group in *para* position of the pyridine ligand led to highly luminescent [(RC^N^C)Au(NHC)] complexes **12** with quantum yields up to 11% and long emission life time up to 506 μs.[41] DFT and TDFT calculations suggest that the π-extension on the (C^N^C) ligand results in an enhanced radiative decay while suppressing the non-radiative ones through minimization of the structural excited-state distortion. The long-lived triplet states observed for these complexes points towards their potential application in photochemical reactions. Indeed, excited state E(***12a**$^{+/0}$) was found to be a powerful oxidant (ca. 0.75 V vs $Cp_2Fe^{+/0}$ (1.43 vs NHE)) resulting in the use of **12a** as photocatalyst in the oxidative functionalization of secondary and tertiary amines (Scheme 2).[42]

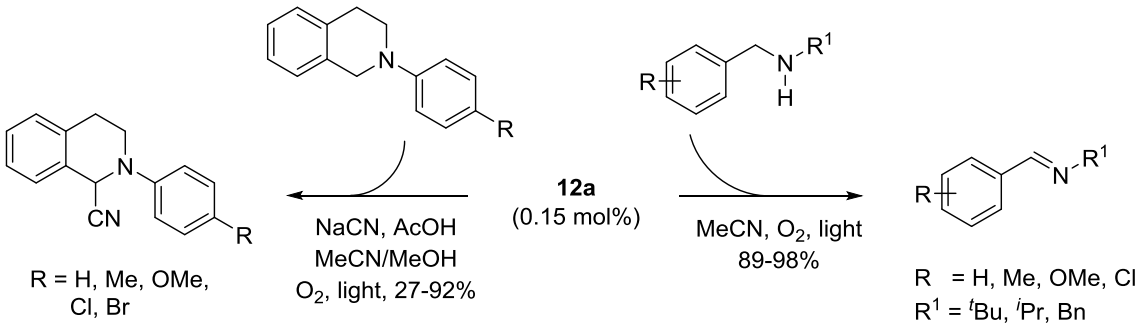

Scheme 2. [(C^N^C)Au(NHC)] complexes in photocatalyzed reactions.

1.1.2 [(C^N^C)AuOH] Complexes

Given the importance of [(C^N^C)Au^{III}] complexes, additional methods towards their straightforward derivatization have continued to flourish. In 2012, Bochmann and co-workers identified [(C^N^C)AuOH] complex **15** ((C^N^C) = 2,6-bis(4-*tert*-butylphenylpyridine)) as a suitable precursor to activate both Csp^2-, Csp- as well as N-H bonds under mild reaction conditions.[43] Compound **15** was initially prepared in two steps by reaction of the corresponding chloro derivative **13** with silver trifluoroacetate to give [(C^N^C)AuOAc^F] **14** followed by basic hydrolysis with KOH in toluene/water. Alternatively, a one-step procedure could be devised by treatment of **13** with $CsOH{\cdot}H_2O$ in THF/toluene/H_2O (1:1:1). The reaction of the resulting Au^{III}-OH complex with phenylacetylene in the absence of any additive furnished [(C^N^C)Au(C≡C-C_6H_5)] **16** in excellent yield. Treatment with 3,5-dimethylpyrazole and imidazole delivered the corresponding [(C^N^C)Au(NHet)] complexes **17a-b** in 95 and 92% yields, respectively. In refluxing toluene, **15** undergoes direct auration with fluoroarenes (pentafluorobenze and 2,3,5,6-tetrafluorobenzene) to form luminescent Au^{III}-aryl complexes [(C^N^C)Au($C_6H_xF_y$)] **18a-b**. Interestingly, [(C^N^C)Au(Aryl)] complexes **19a-d** were also obtained in high yields by reaction of **15** with the corresponding arylboronic acids under neutral conditions (Scheme 3).

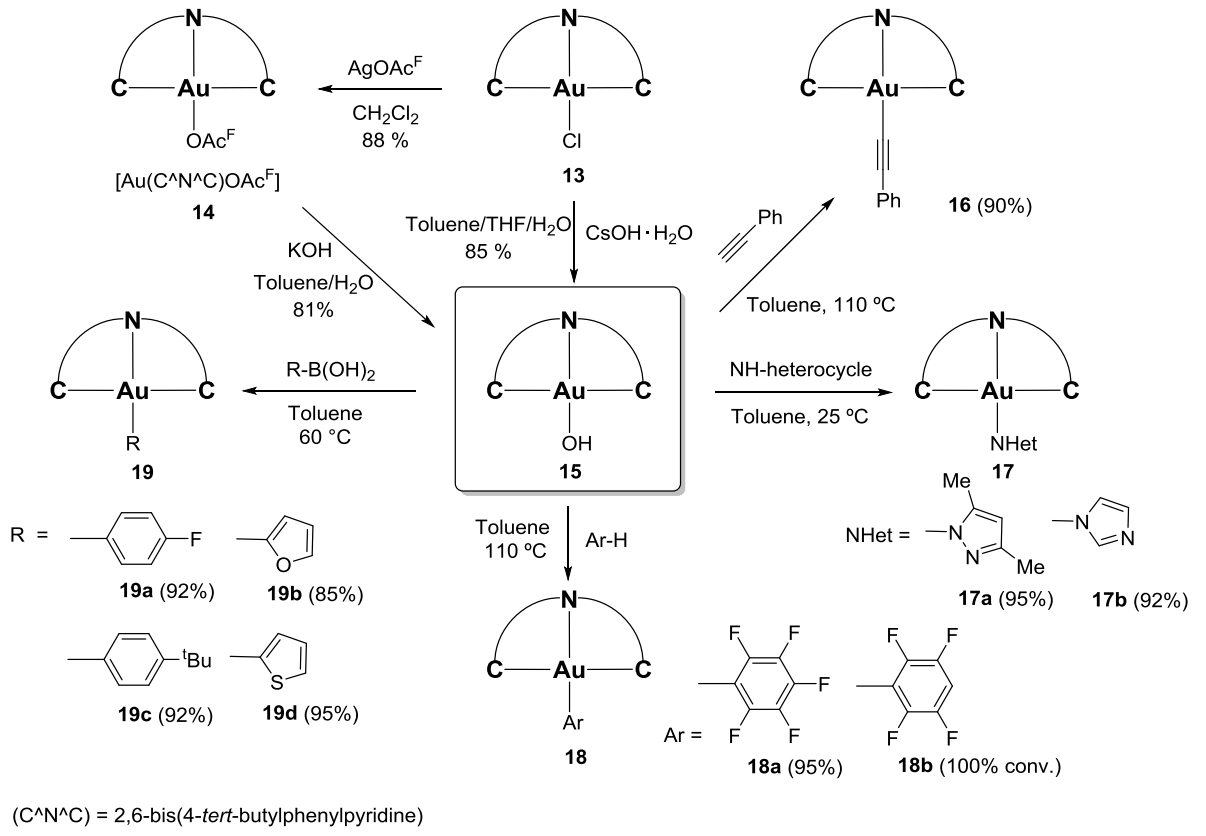

Scheme 3. [(C^N^C)AuOH] complex **15**: Synthesis and reactivity.

Cleavage of the Csp^2-Au bonds in these complexes has also been studied. Treatment of **18a** with trifluoroacetic acid ($HOAc^F$) delivered monocyclometalated [(C^N)$AuOAc^F$] complex **20a** in 90% yield. On the other hand, the reaction of [(C^N^C)$AuOAc^F$] **14** with $AgOAc^F$ in the presence of (*p*-fluorophenyl)boronic acid yielded analogous complex **20b** in 76% yield.[44]

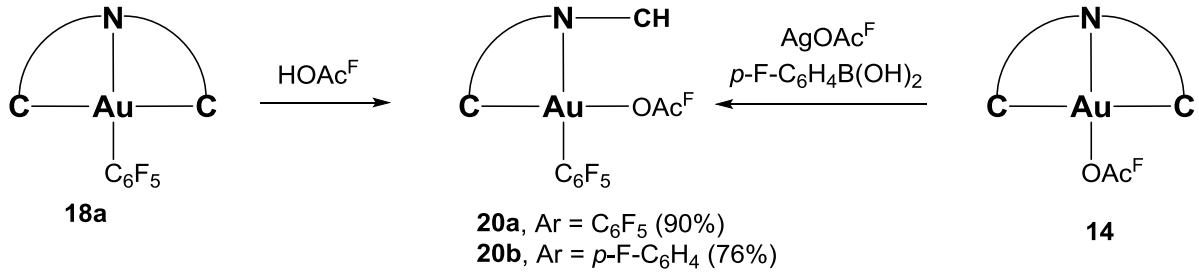

(C^N^C) = 2,6-bis(4-*tert*-butylphenylpyridine)

Scheme 4. [(C^N^C)Au^{III}] complexes as precursors of monocyclometalated [(C^N)$Au^{III}(OAc^F)$(Aryl)] complexes **20**.

1.1.3 [(C^N^C)Au(Olefin)] Complexes

In contrast to Au^I-alkene and alkyne complexes, which have been widely characterized,[45] Au^{III} complexes of olefin or diene are much more rare. Initial attempts to obtain Au^{III}-alkene species met with failure regardless of the gold source ($AuCl_3$, $AuBr_3$, $HAuCl_4$ and $NaAuCl_4$), as invariably reduction to Au^I or Au^0 was concomitantly observed. Taking advantage of the additional stability associated with the (C^N^C) pincer template, Bochmann and co-workers succeeded in the synthesis of Au^{III}-alkene complexes by reaction of [(C^N^C)$AuOAc^F$] **14** with cyclopentene, norbornene and ethylene as summarized in Scheme 5. Au^{III}-η^2-olefin complexes **21a-c** were efficiently obtained from reactions carried out in dichloromethane at -40 °C in the presence of $B(C_6F_5)_3$.[46] Coordination of the metal to the double bond is reversible since addition of dimethyl sulfide to an NMR sample of these complexes triggered a fast ligand exchange producing $[(C^N^C)AuSMe_2]^+$ together with the corresponding alkene. Interestingly, the reaction of [(C^N^C)$AuOAc^F$] **14** with ethylene in the absence of $B(C_6F_5)_3$ led to the quantitative insertion of ethylene into Au-OAc^F bond producing complex **22**. Likewise, the reaction of **14** with norbornene in the presence of MeOH yields monocyclometalated complex **23**, signalizing the selective Csp^2-Au^{III} cleavage in line with the results described in Scheme 4.

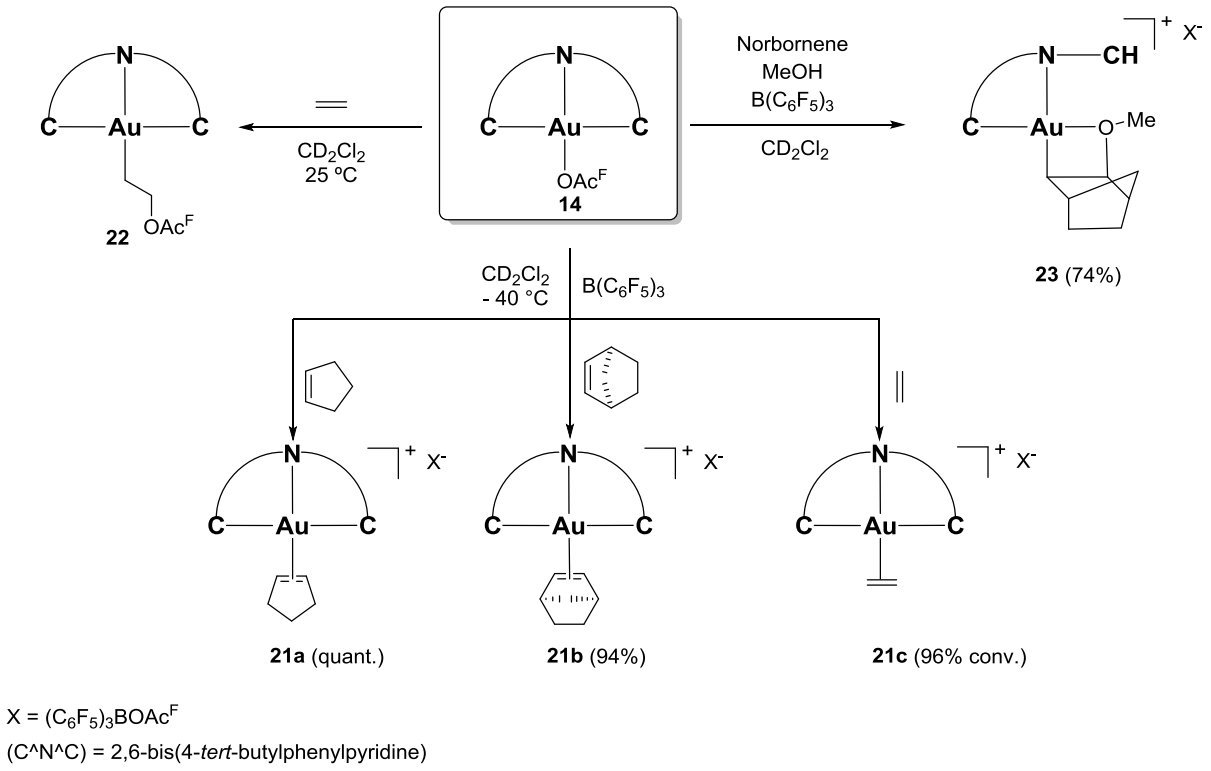

Scheme 5. [(C^N^C)Au^{III}(olefin)] complexes. Synthesis and reactivity.

1.1.4 [(C^N^C)AuH] Complexes

Au^{III}-hydroxo complex **15** served as suitable precursor for the first example of an isolated Au^{III}-hydride reported in the literature.[47] Complex **24** could be prepared as a dark yellow crystalline solid by the reaction of **15** with $LiHBEt_3$ in toluene at -78 °C. Surprisingly, **24** is stable towards air and moisture in solid state, whereas toluene and CH_2Cl_2 solutions darkened rapidly when exposed to light producing [(C^N^C)AuCl] **13** by activation of the solvent in the latter case. The rigidity of the (C^N^C) pincer ligand, which suppresses the otherwise expected reductive elimination to form Csp^2-H bonds, seems to be responsible for the stability of this complex. Complex **24** reacted with 1,1-dimethylallene and cyclohexylallene to produce the corresponding Au^{III}-vinyl complexes **25a-b** in high chemo- and regioselective fashion.[47] Recently, the hydroauration of internal and terminal alkynes has also been demonstrated.[48] In this case, the reaction seems to be mediated by radicals and a binuclear outer-sphere mechanism is proposed to justify the formation of the observed *trans*-insertion products **25**. Interestingly, the reaction of **24** with the analogous Au^{III}-OAc^F **14** (fast) and Au^{III}-OH complex **15** (slow) produced, via reductive condensation, Au^{II}-dimer **26**. The molecular arrangement of this binuclear complex was confirmed by X-Ray diffraction analysis which revealed a Au^{II}-Au^{II} bond distance of 2.4941(4) Å (Scheme 6).

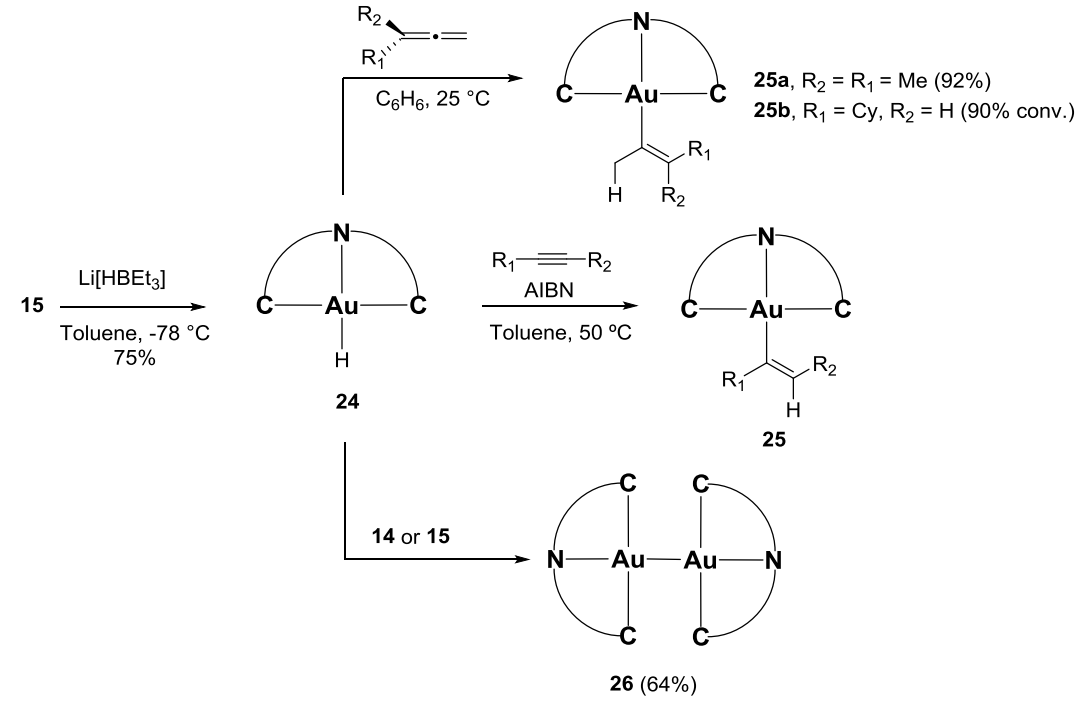

Scheme 6. [(C^N^C)AuH]. Synthesis and reactivity.

1.1.5 [(C^N^C)Au(Oxo) and (Peroxo)] Complexes

Au^{III}-oxo and -hydrperoxo complexes have been proposed as intermediates in numerous industrially relevant processes including the oxidation of CO as well as the electrochemical splitting of water. However, and despite extensive experimental and computational work, evidence for the formation of Au^{III}-O species, as well as in depth understanding of their stability and synthetic potential within this type of processes has been missing. Taking advantage of the stable Au^{III}-hydroxo complex [(C^N^C)AuOH] **15** and [(C^N^C)AuH] complex **24**, Bochmann and co-workers set out to study in depth the intrinsic reactivity of Au^{III}-O bonds in this context (Scheme 7).[49] First, Au^{III}-peroxo complex [(C^N^C)AuOO^{t}Bu] **27** could be synthesized by the reaction of [(C^N^C)AuOH] **15** with *tert*-butyl hydroperoxide in toluene at room temperature. Similarly, the reaction of **15** with 30% aqueous hydrogen peroxide produced the Au^{III}-hydroperoxide complex [(C^N^C)AuOOH] **28**. After prolonged time in solution (CD_2Cl_2 or THF), hydroperoxide **28** evolves into bridging peroxide **29** in a process that seems to be reversible as, in fact, **29** goes back to **28** and **15** in aqueous dichloromethane. It was also found that hydroxide **15** in dry solvents (acetone or THF) undergoes dehydration to form a bridging oxide complex **30**. The oxidizing character of Au^{III}-oxo and -peroxo complexes **27**-**30** was examined with [(*p*-tolyl)$_3$P] as reducing agent. The reaction of peroxide **27** with one equivalent of phosphine in dichloromethane produced [(C^N^C)AuO^{t}Bu] **31** and phosphine oxide [O=P(*p*-tolyl)$_3$] after 16 h at room temperature. In contrast, hydroperoxide **28** interacts with [(*p*-tolyl)$_3$P] to give hydroxide **15**

together with the corresponding phosphine oxide in a very fast reaction. When binuclear peroxide complex **29** was treated with [(*p*-tolyl)$_3$P], the phosphine is slowly oxidized reaching full conversion after 36 hours. A stepwise mechanism involving the abstraction of oxygen was proposed from **29→30→26**, although **30** could not be detected when the reaction progress was monitored by ^{1}H NMR, indicating that reduction of Au^{III} (**30**) to Au^{II} **26** is a fast process.

More importantly, when hydroxide **15** was treated with phosphine (excess) in dichloromethane at room temperature, the corresponding hydride [(C^N^C)AuH] **24** along with dimeric product **26** were detected in the reaction mixture.

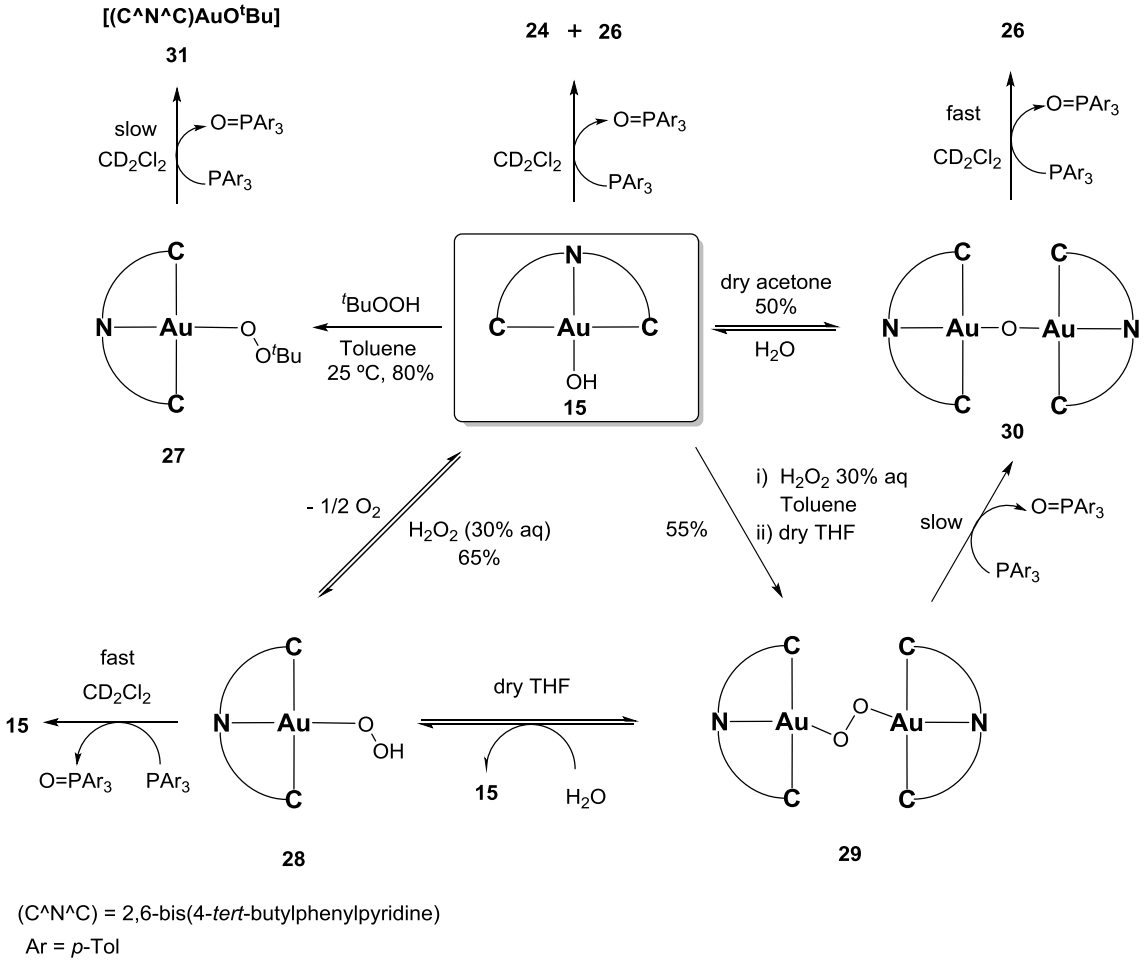

Scheme 7. [(C^N^C)Au^{III}(Oxo)] complexes. Synthesis and reactivity.

1.1.6 [(C^N^C) Au^{III}(CO)/(CO$_2$)] Complexes

In analogy to Au^{III}-hydrido or -oxo species, examples of gold-CO complexes had been mostly limited to Au^{I} species.[50] The interest in Au^{III}-CO complexes has recently spiked due to the good levels of activity that heterogeneous gold catalysts exhibit in water-gas shift reaction (WGS),[51-53] one of the most prominent processes for the sustainable generation of hydrogen. Mechanistic understanding of

these transformations relies on the ability to translate the heterogeneous processes to homogeneous set-ups so that the nature of the individual steps of the catalytic cycle can be fully unraveled based on the isolation and reactivity of the proposed reaction intermediates.

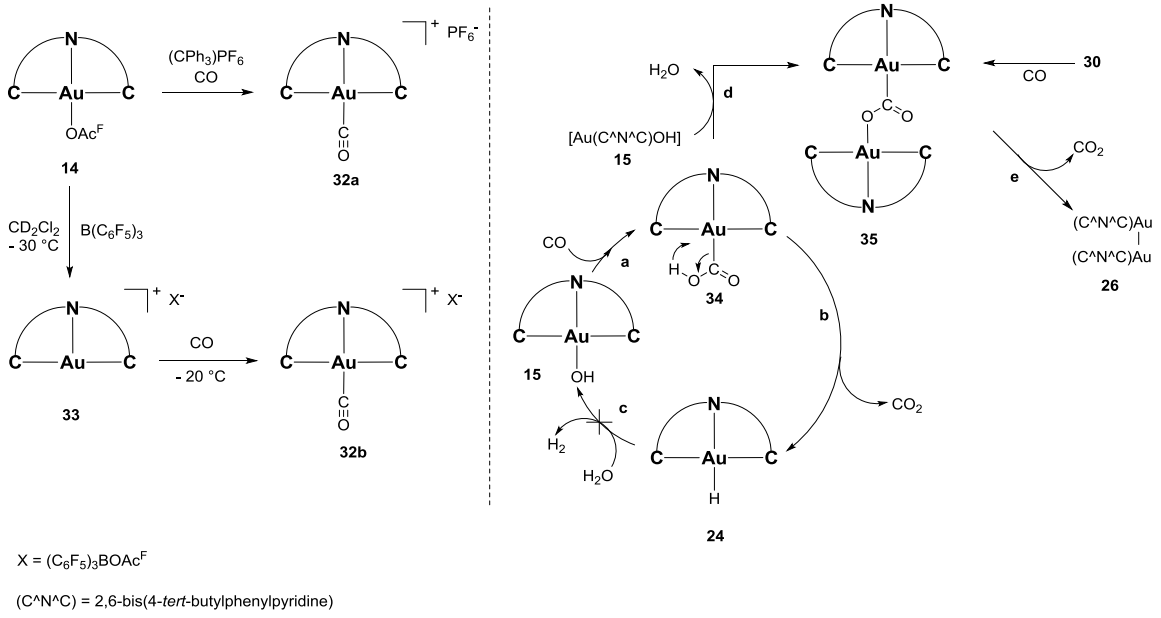

Scheme 8. (C^N^C)Au^{III}-CO complexes. Synthesis and reactivity.

Bochmann's group reported the successful synthesis of the first isolable Au^{III}-CO complexes $[(C^N^C)AuCO]^+X^-$ **32a** (X = PF_6) and **32b** (X = $B(C_6F_5)_3$) (Scheme 8).[50] Complex **32b** was synthesized in two steps by reaction of $[(C^N^C)AuOAc^F]$ **14** with $B(C_6F_5)_3$ in dichloromethane at -30 °C to generate complex **33** followed by treatment with CO at -20 °C to deliver $[(C^N^C)AuCO][B(C_6F_5)_3OAc^F]$ **32b**. Alternatively, the reaction of **14** with $(CPh_3)PF_6$ and CO in dichloromethane at -30 °C furnished complex **32a** in a single step process. Both Au^{III}-CO complexes are stable up to -10 °C and were characterized by both NMR and IR. Interestingly, a stretching ν_{CO} band for **32b** was observed at 2167 cm^{-1} compared to free CO (2143 cm^{-1}). Apparently, IR frequencies of Au^{III} carbonyls are very high compared to those of isoelectronic Pt^{II} congeners $[(N^N^C)PtCO]^+$ (ν_{CO} at 2094 cm^{-1}), suggesting that the back bonding donation in Au^{III}-CO is weaker than that in Pt^{II}-CO species.[54, 55] The difference in reactivity between Pt^{II}- and Au^{III}-CO complexes **32a-b** might also be explained on the same basis: while $[(N^N^C)PtCO]^+$ is stable at elevated temperature, analogous Au^{III}-CO complexes are highly sensitive towards both temperature or nucleophiles that react onto the electrophilic CO bond.

Different mechanisms (namely redox, formate or carboxylate pathways) have been proposed in metal-catalyzed WGS reactions.[51, 53, 56] The expected steps according to a carboxylate mechanism (**a**: CO insertion **b:** decarboxylation and **c**: water activation) are shown on the right hand side of Scheme 8. Hydroxide complex $[(C^N^C)AuOH]$ **15** was used as model system to probe this reaction pathway but replacing water to ensure a precise stoichiometry as well as reaction monitoring by ^1H NMR. Steps **a**

and **b** could be corroborated by detection of gold hydride **24** when CO was bubbled in a solution of **15** for 30 seconds at room temperature, suggesting the formation of unstable intermediate [(C^N^C)AuCO$_2$H] **34** which might undergo β-hydride elimination to liberate CO_2 and complex **24**. Unfortunately step **c**, needed to close the putative catalytic cycle, does not work under neutral conditions as hydride **24** is stable to water and weak acids as described in the previous section. The first gold-CO_2 complex **35** (step **d**) was obtained as a result of the reaction of **15** with CO when the mixture was left to crystalize in the dark for 20 h. Treatment of **30** with CO also gave the same complex **35** which undergoes CO_2 elimination (step **e**) in solution to form dimeric Au^{II} complex **26**.

1.2 [(C^N^N)Au^{III}] Complexes

The synthesis of stable [(C^N^N)Au^{III}] complexes has relied on monoanionic 6-substituted-2,2'-bipyridine and 2,9-diphenyl-1,10-phenanthroline ligands which are combined with suitable Au^{III} precursors in the presence or absence of silver salts to ensure a smooth Csp^2-H activation.[57-59] Representative members of this class of cationic complexes [(N^N^C)AuX] (**36-39**) have been summarized in Scheme 9.

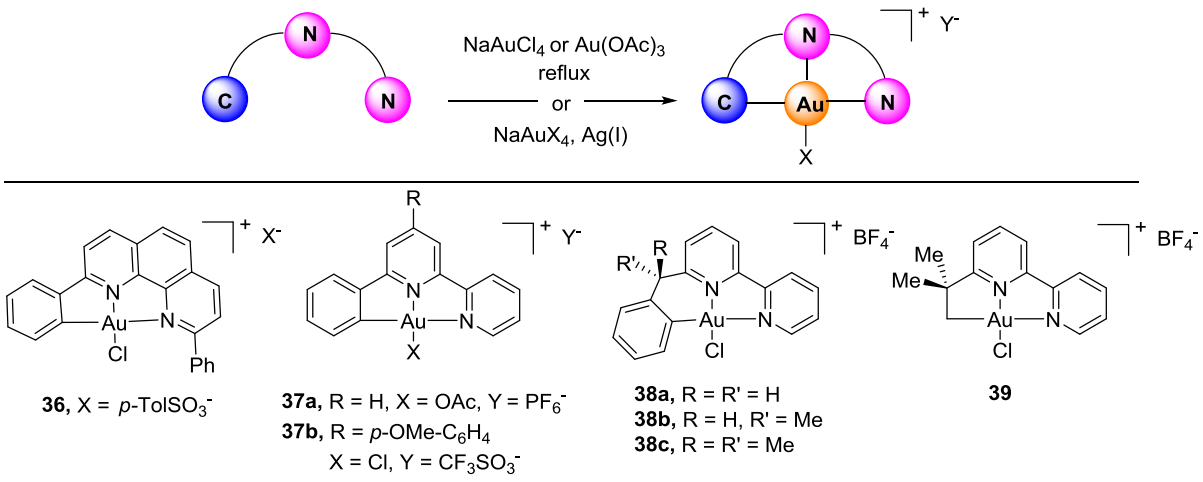

Scheme 9. Representative examples of [(C^N^C)AuX] complexes.

Ligand exchange reactions of the chlorido ligand have been explored although some of the resulting compounds proved to be unstable in solution. For example, direct treatment of **38c** with Ph_3P preferentially triggers the decoordination of one of the pyridine ligands to give monocyclometalated complex **40**. In contrast, abstraction of the chlorido ligand in the presence of silver acetate produced the corresponding [(C^N^C)AuOAc] derivative **41**, much more prone to exchange reactions, thus broadening the scope of nucleophiles that can be incorporated in these transformations as shown by the smooth formation of sulfide **42** (Scheme 10).

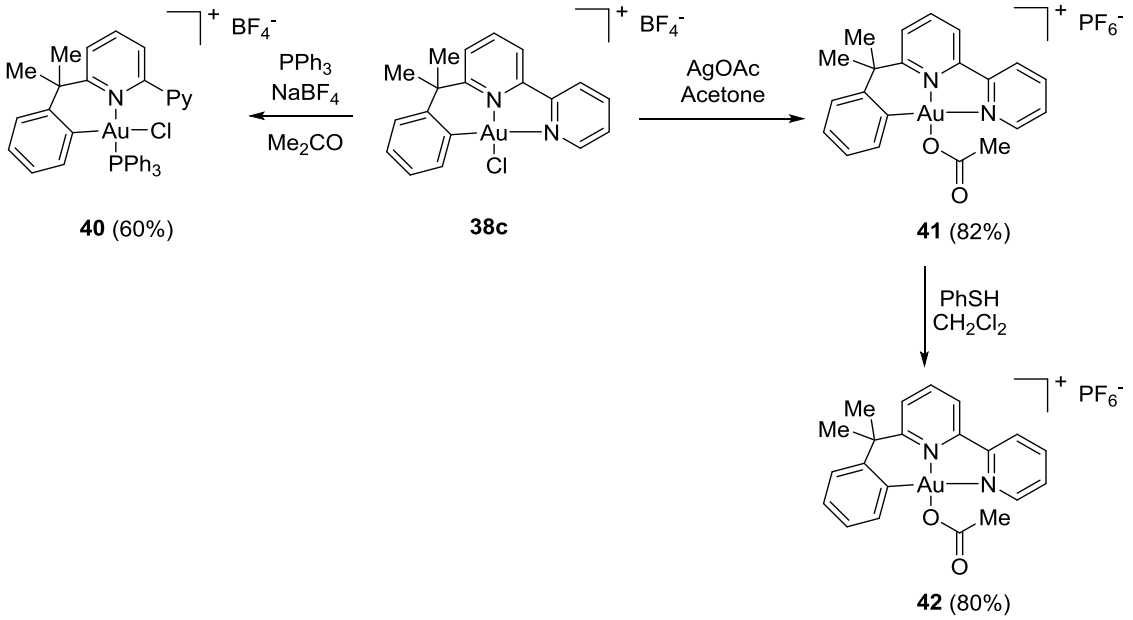

Scheme 10. [(C^N^C)AuCl] complex **38c**. Ligand exchange reactivity.

Complex **37a** could be used as a viable precursor of [(C^N^N)Au(alkynyl)] complexes **43a-e** by simple treatment with terminal alkynes under basic conditions (Scheme 11).[60] The luminescence of this class of complexes has been the focus of detailed studies, which reveal promising emissive properties in the solid state, likely stemming from IL states of the cyclometalated ligand.[60, 61] Additionally, the presence of strong aurophilic interactions between two discrete gold cationic complexes has also concealed increasing attention, particularly in the case of **43e** which, in contrast to some of the other members of this family, proved to be stable both as a solid as well as in solution. Single crystal analysis showed the shortest intermolecular $Au^{III}\cdots Au^{III}$ distance determined thus far between two Au^{III} complex cations (3.495 Å), which is comparable to that reported for intramolecular intermetal $Au^{III}\cdots Au^{III}$ systems (3.434 Å). The aurophilic interactions bring unique spectroscopic and photochemical properties as a consequence of metal-metal bonding interactions in the ground- and excited state.[62]

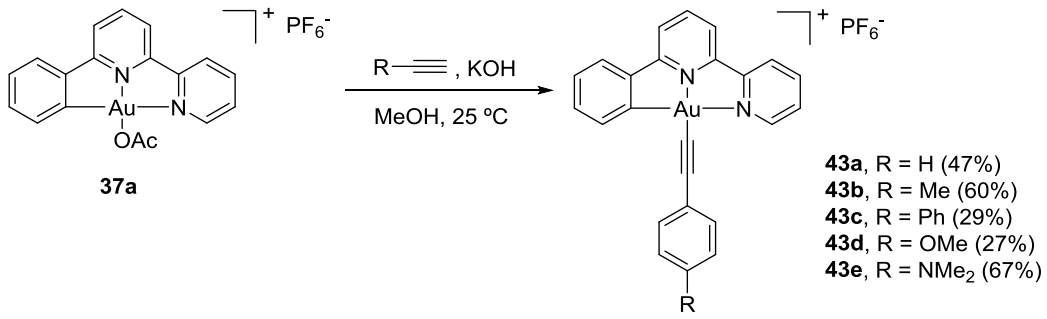

Scheme 11. [(C^N^C)Au(alkynyl)] complexes.

1.3 [(N^C^N)Au^{III}] Complexes

Among the biscyclometalated-Au^{III} pincer complexes, [(N^C^N)Au^{III}] species have remained largely unexplored due to their troublesome synthesis, even if the monoanionic (N^C^N) ligand has been broadly employed to stabilize d^8 transition metals like Ni^{II}, Pd^{II} and Pt^{II}. Transmetalation with the corresponding Hg precursor remains the most common strategy to access this class of cationic complexes, even in the case of six-membered biscyclometalated complexes.[63] Alternatively, direct auration in the presence of $HAuCl_4$ has also been successfully employed in a few cases.[64] In the case of tertiary alkylamines as a coordinating sites, transmetalation of the corresponding Aryl-Au^{I} has also been proven a viable pathway that avoids the use of toxic or sensitive reagents.[65] Representative examples of this complex class (**44-47**) have been summarized in Scheme 12.

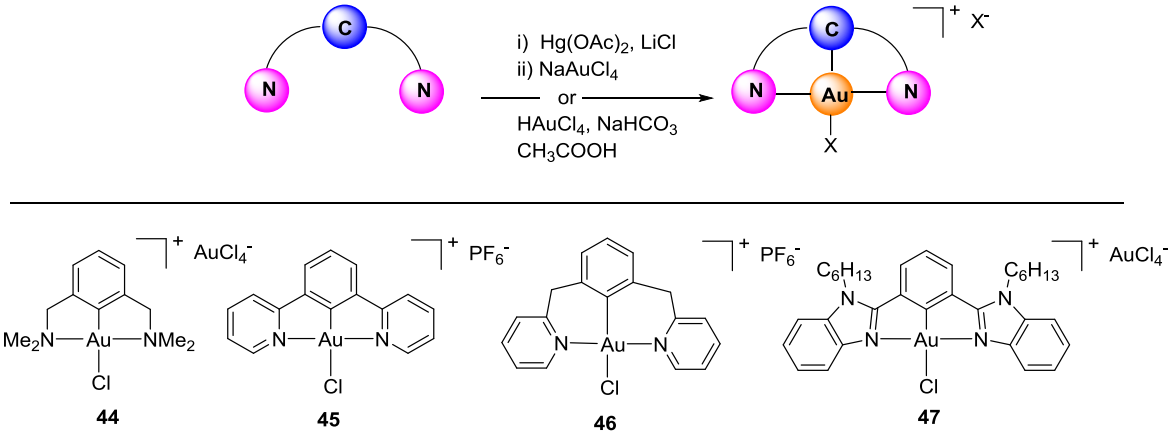

Scheme 12. Synthesis and representative examples of [(N^C^N)AuCl] complexes.

As shown in Scheme 13, replacement of the chlorido ligand in some of these complexes turned out to be rather challenging task. Attempts to abstract the chloride in [(N^C^N)AuCl]PF_6 **45,** even in the presence of silver salts, were not successful despite the clear elongation of the Au-Cl bond observed by X-Ray diffraction analysis. The reaction of **45** with triphenylphosphine resulted in the cleavage of the Au^{III}-N bonds to form complex **48** in which both phosphines are arranged in *trans* relative configuration whereas 6-membered ring biscyclometalated complex **46** reacted with PPh_3 to form a pentacoordinated Au^{III}-complex **49**.[63b] In contrast to these examples, the removal or exchange of the chlorido ligand on **44** took place smoothly in the presence of silver salts. It is thus clear that although all [(N^C^N)Au^{III}] complexes shown in Scheme 12 entitle a Au-Cl bond *trans* to a Csp^2-anionic carbon ligand, a completely different reactivity regarding chloride exchange is observed as a result of subtle effects of the ancillary ligand framework.

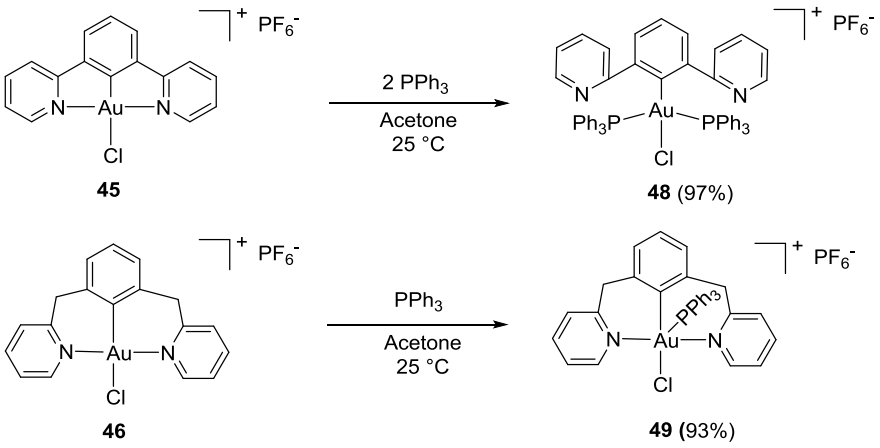

Scheme 13. Reactivity of [(N^C^N)AuCl] complexes.

Despite their sensitivity, the photophysical properties of [(N^C^N)Au^{III}] complexes could also be determined. Wenger and co-workers studied 1,3-bis(1-hexyl-2-benzimidazoyl)-benzene complexes **47** as the analogous Pd^{II} and Pt^{II} complexes were known,[66] with Pt^{II}-complexes being highly emissive. Compound **47** is non-emissive in solution but emits in solid state with λ_{max} at 427 nm at room temperature. The alkynyl derivative **50** could not be prepared using classical Sonogashira cross-coupling conditions and thus slow addition of [Au(L)Cl][$AuCl_4$] **47** to lithiated alkyne (4-ethynyltoluene) in THF had to be performed to produce **50** in very low yield. Although compound **50** [Au(L)(C≡C$C_6H_4CH_3$)][$AuCl_4$] could not be purified, it seemed to be emissive in dichloromethane at room temperature (Scheme 14).

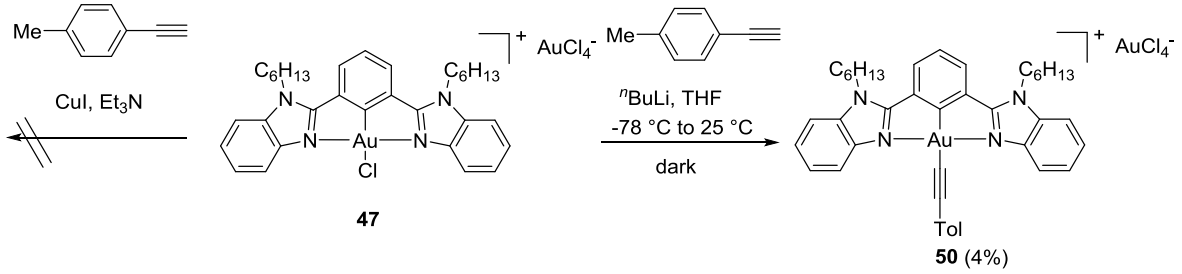

Scheme 14. Synthesis of [(N^C^N)Au(alkynyl)] complexes.

1.4 [(N^C^C)Au^{III}]Complexes

Recently, a new class of neutral pincer complexes based on 3,5-diarylsubstituted phenylpyridine ligands has also been reported.[67] [(N^C^C)Au^{III}] species were synthesized in two steps starting by coordination of $NaAuCl_4$ with the (N^C^C) ligand followed by biscyclometalation in acetonitrile:water mixtures under microwave conditions. The desired complexes were produced in good yields avoiding the use of Hg or any other hazardous metal. Representative members of this compound class (**51-53**) are shown in Scheme 15.

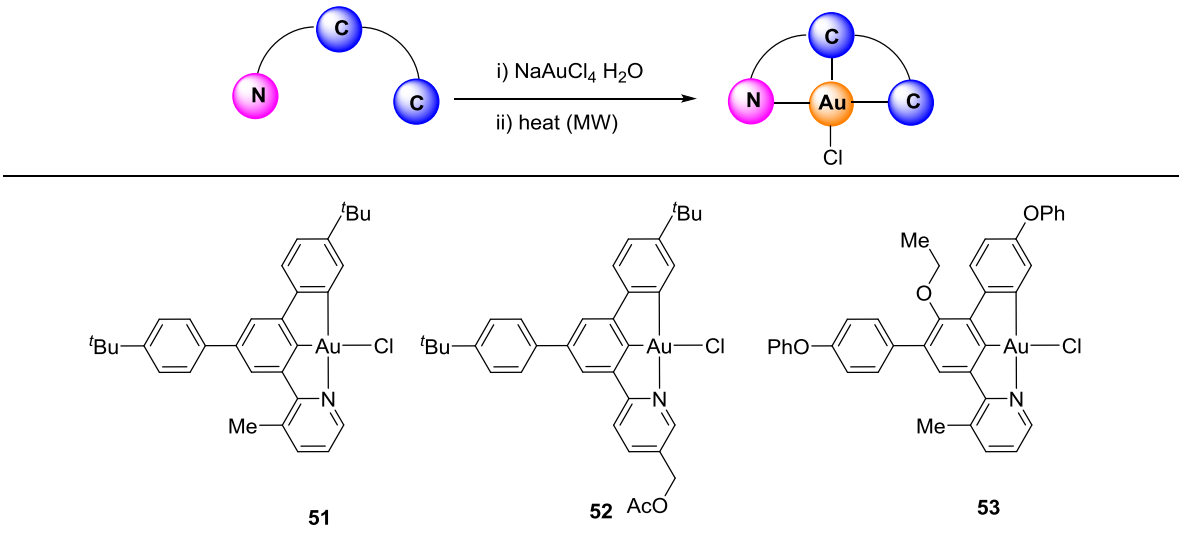

Scheme 15. Synthesis of [(N^C^C)AuCl] complexes. Representative examples.

The degree of stabilization provided by the (N^C^C) framework was assessed with the synthesis of highly electron-deprived Au^{III} species. Recently, gold-catalyzed oxidative cross-coupling reactions have been reported offering new venues for the formation C-C or C-X bonds.[8-13] These transformations rely on the use of strong oxidants such as Selectfluor to perform the key Au^{I}/Au^{III} redox turnover. Given the large number of reports invoking Au^{III}-fluorides as putative reaction intermediates and the lack of solid experimental evidence on their participation in these transformations [(N^C^C)AuF] complexes were sought in this study. Stable Au^{III}-F complexes could be prepared through a mild Cl/F ligand exchange reaction in the presence of AgF (Scheme 16). Complex **54** was found to be thermally stable (in solid state as well as in solution) and not sensitive to air, in contrast to the previously reported gold(III) fluorido complexes.[68]

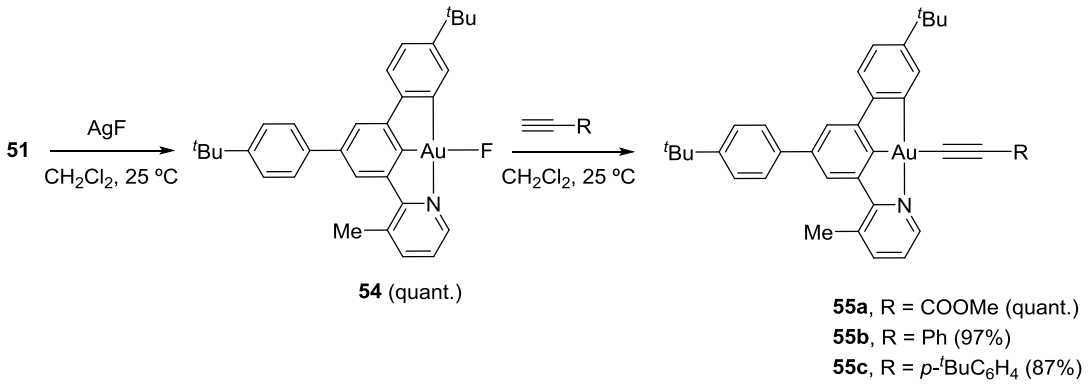

Scheme 16. Synthesis of [(N^C^C)AuF] and [(N^C^C)Au(alkynyl)] complexes.

As discussed in the previous sections, one of the main challenges in the development of highly phosphorescent Au^{III} complexes is the need to overcome the high electrophilicity of the Au^{III} center which renders the unoccupied dσ* (dx^2-y^2) orbital low-lying as a result low-energy ligand-to-metal

charge transfer (LMCT). As a result, excited states close to the emissive IL excited states, lead to effective luminescence quenching. Theoretical calculations had predicted that the rigidity of the (N^C^C) framework, with two consecutive C_{sp}^2 anionic carbons stabilizing the electrophilic Au^{III} center could help to overcome these limitations.[31a, 31c, 31d] Thus, Au^{III}-alkynyl complexes [(N^C^C)Au(C≡CR)] **55a-c** could be obtained in very good yields when **54** was treated with terminal alkynes in dichloromethane at room temperature. These complexes were found to be highly luminescent in degassed dichloromethane solution. Here, it is important to mention that even the chlorido complexes **51** show intense luminescence (with PL quantum yield up to 17% and emission lifetime of 56 μs, this is in stark contrast to their analogous [(C^N^C)AuCl] **1** and **13** which are not emissive even at 77 K. Moreover, complex **55b** shows an emission quantum yield up to 28% with 80 μs lifetime, which compares positively with that of [(C^N^C)Au(alkynyl)] complexes **5**. Keeping in mind the facile synthesis, great stability and highly luminescent nature, improved versions of these complexes might hold potential as candidates for the development of new OLEDs.

2. Monocyclometalated Gold Complexes

2.1 [(C^N)Au^{III}] Complexes

2-Aryl substituted pyridine ligands have been predominantly used to prepare [(C^N)Au^{III}] neutral monocyclometalated gold complexes. However, metalation sites have also been extended to Csp^3-hybridized atoms and N-centers from amines, imines and diazo compounds so that five- as well as six-membered ring monocyclometalated complexes have been successfully obtained. Three main strategies have been broadly applied to enable the key cycloauration process: a) transmetalation with the corresponding organomercury intermediates; b) N-coordination followed by chloride abstraction in presence of Ag^I salt; c) direct coordination and auration upon strong heating or microwave conditions. Selected examples of this compound class (**56**-**73**) are presented in Scheme 17.[69,70, 63a, 71-73] In 2007, Henderson reviewed this highly abundant class of complexes, with particular emphasis on the synthesis of the dichloro derivatives and their reactivity towards ligand displacements with phosphines, halide, pseudohalides and carboxylates.[74] As such, only the most recent developments on this class of complexes will be described herein.

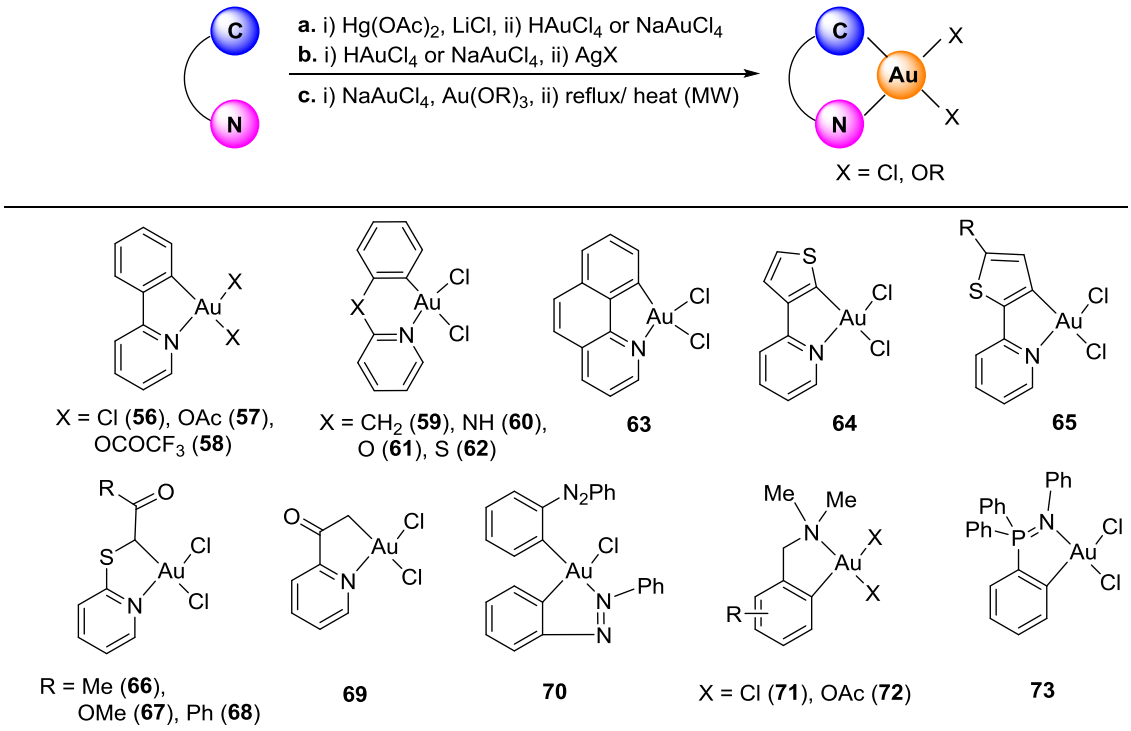

Scheme 17. Synthesis and representative examples of [(C^N)AuX$_2$] complexes.

2.1.1 [(C^N)Au(Aryl)] Complexes

Earlier investigations by Vicente and co-workers on 2-phenyl-azophenyl based ligands enabled the synthesis of a broad spectrum of [(C^N)Au^{III}] mono- and-diaryl complexes.[75] These species were recognized as highly prone to undergo reductive elimination yielding Csp^2-Csp^2 bonds and Au^I species, thus fostering efforts towards the development of more stable templates. Taking advantage of stable, cyclometalated 2-phenylpyridine [(C^N)AuCl$_2$] precursors, [(C^N)Au^{III}]-biaryl complexes could be synthesized by reaction with the corresponding lithiated arenes in dry diethyl ether at -78 °C (Method A, Scheme 18). Yields were only moderate due to partial decomposition of these compounds via reductive elimination. As such, higher stability was sought by employing electron deficient arene species as shown by compounds **74a-d**.[76] Very recently Gray *et al*. reported an alternative method, via a Suzuki-Miyaura coupling of arylboronic acids on the corresponding Au^{III}-dichloro complex (Method B, Scheme 18).[77] Catalytic amounts of Pd(OAc)$_2$ in the presence of K$_2$CO$_3$ in toluene:^{i}PrOH at room temperature furnished diaryl complexes **75a-d** in good yields. The protocol is quite general and tolerates a wide range of substituents from EDG (Me, OMe) to EWG ones (esters, CF$_3$, NO$_2$) on the aryl boronic acid counterpart.

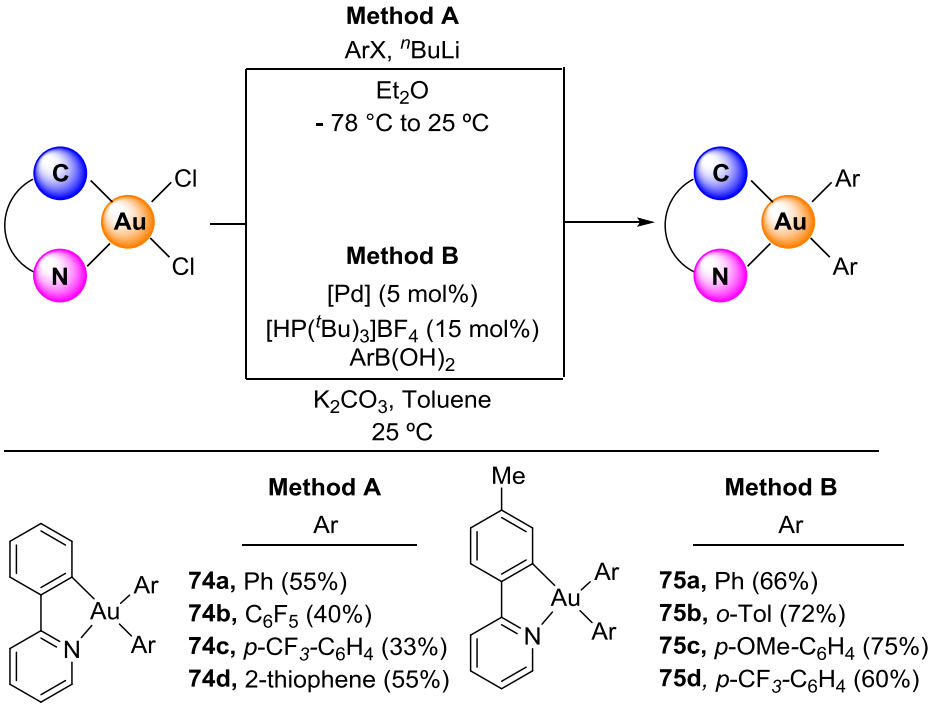

Scheme 18. Synthesis of [(C^N)Au(Ar)$_2$] complexes.

The introduction of strong field aromatic stabilized carbanions ligands aimed to destabilize the metal centered (MC) transition to higher energies thereby creating a conductive metal-ligand environment for effective mixing of singlet-triplet states and radiative relaxation from the triplet manifold. [(C^N)Au^{III}]-Biaryl complexes **74b-d** turned out to be emissive with PL quantum yield up to 1%. As the different aryl moieties showed no significant effect on the absorption or the emission wavelengths of these complexes, the observed emission bands are assigned to a metal perturbed intraligand charge transfer (^{3}ILCT) [π-π*].

To improve the emission as well as the stability and quantum yields of these species, analogous [(C^N)Au^{III}]-monoaryl complexes were sought combining highly electron deficient ancillary ligands with strong field donors (Scheme 19).[78] The reaction of lithiated 2,4,6-tris(trifluoromethyl)phenyl (LiFMes) with Au^{III}-dichloro complex **56** in dry diethyl ether afforded monoarylated product **76** in 77% yield. The chlorido group could be displaced by terabutylammonium cyanide, NaI, Ph-C≡C-Ag and *p*-(NPh$_2$)-C$_4$H$_4$-C≡C-Cu respectively delivering complexes **77a-d** in moderate to good yields. Unlike diaryl complexes **75a-d**, both the ancillary (C^N) and the anionic (Y = CN, I, alkynyl) ligand showed significant influence on both the absorption as well as on the emission wavelengths of these complexes. Interestingly, a highly efficient interligand charge transfer in **77d** results in a solvent-dependent emission behavior ranging from deep blue to red. A photoluminescence emission quantum yield of 30% (441 nm) in solution and 39% (622 nm) in solid state could be observed, which is comparable to that of the most efficient (C^N^C) biscyclometalated Au^{III} complexes described in the previous sections.[38-39]

Aquo complex **78** was obtained in 93% yield by reaction of **76** with AgOTf in chloroform at room temperature. The weakly coordinating water could be displaced by different weak nucleophiles like PPh_3 (**79a**), $P(OMe)_3$ (**79b**), 4-fluoroaniline (**79c**), 4-fluoropyridine (**79d**) and quinoline (**79e**). These complexes exhibit a PL quantum yield up to 17.8% with emission lifetimes of ca. 150 μs in poly(methylmethacrylate) (PMMA) matrix. Their photocatalytic behavior was examined towards the photooxidation of benzylic amines to the corresponding imines. Complex **79b** proved to be the best catalyst so that a 0.5 mol% load sufficed to perform the quantitative conversion of N-benzyl-*tert*-butylamine to the corresponding N-benzylidene-imines within 4 h in the presence of molecular oxygen.[79]

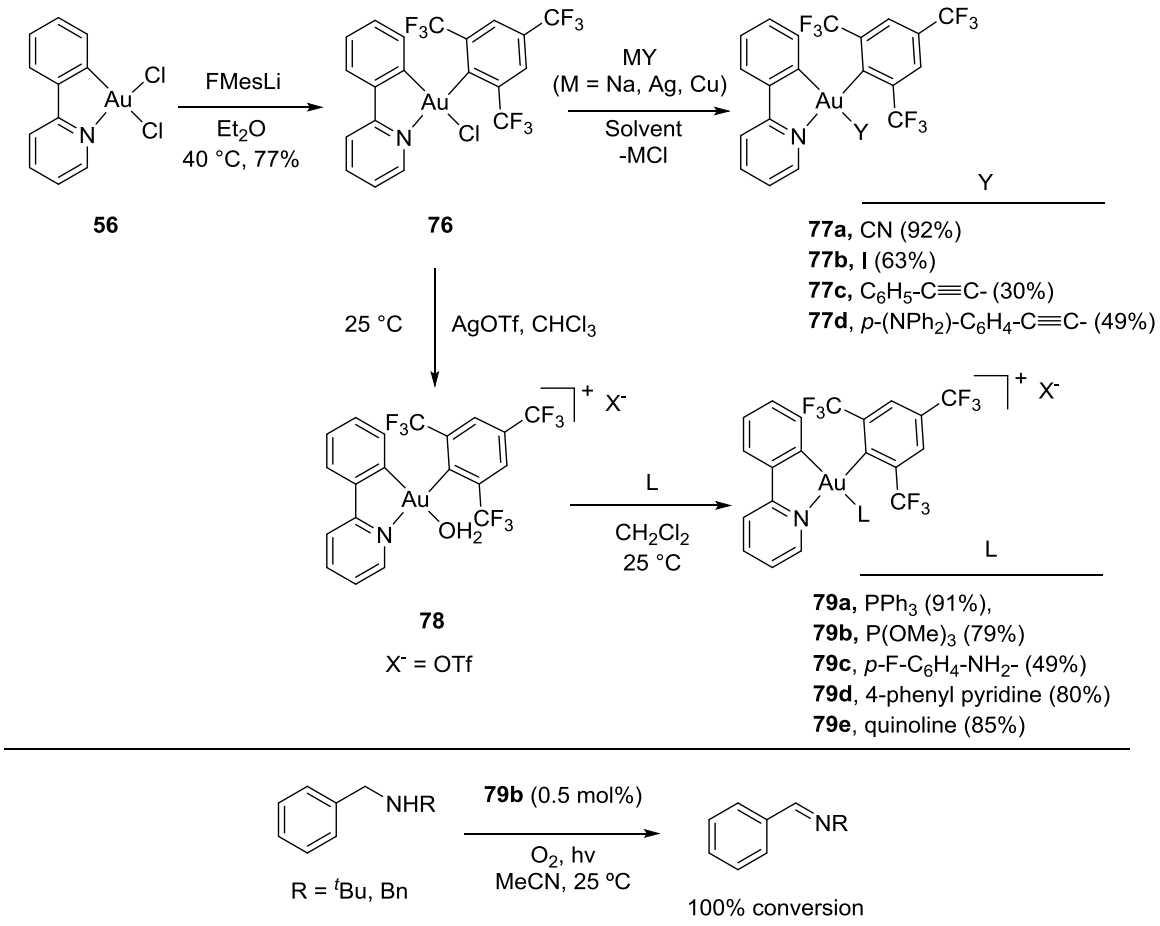

Scheme 19. Synthesis of [(C^N)Au(Ar)(Y)] complexes.

2.1.2 [(C^N)Au(Alkynyl)] Complexes

As discussed in the previous section, a well-established strategy to enhance the luminescence of Au^{III} complexes is the incorporation of strong σ-donor ligands in order to enlarge the d-d ligand-field-spliting. To this end, Yam and co-workers followed a similar approach to that described in the preceding section but using Li-alkynyl species to produce monocyclometalated [(C^N)Au^{III}]-dialkynyl complexes **80-82** (Scheme 20, Method A).[80] An analogous series (**83-85**) was reported by Koushik and

co-workers using terminal alkynes in the presence of Et_3N and a catalytic amount of CuI to attain the required ligand exchange (Scheme 20, Method B).[81] These complexes, with the exception of **83**, exhibited luminescence at room temperature in solution, which is ascribed to a metal-perturbed ^{3}IL(π-π*) transition of the cyclometalated (N^C) ligand.

Interesting lessons can also be learnt from the photoluminescence properties determined for these compounds. For example, complex **85** showed higher quantum yield compare to **83a** indicating that the structural rigidification leads to partial decrease in non-radiative decay rates (κ_{nr}). Quantum yields up to 10.3% and emission lifetimes up to ca. 30 μs were observed surpassing the analogous diaryl complexes **77a-d** and approaching the efficiency of high order biscyclometalated [(C^N^C))Au(alkynyl)] complexes seen in the previous sections.

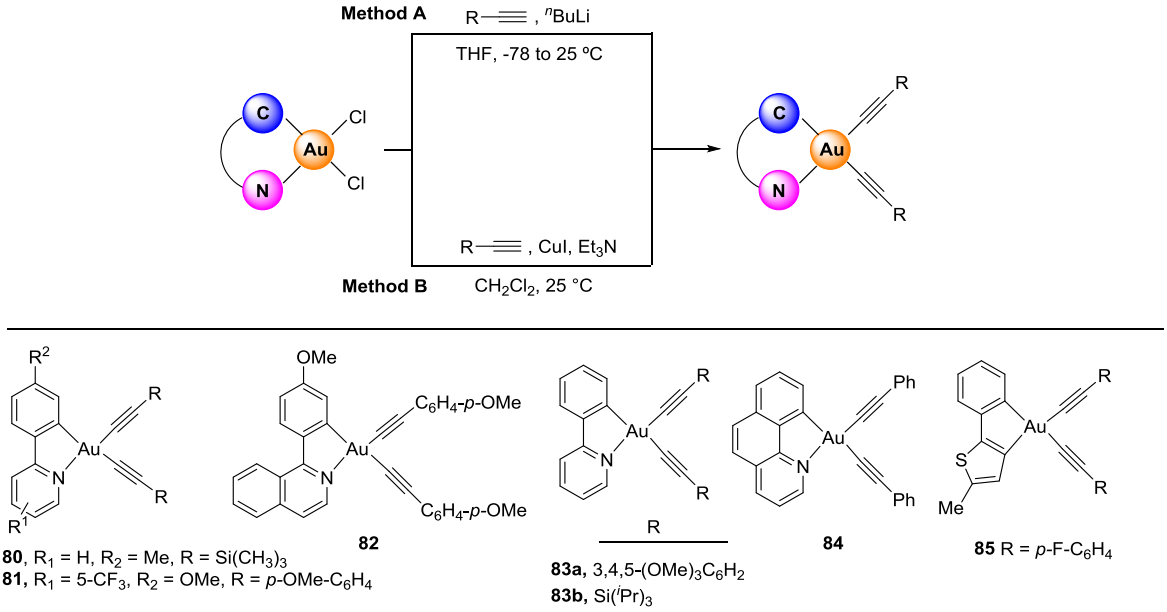

Scheme 20. Synthesis of of [(C^N)Au(C≡CR)$_2$] complexes

2.1.3 [(C^N)Au(CN)$_2$] Complexes

As described earlier, the lack of stability of monocyclometalated [(C^N)Au^{III}]-mono-, bisaryl and bisalkynyl complexes due to facile reductive elimination poses serious challenge for their development as doping agents in OLEDs. The use of cyanides as strong σ-donor ligands in this context represents an attractive strategy: first, the resulting compounds would have an enhanced stability as reductive elimination would be disfavored and π-back donation could also enhance the complex stability. Second, as strong σ-donors, an enhanced splitting of non-emissive d-d states is to be expected. In fact, luminescent cyclometalated Ir^{III}- and Pt^{II}-dicyano complexes are known[82] but only recently luminescent [(C^N)Au^{III}]-dicyano complexes have been reported **86**-**88** (Scheme 21).[83] These complexes were easily prepared by reaction of corresponding Au^{III}-dichlorido precursors with

tetrabutylammonium cyanide in MeCN/MeOH solvent mixtures. Unlike diaryl (**74-75**) or dialkynyl complexes (**80-85**), where electronic tuning was required to get stable complexes, all these compounds are stable and easy to handle. Each complex shows a different emission maxima which signalize the participation of the (C^N) ligand in the excited state and the minimal involvement of cyanide ligand, in sharp contrast to the behavior observed in Ir^{III}- and Pt^{II}-dicyano complexes. Although in solution the compounds are not powerful emitters, PL quantum yields up to 30% were achieved in PMMA films making these complexes a potential alternative to less stable diaryl or dialkynyl Au^{III} complexes described in Schemes 18 and 20.

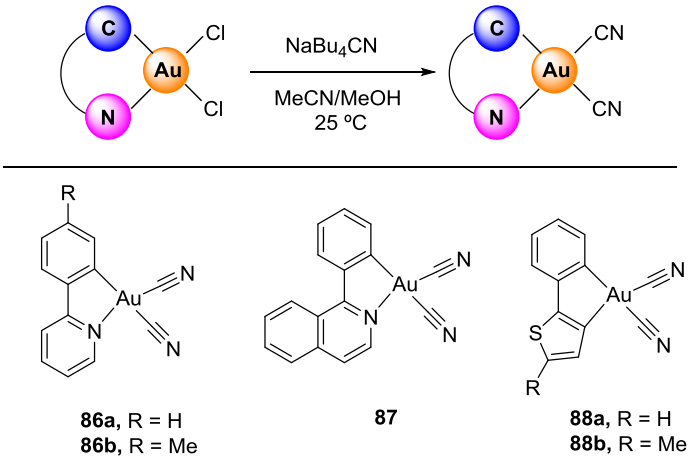

Scheme 21. Synthesis of [(C^N)Au(CN)$_2$] complexes.

2.1.4 [(C^N)Au(NHC)] Complexes

In 2014, Che and co-workers presented the synthesis of cyclometalated [(C^N)Au(NHC)$_2$] complexes **89** and **90** by transmetalation of the corresponding [(C^N)AuCl$_2$] precursor with (NHC)Ag^{I} salts (Scheme 22).[84] Complexes of type **89** show luminescence in solution (CH_3CN) at room temperature with quantum yields up to ca. 10%. As in the previous cases, the emissions are assigned to a triplet intraligand ^{3}IL(π-π*) transition of the cyclometalated (C^N) moiety. Importantly, sulfonate-functionalized complexes **90** are water soluble and present both fluorescence and phosphorescence properties.

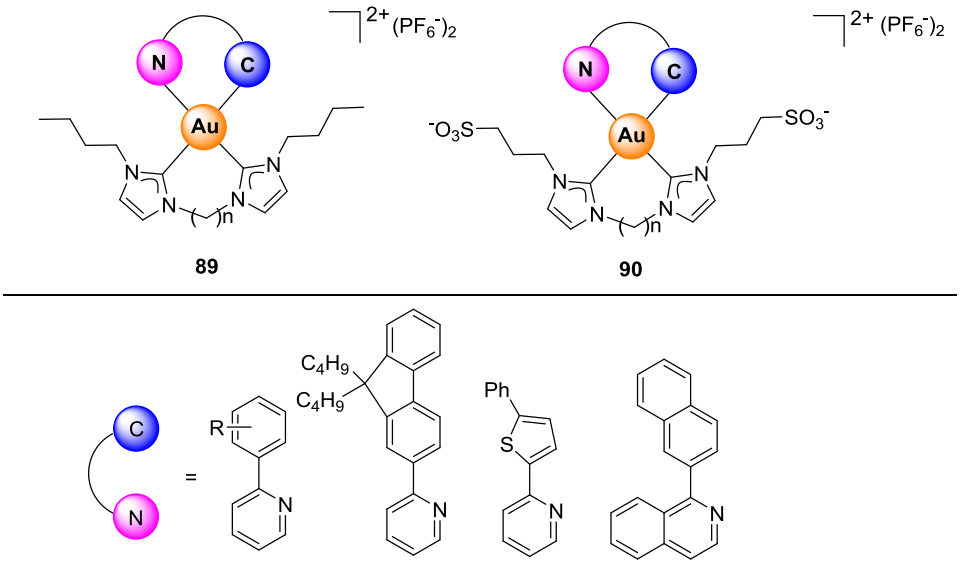

Scheme 22. Examples of [(C^N)Au(NHC)$_2$] complexes.

2.1.5 [(C^N)Au(Oxo)] Complexes

The lability of acetato and trifluoroacetato ligands confers [(C^N)Au(OR)$_2$] complexes a higher reactivity compared to the corresponding dichloro counterparts. In a representative example, Au^{III}-diacetato complex **91** has been shown to activate the C-H bond of acetone delivering the corresponding σ-acetonyl complex **92**,[72b] a process that has been previously observed in Au^{III} species (Scheme 23).[85] Trifluoroacetato ligands are even more labile and reactive,[86] and thus the reactions with Grignard or lithium reagents at low temperature produce, selectively mono- and dialkylated compounds **94** and **95** respectively in higher yields compared to methods based on the reaction of the corresponding dichloro precursors (Scheme 23).

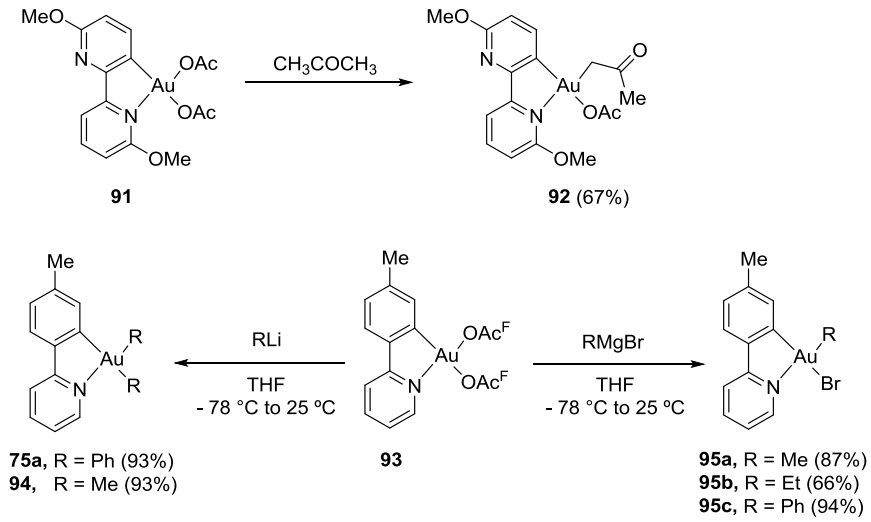

Scheme 23. Reactivity of [(C^N)Au(OR)$_2$] complexes.

Compound **94** proved to be a suitable precursor for one of the few Au^{III}-diolefinic complexes reported up to date.[87] Upon treatment with triflic acid (TfOH) at -78°C in dichloromethane, complex **96** was formed in 85% yield. Addition of 1,5-cyclooctadiene (COD) furnished Au^{III}-olefin complex **97a** which could only be characterized by a down-field ^{1}H-NMR shift in the COD vinylic protons (from δ = 5.56 ppm to δ = 6.39 ppm). Attempts to grow crystals of this compound met with failure, therefore complex **97b** was synthesized by the reaction of **94** with $[\{3,5\text{-}(CF_3)_2\text{-}C_3H_3\}_4B^-][(Et_2O)_2H^+]$ ($HBArf{\bullet}2OEt_2$) followed by the addition of COD (Scheme 24). Complex **97b** gave suitable crystals for X-Ray diffraction analysis, which showed a rather long Au^{III}-C_{cod} distance compared to those found in Au^{I}-C_{alkene} complexes[88] or in isoelectronic $[(cod)PtMe_2]$ complex previously reported.[89]

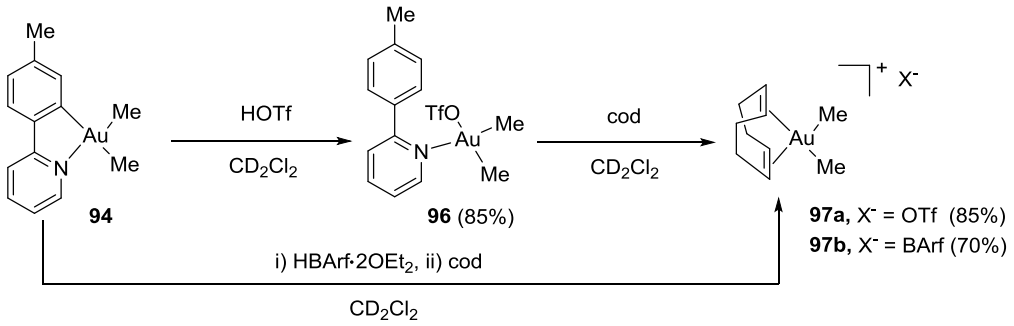

Scheme 24. [(C^N)Au(di-olefinic)] complexes.

In 2014, Tilset's group conducted a detailed mechanistic study on the reversible insertion of ethylene into $[(C\text{^}N)Au^{III}(OR)_2]$ bonds.[90] When a solution of complex **93** in trifluoroacetic acid (TFA) was bubbled with ethylene, formation of inserted product **98** was immediately observed. The reaction of **93** with ethylene in trifluoroethanol (TFE) as solvent delivered the ethylene inserted product **99** within 30 minutes. The structures of both **98** and **99** could be confirmed by X-Ray diffraction analysis. The products observed reflect a formal insertion of ethylene into the Au-O bond in *trans* selective fashion to the pyridine (weakest *trans* effect) rather than to the C (strongest *trans* effect) ligand. This initially counterintuitive result could be successfully rationalized by means of a two-step mechanism corroborated by DFT calculations: in the first step, the substitution of one of the OAc^F ligands by ethylene takes place. Although this process would be more favored to occur *trans* to the C ligand, the subsequent step, i.e. the attack of the liberated OAc^F at the coordinated ethylene in *trans* fashion is both thermodynamically and kinetically more favorable on the ethylene precursor stemming from ligand displacement *trans* to the pyridine ligand, thus explaining the selective formation of **98** and **99**. This study also revealed that the attack of the OAc^F to ethylene is a reversible processes, a well-established reactivity for Au^I but not for Au^{III} complexes. The higher reaction rates observed in TFA and TFE compared with DCM seem to correlated with the rate determining substitution of the OAc^F ligand due to the different abilities of these solvents to stabilize the corresponding anions. This work set the ground

for the development of catalytic version of the reaction, for which the dichotomy between *trans* to N vs. *trans* to C in the protodeauration step will need to be exquisitely sorted out.

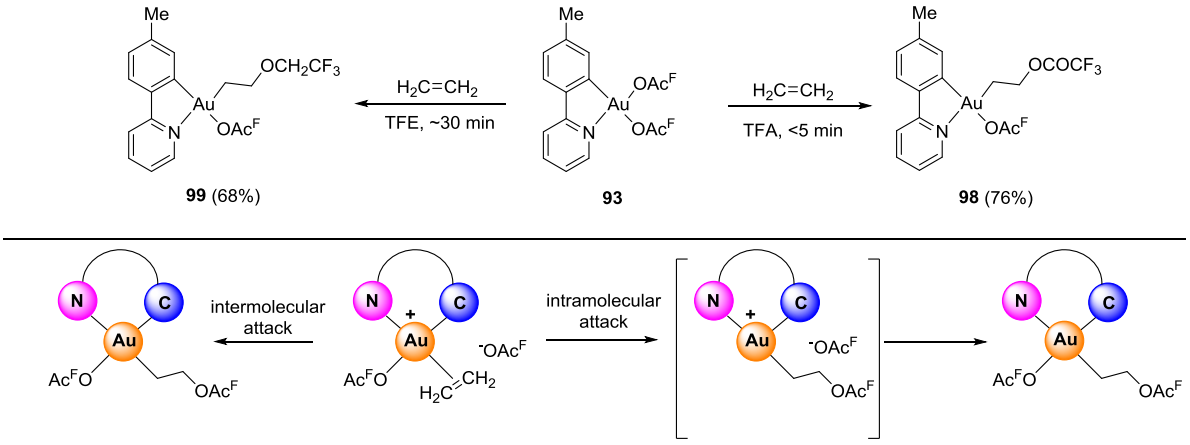

Scheme 25. [(C^N)Au(OR)$_2$]: alkene insertion complexes.

An interesting extension of the reactivity of [(C^N)Au(OAc^F)$_2$] complexes was recently reported by Gray and co-workers. Treatment of **58** and **93** with boronic acids in the presence of potassium *tert*-butoxide led to the formation of cylometalated Au^{III} boroxinato complexes **100** in good yields via a arrested transmetalation reaction (Scheme 26).[91]

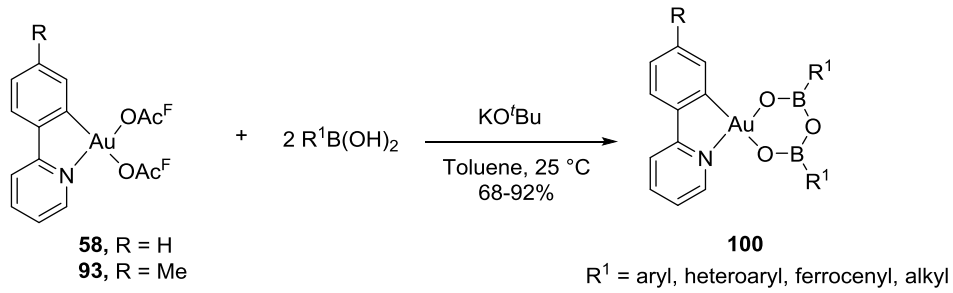

Scheme 26. [(C^N)Au(OB-R$_1$)$_2$O]: boronic acid complexes.

2.1.6 [(C^N)Au(X)(Y)] Complexes as Catalysts

[(C^N)Au(X)(Y)] complexes have also found application in catalysis. In particular, [(C^N)AuCl$_2$] dichlorido complex **56** was successfully used as carbophilic Lewis acid for the efficient π-activation of alkynes in a three component reaction involving aldehydes, secondary amines and terminal alkynes to produce propagylamines as shown in Scheme 27.[92] Complex **56** proved to be highly robust so that 10 successive cycles could be performed with overall turnover numbers > 800. More recently, investigations have also showcased catalytic applications of these complexes towards the synthesis of chiral allenes, oxazoles and isoxazoles respectively.[93, 94]

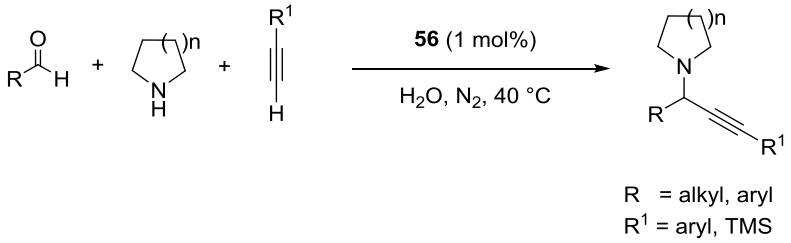

Scheme 27. Application of **56** as catalyst in a multicomponent reaction.

In 2015, You *et al*. described the utilization of cyclometalated [(C^N)Au(X)(Y)] complexes **101a-b** to study the mechanism of gold-catalyzed oxidative C-H arylation of 2-arylpyridines with arylboronic acids (Scheme 28).[95] The stoichiometric reaction of **101a-b** with phenylboronic acid in the presence of KF delivered the desired cross-coupled product **102** in excellent yield. Since no halogen-fluorido (Halogen = Cl, Br) exchange on Au^{III} could be observed by ^{19}F NMR, KF is considered a Lewis base that activates the C-B bond towards trasmetalation. A catalytic version of this transformation could be devised with NFSI as stoichiometric oxidant. Formation of a [(C^N)AuPhCl] complex could be confirmed by ESI-HRMS whereas a signal at δ = -210.4 ppm in the ^{19}F NMR is proposed to signalize the formation of a Au^{III}-F bond during the course of reaction. A detailed investigation on the synthesis and isolation of (C^N)-gold(III) fluorido complexes [(C^N)AuFR] (R = F, Aryl) and their reactivity towards transmetalation with aryl boronic acids has also been recently reported.[96]

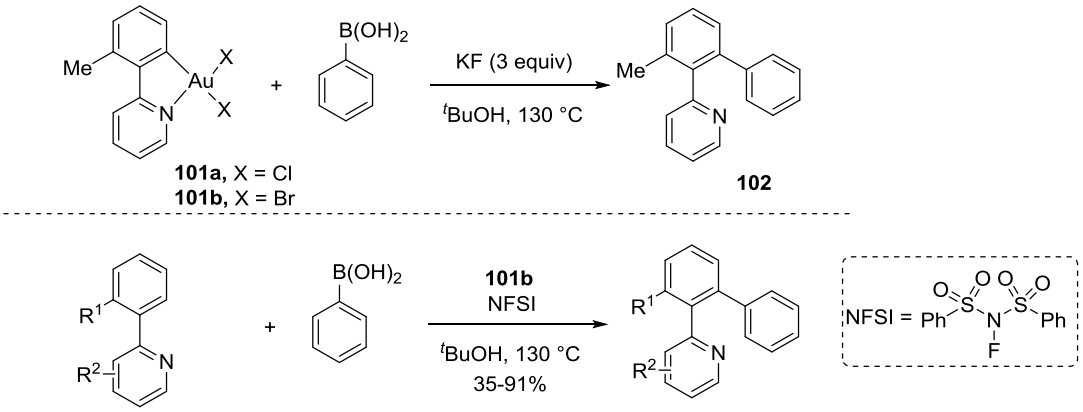

Scheme 28. Application of **101** in oxidative cross-coupling.

2.2 [(C^C)Au(X)(Y)] Complexes

Au^{III} complexes containing a chelating dicarbanionic biphenyl-type ligand are rare. Recently, Mohr and co-workers reported an oligomeric [(C^C)AuXL] complex [(C^C) = 4,4'-di-*tert*-butylbiphenyl] complex (**103**) by transmetalation of [(C^C)Sn(^{t}Bu)$_2$] with $HAuCl_4$.[97] Due to its poor solubility, **103** could not be characterized by solution NMR spectroscopy but formation of the corresponding dimer (n = 2) could be confirmed by MALDI spectrometry. Reaction with donor ligands (e.g. pyridine (Py),

1,3,5-triaza-7-phosphaadmantane (PTA) and xylyl isonitrile (XyNC)) or nucleophiles (selenoureas, carbanions) delivered the corresponding soluble complexes [(C^C)AuCl(L/Nu)] in good yields (**104a-f**). Interestingly, **104a-c** display a very weak emission at room temperature in solution whereas an intense luminescence was observed in glass matrix at 77K (Scheme 29).

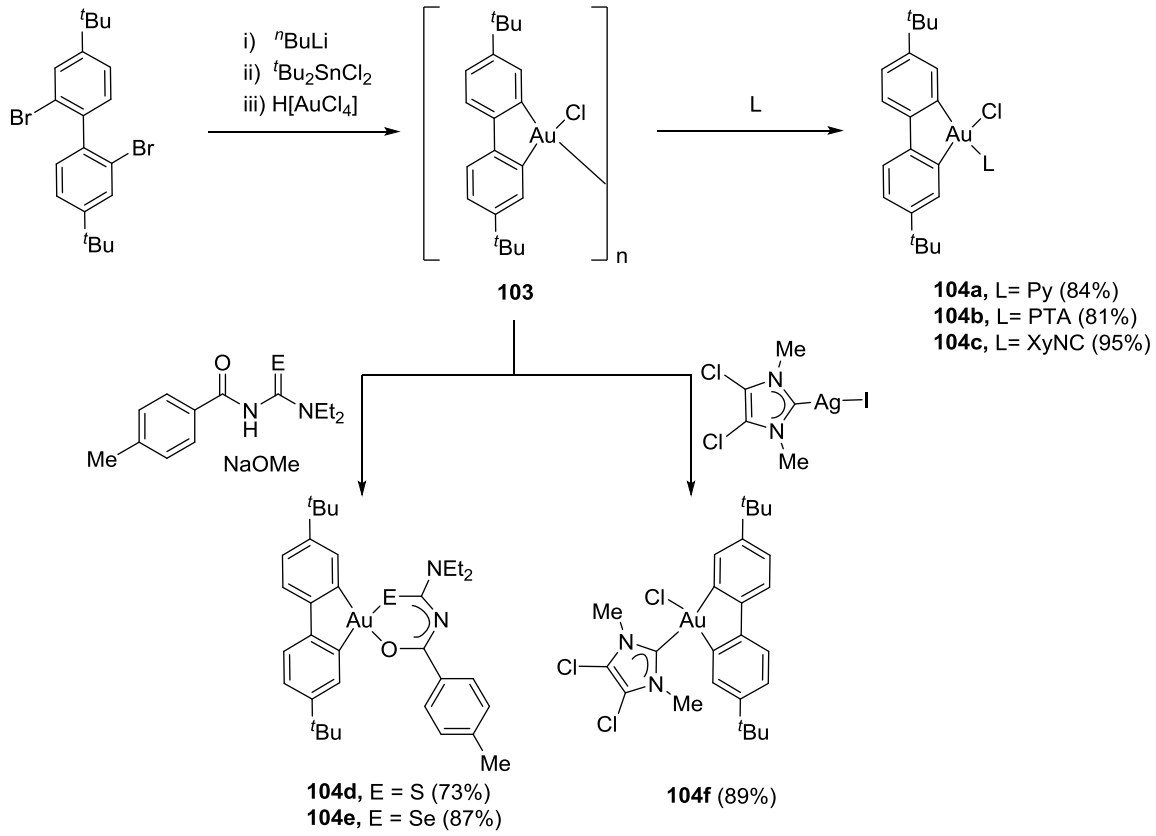

Scheme 29. Reactivity of [(C^C)Au(X)(Y)] complexes.

Shortly thereafter, Toste and co-workers reported the synthesis of stable, yet catalytically active [(C^C)AuIPrCl] complex **107** by oxidative addition of biphenylene to cationic IPrAu^{I} via aqua-complex **106.**[98] Unlike other methods, no external oxidant or harsh reaction conditions were required to access **107** which is isolated as a yellow powder in 80% yield (Scheme 30). The rate of C-C bond cleavage or oxidative addition is highly dependent on the counteranion, as longer reaction times were observed for more coordinating TfO^- anion. Complex **107** was examined in various transformations including conjugate additions to α,β-unsaturated aldehydes as well as [2+2] cycloadditions reactions with unsaturated aldehyde-allenes with very positive results in all cases (Scheme 30, bottom). The improved performance of **107** compared to Au^{I} catalysts in some of these transformations highlights the hard Lewis-acid character of **107** complementary to the soft Lewis-acidic nature of Au^{I} species.

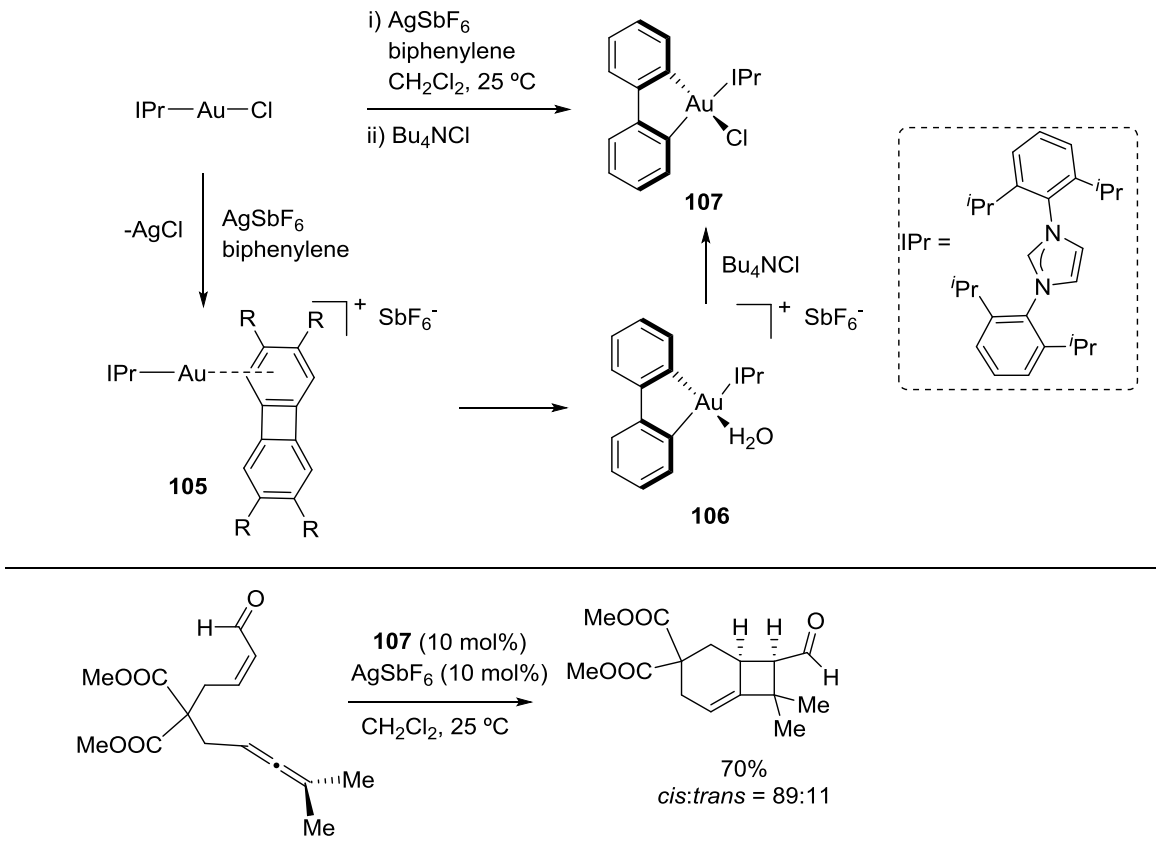

Scheme 30. Synthesis and catalytic application of [(C^C)Au(X)(Y)] complexes.

2.3 [(P^C)Au(X)(Y)] Complexes

Dinuclear cycloaurated complexes with a bridging (P^C) ligand ((P^C) = 2-(dialkyl/diarylphosphino)phenyl) have been studied by Bennett and Bhargava who demonstrated that dinuclear Au^{II} species **108** produced via oxidation of the corresponding dinuclear Au^{I} complexes can be stabilized with this type of ligand frameworks.[99] Rearrangement of cyclometalated Au^{II}-Au^{II} dimer **108** to Au^{I}-Au^{III} complex **109** leads to the formation of **110** (minor) and C-C coupling **111** as major reaction product (Scheme 31).[100]

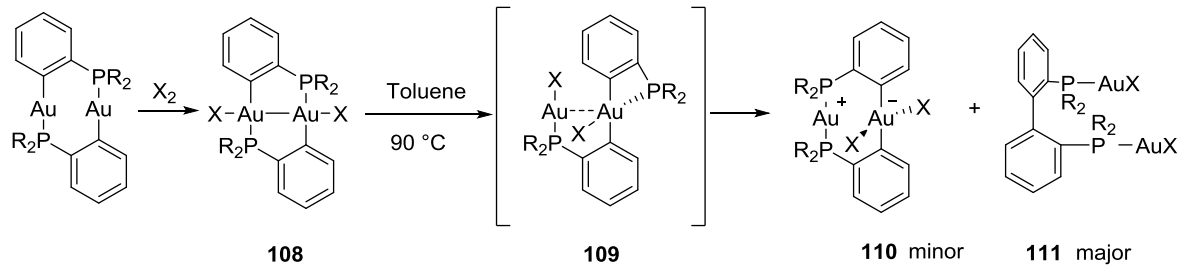

Scheme 31. Synthesis and reactivity of [(P^C)Au(X)(Y)] complexes.

More recently, (P^C) ligands have come to the front in the context of Au^{I}/Au^{III} catalytic cycles. Although the ability of gold to undergo oxidative addition onto Csp^2-X has been the subject of intensive research efforts,[101] its occurrence under homogeneous conditions could never be secured, in contrast to evidence found under heterogeneous conditions.[102] In 2014, Bourissou and co-workers showed that (P^C) cyclometalated Au^{III} complexes **114** and **116** can be accessed by oxidative addition of Au^{I} onto 8-halo naphthyl phosphines **112a-c** (Scheme 32).[103] Key for the success of these transformations was the design of the (P^C) ligands which permit the disposition of the C_{sp}^2-X bond and the metal center in close proximity. The cyclometalation (via oxidative addition) works at room temperature for iodo (**113**), and at 130 °C for bromoarenes (**115**), whereas no reaction was observed in the case of chloro complex **117** even at elevated temperature.

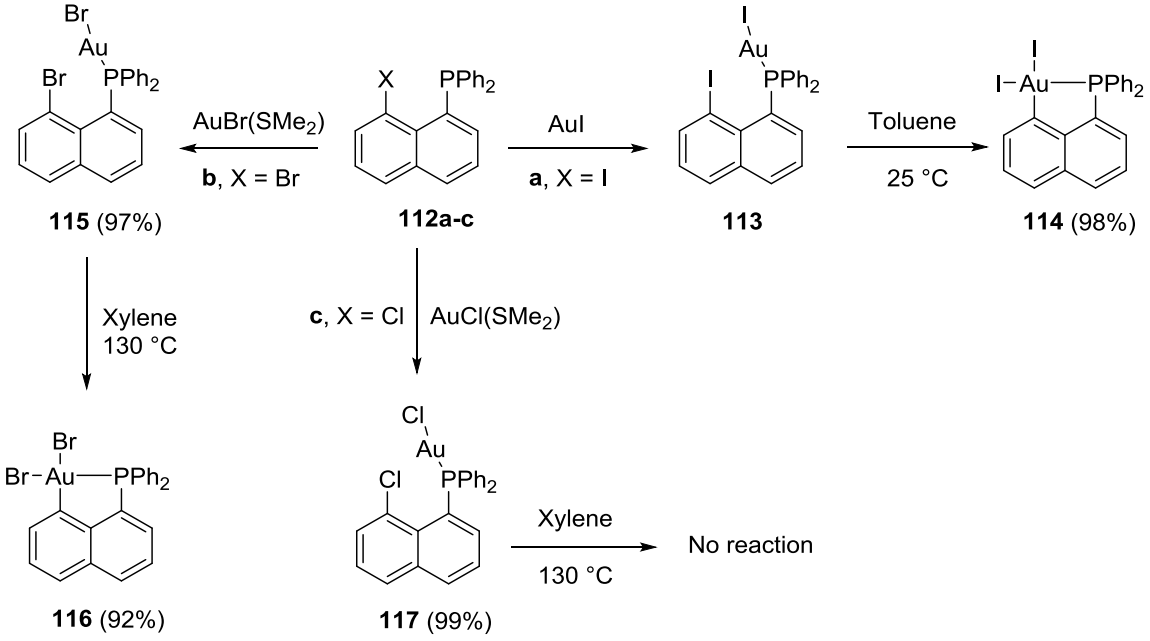

Scheme 32. Synthesis of [(P^C)Au(X)(Y)] complexes.

The reactivity of these compounds was also studied.[104] [(P^C)$AuMe_2$]complex **119** was prepared by treatment of **118** with MeMgBr in dry tetrahydrofuran. Tricoordinated Au^{III} cationic species **120** were generated upon methide abstraction using $B(C_6F_5)_3$. These compounds can undergo a subsequent abstraction of C_6F_5 from the boron center to afford complexes **121** and **122** in 35 and 53% yield respectively. In the presence of $B(C_6F_5)_3$, **120** reacts with norbornene (3 equiv) at -80 °C followed by addition of a donor ligand like pyridine/chloride to furnish a stable complex **123** (Scheme 33). In analogy to Pt^{II}-Me complexes, double insertion of norbornene into Au-Me bond was observed. X-Ray diffraction analysis confirmed that the insertion of the olefin takes place from *exo* face and in a *syn* manner unlike *anti* addition observed in previously described [(N^C)Au^{III}] systems.[90]

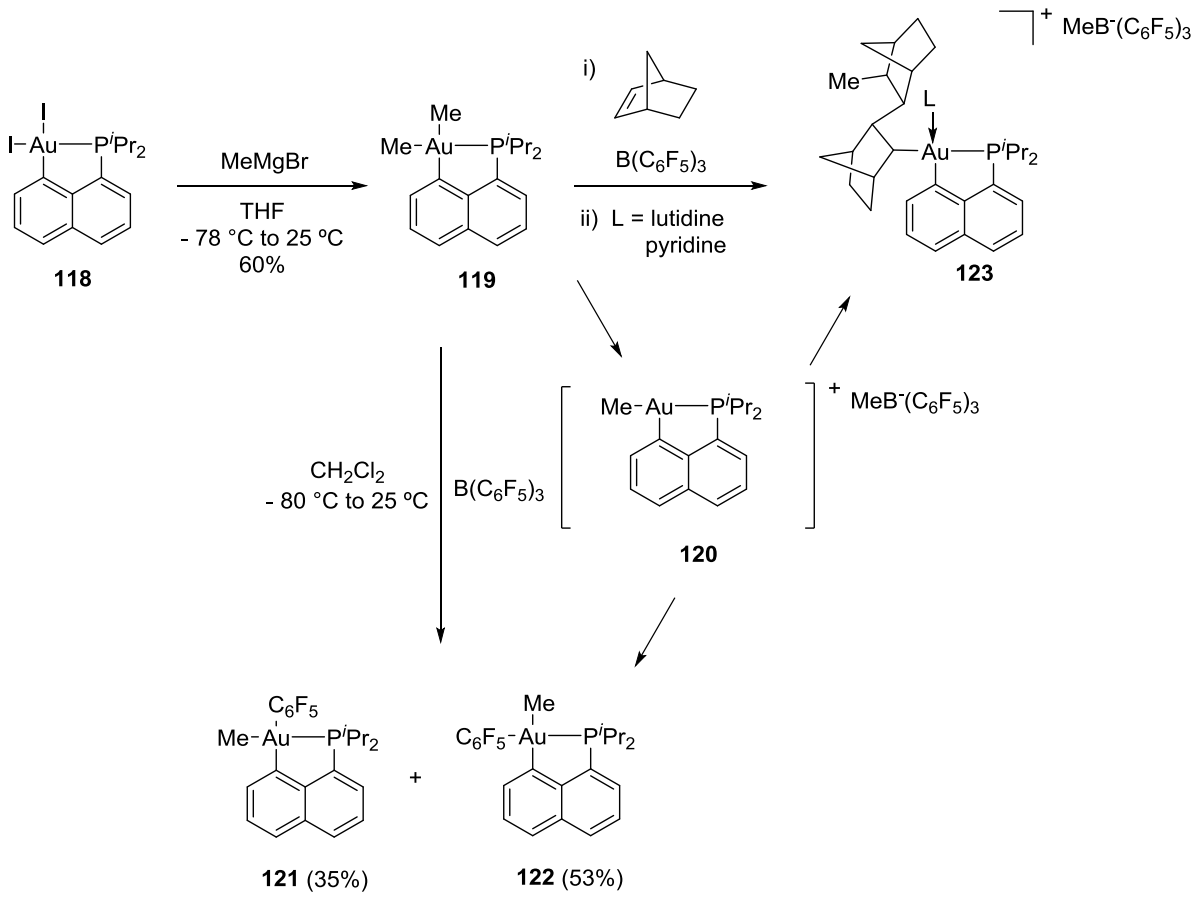

Scheme 33. Synthesis and reactivity of [(P^C)Au(X)(Y)] complexes.

2.4 [(N^N)Au^{III}] Complexes

Stable cyclometalated Au^{III} complexes based on (N^N) ligands (**124-131**) have been known for more than 60 years.[105] The most common strategies to access these compounds rely on the reaction of the corresponding (N^N) ligands with $NaAuCl_4$ or $HAuCl_4$ in polar solvents (H_2O, ROH, etc) followed by thermal or silver-induced coordination of the second N moiety (Scheme 34). From a purely structural point of view these complexes present interesting features. For instance, rare pentacoordinated Au^{III} complex **124b** could be synthesized by the reaction of substituted 2,9-dimethyl-1,10-phenanthroline with $KAuCl_4$ in methanol,[106] whereas μ–oxo complex **125** was obtained by treating bipy-$AuCl_3$ adduct in presence of $AgBF_4$.[107] Tris-(pyrazolyl) Au^{III} complex **126** was prepared in excellent yield upon reaction of $Na[B(pz)_4]$ with $NaAuCl_4$ in water at room temperature for 5 min and the structure was confirmed by X-Ray diffraction analysis.[108] The reaction of picolinamide and $NaAuCl_4$ in water at ambient temperature afforded **127** in excellent yield.[109]

In 2010, Jurisson and co-workers demonstrated the synthesis and radiotherapeutic study of bis-thiosemicarbazonato Au^{III} complex **129** which was prepared by the reaction of thiosemicarbazone ligand with $NaAuCl_4$ in ethanol.[110] In vivo study this complex found to be unstable, therefore further

modifications to enhance the stability are required. Tilset and Swag synthesized [(N^N)$AuCl_3$] (N^N = 6,6'-dimethyl-2,2'-bipyridine) complex **130** using microwave method and demonstrated its fluxional behavior (in solution, the (N^N) ligand *rocks and rolls* with gold(III) center) by variable temperature ^{1}H NMR spectroscopy.[111] In 2014, Larsen and co-workers shown that reaction of 6-methoxy-4-phenyl-2-(2'-pyridil)quinoline (MeO-Py-Quin) with $NaAuCl_4$ in presence of $AgBF_4$ (1 equiv) at 90 °C in acetonitrile delivered complex [(N^N)$AuCl_3$] (N^N = MeO-Py-Quin) **131**. Addition of two equivalent of $AgBF_4$ afforded a cationic gold(III) complex.[112] Recently You *et al*. has reported that [Au(bpy)Cl_2]$^+$Cl complexes proved to be the best catalyst for the synthesis of 3-alkynyl furans/pyrroles.[113]

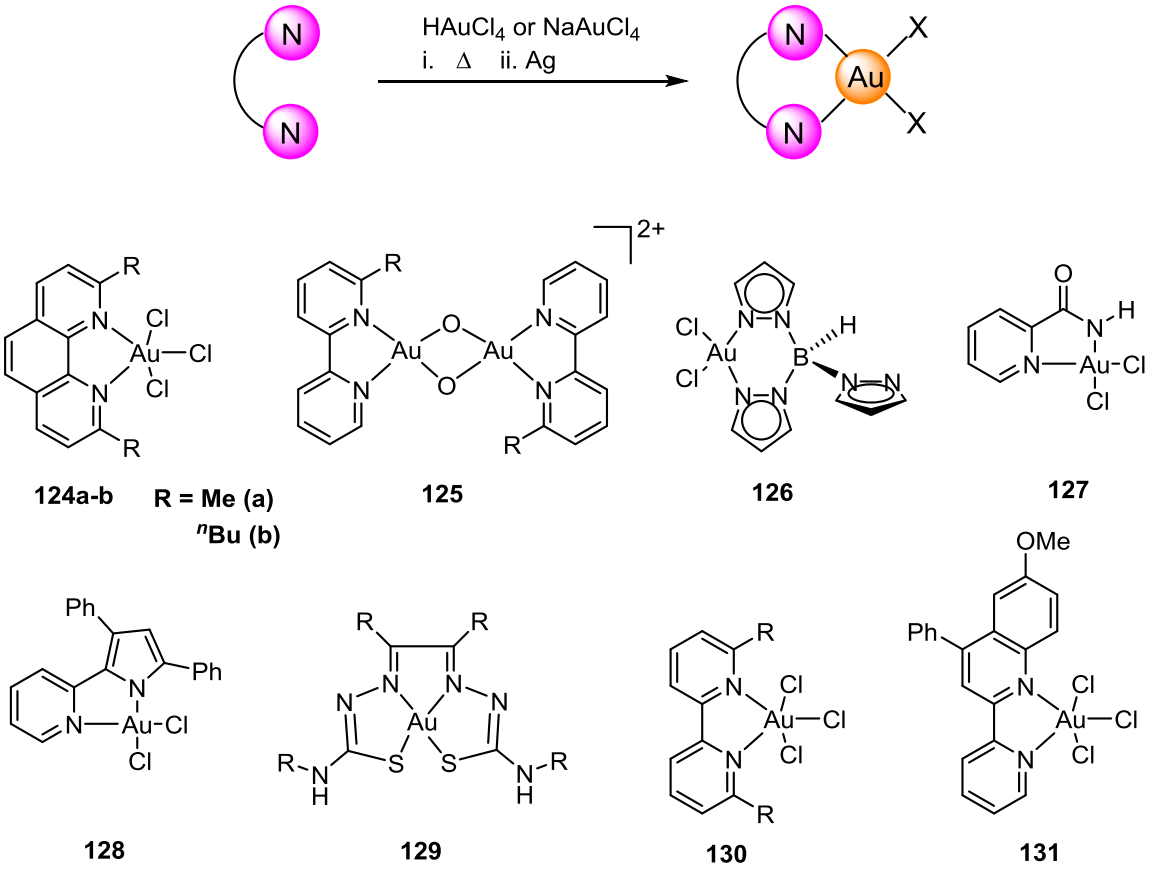

Scheme 34. Representative examples of [(N^N)Au^{III}] complexes.

Some of these complexes have also been used as chemical probes to study reductive elimination as shown by Vicic and co-workers.[114] Unlike dimethyl complexes [(C^N)$AuMe_2$] **94** or [(P^C)$AuMe_2$] **119**, which can be prepared in excellent yield using MeLi or MeMgBr respectively, complex **132** was obtained by a transmetalation reaction of **128** with $SnMe_4$ at -78 °C in dry THF. In contrast to [(R_3P)AuXMe_2], which show fast loss of ethane (from tricoordinated gold(III) species which formed after ligand dissociation) at 45 to 75 °C,[115] **132** found to be thermally stable (Scheme 35).

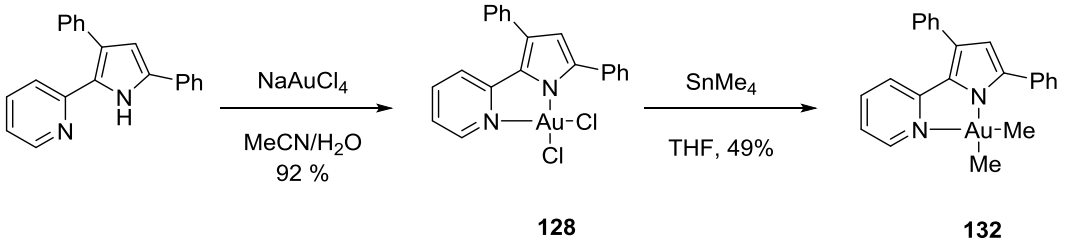

128 132

Scheme 35. Synthesis of [(N^N)AuMe$_2$] complex **132**.

2.4.1 [(N^N)Au(Olefin)] Complexes

In 2004, Cinellu *et al.* demonstrated that when oxo complex [(N^N^R)$_2$Au$_2$(μ-O)$_2$][PF$_6$] **125** was exposed to olefins (ethylene, styrene and norbornene) in different solvents stable [(N^N^R)Au(olefin)][PF$_6$] complexes **133** could be produced.[116] Unlike [(COD)AuMe$_2$] complex **97**, in ^{1}H NMR, an up-field shifts were observed for CH and CH$_2$ resonance of styrene indicating that back donation is compensating the π-electron activation upon coordination to the metal center. Interestingly, auraoxetane complex **135** could be isolated as a minor product along with **134** from the reaction of oxo-complex **125** with norbornene (Scheme 36).[117]

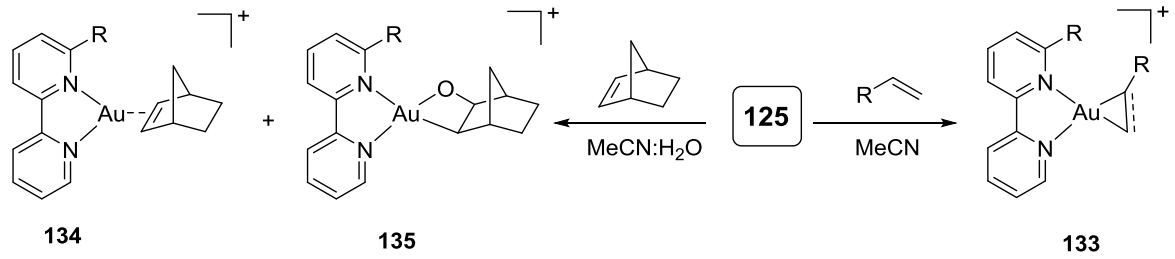

134 135 133

Scheme 36. Synthesis of [(N^N)Au(olefinic)] complexes.

In contrast, Atwood *et al.* demonstrated that [Au(bpy)Cl$_2$]$^+$X complexes do not react with ethylene and propylene at room temperature in water but at 50 °C formation of β-(hydroxyalkyl)Au^{III} complexes were observed.[118]

2.5 [(N^O)Au^{III}] Complexes

In 1992, Parish and co-workers investigated cyclometalated gold(III) derivatives with different (N^O) donor ligands.[119] Complex **136** was synthesized by reaction of 2-picolinic acid with NaAuCl$_4$ in water at room temperature and its structure was confirmed by X-Ray diffraction analysis (Scheme 37).

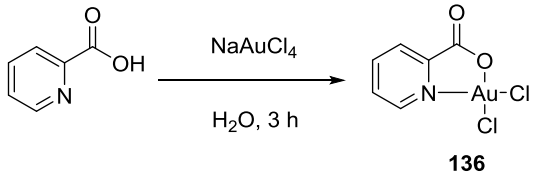

Scheme 37. Synthesis of [(N^O)Au^{III}] complexes.

In the past decade, (N^O) based cyclometalated gold(III) complexes have been used as catalysts in a wide variety of transformations showing comparable abilities to that of gold(I) species to activate all kinds of π-systems.[120-122] Some representative examples have been summarized in Scheme 38. Furans containing triple bonds (**137**) could be transformed into phenols **139** in the presence of complex **136** via arene oxide intermediates **138A-B** (Scheme 38A).[123] Complex **136** was also able to produce imidazole[1-,2-α]pyridines from the reaction of alkynes and 2-aminopyridine *N*-oxides (Scheme 38B).[124] Starting from diynes and alkenes, a strategy to access cyclopropylnaphthalenes was also developed using **136** as catalyst (Scheme 38C).[125] Very recently the synthesis of 3-hydroxyisoxazoles from the corresponding O-allyl hydroxamates in presence of **136** (5 mol%) in refluxing dichloroethane has been also reported (Scheme 38D).[126]

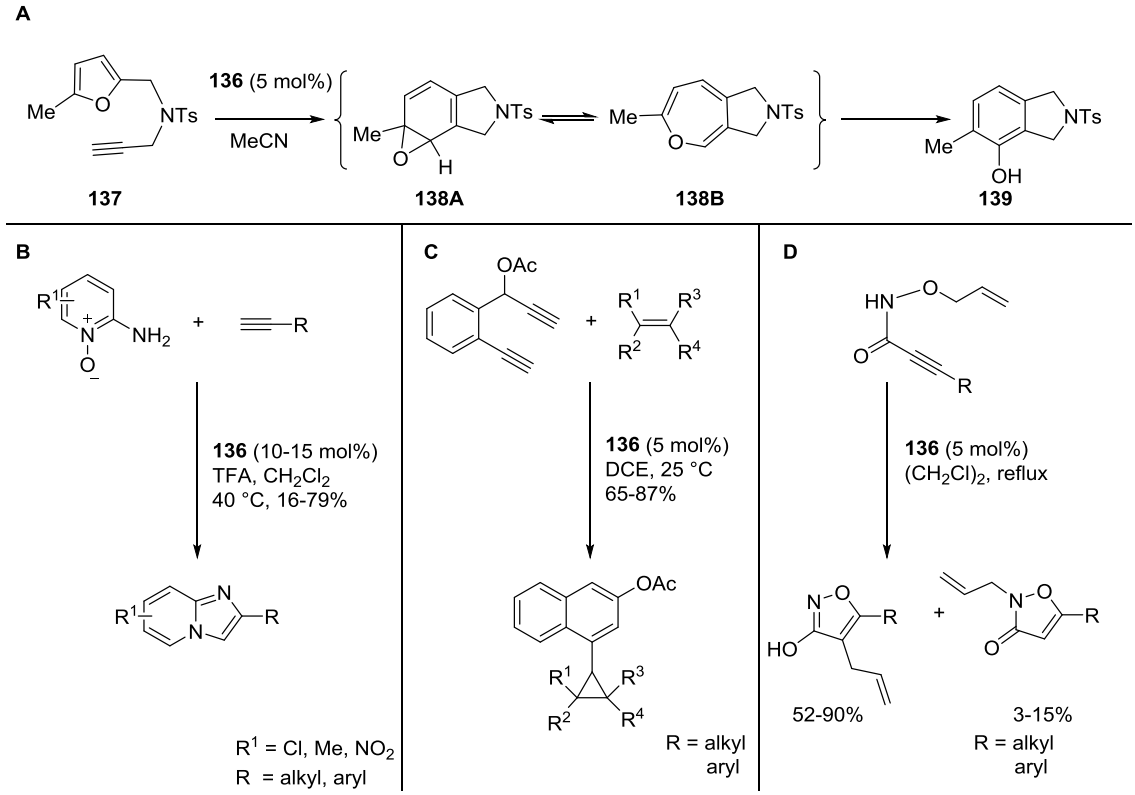

Scheme 38. Catalytic reactivity of [(N^O)Au^{III}] complex **136**.

2.6 [(N^P)Au^{III}] Complexes

Although (N^P) templates have been used to stabilize Pd and Ni complexes,[127] this type of ligand systems have not been widely used in gold chemistry. Recently though, the oxidative addition of aryldiazonium salt to (N^P)Au^{I}Cl precursors **140** has been proved producing the corresponding [(N^P)Au^{III}ArCl] complexes **141** in the presence of light (Scheme 39).[128] These processes are relevant in the context of recently developed light-driven, gold-catalyzed 1,2-difunctionalization of alkynes that use aryldiazonium salts in the absence of photosensitizer or external oxidants.

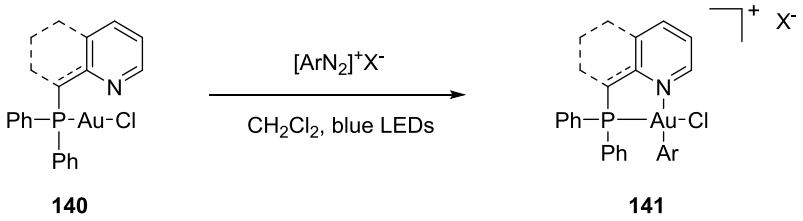

140 **141**

Scheme 39. Synthesis of [(N^P)Au^{III}] complexes.

Conclusions

Formation of mono- and bis-cyclometalated gold(III) complexes results in stabilized species that have enabled not only the isolation but also the in depth study of the intrinsic reactivity of gold(III) species typically proposed in the literature but rather elusive under catalytic conditions due to their highly reactive nature. Gold(III)-hydrides, alkoxides, carboxylates etc. have been characterized for the first time taking advantage of multi-coordinating ligand templates. Fundamental aspects of the reactivity associated with these putative catalytic intermediates have also been revealed. The careful balance between stabilization and reactivity provided by cyclometalating ligands has also resulted in the successful development of new, highly efficient, gold(III) catalysts.

In addition, in depth understanding of both, the tridimensional structure and inherent electronic features of cyclometalated gold(III) species has paved the venue for the development of new materials with improved, easily tunable photophysical properties which will continue to impact technological developments in the field of emissive materials.

Finally, one can argue that, without question, the chemistry of gold(III) cyclometalated complexes transcends and interconnects not one but multiple research disciplines including catalysis, inorganic and bioinorganic chemistry, ligand design and material science, which certainly warrantees exciting developments in these areas in the years to come.

Objectives

The aim of this thesis was to develop novel ligand templates which enable synthesis and isolation of stable cyclometalated gold(III) fluorido complexes in order to explore their reactivity. And to understand the mechanisms of gold catalyzed transformations in which gold(III)-fluorido complexes have been proposed as reactive intermediates. Finally to develop new transformationS using these stable Au^{III}-F as catalysts. Towards this objective we proceed as follows:

i. Di-substituted phenyl-pyridine based N^C^C type ligand template was designed and prepared which enabled the synthesis of first stable (N^C^C)Au^{III}-F and their reactivity with terminal alkynes was studied (Chapter 2).

ii. Next, phenyl-pyridine based C^N type ligand was used to acceess (C^N)Au^{III}-F_2 as well (C^N)Au^{III}-aryl-F in monomeric form. These complexes were used to investigated the long standing puzzle that how Au^{III}-F react with aryl boronic acids (Chapter 3).

iii. (N^C^C)Au^{III}-F was found to catalyze the dehydrogenation of formic acid. A gold(III)-formate to gold(III)-hydride to gold(III)-formate catalytic cycle was proposed. This gold(III)-hydride undergo hydroauration of alkyne to result (*Z*)-vinyl gold(IIII) complexes (Chapter 4).

iv. A detailed mechanistic investigation was carried out to understand how the hydroauration proceed to result (*Z*)-vinyl gold(IIII) complexes (Chapter 5).

References

[1] M. Pernpointner, A. S. K. Hashmi, *J. Chem. Theory Comput.* **2009**, *5*, 2717-2725.

[2] A. Leyva-Pérez, A. Corma, *Angew. Chem. Int. Ed.* **2012**, *51*, 614-635.

[3] A. S. K. Hashmi, *Angew. Chem. Int. Ed.* **2010**, *49*, 5232-5241.

[4] R. Dorel, A. M. Echavarren, *Chem. Rev.* **2015**, *115*, 9028-9072.

[5] J. Xiao, X. Li, *Angew. Chem. Int. Ed.* **2011**, *50*, 7226-7236.

[6] D. J. Gorin, F. D. Toste, *Nature* **2007**, *446*, 395-403.

[7] A. Fürstner, P. W. Davies, *Angew. Chem. Int. Ed.* **2007**, *46*, 3410-3449.

[8] H. A. Wegner, M. Auzias, *Angew. Chem. Int. Ed.* **2011**, *50*, 8236-8247.

[9] P. Garcia, M. Malacria, C. Aubert, V. Gandon, L. Fensterbank, *ChemCatChem* **2010**, *2*, 493-497.

[10] C. Nevado, T. d. Haro, in *New Strategies in Chemical Synthesis and Catalysis*, Wiley-VCH Verlag GmbH & Co. KGaA, **2012**, pp. 247-272.

[11] M. Joost, A. Amgoune, D. Bourissou, *Angew. Chem. Int. Ed.* **2015**, *54*, 15022-15045.

[12] T. de Haro, C. Nevado, *Synthesis* **2011**, *2011*, 2530-2539.

[13] T. C. Boorman, I. Larrosa, *Chem. Soc. Rev.* **2011**, *40*, 1910-1925.

[14] H. Schmidbaur, A. Schier, *Arab. J. Sci. Eng.* **2012**, *37*, 1187-1225.

[15] D.-A. Rosca, J. A. Wright, M. Bochmann, *Dalton. Trans.* **2015**, *44*, 20785-20807.

[16] M. A. Baldo, D. F. O'Brien, Y. You, A. Shoustikov, S. Sibley, M. E. Thompson, S. R. Forrest, *Nature* **1998**, *395*, 151-154.

[17] H. Yersin, in *Highly Efficient OLEDs with Phosphorescent Materials*, Wiley-VCH Verlag GmbH & Co. KGaA, **2008**, pp. I-XVIII.

[18] C. Fan, C. Yang, *Chem. Soc. Rev.* **2014**, *43*, 6439-6469.

[19] V. W.-W. Yam, E. C.-C. Cheng, *Chem. Soc. Rev.* **2008**, *37*, 1806-1813.

[20] V. W. Yam, K. M. Wong, *Chem. Commun.* **2011**, *47*, 11579-11592.

[21] C. Bronner, O. S. Wenger, *Dalton. Trans.* **2011**, *40*, 12409-12420.

[22] A. Y.-Y. Tam, V. W.-W. Yam, *Chem. Soc. Rev.* **2013**, *42*, 1540-1567.

[23] K.-H. Wong, K.-K. Cheung, M. C.-W. Chan, C.-M. Che, *Organometallics* **1998**, *17*, 3505-3511.

[24] V. W. Yam, K. M. Wong, L. L. Hung, N. Zhu, *Angew. Chem. Int. Ed.* **2005**, *44*, 3107-3110.

[25] K. M.-C. Wong, L.-L. Hung, W. H. Lam, N. Zhu, V. W.-W. Yam, *J. Am. Chem. Soc.* **2007**, *129*, 4350-4365.

[26] V. K. Au, K. M. Wong, N. Zhu, V. W. Yam, *J. Am. Chem. Soc.* **2009**, *131*, 9076-9085.

[27] J. L.-L. Tsai, A. O.-Y. Chan, C.-M. Che, *Chem. Commun.* **2015**, *51*, 8547-8550.

[28] C. K.-L. Li, R. W.-Y. Sun, S. C.-F. Kui, N. Zhu, C.-M. Che, *Chem. Eur. J.* **2006**, *12*, 5253-5266.

[29] J. J. Yan, A. L.-F. Chow, C.-H. Leung, R. W.-Y. Sun, D.-L. Ma, C.-M. Che, *Chem. Commun.* **2010**, *46*, 3893-3895.

[30] R. W.-Y. Sun, C.-N. Lok, T. T.-H. Fong, C. K.-L. Li, Z. F. Yang, T. Zou, A. F.-M. Siu, C.-M. Che, *Chem. Sci.* **2013**, *4*, 1979-1988.

[31] (a) B.-Z. Yang, X. Zhou, T. Liu, F.-Q. Bai, H.-X. Zhang, *J. Phy. Chem. A* **2009**, *113*, 9396-9403; (b) G. S. Ming Tong, K. T. Chan, X. Chang, C.-M. Che, *Chem. Sci.* **2015**, *6*, 3026-3037; (c) E. S.-H. Lam, W. H. Lam, V. W.-W. Yam, *Inorg. Chem.* **2015**, *54*, 3624-3630; (d) M. C. Tang, C. K. Chan, D. P. Tsang, Y. C. Wong, M. M. Chan, K. M. Wong, V. W. Yam, *Chem. Eur. J.* **2014**, *20*, 15233-15241.

[32] K. M.-C. Wong, X. Zhu, L.-L. Hung, N. Zhu, V. W.-W. Yam, H.-S. Kwok, *Chem. Commun.* **2005**, 2906-2908.

[33] V. K.-M. Au, K. M.-C. Wong, D. P.-K. Tsang, M.-Y. Chan, N. Zhu, V. W.-W. Yam, *J. Am. Chem. Soc.* **2010**, *132*, 14273-14278.

[34] V. K. Au, D. Wu, V. W. Yam, *J. Am. Chem. Soc.* **2015**, *137*, 4654-4657.

[35] M. C. Tang, D. P. Tsang, M. M. Chan, K. M. Wong, V. W. Yam, *Angew. Chem. Int. Ed.* **2013**, *52*, 446-449.

[36] M. C. Tang, D. P. Tsang, Y. C. Wong, M. Y. Chan, K. M. Wong, V. W. Yam, *J. Am. Chem. Soc.* **2014**, *136*, 17861-17868.

[37] V. K. Au, D. P. Tsang, K. M. Wong, M. Y. Chan, N. Zhu, V. W. Yam, *Inorg. Chem.* **2013**, *52*, 12713-12725.

[38] W. P. To, K. T. Chan, G. S. Tong, C. Ma, W. M. Kwok, X. Guan, K. H. Low, C. M. Che, *Angew. Chem. Int. Ed.* **2013**, *52*, 6648-6652.

[39] G. Cheng, K. T. Chan, W. P. To, C. M. Che, *Adv. Mater.* **2014**, *26*, 2540-2546.

[40] J. Fernandez-Cestau, B. Bertrand, M. Blaya, G. A. Jones, T. J. Penfold, M. Bochmann, *Chem Commun.* **2015**, *51*, 16629-16632.

[41] W. P. To, G. S. Tong, W. Lu, C. Ma, J. Liu, A. L. Chow, C. M. Che, *Angew. Chem. Int. Ed.* **2012**, *51*, 2654-2657.

[42] C.-Y. Sun, W.-P. To, X.-L. Wang, K.-T. Chan, Z.-M. Su, C.-M. Che, *Chem. Sci.* **2015**, *6*, 7105-7111.

[43] D. A. Rosca, D. A. Smith, M. Bochmann, *Chem. Commun.* **2012**, *48*, 7247-7249.

[44] D. A. Smith, D.-A. Roşca, M. Bochmann, *Organometallics* **2012**, *31*, 5998-6000.

[45] H. Schmidbaur, A. Schier, *Organometallics* **2010**, *29*, 2-23.

[46] N. Savjani, D. A. Rosca, M. Schormann, M. Bochmann, *Angew. Chem. Int. Ed.* **2013**, *52*, 874-877.

[47] D. A. Rosca, D. A. Smith, D. L. Hughes, M. Bochmann, *Angew. Chem. Int. Ed.* **2012**, *51*, 10643-10646.

[48] A. Pintus, L. Rocchigiani, J. Fernandez-Cestau, P. H. M. Budzelaar, M. Bochmann, *Angew. Chem. Int. Ed.* **2016**, *55*, 12321-12324.

[49] D. A. Rosca, J. A. Wright, D. L. Hughes, M. Bochmann, *Nature. Commun.* **2013**, *4*, 2167.

[50] D.-A. Roşca, J. Fernandez-Cestau, J. Morris, J. A. Wright, M. Bochmann, *Sci. Adv.* **2015**, *1*, e1500761.

[51] W. Song, E. J. M. Hensen, *ACS Cat.* **2014**, *4*, 1885-1892.

[52] M. Flytzani-Stephanopoulos, *Acc. Chem. Res.* **2014**, *47*, 783-792.

[53] M. Yang, S. Li, Y. Wang, J. A. Herron, Y. Xu, L. F. Allard, S. Lee, J. Huang, M. Mavrikakis, M. Flytzani-Stephanopoulos, *Science* **2014**, *346*, 1498-1501.

[54] T. G. Appleton, R. D. Berry, J. R. Hall, D. W. Neale, *J. Organomet. Chem.* **1989**, *364*, 249-273.

[55] S.-W. Lai, H.-W. Lam, W. Lu, K.-K. Cheung, C.-M. Che, *Organometallics* **2002**, *21*, 226-234.

[56] (a) G. Bond, *Gold. Bull.*, *42*, 337-342; (b) Q. Fu, H. Saltsburg, M. Flytzani-Stephanopoulos, *Science* **2003**, *301*, 935-938.

[57] C.-W. Chan, W.-T. Wong, C.-M. Che, *Inorg. Chem.* **1994**, *33*, 1266-1272.

[58] H.-Q. Liu, T.-C. Cheung, S.-M. Peng, C.-M. Che, *J. Chem. Soc., Chem. Commun.* **1995**, 1787-1788.

[59] M. A. Cinellu, A. Zucca, S. Stoccoro, G. Minghetti, M. Manassero, M. Sansoni, *J. Chem. Soc., Dalton Trans.* **1996**, 4217-4225.

[60] V. K. Au, W. H. Lam, W. T. Wong, V. W. Yam, *Inorg. Chem.* **2012**, *51*, 7537-7545.

[61] X. S. Xiao, W. L. Kwong, X. Guan, C. Yang, W. Lu, C. M. Che, *Chem. Eur. J.* **2013**, *19*, 9457-9462.

[62] W. Lu, K. T. Chan, S.-X. Wu, Y. Chen, C.-M. Che, *Chem. Sci.* **2012**, *3*, 752-755.

[63] (a) P. A. Bonnardel, R. V. Parish, R. G. Pritchard, *J. Chem. Soc., Dalton Trans.* **1996**, 3185-3193; (b) G. Alesso, M. A. Cinellu, S. Stoccoro, A. Zucca, G. Minghetti, C. Manassero, S. Rizzato, O. Swang, M. K. Ghosh, *Dalton. Trans.* **2010**, *39*, 10293-10304.

[64] S. Stoccoro, G. Alesso, M. A. Cinellu, G. Minghetti, A. Zucca, M. Manassero, C. Manassero, *Dalton. Trans.* **2009**, 3467-3477.

[65] M. Contel, M. Stol, M. A. Casado, G. P. M. van Klink, D. D. Ellis, A. L. Spek, G. van Koten, *Organometallics* **2002**, *21*, 4556-4559.

[66] A. Herbst, C. Bronner, P. Dechambenoit, O. S. Wenger, *Organometallics* **2013**, *32*, 1807-1814.

[67] R. Kumar, A. Linden, C. Nevado, *Angew. Chem. Int. Ed.* **2015**, *54*, 14287-142290

[68] (a) N. P. Mankad, F. D. Toste, *J. Am. Chem. Soc.* **2010**, *132*, 12859-12861; (b) N. P. Mankad, F. D. Toste, *Chem. Sci.* **2012**, *3*, 72-76.

[69] (a) J. Vicente, M.-T. Chicote, M.-D. Bermuadez, X. Solans, M. Font-Altaba, *J. Chem. Soc., Dalton Trans.* **1984**, 557-562; (b) J. Vicente, M. T. Chicote, M. I. Lozano, S. Huertas, *Organometallics* **1999**, *18*, 753-757.

[70] E. C. Constable, T. A. Leese, *J. Organomet. Chem.* **1989**, *363*, 419-424.

[71] (a) Y. Fuchita, H. Ieda, Y. Tsunemune, J. Kinoshita-Nagaoka, H. Kawano, *J. Chem. Soc., Dalton Trans.* **1998**, 791-796; (b) Y. Fuchita, H. Ieda, S. Wada, S. Kameda, M. Mikuriya, *J. Chem. Soc., Dalton Trans.* **1999**, 4431-4435.

[72] (a) M. A. Cinellu, A. Zucca, S. Stoccoro, G. Minghetti, M. Manassero, M. Sansoni, *J. Chem. Soc., Dalton Trans.* **1995**, 2865-2872; (b) F. Cocco, M. A. Cinellu, G. Minghetti, A. Zucca, S. Stoccoro, L. Maiore, M. Manassero, *Organometallics* **2010**, *29*, 1064-1066.

[73] A. P. Shaw, M. Tilset, R. H. Heyn, S. Jakobsen, *J. Coord. Chem.* **2011**, *64*, 38-47.

[74] W. Henderson, in *Adv. Organomet. Chem., Vol. Volume 54* (Eds.: W. Robert, F. H. Anthony), Academic Press, **2006**, pp. 207-265.

[75] (a) J. Vicente, M.-T. Chicote, M. D. Bermudez, M. J. Sanchez-Santano, P. G. Jones, C. Fittschen, G. M. Sheldrick, *J. Organomet. Chem.* **1986**, *310*, 401-409; (b) J. Vicente, M. D. Bermudez, J. Escribano, M. P. Carrillo, P. G. Jones, *J. Chem. Soc., Dalton Trans.* **1990**, 3083-3089; (c) J. Vicente, M. Dolores Bermudez, J. Escribano, *Organometallics* **1991**, *10*, 3380-3384.

[76] J. A. Garg, O. Blacque, T. Fox, K. Venkatesan, *Inorg. Chem.* **2010**, *49*, 11463-11472.

[77] A. Maity, A. N. Sulicz, N. Deligonul, M. Zeller, A. D. Hunter, T. G. Gray, *Chem. Sci.* **2015**, *6*, 981-986.

[78] A. Szentkuti, M. Bachmann, J. A. Garg, O. Blacque, K. Venkatesan, *Chem. Eur. J.* **2014**, *20*, 2585-2596.

[79] T. N. Zehnder, O. Blacque, K. Venkatesan, *Dalton. Trans.* **2014**, *43*, 11959-11972.

[80] V. K. Au, K. M. Wong, N. Zhu, V. W. Yam, *Chem. Eur. J.* **2011**, *17*, 130-142.

[81] J. A. Garg, O. Blacque, K. Venkatesan, *Inorg. Chem.* **2011**, *50*, 5430-5441.

[82] (a) M. K. Nazeeruddin, R. Humphry-Baker, D. Berner, S. Rivier, L. Zuppiroli, M. Graetzel, *J. Am. Chem. Soc.* **2003**, *125*, 8790-8797; (b) J. Forniés, S. Fuertes, J. A. López, A. Martín, V. Sicilia, *Inorg. Chem.* **2008**, *47*, 7166-7176.

[83] A. Szentkuti, J. A. Garg, O. Blacque, K. Venkatesan, *Inorg. Chem.* **2015**, *54*, 10748-10760.

[84] F. F. Hung, W. P. To, J. J. Zhang, C. Ma, W. Y. Wong, C. M. Che, *Chem. Eur. J.* **2014**, *20*, 8604-8614.

[85] J. Vicente, M.-D. Bermudez, M.-T. Chicote, M.-J. Sanchez-Santano, *J. Chem. Soc., Chem. Commun.* **1989**, 141-142.

[86] E. Langseth, C. H. Görbitz, R. H. Heyn, M. Tilset, *Organometallics* **2012**, *31*, 6567-6571.

[87] E. Langseth, M. L. Scheuermann, D. Balcells, W. Kaminsky, K. I. Goldberg, O. Eisenstein, R. H. Heyn, M. Tilset, *Angew. Chem. Int. Ed.* **2013**, *52*, 1660-1663.

[88] (a) M. A. Cinellu, G. Minghetti, S. Stoccoro, A. Zucca, M. Manassero, *Chem. Commun.* **2004**, 1618-1619; (b) M. A. Cinellu, G. Minghetti, F. Cocco, S. Stoccoro, A. Zucca, M. Manassero, M. Arca, *Dalton. Trans.* **2006**, 5703-5716; (c) T. J. Brown, M. G. Dickens, R. A. Widenhoefer, *J. Am. Chem. Soc.* **2009**, *131*, 6350-6351; (d) T. J. Brown, M. G. Dickens, R. A. Widenhoefer, *Chem. Commun.* **2009**, 6451-6453; (e) T. N. Hooper, M. Green, J. E. McGrady, J. R. Patel, C. A. Russell, *Chem. Commun.* **2009**, 3877-3879; (f) R. E. M. Brooner, R. A. Widenhoefer, *Organometallics* **2011**, *30*, 3182-3193.

[89] R. P. Hughes, J. S. Overby, K.-C. Lam, C. D. Incarvito, A. L. Rheingold, *Polyhedron* **2002**, *21*, 2357-2360.

[90] E. Langseth, A. Nova, E. A. Traseth, F. Rise, S. Oien, R. H. Heyn, M. Tilset, *J. Am. Chem. Soc.* **2014**, *136*, 10104-10115.

[91] A. R. Browne, N. Deligonul, B. L. Anderson, M. Zeller, A. D. Hunter, T. G. Gray, *Chem. Commun.* **2015**, *51*, 15800-15803.

[92] V. K.-Y. Lo, K. K.-Y. Kung, M.-K. Wong, C.-M. Che, *J. Organomet. Chem.* **2009**, *694*, 583-591.

[93] K. K.-Y. Kung, V. K.-Y. Lo, H.-M. Ko, G.-L. Li, P.-Y. Chan, K.-C. Leung, Z. Zhou, M.-Z. Wang, C.-M. Che, M.-K. Wong, *Adv. Synth. Catal.* **2013**, *355*, 2055-2070.

[94] H. von Wachenfeldt, A. V. Polukeev, N. Loganathan, F. Paulsen, P. Rose, M. Garreau, O. F. Wendt, D. Strand, *Dalton. Trans.* **2015**, *44*, 5347-5353.

[95] Q. Wu, C. Du, Y. Huang, X. Liu, Z. Long, F. Song, J. You, *Chem. Sci*. **2015**, *6*, 288-293.

[96] R. Kumar, A. Linden, C. Nevado, *J. Am. Chem. Soc.* **2016**, *138*, 13790-13793.

[97] B. David, U. Monkowius, J. Rust, C. W. Lehmann, L. Hyzak, F. Mohr, *Dalton. Trans.* **2014**, *43*, 11059-11066.

[98] C. Y. Wu, T. Horibe, C. B. Jacobsen, F. D. Toste, *Nature* **2015**, *517*, 449-454.

[99] S. K. Bhargava, F. Mohr, J. D. Gorman, *J. Organomet. Chem.* **2000**, *607*, 93-96.

[100] M. A. Bennett, D. C. R. Hockless, A. D. Rae, L. L. Welling, A. C. Willis, *Organometallics* **2001**, *20*, 79-87.

[101] (a) C. González-Arellano, A. Abad, A. Corma, H. García, M. Iglesias, F. Sánchez, *Angew. Chem. Int. Ed.* **2007**, *46*, 1536-1538; (b) T. Lauterbach, M. Livendahl, A. Rosellón, P. Espinet, A. M. Echavarren, *Org. Lett.* **2010**, *12*, 3006-3009; (c) P. S. D. Robinson, G. N. Khairallah, G. da Silva, H. Lioe, R. A. J. O'Hair, *Angew. Chem. Int. Ed.* **2012**, *51*, 3812-3817.

[102] (a) S. K. Beaumont, G. Kyriakou, R. M. Lambert, *J. Am. Chem. Soc.* **2010**, *132*, 12246-12248; (b) G. Kyriakou, S. K. Beaumont, S. M. Humphrey, C. Antonetti, R. M. Lambert, *ChemCatChem* **2010**, *2*, 1444-1449; (c) A. Corma, R. Juarez, M. Boronat, F. Sanchez, M. Iglesias, H. Garcia, *Chem. Commun.* **2011**, *47*, 1446-1448.

[103] J. Guenther, S. Mallet-Ladeira, L. Estevez, K. Miqueu, A. Amgoune, D. Bourissou, *J. Am. Chem. Soc.* **2014**, *136*, 1778-1781.

[104] F. Rekhroukh, R. Brousses, A. Amgoune, D. Bourissou, *Angew. Chem. Int. Ed.* **2015**, *54*, 1266-1269.

[105] (a) A. C. Davis, R. F. Hunter, C. M. Harris, T. N. Lockyer, J. N. Chaudhuri, S. Basu, N. V. S. Rao, C. V. Ratnam, A. F. Trotman-Dickenson, D. B. Powell, N. Sheppard, R. H. Burnell, H. R. Arthur, Y. L. Ng, N. P. Buu-Hoi, P. Jacquignon, E. W. Abel, A. Singh, G. Wilkinson, E. E. Aynsley, S. Sampath, P. F. G. Praill, D. M. Heinekey, I. T. Millar, K. J. M. Andrews, F. N. Woodward, *J. Chem. Soc.* **1959**, 3081-3102; (b) W. T. Robinson, E. Sinn, *J. Chem. Soc., Dalton Trans.* **1975**, 726-731.

[106] G. Marangoni, B. Pitteri, V. Bertolasi, G. Gilli, V. Ferretti, *J. Chem. Soc., Dalton Trans.* **1986**, 1941-1944.

[107] M. Agostina Cinellu, G. Minghetti, M. Vittoria Pinna, S. Stoccoro, A. Zucca, M. Manassero, M. Sansoni, *J. Chem. Soc., Dalton Trans.* **1998**, 1735-1742.

[108] J. Vicente, M. T. Chicote, R. Guerrero, U. Herber, D. Bautista, *Inorg. Chem.* **2002**, *41*, 1870-1875.

[109] D. T. Hill, K. Burns, D. D. Titus, G. R. Girard, W. M. Reiff, L. M. Mascavage, *Inorg. Chim. Acta* **2003**, *346*, 1-6.

[110] B. N. Bottenus, P. Kan, T. Jenkins, B. Ballard, T. L. Rold, C. Barnes, C. Cutler, T. J. Hoffman, M. A. Green, S. S. Jurisson, *Nucl. Med. Biol.* **2010**, *37*, 41-49.

[111] A. P. Shaw, M. K. Ghosh, K. W. Törnroos, D. S. Wragg, M. Tilset, O. Swang, R. H. Heyn, S. Jakobsen, *Organometallics* **2012**, *31*, 7093-7100.

[112] E. M. Laguna, P. M. Olsen, M. D. Sterling, J. F. Eichler, A. L. Rheingold, C. H. Larsen, *Inorg. Chem.* **2014**, *53*, 12231-12233.

[113] S. Zhang, Y. Ma, J. Lan, F. Song, J. You, *Org. Biomol. Chem.* **2015**, *13*, 5867-5870.

[114] S. Schouteeten, O. R. Allen, A. D. Haley, G. L. Ong, G. D. Jones, D. A. Vicic, *J. Organomet. Chem.* **2006**, *691*, 4975-4981.

[115] (a) S. Komiya, A. Shibue, *Organometallics* **1985**, *4*, 684-687; (b) S. Komiya, T. Sone, S. Ozaki, M. Ishikawa, N. Kasuga, *J. Organomet. Chem.* **1992**, *428*, 303-313; (c) O. Schuster, R.-Y. Liau, A. Schier, H. Schmidbaur, *Inorg. Chim. Acta* **2005**, *358*, 1429-1441.

[116] M. A. Cinellu, G. Minghetti, S. Stoccoro, A. Zucca, M. Manassero, *Chem. Commun.* **2004**, 1618-1619.

[117] M. A. Cinellu, G. Minghetti, F. Cocco, S. Stoccoro, A. Zucca, M. Manassero, *Angew. Chem. Int. Ed.* **2005**, *44*, 6892-6895.

[118] C. E. Rezsnyak, J. Autschbach, J. D. Atwood, S. Moncho, *J. Coord. Chem.* **2013**, *66*, 1153-1165.

[119] A. Dar, K. Moss, S. M. Cottrill, R. V. Parish, C. A. McAuliffe, R. G. Pritchard, B. Beagley, J. Sandbank, *J. Chem. Soc., Dalton Trans.* **1992**, 1907-1913.

[120] A. S. Hashmi, J. P. Weyrauch, M. Rudolph, E. Kurpejovic, *Angew. Chem. Int. Ed.* **2004**, *43*, 6545-6547.

[121] C. Ferrer, C. H. M. Amijs, A. M. Echavarren, *Chem. Eur. J.* **2007**, *13*, 1358-1373.

[122] E. Tomas-Mendivil, J. Starck, J. C. Ortuno, V. Michelet, *Org. Lett.* **2015**, *17*, 6126-6129.

[123] A. S. K. Hashmi, M. Rudolph, J. P. Weyrauch, M. Wölfle, W. Frey, J. W. Bats, *Angew. Chem. Int. Ed.* **2005**, *44*, 2798-2801.

[124] E. P. A. Talbot, M. Richardson, J. M. McKenna, F. D. Toste, *Adv. Synth. Catal.* **2014**, *356*, 687-691.

[125] T. Lauterbach, M. Ganschow, M. W. Hussong, M. Rudolph, F. Rominger, A. S. K. Hashmi, *Adv. Synth. Catal.* **2014**, *356*, 680-686.

[126] S. Sugita, M. Ueda, N. Doi, N. Takeda, O. Miyata, *Tetrahedron Lett.* **2016**, *57*, 1786-1789.

[127] (a) O. Daugulis, M. Brookhart, *Organometallics* **2002**, *21*, 5926-5934; (b) J. Flapper, H. Kooijman, M. Lutz, A. L. Spek, P. W. N. M. van Leeuwen, C. J. Elsevier, P. C. J. Kamer, *Organometallics* **2009**, *28*, 1180-1192; (c) Z. Guan, W. J. Marshall, *Organometallics* **2002**, *21*, 3580-3586.

[128] (a) L. Huang, F. Rominger, M. Rudolph, A. S. K. Hashmi, *Chem. Commun.* **2016**, *52*, 6435-6438; (b) L. Huang, M. Rudolph, F. Rominger, A. S. K. Hashmi, *Angew. Chem. Int. Ed.* **2016**, *55*, 4808-4813; (c) C. Khin, A. S. K. Hashmi, F. Rominger, *Eur. J. Inorg. Chem.* **2010**, *2010*, 1063-1069.

CHAPTER 2

LUMINESCENT (N^C^C)-GOLD(III) COMPLEXES: STABILIZED GOLD(III) FLUORIDE

CHAPTER 2

Luminescent (N^C^C)-Gold(III) Complexes: Stabilized Gold(III) Fluorides

Roopender Kumar, Anthony Linden and Cristina Nevado

(*Angew. Chem. Int. Ed.* **2015**, *54*, 14287-14290)

Au(III) complexes have been underutilized compared to isoelectronic Pt(II) and Ir(III) species as additives to enhance the efficiency of organic light-emitting diodes (OLEDs).[1] The reason is two-fold: on the one hand, the Au(III) center is highly electrophilic and secondly, the presence of a low-energy d-d ligand field state that could quench the luminescence of the excited state by thermal equilibration or energy transfer represents an additional challenge. Among several others, pincer ligands based on dianionic 2,6-diphenylpyridine frameworks (C^N^C) have become excellent platforms for the stabilization of gold in high oxidation states as demonstrated by the seminal work of Che,[2] Yam[3] and Bochmann.[4] Phenylpyridine (N^C)-Au(III) species have also received increasing attention in this context (Scheme 1a).[5] Promising emissive properties have been determined for many of these complexes.[2-3, 4a, 5b]

Transition metal fluorido complexes lie at the heart of some of the most synthetically useful transformations in modern catalysis. While both, Pd(II)- and Pd(IV)-F complexes have been isolated and characterized as intermediates in fluorination and cross-coupling reactions,[6] reports on gold fluorido complexes are, in contrast, extremely limited. In 2005, the first stabilized *N*-heterocyclic carbene (NHC)Au(I)-F complex was reported by Sadighi *et al.* (Scheme 1b).[7,8] Recently, gold catalysts and electrophilic fluorinating agents have been effectively combined not only to produce new C-F bonds,[9a-c] but also C-C bonds via Au(I)/Au(III) redox catalytic cycles.[9d-m] Although both, Csp^2- and Csp^3-Au(III)-F intermediates have been postulated, experimental evidence to substantiate the participation of these species in the above-mentioned transformations is to-date scarce. The major challenges include the need for strong oxidants to access gold in a high oxidation state, thus limiting the functional group compatibility, and the instability of the resulting oxidized metal complexes. Pioneering work from Toste *et al* has shown that *cis*-(NHC)Au(III)AlkylF_2 complexes, in equilibrium with the corresponding dimeric forms, can be obtained by oxidation of (NHC)Au(I)Alkyl with XeF_2 (Scheme 1b).[10] Interestingly though, a synthesis of gold(III) fluorido complexes using classical pincer or phenylpyridine templates, devoid of oxidative conditions is yet to be reported, likely due to the insufficient stabilization of the electron deprived metal. We hypothesized that two consecutive C-anionic centers on the ancillary ligand could donate sufficient electron density to stabilize a highly electrophilic Au(III) center and thus, 3,5-disubstituted phenylpyridine ligands were designed with the aim of simultaneous double Csp^2-H functionalization of the aromatic rings (Scheme 1c). We also envisioned that the central aromatic ring in such (N^C^C) ligand would exert a strong *trans* effect that facilitate a direct anionic ligand exchange to produce the corresponding Au(III)-F complexes from the corresponding chlorido complexes. Here, the first examples of monomeric, bench-stable Csp^2-Au(III)-F complexes are presented and the unique properties and intrinsic

reactivity of Au-F bonds have been studied. Notably, (N^C^C)-Au(III) species present enhanced emissive properties compared to the classical (C^N^C)-Au(III) systems.

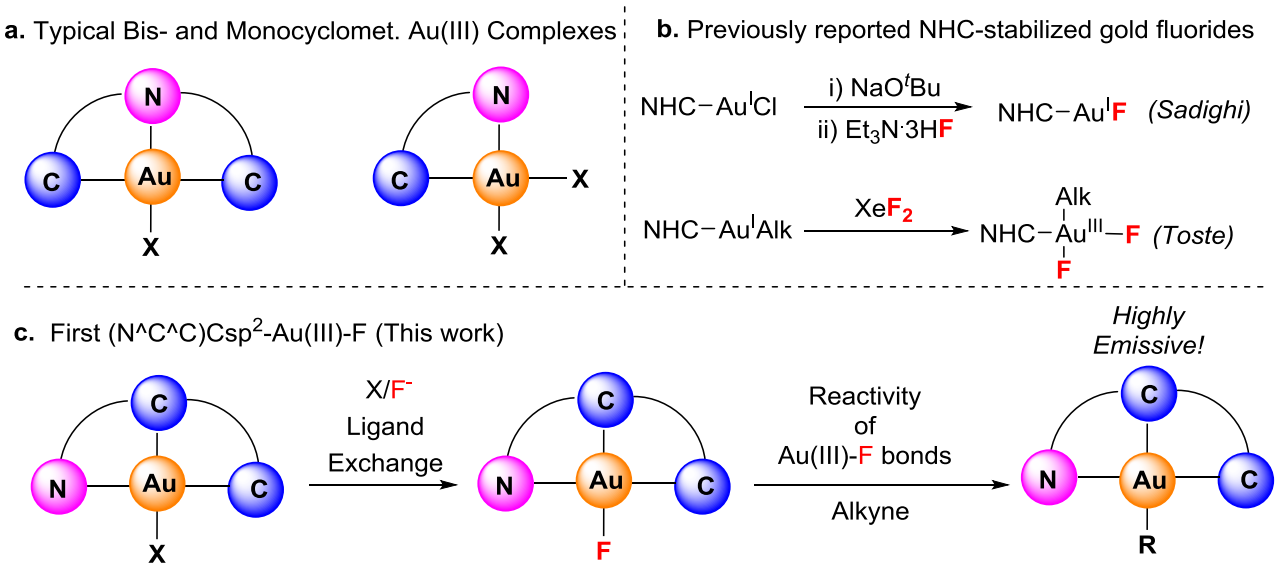

Scheme 1. a. Classical (C^N^C)-pincer and bidentate (N^C)-phenylpyridine gold(III) stabilized complexes (X = Halide, Csp, Csp^2). b. Previously reported (NHC)Au(I)F and (NHC)Au(III)AlkF_2 complexes. c. Novel (N^C^C)-Au(III)-F complexes via anionic ligand exchange reaction.

Ligands **La-j** (Table 1) were prepared by Suzuki-Miyaura cross-coupling between commercially available 2-bromo-3-substituted pyridines and 3,5-bisaryl-substituted phenyl boronic acids.[11] Treatment of **La-j** with $NaAuCl_4{\cdot}2H_2O$ in an acetonitrile/water mixture at 25°C for 2 hours resulted in the formation of **La-j**$AuCl_3$ complexes **1a-j** in 70-99% yields. X-Ray diffraction analysis of compound **1a** validated the proposed structure (Figure 1).[11] Next, the reactions of complexes **1** in acetonitrile/water 1:1 at 170 °C in the microwave for 70 minutes delivered bis-cyclometalated products **2a-j** in 40-72% yields.[12]

Substituents on the pyridine ring were well tolerated although slightly lower yields were observed for electron-withdrawing groups (**2a-d**). The substitution pattern on the 3,5-aryl moieties was also studied: *p*-isopropoxy- (**1e**), *p*-phenoxy- (**1f**), 2,3,4-trimethoxy- (**1g**) and *p*-cyclohexyl- (**1h**) substituted bis-cycloaurated adducts **2e-h** could be prepared in good yields. Substitution on the central phenyl ring could also be accommodated, as shown in compounds **2i** and **2j**. Single crystals of complexes **2a** and **2d** confirmed the structural assignments (Figure 1).[11] This two-step procedure to access chlorides **2** avoids the use of mercury compounds, which are employed as precursors for the synthesis of classical pincer (C^N^C)-Au(III)Cl complexes, by transmetalation between the mercury precursors and $HAuCl_4$.[2-4, 13]

Table 1. Synthesis of (N^C^C)-Au(III)-F complexes

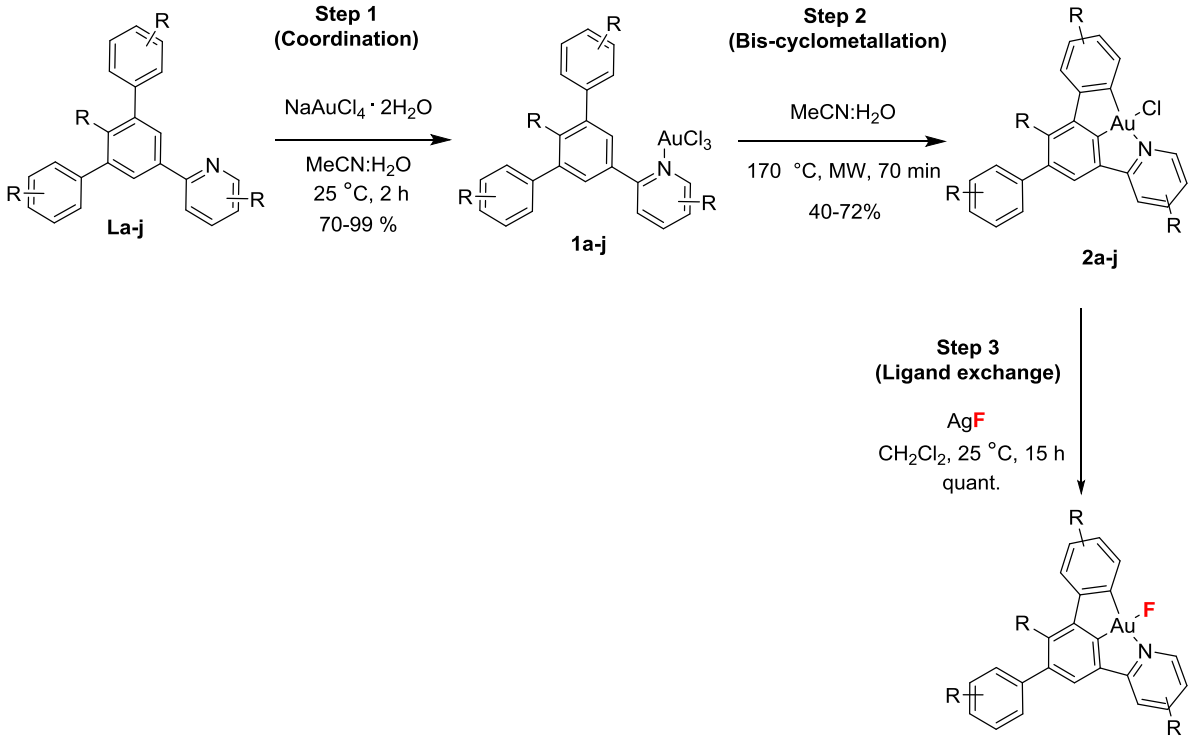

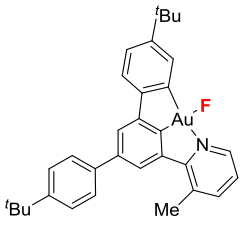

Step 1: **1a,** 99% (X-Ray)
Step 2: **2a,** 72% (X-Ray)
Step 3: **3a**, quant.

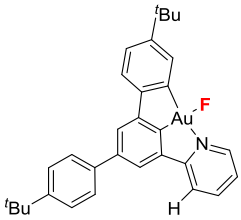

Step 1: **1b,** 98%
Step 2: **2b,** 57%
Step 3: **3b**, quant.

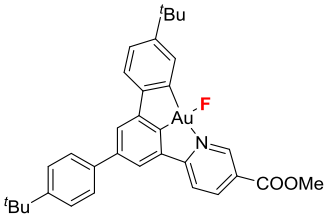

Step 1: **1c,** 70%
Step 2: **2c,** 44%
Step 3: **3c**, quant.

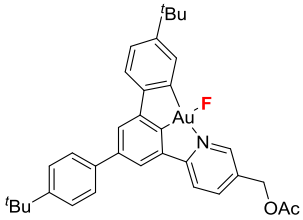

Step 1: **1d,** 80%
Step 2: **2d,** 51% (X-Ray)
Step 3: **3d**, quant. (X-Ray)

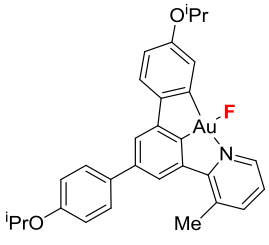

Step 1: **1e,** 95%
Step 2: **2e,** 63%
Step 3: **3e**, quant.

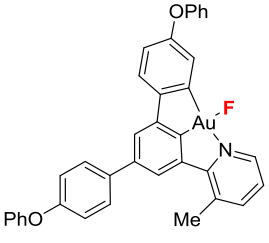

Step 1: **1f,** 97%
Step 2: **2f,** 59%
Step 3: **3f**, quant.

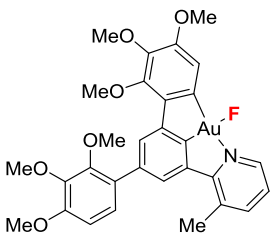

Step 1: **1g,** 92%
Step 2: **2g,** 55%
Step 3: **3g**, quant.

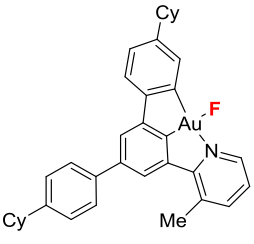

Step 1: **1h,** 96%
Step 2: **2h,** 47%
Step 3: **3h**, quant.

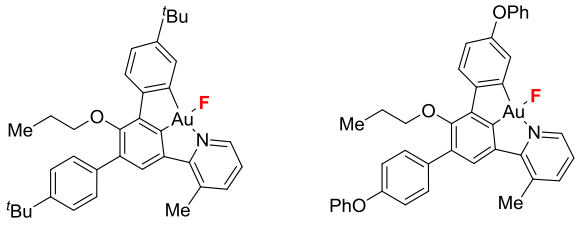

Step 1: **1i,** 94%
Step 2: **2i,** 40%
Step 3: **3i**, quant.

Step 1: **1j,** 98%
Step 2: **2j,** 40%
Step 3: **3j**, quant.

Exchange of the chlorido ligand to produce the desired (N^C^C)-Au(III)-F **3** was carried out by treatment with silver fluoride in dry CH_2Cl_2 at room temperature providing full conversion of the starting materials after 12 h. The reactions were monitored by both ^{1}H and ^{19}F NMR, which indicated the clean formation of the Au-F bond with a characteristic ^{19}F NMR resonance in the δ –(230-225) ppm range (C_6D_6). Complexes **3** were insensitive towards light, air or even water and proved to be stable in its monomeric form for weeks at room temperature in the solid state as well as in solution in chlorinated solvents. Suitable, albeit disordered, crystals of compound **3d** could be obtained by slow diffusion of hexane into a concentrated solution of the complex in dichloromethane, enabling the confirmation of both composition and structure (Figure 1).[11] These results confirmed that the (N^C^C) framework can overcome the weak *trans* ligand-directing effect[14] of the pyridine moiety in classical (C^N^C) systems in which a direct ligand exchange reaction on the gold(III)-chlorido bond, even in the presence of silver salts, is sometimes difficult to attain.[4a]

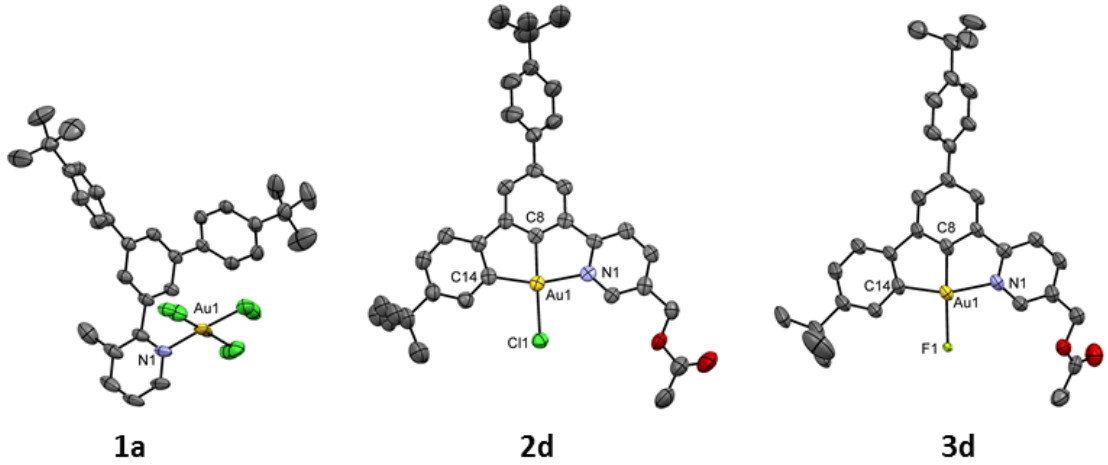

1a **2d** **3d**

Figure 1. The solid-state molecular structures of **1a**, **2d**, and **3d** are shown with atoms drawn using 50% probability ellipsoids. The trans-effect of the central Csp^2-atom of the ligand results in an elongated Au(1)-X(1) bond.[2c,10a] **2d**: Au(1)-Cl(1) = 2.3602(19) Å. **3d**: Au(1)-F(1) = 2.264(3) Å. A distorted square planar geometry was confirmed with the trans angles around the Au(III) center deviating significantly from ideal values. **2d**: N(1)-Au(1)-C(14) = 160.5(3). **3d**: N(1)-Au(1)-C(14) = 160.3(3).

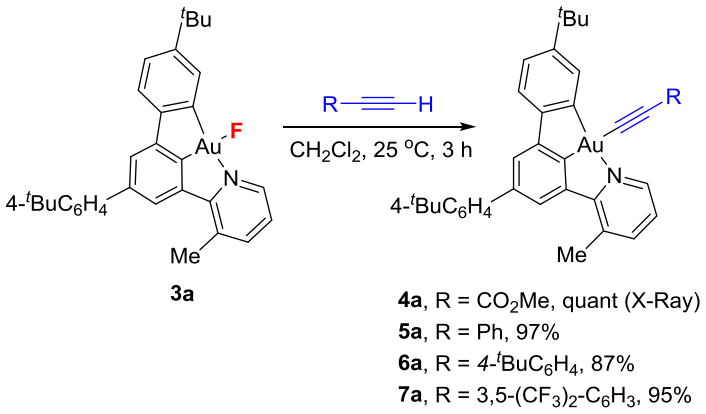

Scheme 2. Synthesis of (N^C^C)-Au(III)-alkynyl complexes **4-7a**.

The reaction of complex **3a** with terminal alkynes was investigated. Treatment with methyl propiolate in dichloromethane at 25 °C for 3 hours yielded, after evaporation of the solvent, Au(III)-akynyl complex **4a**, whose structure was confirmed by X-Ray diffraction analysis.[11] Phenyl acetylene produced the corresponding alkynyl complex **5a** in almost quantitative yield. Other aryl substituted alkynes reacted in an analogous manner so that (N^C^C)-Au(III)-alkynyl complexes **6-7a** could be obtained in high yields as summarized in Scheme 2. The intrinsic lability of the Au-F bond can be compared to that of previously reported weakly bound Au-alkoxide ligands.[4a]

We recognized that the (N^C^C) ligand framework, could not only render the Au(III) more electron rich, but also raise the energy of the d-d states and thereby increase the chances of populating emissive states, in turn, fostering luminescence properties as predicted by DFT calculations.[15] For this reason, the photophysical properties of **2a**, **3a**, **4-7a** were also studied (Figure 2). These complexes showed intense absorption bands at 320-337 nm and a broad vibronic-structured moderately intense absorption band at 375-381 nm with extinction coefficients ε in the order of $> 10^3$ $M^{-1}cm^{-1}$ in dichloromethane solution at 25°C. Given the similar absorption bands detected for all complexes despite the different non-ancillary anionic ligand (Cl-, F-, and acetylides), the possibility of ligand-to-metal or ligand-to-ligand charge transfer transitions (LMCT and LLCT, respectively) can be excluded. Hence, the characteristic absorption bands can be assigned to metal-perturbed intraligand (IL) transitions localized on the (N^C^C) ligand. As no Au(III)•••Au(III) interaction was observed in any of the crystal structure analyses,[11] the presence of metal-to-metal-to-ligand charge transfer (MMLCT) transitions can also be discarded.

Interestingly, complexes **2-7a** showed a strong luminescence upon excitation at λ ≥335 nm in degassed dichloromethane at room temperature. All of these compounds exhibit almost similar intense vibronic-structured emission bands with peak maxima at 489-497 nm. These emissions are assigned to a metal-perturbed ^{3}IL (π-π*) transition of the (N^C^C) ligand. Their solution emission quantum yields are in most cases over 0.16 and up to 0.28, a remarkable value in the arena of gold(III) emissive compounds. Besides the commonly encountered acetylides or NHC σ donor ligands, also chlorido and even a fluorido ligand are able to activate

the intraligand state (^{3}IL) emission of the corresponding cyclometalated Au(III) complexes, with 0.17 and 0.27 quantum yields, respectively.

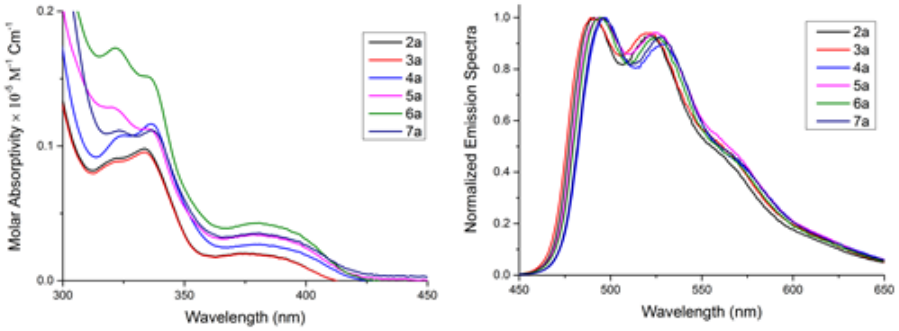

Cmp.	Absorption λ_{max} [nm] (ϵ_{max} [M^{-1} cm^{-1}])	Emisssion λ_{max} [nm] (τ_0 [µs])[a]	φ_{em} [b]	k_r 10^3x[s^{-1}][c]	k_{nr} 10^4x[s^{-1}][d]
2a	322(9093), 334(9797), 375(2039)	491, 522 (56)	0.17	3.0	1.4
3a	322(8857), 334(9542), 375(1986)	489, 522 (55)	0.27	4.9	1.3
4a	325(10781), 336(11644), 381(2705)	497, 528 (54)	0.16	2.9	1.5
5a	320(12880), 334(11282), 378(3478)	494, 526 (63)	0.27	4.2	1.1
6a	323 (11158), 337(11165), 381(3531)	496, 527 (80)	0.16	2.0	1.0
7a	322(17268), 335(15157), 381(4248)	494, 526 (60)	0.28	4.6	1.2

Figure 1. Absorption and emission spectra (top left to top right). [a] Phosphorescence lifetime. [b] Phosphorescence quantum yield measured at 1 x 10^{-5} mol dm^{-3} at room temperature. [c] Radiative decay rate constant estimated by $k_r = \varphi/\tau$. [d] Non-radiative decay rate constant estimated by $k_{nr} = (1-\varphi)/\tau$.

As such, the remarkable luminescent behavior of these compounds needs to stem from the special arrangement of the (N^C^C) scaffold.[16] Unlike most Au(III) compounds, which exhibit luminescence only at low temperature or are non-emissive, complexes **2-7a** display luminescence in solution at ambient temperature and are comparable or even improve the performance of emissive classical (C^N^C)-pincer and (N^C)-phenylpyridine Au(III) complexes.[2,3, 4a, 5b, 17]

In summary, a novel (N^C^C) pincer framework, able to stabilize gold in high oxidation state, is reported here. The first examples of Csp^2-gold(III) fluorido complexes obtained through a mild Cl/F ligand exchange reaction have been described. These new Au(III)-F species are stabilized through a carefully designed ligand system, that balances the electronic needs of the metal yielding monomeric, bench-stable, complexes. Discrete (N^C^C)-Au(III)-F species were used as chemical probes to gain a deeper understanding of elementary reactivity of Au-F bonds. The improved photophysical properties measured for the (N^C^C)-Au(III) complexes represent a valuable addition to the current portfolio of classical pincer (C^N^C)- and (N^C)-Au(III) emissive species.

References

[1] M. A. Baldo, M. E. Thompson, S. R. Forrest, *Nature*, **2000**, *403*, 750-553.

[2] (a) W.-T. To, G. S.-M. Tong, W. Lu, C. Ma, J. Liu, A. L.-F. Chow, C.-M. Che, *Angew. Chem. Int. Ed*. **2012**, *51*, 2654-2657. (b) W.-P. To, K. T. Chan, G. S. M. Tong, C. Ma, W.-M. Kwok, X. Guan, K.-H. Low, C.-M. Che, *Angew. Chem. Int. Ed.* **2013**, *52*, 6648-6652. (c) C. K.-L. Li, R. W. –Y. Sun, S. C.-F. Kui, N. Zhu, C. –M. Che, *Chem. Eur. J*. **2006**, *12*, 5253.

[3] (a) V. W.-W. Yam, K. M.-C. Wong, L.-L. Hung, N. Zhu, *Angew. Chem. Int. Ed*. **2005**, *44*, 3107-3110. (b) K. M.-C. Wong, L.-L. Hung, W. H. Lam, N. Zhu, V. W.-W. Yam, *J. Am. Chem. Soc*. **2007**, *129*, 4350-4345.

[4] (a) D.-A. Rosca, D. A. Smith, M. Bochmann, *Chem. Commun.* **2012**, *46*, 7247-7249. (b) D.-A. Rosca, J. A. Wright, D. L. Hughes, M. Bochmann, *Nat. Commun*. **2013**, *4*, 2167.

[5] (a) Q. Wu, C. Du, Y. Huang, X. Liu, Z. Long, F. Song, J. You, *Chem. Sci*., **2014**, 6, 288-293. (b) A. Szentkuti, M. Bachmann, J. A. Garg, O. Blacque, V. Koushik, *Chem. Eur. J.* **2014**, *20*, 2585-2596.

[6] (a) D. A. Watson, M. Su, G. Teverovskiy, Y. Zhang, J. García-Fortanet, T. Kinzel, S. L. Buchwald, *Science* **2009**, *325*, 1661-1664. (b) N. D. Ball, M. S. Sanford, *J. Am. Chem. Soc.* **2009**, *131*, 3796–3797. (c) A. J. Hickman, M. S. Sanford, Nature **2012**, *484*, 177-185.

[7] D. S. Laitar, P. Muller, T. Gray, J. P. Sadighi, *Organometallics* **2005,** *24*, 4503-4505.

[8] (a) J. A. Akana, K. X. Bhattachayya, P. Muller, J. P. Sadighi, *J. Am. Chem. Soc*. **2007**, *129*, 7736-7737. (b) O. E. Okoromoba, J. Han, G.B. Hammond, B. Xu, *J. Am. Chem. Soc.* **2014**, *136*, 14381–14384.

[9] (a) M. Schuler, F. Silva, C. Bobbio, A. Tessier, V. Gouverneur, *Angew. Chem. Int. Ed*. **2008**, *47*, 7927-7930. (b) T. de Haro, C. Nevado, *Chem. Commun.* **2011**, *47*, 248-249. (c) J. Qian, Y. Liu, J. Zhu, B. Jiang, Z. Xu, *Org. Lett.*, **2011**, *13*, 4220–4223. (d) M. Hofer, E. Gomez-Bengoa, C. Nevado *Organometallics* **2014**, *33*, 1328-1332. (e) S. Carrettin, J. Guzman, A. Corma, *Angew. Chem. Int. Ed*. **2005**, *44*, 2242-2245. (f) Zhang, G., Peng, Y., Cui. L., Zhang, L. *Angew. Chem. Int. Ed.* **2009**, *48*, 3112–3115. (g) Brenzovich, W. E., Benitez, D., Lackner, A. D., Shunatona, H. P., Tkatchouk, E., Goddard, W. A., Toste, F. D. *Angew. Chem. Int. Ed.* **2010**, *49*, 5519-5522. (h) E. Tkatchouk, N. P. Mankad, D. Benitez, W. A. Goddard, F. D. Toste *J. Am. Chem. Soc.* **2011**, *133*, 14293-14300. (i) A. D. Melhado, W. E. Brenzovich, A. D. Lackner, F. D. Toste *J. Am. Chem. Soc.* **2010**, *132*, 8885-8887. (j) M. N.

Hopkinson, A. Gee, V. Gouverneur, *Isr. J. Chem*. **2010**, 675-690. (k) H. A. Wegner, M. Auzias, *Angew. Chem. Int. Ed*. **2011**, *50*, 8236-2247. (l) T. C. Boorman, I. Larrosa, *Chem. Soc. Rev.* **2011**, *40*, 1910-1925. (m) C. Nevado, T. de Haro In *New Strategies in Chemical Synthesis and Catalysis*; Pignataro, B., Ed.; Wiley-VCH: Weinheim, **2012**, p 247.

[10] (a) N. P. Mankad, F. D. Toste, *J. Am. Chem. Soc.* **2010**, *132*, 12859-12861. (b) N. P., Mankad, F. D. Toste, *Chem. Sci.* **2012**, *3*, 72-76.

[11] For further details, please, see the Supporting Information. X-Ray diffraction analysis data are available from the CCDC database: **1a** (CCDC-1033830), **2a** (CCDC-1033772), **2d** (CCDC-1058552), **3d** (CCDC-1033763) and **4a** (CCDC-1033775).

[12] E. C. Constable, T. A. Leese, *J. Organomet. Chem.* **1989**, *363*, 419-424.

[13] K. H. Wong, K.-K. Cheung, M. C.-W. Chan, C.-M. Che, *Organometallics* **1998**, *17*, 3505-3511.

[14] A. Hofmann, L. Dahlenburg, R. van Eldik, *Inorg. Chem.* **2013**, *42*, 6528-6538.

[15] (a) B.-Z. Yang, X. Zhou, T. Liu, F.-Q. Bai, H.-X. Zhang, *J. Phys. Chem. A* **2009**, *113*, 9396-9403. (b) C. Bronner, O. S. Wenger, *Dalton Trans.* **2011**, *40*, 12409-12420. (c) G. S. M. Tong, K. T. Chan, X. Chang, C.-M. Che, *Chem. Sci.* **2015**, *6*, 3026-3037. (d) E. S.-H. Lam, Lam, V. W. -W. Yam *Inorg. Chem.* **2015**, *54*, 3624-3630.

[16] For an example of (N^C^C)-Ir complex, see: Y. Koga, M. Kamo, Y. Yamada, T. Matsumoto, K. Matsubara, *Eur. J. Inorg. Chem*. **2011**, 2869.

[17] (a) K. M. –C. Wong, X. Zhu, L.-L. Hung, N. Zhu, V. W. –W. Yam, H. –S. Kwok, *Chem. Commun.* **2005**, 2906-2908. (b) V. K. –M. Au, K. M. –C. Wong, D. P. –K. Tsang, M. –Y. Chan, N. Zhu, V. W. –W. Yam, *J. Am. Chem. Soc.* **2010**, *132*, 14273-14278. (c) M.-C. Tang, D. P.-K. Tsang, Y.-C. Wong, M.-Y. Chan, K. M.-C. Wong, V. W.-W. Yam *J. Am. Chem. Soc.* **2014**, *136*, 17861-17868.

CHAPTER 2

EXPERIMENTAL SECTION

Table of Contents

1. General Information

NMR spectra were recorded on AV2 400 or AV2 500 MHz Bruker spectrometers. Chemical shifts are given in ppm. The spectra were calibrated to the residual ^{1}H and ^{13}C signals of the solvents. Multiplicities are abbreviated as follows: singlet (s), doublet (d), triplet (t), quartet (q), doublet-doublet (dd), quintet (quint), septet (sept), multiplet (m), and broad (b). The compounds were characterized by ^{1}H, ^{13}C, and ^{19}F NMR spectroscopy. Infrared spectra were recorded on a JASCO FT/IR-4100 spectrometer. High-resolution electrospray ionization and electronic impact mass spectrometry was performed on a Finnigan MAT 900 (Thermo Finnigan, San Jose, CA; USA) double focusing magnetic sector mass spectrometer. Ten spectra were acquired. A mass accuracy ≤ 2 ppm was obtained in the peak matching acquisition mode by using a solution containing 2 <l PEG200, 2 <l PPG450, and 1.5 mg NaOAc (all obtained from Sigma-Aldrich, CH-Buchs) dissolved in 100 mL MeOH (HPLC Supra grade, Scharlau, E-Barcelona) as internal standard. GC-MS analysis was done on a Finnigan Voyager GC8000 Top. Elemental microanalysis was carried out with Leco Tru Spec Micro-CHNS analyser. Microwave reaction was done in Discover & Explorer SP (CEM). UV-Vis measurements were carried out on a Perkin-Elmer Lambda 19 UV-Vis spectrophotometer. Emission spectra were acquired on Perkin Elmer spectrophotometer using 450 W Xenon lamp excitation by exciting at the longest-wavelength absorption maxima with the excitation slit width 3 nm and emission slit width 5 nm. All samples for emission spectra were degassed by at least three freeze-pump-thaw cycles in an anaerobic cuvette and were pressurized with N_2 following each cycle. Absolute quantum yields ϕ_{em} were determined at 298 K in dichloromethane using an integrating sphere on the Edinburgh spectrophotometer FLS920 (estimated uncertainty ± 15%). YAG:Ce (powder) was used as a calibration reference with ϕ_{em} = 97%. Phosphorescent lifetimes in dichloromethane were measured on the Edinburgh laser flash photolysis spectrophotometer LP920 with a Nd:YAG 355 nm laser as an excitation source fitted with a single monochromator.

Materials and Methods:

Unless otherwise stated, starting materials were purchased from Aldrich and/or Fluka. Solvents were purchased in HPLC quality, degassed by purging throughly with nitrogen and dried over activated molecular sieves of appropriate size. Alternatively, they were purged with argon and passed through alumina columns in a solvent purification system (Innovative Technology). Conversion was monitored by thin layer chromatography (TLC) using Merck TLC silica gel 60 F254. Compounds were visualized by UV-light at 254 nm and by dipping the plates in an ethanolic vanillin/sulfuric acid solution or an aqueous potassium permanganate solution followed by heating. Flash column chromatography was performed over silica gel (230-400 mesh).

2. General Procedures

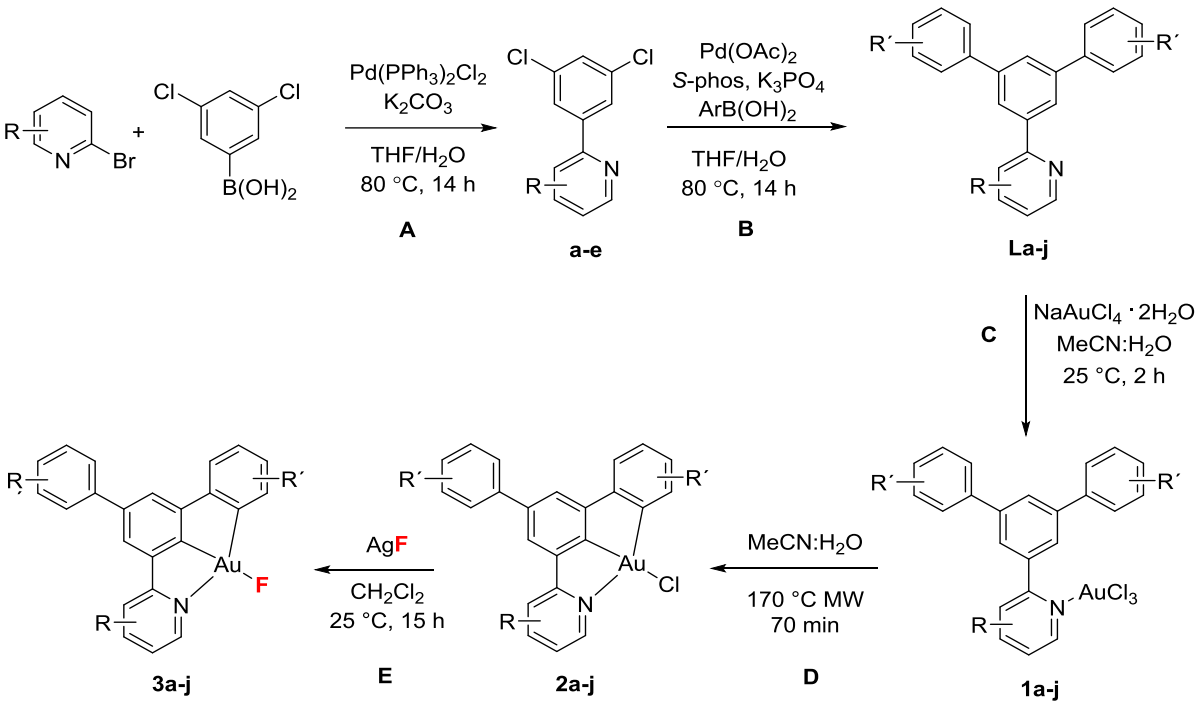

General Procedure A:

In a schlenk tube, the corresponding bromopyridine (1 equiv), boronic acid (1.2 equiv) and potassium carbonate (2 equiv) were dissolved in a mixture of THF/H_2O (3/1). The reaction mixture was degassed for 20-30 minutes. $Pd(PPh_3)_2Cl_2$ (5mol%) was added and reaction mixture was stirred at 80 °C for 14h. Ethyl acetate (20 ml) was added, organic layer was washed with distilled water and dried over anhydrous magnesium sulfate. After filtration the solvent was evaporated and the reaction crude was purified by silica gel chromatography using EtoAc/Hexane as eluent. Compounds **a** to **e** were prepared using general procedure **A**.

General Procedure B:

In a schlenk tube, a mixture of 3,5-dichlorophenyl pyridine **a-e** (1equiv), boronic acid (3 equiv) and K_3PO_4 tribasic (6 equiv) were dissolved in a mixture of THF/H_2O (3/1). The reaction mixture was degassed for 15-20 minutes. $Pd(OAc)_2$ (5 mol%) and *S*-Phos (10 mol%) was added. The reaction was stirred at 80 °C for 14 h. Ethyl acetate (20 ml) was added, organic layer was washed with distilled water and dried over anhydrous magnesium sulfate. After filtration solvent was evaporated and reaction crude was purified by silica gel chromatography using EtoAc/Hexane as eluent. Compounds **La** to **Lj** were prepared using general procedure **B**.

General Procedure C:

A solution of ligand **La-Lj** (1 equiv) in acetonitrile (5 ml) was slowly added to a sodium tetrachloroaurate dihydrate (1 equiv) solution in water (5 ml). Immediate formation of a yellow solid was observed. Reaction was stirred at 25 °C for 2 to 3 hours. Resulting solid was filtered, washed with cold distilled water and dried or the reaction mixture was diluted with distilled water and organic compound was extracted with CH_2Cl_2 (15 x 3 ml). The organic phases were combined and dried over anhydrous magnesium sulfate. After evaporation of the solvent, the product was obtained in reported yields. Compounds **1a-1j** were prepared by using general procedure **C**.

General Procedure D for compound 2a-2j:

In a 20 ml microwave vial, compound **1a-1j** (1 equiv) was dissolved in a mixture of acetonitrile:water (1:1). The reaction mixture was refluxed at 170 °C for 70 minutes in a microwave oven. The reaction mixture was diluted with distilled water and the aqueous layer was extracted with CH_2Cl_2 (15 x 3 ml). The organic phases were combined and dried with anhydrous magnesium sulfate. After evaporation of solvent, the residue was purified by column chromatography on silica gel to furnish the pure product. Compounds **2a-2j** were prepared by using general procedure **D**.

General Procedure E for compound 3a-3j:

In a glovebox, a mixture of cyclometalated gold chloride (1 equiv) and silver fluoride (6 equiv) was dissolved in dry CH_2Cl_2 in a scintillation vial. The reaction mixture was stirred for 16 hours at 25 °C and the reaction progress was monitored by NMR. The reaction mixture was filtered over cotton path and the corresponding gold fluoride was obtained after evaporation of the solvent under reduced pressure by crystallization from a saturated dichloromethane solution by diffusion of hexane or pentane as co-solvent. Compounds **3a-3j** were prepared by using general procedure **E**.

3. Characterization of compounds

2-(3,5-Dichlorophenyl)-3-methylpyridine (a)

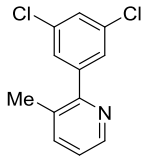

This compound was synthesized by following general procedure **A** using 2-bromo-3-methylpyridine (600 mg, 3.49 mmol), 3,5-dichloro phenyl boronic acid (1.08 g, 4.18 mmol), potassium carbonate (964 mg, 6.96 mmol) and $Pd(PPh_3)_2Cl_2$ (122 mg, 0.17 mmol) in THF/H_2O (15/5 ml). A white solid (738 mg, 89%) was isolated; m.p. 71-73 °C; ^{1}H NMR (400 MHz, CD_2Cl_2): δ 8.50 – 8.48 (m,1H), 7.63 – 7.61 (m, 1H), 7.45 (d, *J* = 1.9 Hz, 2H), 7.43 – 7.40 (m, 1H), 7.23 (dd, *J* = 7.7, 4.7 Hz, 1H), 2.35 (s, 3H); ^{13}C NMR (101 MHz, CD_2Cl_2): δ 156.27, 147.75, 144.33, 139.33, 135.12, 131.58, 128.34, 128.26, 123.50, 20.22; IR (film) ν (cm^{-1}) 1584, 1556, 1455, 1405, 1381, 1283, 1264, 1126, 1097, 1054, 854, 801, 791, 765, 682, 634 cm^{-1}; HR-MS (ESI) *m/z* calcd for $C_{12}H_{10}Cl_2N$ [M+H$^+$] 238.0185, found 238.0181.

2-(3,5-Dichlorophenyl)pyridine (b)

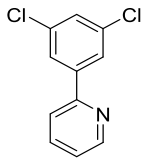

This compound was synthesized by following general procedure **A** using 2-bromopyridine (600 mg, 3.79 mmol), 3,5-dichloro phenyl boronic acid (1.08 g, 5.69 mmol), potassium carbonate (1.05 g, 6.47 mmol) and $Pd(PPh_3)_2Cl_2$ (133 mg, 0.19 mmol) in THF/H_2O (15/5 ml). A white solid (785 mg, 92%) was isolated; m.p. 39-41 °C; ^{1}H NMR (400 MHz, CD_2Cl_2): δ 8.68 (d, *J* = 3.2 Hz, 1H), 7.94 (s, 2H), 7.84 – 7.76 (m, 1H), 7.72 (d, *J* = 7.8 Hz, 1H), 7.41 (s, 1H), 7.35 – 7.25 (m, 1H); ^{13}C NMR (101 MHz, CD_2Cl_2): δ 154.78, 150.44, 142.92, 137.61, 135.86, 129.14, 125.87, 123.85, 121.00; IR (film) ν (cm^{-1}) 3031, 1584, 1575, 1557, 1473, 1407, 1278, 1125, 1092, 991, 850, 799, 735 cm^{-1}; HR-MS (ESI) *m/z* calcd for $C_{11}H_8Cl_2N$ [M+H$^+$] 224.0028, found 224.0030.

Methyl 6-(3,5-dichlorophenyl)nicotinate (c)

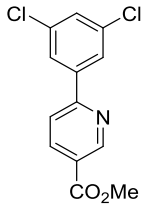

This compound was synthesized by following general procedure **A** using methyl-6-bromo-nicotinate (600 mg, 2.71 mmol), 3,5-dichloro phenyl boronic acid (688 g, 3.61 mmol), potassium carbonate (768 mg, 5.55 mmol)

and $Pd(PPh_3)_2Cl_2$ (97 mg, 0.14 mmol) in THF/H_2O (15/5 ml). A white solid (601 mg, 77%) was isolated; m.p. 106-108 °C; ^{1}H NMR (400 MHz, CD_2Cl_2): δ 9.23 (dd, *J* = 2.2, 0.8 Hz, 1H), 8.36 (dd, *J* = 8.3, 2.2 Hz, 1H), 7.99 (d, *J* = 1.9 Hz, 2H), 7.80 (dd, *J* = 8.3, 0.8 Hz, 1H), 7.46 (t, *J* = 1.9 Hz, 1H), 3.95 (s, 3H); ^{13}C NMR (101 MHz, CD_2Cl_2): δ 165.96, 158.17, 151.46, 141.76, 138.69, 136.09, 130.09, 126.33, 126.00, 120.53, 52.91; IR (film) ν (cm^{-1}) 1725, 1595, 1556, 1430, 1368, 1307, 1279, 1196, 1143, 1115, 1022, 855, 846, 799, 781, 730, 669, 581, 506 cm^{-1}; HR-MS (ESI) *m/z* calcd for $C_{13}H_{10}Cl_2NO_2$ [M+H^+] 282.0083, found 282.0084.

[6-(3,5-Dichlorophenyl)pyridin-3-yl]methanol (d)

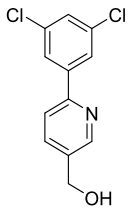

This compound was synthesized by following general procedure **A** using 6-bromopyridine-3-methanol (600 mg, 3.19 mmol), 3,5-dichloro phenyl boronic acid (791 mg, 4.14 mmol), potassium carbonate (882 mg, 6.38 mmol) and $Pd(PPh_3)_2Cl_2$ (111 mg, 0.16 mmol) in THF/H_2O (15/5 ml). A white solid (486 mg, 60%) was isolated; m.p. 125-127 °C; ^{1}H NMR (400 MHz, CD_2Cl_2): δ 8.63 (d, *J* = 1.6 Hz, 1H), 7.93 (d, *J* = 1.9 Hz, 2H), 7.80 (dd, *J* = 8.1, 2.2 Hz, 1H), 7.71 (d, *J* = 8.2 Hz, 1H), 7.41 (t, *J* = 1.9 Hz, 1H), 4.76 (s, 1H), 2.24 (s, 1H); ^{13}C NMR (101 MHz, CD_2Cl_2): δ 154.01, 149.13, 142.68, 136.74, 136.30, 135.88, 129.11, 125.84, 120.77, 62.84; IR (film) ν (cm^{-1}) 3239, 1589, 1555, 1485, 1419, 1379, 1121, 856, 831, 734, 676, 582 cm^{-1}; HR-MS (ESI) *m/z* calcd for $C_{12}H_{10}Cl_2NO$ [M+H^+] 254.0134, found 254.0135.

2-(3,5-Dichloro-4-propoxyphenyl)-3-methylpyridine (e)

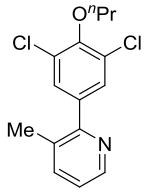

This compound was synthesized by following general procedure **A** using 2-bromo-3-methylpyridine (600 mg, 3.49 mmol), 3,5-dichloro-4-propoxyphenyl boronic acid (1.04 g, 4.18 mmol), potassium carbonate (964 mg, 6.96 mmol) and $Pd(PPh_3)_2Cl_2$ (122 mg, 0.17 mmol) in THF/H_2O (15/5 ml). A colorless oil (811 mg, 78%) was isolated; ^{1}H NMR (400 MHz, CD_2Cl_2): δ 8.47 (dd, *J* = 4.7, 1.1 Hz, 1H), 7.63 – 7.58 (m, 1H), 7.50 (s, 2H), 7.20 (dd, *J* = 7.7, 4.7 Hz, 1H), 4.05 (t, *J* = 6.6 Hz, 2H), 2.36 (s, 3H), 1.94 – 1.84 (m, 2H), 1.10 (t, *J* = 7.4 Hz, 3H); ^{13}C NMR (101 MHz, CD_2Cl_2): δ 156.13, 151.87, 147.69, 139.29, 138.46, 131.49, 130.16, 129.57, 123.25, 75.99, 24.03, 20.33, 10.79; IR (film) ν (cm^{-1}) 2965, 2937, 2878, 1583, 1568, 1545, 1480, 1459, 1446, 1418, 1383,

1298, 1268, 1246, 1123, 1058, 987, 952, 805, 788, 766, 624 cm^{-1}; HR-MS (ESI) *m/z* calcd for $C_{15}H_{16}Cl_2NO$ [M+H$^+$] 296.0604, found 296.0606.

2-[4,4''-Di-*tert*-butyl-(1,1':3',1''-terphenyl) -5'-yl]-3-methylpyridine (La)

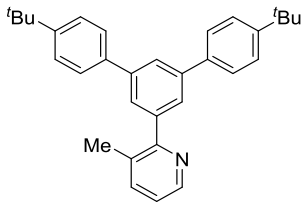

This compound was synthesized by following general procedure **B** using **a** (200 mg, 0.84 mmol), 4-*tert*-butylphenylboronic acid (488 mg, 2.51 mmol), K_3PO_4 tribasic (1.06 g, 5.03 mmol), $Pd(OAc)_2$ (9 mg, 0.04 mmol) and *S*-Phos (33 mg, 0.08 mmol) in THF/H_2O (12/4 ml). A white solid (254 mg, 70%) was isolated; m.p. 154-156 °C; ^{1}H NMR (500 MHz, CD_2Cl_2): δ 8.54 (d, *J* = 4.6 Hz, 1H), 7.86 (s, 1H), 7.71 (d, *J* = 1.0 Hz, 2H), 7.65 (d, *J* = 8.2 Hz, 4H), 7.65 – 7.63 (m, 1H), 7.51 (d, *J* = 8.3 Hz, 4H), 7.23 (dd, *J* = 7.7, 4.7 Hz, 1H), 2.43 (s, 3H), 1.37 (s, 18H); ^{13}C NMR (101 MHz, CD_2Cl_2): δ 159.15, 151.24, 147.55, 142.37, 141.89, 139.03, 138.61, 131.59, 127.42, 126.98, 126.39, 125.66, 122.80, 35.04, 31.69, 20.56; IR (film) ν (cm^{-1}) 2958, 1594, 1583, 1565, 1514, 1458, 1422, 1390, 1362, 1269, 1120, 888, 829, 788, 773 cm^{-1}; HR-MS (ESI) *m/z* calcd for $C_{32}H_{35}NNa$ [M+Na$^+$] 456.2662, found 456.2656.

2-[4,4''-Di-*tert*-butyl-(1,1':3',1''-terphenyl)-5'-yl]pyridine (Lb)

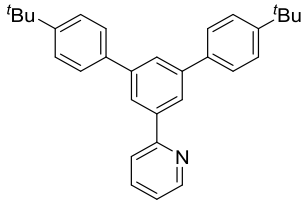

This compound was synthesized by following general procedure **B** using **b** (400 mg, 1.79 mmol), 4-*tert*-butylphenylboronic acid (953 mg, 5.35 mmol), K_3PO_4 tribasic (2.27 g, 10.71 mmol), $Pd(OAc)_2$ (20 mg, 0.09 mmol) and *S*-Phos (73 mg, 0.18 mmol) in THF/H_2O (12/4 ml). A white solid (605 mg, 81%) was isolated; m.p. 79-81 °C; ^{1}H NMR (400 MHz, CD_2Cl_2): δ 8.77 – 8.71 (m, *J* = 4.7, 1.8, 0.9 Hz, 1H), 8.24 (d, *J* = 1.7 Hz, 2H), 7.92 – 7.86 (m, 2H), 7.81 (dt, *J* = 5.6, 1.8 Hz, 1H), 7.71 (d, *J* = 8.6 Hz, 4H), 7.55 (d, *J* = 8.5 Hz, 4H), 7.32 – 7.26 (m, 1H), 1.40 (s, 18H); ^{13}C NMR (101 MHz, CD_2Cl_2): δ 157.74, 151.34, 150.32, 142.57, 141.03, 138.66, 137.33, 127.47, 126.78, 126.42, 124.88, 122.94, 121.17, 35.07, 31.72; IR (film) ν (cm^{-1}) 743, 832, 1113, 1250, 1268, 1362, 1391, 1391, 1460, 1473, 1513, 1566, 1584, 2865, 2901, 2959, 2901, 2865, 1584, cm^{-1}; HR-MS (ESI) *m/z* calcd for $C_{31}H_{34}N$ [M+H$^+$] 420.2686, found 420.2683.

Methyl 6-[4,4''-di-*tert*-butyl-(1,1':3',1''-terphenyl)-5'-yl]nicotinate (Lc)

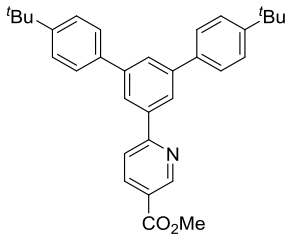

This compound was synthesized by following general procedure **B** using **c** (200 mg, 0.71 mmol), 4-*tert*-butylphenylboronic acid (377 mg, 2.72 mmol), K_3PO_4 tribasic (901 mg, 4.28 mmol), $Pd(OAc)_2$ (8 mg, 0.03 mmol) and *S*-Phos (28 mg, 0.07 mmol) in THF/H_2O (12/4 ml). A white solid (269 mg, 79%) was isolated; m.p. 139-141 °C; ^{1}H NMR (400 MHz, CD_2Cl_2): δ 9.29 (dd, *J* = 2.2, 0.8 Hz, 1H), 8.38 (dd, *J* = 8.3, 2.2 Hz, 1H), 8.28 (d, *J* = 1.7 Hz, 2H), 7.97 (dd, *J* = 8.3, 0.8 Hz, 1H), 7.93 (t, *J* = 1.7 Hz, 1H), 7.69 (d, *J* = 8.4 Hz, 4H), 7.54 (d, *J* = 8.4 Hz, 4H), 3.96 (s, 3H), 1.39 (s, 18H); ^{13}C NMR (101 MHz, CD_2Cl_2): δ 166.34, 161.17, 151.49, 151.42, 142.74, 139.88, 138.39, 138.36, 127.71, 127.44, 126.45, 125.25, 125.13, 120.56, 52.78, 35.07, 31.68; IR (film) ν (cm^{-1}) 2960, 1721, 1595, 1289, 1117, 830, 786, 561 cm^{-1}; HR-MS (ESI) *m/z* calcd for $C_{33}H_{36}NO_2$ [M+H$^+$] 478.2741, found 478.2738.

[6-(4,4''-Di-*tert*-butyl-(1,1':3',1''-terphenyl)-5'-yl)pyridin-3-yl]methanol (Ld')

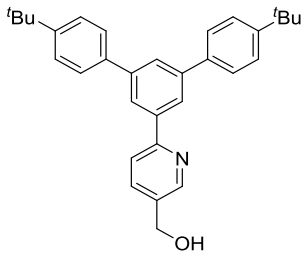

This compound was synthesized by following general procedure **B** using **d** (400 mg, 1.57 mmol), 4-*tert*-butylphenylboronic acid (840 mg, 4.71 mmol), K_3PO_4 tribasic (2.04 g, 9.42 mmol), $Pd(OAc)_2$ (18 mg, 0.08 mmol) and *S*-Phos (66 mg, 0.16 mmol) in THF/H_2O (12/4 ml). A white solid (467 mg, 66%) was isolated; m.p. 199-201 °C; ^{1}H NMR (400 MHz, CD_2Cl_2): δ 8.62 (d, *J* = 1.1 Hz, 1H), 8.17 (d, *J* = 1.7 Hz, 2H), 7.91 (t, *J* = 1.7 Hz, 1H), 7.79 – 7.74 (m, 2H), 7.71 (d, *J* = 8.5 Hz, 4H), 7.56 (d, *J* = 8.5 Hz, 4H), 4.07 (s, 1H), 1.42 (s, 18H); ^{13}C NMR (101 MHz, CD_2Cl_2): δ 156.81, 151.31, 148.79, 142.54, 140.55, 138.54, 136.43, 136.18, 127.47, 126.75, 126.42, 124.89, 121.18, 62.65, 35.06, 31.74; IR (film) ν (cm^{-1}) 2959, 1597, 1486, 1362, 1270, 1017, 827, 691, 559 cm^{-1}; HR-MS (ESI) *m/z* calcd for $C_{32}H_{36}NO$ [M+H$^+$] 450.2791, found 450.2790.

[6-(4,4''-Di-*tert*-butyl-(1,1':3',1''-terphenyl)-5'-yl)pyridin-3-yl]methyl acetate (Ld)

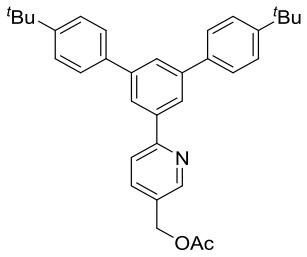

In a schlenk tube, a mixture of **Ld'** (150 mg, 0.33 mmol) and DMAP (4 mg, 0.03 mmol) were dissolved in dichloromethane (4 ml). Ac_2O (41 mg, 0.40 mmol) was added slowly and the reaction mixture was stirred at 25 °C. After 15 minutes the reaction was finished and CH_2Cl_2 (10 ml) was added. Organic layer was washed with distilled water (3 x 5 ml) and dried over anhydrous magnesium sulfate. After filtration solvent was evaporated. The product was isolated by silica gel chromatography as a white solid in 98% yield. m.p. 63-65 °C; ^{1}H NMR (400 MHz, CD_2Cl_2): δ 8.73 (d, *J* = 1.9 Hz, 1H), 8.23 (d, *J* = 1.7 Hz, 2H), 7.90 (d, *J* = 1.3 Hz, 1H), 7.89 – 7.87 (m, 1H), 7.82 (dd, *J* = 8.2, 2.3 Hz, 1H), 7.70 (d, *J* = 8.6 Hz, 4H), 7.54 (d, *J* = 8.5 Hz, 4H), 5.18 (s, 2H), 2.12 (s, 3H), 1.40 (s, 18H); ^{13}C NMR (101 MHz, CD_2Cl_2): δ 171.16, 157.61, 151.38, 150.19, 142.61, 140.51, 138.57, 137.46, 131.08, 127.45, 126.95, 126.42, 124.90, 120.86, 64.13, 35.07, 31.70, 21.27; IR (film) ν (cm^{-1}) 2960, 1740, 1599, 1486, 1362, 1225, 1023, 828, 801, 691, 559 cm^{-1}; HR-MS (ESI) *m/z* calcd for $C_{34}H_{38}NO_2$ [M+H$^+$] 492.2897, found 492.2894.

2-[4,4''-Dipropoxy-(1,1':3',1''-terphenyl)-5'-yl]-3-methylpyridine (Le)

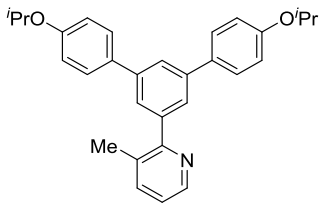

This compound was synthesized by following general procedure **B** using **a** (200 mg, 0.84 mmol), 4-isopropoxyphenylboronic acid (453 mg, 2.51 mmol), K_3PO_4 tribasic (1.06 g, 5.03 mmol), $Pd(OAc)_2$ (9 mg, 0.04 mmol) and *S*-Phos (33 mg, 0.08 mmol) in THF/H_2O (12/4 ml). A white solid (282 mg, 77%) was isolated; m.p. 49-51 °C; ^{1}H NMR (400 MHz, CD_2Cl_2): δ 8.53 (dd, *J* = 4.7, 1.0 Hz, 1H), 7.78 (t, *J* = 1.7 Hz, 1H), 7.65 – 7.61 (m, 3H), 7.62 (d, *J* = 8.6 Hz, 4H), 7.22 (dd, *J* = 7.7, 4.7 Hz, 1H), 6.98 (d, *J* = 8.8 Hz, 4H), 4.61 (sept, *J* = 6.0 Hz, 2H), 2.43 (s, 3H), 1.36 (d, *J* = 6.1 Hz, 12H); ^{13}C NMR (101 MHz, CD_2Cl_2): δ 159.24, 158.34, 147.53, 142.35, 141.68, 138.98, 133.78, 131.55, 128.82, 126.27, 124.99, 122.75, 116.66, 70.53, 22.41, 20.56; IR (film) ν (cm^{-1}) 2975, 1607, 1508, 1425, 1235, 1182, 1105, 952, 827, 790, 602, 530 cm^{-1}; HR-MS (ESI) *m/z* calcd for $C_{30}H_{32}NO_2$ [M+H$^+$] 438.2428, found 438.2422.

2-[4,4''-Diphenoxy-(1,1':3',1''-terphenyl)-5'-yl]-3-methylpyridine (Lf)

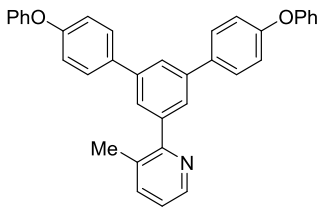

This compound was synthesized by following general procedure **B** using **a** (200 mg, 0.84 mmol), 4-phenoxyphenylboronic acid (539 mg, 2.51 mmol), K_3PO_4 tribasic (1.06 g, 5.03 mmol), $Pd(OAc)_2$ (9 mg, 0.04 mmol) and *S*-Phos (33 mg, 0.08 mmol) in THF/H_2O (12/4 ml). A white solid (347 mg, 82%) was isolated; m.p. 51-53 °C; ^{1}H NMR (500 MHz, CD_2Cl_2): δ 8.54 (d, *J* = 4.6 Hz, 1H), 7.83 (s, 1H), 7.71 – 7.68 (m, 8H), 7.65 (d, *J* = 7.6 Hz, 1H), 7.38 (t, *J* = 7.8 Hz, 4H), 7.23 (dd, *J* = 7.6, 4.8 Hz, 1H), 7.15 (d, *J* = 7.4 Hz, 1H), 7.13 – 7.06 (m, 8H), 2.45 (s, 3H); ^{13}C NMR (126 MHz, CD_2Cl_2): δ 157.72, 147.60, 142.55, 141.49, 139.06, 136.59, 131.57, 130.41, 129.18, 126.96, 125.47, 124.05, 122.87, 119.60, 20.56; IR (film) ν (cm^{-1}) 3040, 1587, 1505, 1487, 1427, 1228, 1167, 870, 834, 790, 745, 690 cm^{-1}; HR-MS (ESI) *m/z* calcd for $C_{36}H_{28}NO_2$ [M+H$^+$] 506.2115, found 506.2107.

2-[2,2'',3,3'',4,4''-Hexamethoxy-(1,1':3',1''-terphenyl)-5'-yl]-3-methylpyridine (Lg)

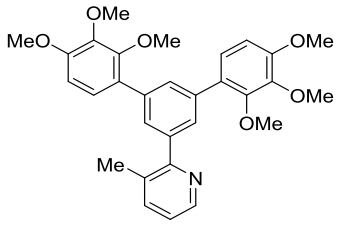

This compound was synthesized by following general procedure **B** using **a** (200 mg, 0.84 mmol), 2,3,4-trimethoxyphenylboronic acid (534 mg, 2.51 mmol), K_3PO_4 tribasic (1.06 g, 5.03 mmol), $Pd(OAc)_2$ (9 mg, 0.04 mmol) and *S*-Phos (33 mg, 0.08 mmol) in THF/H_2O (12/4 ml). A gummy solid (357 mg, 85%) was isolated; ^{1}H NMR (400 MHz, CD_2Cl_2): δ 8.53 – 8.49 (m, 1H), 7.67 (t, *J* = 1.7 Hz, 1H), 7.64 – 7.61 (m, 1H), 7.60 (d, *J* = 1.7 Hz, 2H), 7.20 (dd, *J* = 7.7, 4.8 Hz, 1H), 7.13 (d, *J* = 8.6 Hz, 2H), 6.78 (d, *J* = 8.7 Hz, 2H), 3.89 (s, 6H), 3.88 (s, 6H), 3.72 (s, 6H), 2.45 (s, 3H); ^{13}C NMR (101 MHz, CD_2Cl_2): δ 159.25, 153.96, 152.10, 147.48, 143.21, 141.00, 138.92, 138.42, 131.59, 129.98, 128.97, 128.83, 125.42, 122.59, 108.20, 61.47, 61.33, 56.53, 20.54; IR (film) ν (cm-1) 2934, 1596, 1494, 1463, 1398, 1292, 1233, 1089, 1009, 888, 801, 714 cm^{-1}; HR-MS (ESI) *m/z* calcd for $C_{30}H_{32}NO_6$ [M+H$^+$] 502.2218, found 502.2224.

2-[4,4''-Dicyclohexyl-(1,1':3',1''-terphenyl)-5'-yl]-3-methylpyridine (Lh)

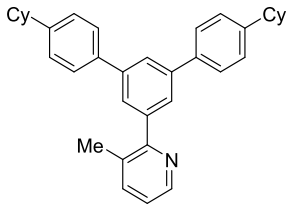

This compound was synthesized by following general procedure **B** using **a** (200 mg, 0.84 mmol), 4-cyclohexylphenylboronic acid (514 mg, 2.51 mmol), K_3PO_4 tribasic (1.06 g, 5.03 mmol), $Pd(OAc)_2$ (9 mg, 0.04 mmol) and *S*-Phos (33 mg, 0.08 mmol) in THF/H_2O (12/4 ml). A white solid (349 mg, 85%) was isolated; m.p. 65-67 °C; ^{1}H NMR (400 MHz, CD_2Cl_2): δ 8.61 – 8. 55 (m, 1H), 7.90 (t, *J* = 1.7 Hz, 1H), 7.76 (d, *J* = 1.7 Hz, 2H), 7.68 (d, *J* = 8.3 Hz, 4H), 7.67 – 7.63 (m, 1H), 7.37 (d, *J* = 8.1 Hz, 4H), 7.24 (dd, *J* = 7.6, 4.8 Hz, 1H), 2.68 – 2.58 (m, 2H), 2.47 (s, 3H), 2.01 – 1.89 (m, 8H), 1.85 – 1.77 (m, 2H), 1.59 – 1.51 (m, 4H), 1.45 (dt, *J* = 12.4, 2.9 Hz, 2H), 1.38 – 1.31 (m, 2H); ^{13}C NMR (101 MHz, CD_2Cl_2): δ 159.16, 148.24, 147.58, 142.38, 142.03, 139.06, 139.01, 131.54, 127.91, 127.70, 126.98, 125.66, 122.78, 44.88, 35.11, 27.54, 26.79, 20.60; IR (film) ν (cm^{-1}) 2923, 2850, 1560, 1513, 1448, 1421, 1121, 874, 825, 789, 766, 737, 700, 626, 574 cm^{-1}; HR-MS (ESI) *m/z* calcd for $C_{36}H_{40}N$ [M+H$^+$] 486.3155, found 486.3151.

2-[4,4''-Di-*tert*-butyl-2'-propoxy-(1,1':3',1''-terphenyl)-5'-yl]-3-methylpyridine (Li)

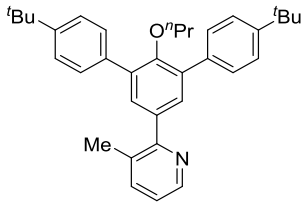

This compound was synthesized by following general procedure **B** using **e** (400 mg, 1.35 mmol), 4-*tert*-butylphenylboronic acid (727 mg, 4.05 mmol), K_3PO_4 tribasic (1.71 g, 8.10 mmol), $Pd(OAc)_2$ (15 mg, 0.07 mmol) and *S*-Phos (55 mg, 0.13 mmol) in THF/H_2O (12/4 ml). A white solid (527 mg, 79%) was isolated; m.p. 154-156 °C; ^{1}H NMR (400 MHz, CD_2Cl_2): δ 8.52 – 8.48 (m, 1H), 7.62 – 7.59 (m, 1H), 7.60 (d, *J* = 8.6 Hz, 4H), 7.50 (s, 2H), 7.49 – 7.45 (m, 4H), 7.18 (dd, *J* = 7.7, 4.7 Hz, 1H), 3.26 (t, *J* = 6.4 Hz, 2H), 2.44 (s, 3H), 1.38 (s, 18H), 1.29 – 1.21 (m, 2H), 0.56 (t, *J* = 7.4 Hz, 3H); ^{13}C NMR (101 MHz, CD_2Cl_2): δ 158.71, 154.69, 150.70, 147.52, 138.96, 137.10, 136.49, 136.11, 131.42, 131.22, 129.74, 125.52, 122.50, 75.25, 35.03, 31.74, 23.60, 20.66, 10.69; IR (film) ν (cm^{-1}) cm^{-1}; HR-MS (ESI) *m/z* calcd for $C_{35}H_{42}NO$ [M+H$^+$] 492.3261, found 492.3255.

2-[4,4''-diphenoxy-2'-propoxy-(1,1'-3',1''-terphenyl)-5'-yl]-3-methylpyridine (Lj)

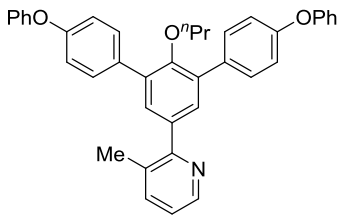

This compound was synthesized by following general procedure **B** using **e** (209 mg, 0.708 mmol), 4-phenoxyphenylboronic acid (458 mg, 2.12 mmol), K_3PO_4 tribasic (901 mg, 4.248 mmol), $Pd(OAc)_2$ (8 mg, 0.035 mmol) and *S*-Phos (28 mg, 0.07 mmol) in THF/H_2O (12/4 ml). A white solid (302 mg, 75%) was isolated; m.p. 142-144 °C; ^{1}H NMR (400 MHz, CD_2Cl_2) δ 8.50 (d, *J* = 4.2 Hz, 1H), 7.66 (d, *J* = 8.8 Hz, 4H), 7.61 (dd, *J* = 7.7, 0.7 Hz, 1H), 7.51 (s, 2H), 7.43 – 7.31 (m, 4H), 7.23 – 7.01 (m, 11H), 3.29 (t, *J* = 6.4 Hz, 2H), 2.45 (s, 3H), 1.36 – 1.25 (m, 2H), 0.65 (t, *J* = 7.4 Hz, 3H).^{13}C NMR (101 MHz, CD_2Cl_2) δ 158.50, 157.95, 157.04, 154.49, 147.53, 139.03, 137.26, 135.64, 134.46, 131.58, 131.43, 131.22, 130.34, 123.83, 122.60, 119.36, 119.04, 75.30, 23.71, 20.64, 10.83. IR (film) ν (cm^{-1}) 1568, 1556, 1409, 1290, 1125, 854, 787 cm^{-1}; HR-MS (ESI) *m/z* calcd for $C_{39}H_{34}NO_3$ [M+H$^+$] 564.2533, found 564.2524.

$LaAuCl_3$ (1a)

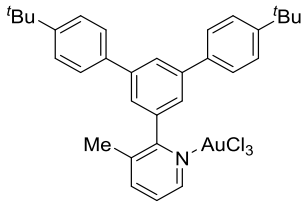

This compound was synthesized by following general procedure **C** using **La** (255 mg, 0.59 mmol) in acetonitrile (10 ml), sodium tetrachloroaurate dehydrate (233 mg, 0.59 mmol) in water (15 ml) to furnish the product as dark yellow solid (428 mg, 99%); m.p. 178-180 °C; ^{1}H NMR (500 MHz, CD_2Cl_2): δ 8.65 (d, *J* = 5.8 Hz, 1H), 8.10 – 8.05 (m, 2H), 7.75 (d, *J* = 0.9 Hz, 2H), 7.71 (d, *J* = 8.4 Hz, 4H), 7.68 – 7.66 (m, 1H), 7.54 (d, *J* = 8.3 Hz, 4H), 2.40 (s, 3H), 1.37 (s, 18H); ^{13}C NMR (126 MHz, CD_2Cl_2): δ 159.68, 151.95, 147.65, 144.18, 143.07, 139.85, 137.54, 137.17, 128.40, 127.53, 127.42, 127.32, 126.61, 35.11, 31.64, 20.91; IR (film) ν (cm^{-1}) 2963, 1598, 1514, 1510, 1467, 1395, 1270, 1235, 1124, 1114, 1014, 893,837, 795, 690, 670, 656 cm^{-1}; HR-MS (ESI) *m/z* calcd for $C_{32}H_{35}AuCl_3NNa$ [M+Na$^+$] 758.1393, found 758.1388. Elem. Anal. Calcd. For $C_{32}H_{35}AuCl_3N$: C, 52.15; H, 4.79; N, 1.90, found: C, 52.12; H, 4.75; N, 1.88.

$LbAuCl_3$ (1b)

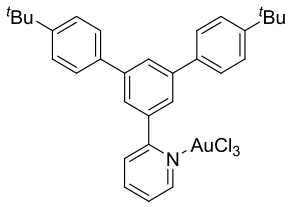

This compound was synthesized by following general procedure **C** using **Lb** (150 mg, 0.35 mmol) in acetonitrile (7 ml), sodium tetrachloroaurate dehydrate (142 mg, 0.35 mmol) in water (10 ml) to furnish the product as dark yellow solid (252 mg, 98%); m.p. 196-198 °C; ^{1}H NMR (400 MHz, CD_2Cl_2): δ 8.85 (ddd, *J* = 6.0, 1.4, 0.6 Hz, 1H), 8.23 (td, *J* = 7.7, 1.5 Hz, 1H), 8.09 (t, *J* = 1.7 Hz, 1H), 8.02 (d, *J* = 1.7 Hz, 2H), 7.95 (ddd, *J* = 7.9, 1.6, 0.6 Hz, 1H), 7.77 – 7.71 (m, 1H), 7.73 (d, *J* = 8.7 Hz, 4H), 7.55 (d, *J* = 8.6 Hz, 4H), 1.38 (s, 18H); ^{13}C NMR (101 MHz, CD_2Cl_2): δ 152.10, 150.41, 143.48, 142.91, 138.83, 137.35, 130.20, 128.82, 127.57, 127.17, 126.69, 126.66, 110.61, 35.14, 31.65; IR (film) ν (cm^{-1}) 2958, 2901, 1593, 1487, 1393, 1270, 1253, 1065, 1052, 1044, 1027, 1017, 834, 771, cm^{-1}; HR-MS (ESI) *m/z* calcd for $C_{31}H_{33}NAuCl_3NNa$ [M+Na^+] 744.1237, found 744.1232. Elem. Anal. Calcd. For: $C_{31}H_{33}AuCl_3N$: C, 51.50; H, 4.60; N, 1.94, found: C, 51.86; H, 4.62; N, 1.98.

$LcAuCl_3$ (1c)

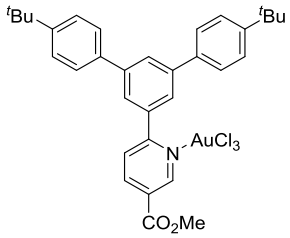

This compound was synthesized by following general procedure **C** using **Lc** (250 mg, 0.57 mmol) in acetonitrile (10 ml), sodium tetrachloroaurate dehydrate (227 mg, 0.57 mmol) in water (15 ml) to furnish the product as orange solid (228 mg, 70%); m.p. 213-215 °C; ^{1}H NMR (400 MHz, CD_2Cl_2): δ 9.48 (d, *J* = 1.8 Hz, 1H), 8.77 (dd, *J* = 8.2, 1.8 Hz, 1H), 8.13 (t, *J* = 1.6 Hz, 1H), 8.07 – 8.04 (m, 1H), 8.05 (d, *J* = 1.6 Hz, 2H), 7.73 (d, *J* = 8.6 Hz, 4H), 7.56 (d, *J* = 8.5 Hz, 4H), 4.07 (s, 3H), 1.38 (s, 18H); ^{13}C NMR (101 MHz, CD_2Cl_2): δ 163.70, 162.93, 152.20, 151.89, 143.66, 143.10, 138.28, 137.11, 129.92, 129.87, 129.41, 127.55, 126.68, 126.56, 54.11, 35.12, 31.61; IR (film) ν (cm^{-1}) 1739, 1594, 1438, 1300, 1128, 836, 773, 558, 528, 508 cm^{-1}; HR-MS (ESI) *m/z* calcd for $C_{33}H_{35}AuCl_3NNaO_2$ [M+Na^+] 802.1291, found 802.1285. Elem. Anal. Calcd. For $C_{33}H_{35}AuCl_3NO_2$: C, 50.75; H, 4.52; N, 1.79, found: C, 50.67; H, 4.44; N, 1.74.

$LdAuCl_3$ (1d)

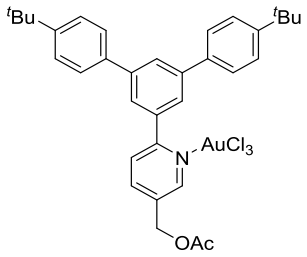

This compound was synthesized by following general procedure **C** using **Ld** (130 mg, 0.26 mmol) in acetonitrile (7 ml), sodium tetrachloroaurate dehydrate (105 mg, 0.26 mmol) in water (10 ml) to furnish the product as yellow solid (167 mg, 80%); m.p. 210-212 °C; ^{1}H NMR (400 MHz, CD_2Cl_2): δ 8.89 (s, 1H), 8.23 – 8.17 (m, 1H), 8.11 – 8.09 (m, 1H), 8.03 – 7.99 (m, 2H), 7.94 (d, *J* = 8.1 Hz, 1H), 7.73 (d, *J* = 8.7 Hz, 4H), 7.56 (d, *J* = 8.7 Hz, 4H), 5.30 (s, 2H), 2.19 (s, 3H), 1.38 (s, 18H); ^{13}C NMR (101 MHz, CD_2Cl_2): δ 170.85, 160.29, 152.12, 149.40, 143.51, 142.36, 138.57, 137.31, 136.63, 129.84, 128.90, 127.57, 126.67, 62.44, 35.13, 31.65, 21.13; IR (film) ν (cm^{-1}) 2961, 2901, 1733, 1596, 1499, 1381, 1362, 1232, 1216, 1027, 1015, 832, 821, 559 cm^{-1}; HR-MS (ESI) *m/z* calcd for $C_{34}H_{37}AuCl_3NNaO_2$ [M+Na^+] 816.1448, found 816.1443. Elem. Anal. Calc. for: $C_{34}H_{37}AuCl_3NO_2$: C, 51.37; H, 4.69; N, 1.76, found: C, 51.23; H, 4.70; N, 1.72.

$LeAuCl_3$ (1e)

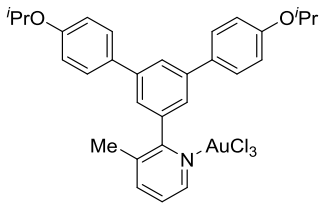

This compound was synthesized by following general procedure **C** using **Le** (200 mg, 0.46 mmol) in acetonitrile (10 ml), sodium tetrachloroaurate dehydrate (181 mg, 0.46 mmol) in water (15 ml) to furnish the product as reddish brown solid (321 mg, 95%); m.p. 181-183 °C; ^{1}H NMR (400 MHz, CD_2Cl_2): δ 8.64 (d, *J* = 5.4 Hz, 1H), 8.06 (d, *J* = 7.8 Hz, 1H), 7.98 (t, *J* = 1.7 Hz, 1H), 7.67 (d, *J* = 8.8 Hz, 4H), 7.69 – 7.64 (m, 3H), 7.00 (d, *J* = 8.8 Hz, 4H), 4.62 (sept, *J* = 6.0 Hz, 2H), 2.39 (s, 3H), 1.36 (d, *J* = 6.1 Hz, 12H); ^{13}C NMR (101 MHz, CD_2Cl_2): δ 159.70, 158.79, 147.58, 144.14, 142.84, 139.83, 137.12, 132.65, 129.01, 127.71, 127.28, 126.66, 116.79, 70.57, 22.37, 20.89; IR (film) ν (cm^{-1}) 2975, 1607, 1508, 1470, 1384, 1285, 1237, 1183, 1107, 953, 834, 792, 711, 603, 532 cm^{-1}; HR-MS (ESI) *m/z* calcd for $C_{30}H_{31}AuCl_3NNaO_2$ [M+Na^+] 762.0978, found 762.0969. Elem. Anal. Calcd. For: $C_{30}H_{31}AuCl_3NO_2$: C, 48.63; H, 4.22; N, 1.89, found: C, 48.57; H, 4.19; N, 1.91.

LfAuCl$_3$ (1f)

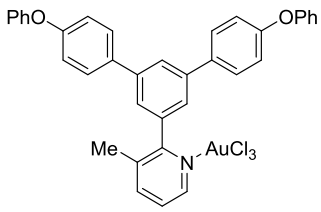

This compound was synthesized by following general procedure **C** using **Lf** (200 mg, 0.39 mmol) in acetonitrile (10 ml), sodium tetrachloroaurate dehydrate (157 mg, 0.39 mmol) in water (15 ml) to furnish the product as orange solid (309 mg, 97%); m.p. 178-180 °C; ^{1}H NMR (400 MHz, CD_2Cl_2): δ 8.66 (d, *J* = 5.3 Hz, 1H), 8.08 (d, *J* = 7.8 Hz, 1H), 8.03 (t, *J* = 1.7 Hz, 1H), 7.74 (d, *J* = 8.8 Hz, 4H), 7.75 - 7.72 (m, 2H), 7.68 (dd, *J* = 7.8, 5.9 Hz, 1H), 7.39 (d, *J* = 7.5 Hz, 2H), 7.37 (d, *J* = 7.5 Hz, 2H), 7.12 (d, *J* = 8.8 Hz, 4H), 7.17 – 7.06 (m, 6H), 2.41 (s, 3H); ^{13}C NMR (101 MHz, CD_2Cl_2): δ 159.41, 158.32, 157.45, 147.67, 144.22, 142.63, 139.82, 137.29, 135.35, 130.44, 129.36, 128.23, 127.42, 127.37, 124.22, 119.80, 119.61, 20.88; IR (film) ν (cm^{-1}) 1588, 1505, 1487, 1446, 1199, 1168, 954, 870, 837, 796, 785, 752, 739, 691, 532 cm^{-1}; HR-MS (ESI) *m/z* calcd for $C_{36}H_{27}AuCl_3NNaO_2$ [M+Na$^+$] 830.0665, found 830.0665. Elem. Anal. Calcd. For: $C_{36}H_{27}AuCl_3NO_2 \cdot CH_2Cl_2$: C, 49.72; H, 3.27; N, 1.57, found: C, 49.42; H, 4.24; N, 1.50.

LgAuCl$_3$ (1g)

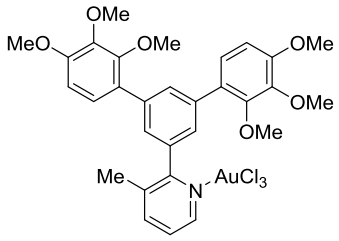

This compound was synthesized by following general procedure **C** using **Lg** (50 mg, 0.09 mmol) in acetonitrile (2.5 ml), sodium tetrachloroaurate dehydrate (39 mg, 0.09 mmol) in water (5 ml) to furnish the product as dark brown solid (73 mg, 92%); m.p. 103-105 °C; ^{1}H NMR (400 MHz, CD_2Cl_2): δ 8.63 (d, *J* = 5.4 Hz, 1H), 8.06 (d, *J* = 7.8 Hz, 1H), 7.98 (t, *J* = 1.6 Hz, 1H), 7.65 (dd, *J* = 7.8, 5.9 Hz, 2H), 7.64 (d, *J* = 1.6 Hz, 1H), 7.22 (d, *J* = 8.6 Hz, 2H), 6.81 (d, *J* = 8.7 Hz, 2H), 3.90 (s, 6H), 3.89 (s, 6H), 3.72 (s, 6H), 2.43 (s, 3H); ^{13}C NMR (101 MHz, CD_2Cl_2): δ 159.78, 154.41, 152.11, 147.61, 144.08, 143.24, 139.91, 139.60, 136.06, 133.12, 129.10, 127.85, 127.14, 125.55, 108.46, 61.76, 61.38, 56.54, 20.95; IR (film) ν (cm^{-1}) 2932, 1594, 1493, 1462, 1424, 1397, 1291, 1232, 1209, 1119, 1088, 1029, 1008, 798 cm^{-1}; HR-MS (ESI) *m/z* calcd for $C_{30}H_{31}AuCl_3NNaO_6$ [M+Na$^+$] 826.0766, found 826.0774. Elem. Anal. Calcd. For: $C_{30}H_{31}AuCl_3NO_6$: C, 44.77; H, 3.88; N, 1.74, found: C, 44.87; H, 3.88; N, 2.07.

LhAuCl$_3$ (1h)

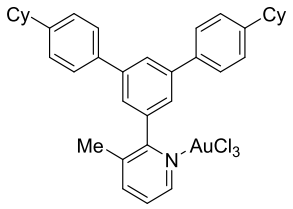

This compound was synthesized by following general procedure **C** using **Lh** (170 mg, 0.35 mmol) in acetonitrile:ethyl acetate (5:5 ml), sodium tetrachloroaurate dehydrate (139 mg, 0.35 mmol) in water (10 ml) to furnish the product as yellow solid (264 mg, 96%); m.p. 105-107 °C (decomposition); ^{1}H NMR (400 MHz, CD_2Cl_2) δ 8.60 (ddd, *J* = 5.9, 1.3, 0.6 Hz, 1H), 8.07 – 8.01 (m, 2H), 7.73 (d, *J* = 1.7 Hz, 2H), 7.69 (d, *J* = 8.4 Hz, 4H), 7.64 (dd, *J* = 7.8, 6.0 Hz, 1H), 7.36 (d, *J* = 8.1 Hz, 4H), 2.61-2.58 (m, 2H), 2.37 (s, 3H), 1.95 – 1.83 (m, 8H), 1.79 – 1.75 (m, 2H), 1.54 – 1.38 (m, 8H), 1.35 – 1.24 (m, 2H); ^{13}C NMR (101 MHz, CD_2Cl_2): δ 159.43, 148.92, 147.58, 144.21, 143.06, 139.75, 137.89, 137.16, 128.32, 128.10, 127.77, 127.38, 127.35, 44.83, 35.01, 34.98, 27.44, 26.70, 20.82; IR (film) ν (cm^{-1}) 2921, 2849, 1593, 1513, 1447, 1134, 999, 826, 788, 551 cm^{-1}; HR-MS (ESI) *m/z* calcd for $C_{36}H_{39}AuCl_3NNa$ [M+Na$^+$] 810.1706, found 810.1696. Elem. Anal. Calcd. For: $C_{36}H_{39}AuCl_3N$: C, 54.80; H, 4.98; N, 1.78, found: C, 54.57; H, 4.96; N, 1.67.

LiAuCl$_3$ (1i)

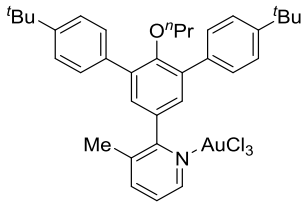

This compound was synthesized by following general procedure **C** using **Li** (140 mg, 0.28 mmol) in acetonitrile:ethyl acetate (5:5 ml), sodium tetrachloroaurate dehydrate (113 mg, 0.28 mmol) in water (10 ml) to furnish the product as yellow to brown solid (213mg, 94%); m.p. 175-177 °C; ^{1}H NMR (400 MHz, CD_2Cl_2) δ 8.62 (dd, *J* = 5.9, 0.6 Hz, 1H), 8.02 (ddd, *J* = 7.8, 1.3, 0.7 Hz, 1H), 7.70 – 7.62 (m, 5H), 7.53 (s, 2H), 7.49 (d, *J* = 8.6 Hz, 4H), 3.26 (t, *J* = 6.4 Hz, 2H), 2.40 (s, 3H), 1.37 (s, 18H), 1.25 – 1.20 (m, 2H), 0.53 (t, *J* = 7.4 Hz, 3H); ^{13}C NMR (101 MHz, CD_2Cl_2): δ 156.90, 151.25, 147.54, 144.01, 139.78, 137.48, 135.39, 131.81, 131.78, 129.83, 127.14, 125.68, 75.51, 35.06, 31.66, 23.45, 20.85, 10.61; IR (film) ν (cm^{-1}) 2961, 1474, 1461, 1442, 1381, 1268, 1239, 1225, 1133, 1103, 949, 837, 799, 662, 568 cm^{-1}; HR-MS (ESI) *m/z* calcd for $C_{35}H_{41}AuCl_3NNaO$ [M+Na$^+$] 816.1812, found 816.1813. Elem. Anal. Calcd. For: $C_{35}H_{41}AuCl_3NO$: C, 52.88; H, 5.20; N, 1.76, found: C, 53.06; H, 5.50; N, 1.65.

$LiAuCl_3$ (1j)

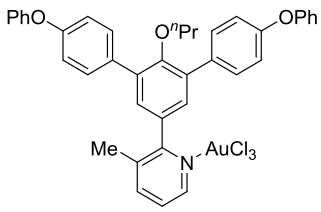

This compound was synthesized by following general procedure **C** using **Lj** (100 mg, 0.177 mmol) in EtOAc:MeCN (2.5:2.5 ml), sodium tetrachloroaurate dehydrate (70 mg, 0.177 mmol) in water (5 ml) to furnish the product as yellow to brown solid (150 mg, 98 %); m.p. 150-152 °C; ^{1}H NMR (400 MHz, CD_2Cl_2) δ 8.61 (d, *J* = 5.9 Hz, 1H), 8.04 (d, *J* = 7.8 Hz, 1H), 7.76 – 7.71 (m, 4H), 7.65 (dd, *J* = 7.8, 6.0 Hz, 1H), 7.54 (s, 2H), 7.40 – 7.34 (m, 4H), 7.16 – 7.04 (m, 10H), 3.32 (t, *J* = 6.4 Hz, 2H), 2.41 (s, 3H), 1.35 – 1.23 (m, 2H), 0.63 (t, *J* = 7.4 Hz, 3H); ^{13}C NMR (101 MHz, CD_2Cl_2) δ 159.30, 157.67, 157.59, 156.76, 147.57, 144.05, 139.81, 137.03, 133.23, 131.94, 131.87, 131.75, 130.38, 127.26, 124.02, 119.58, 118.99, 75.62, 23.60, 20.84, 10.79; IR (film) ν (cm^{-1}) 1587, 1505, 1486, 1230, 1168, 955, 870, 837, 739, 691 cm^{-1}; HR-MS (ESI) *m/z* calcd for $C_{39}H_{33}AuCl_3NNaO_3$ [M+Na$^+$] 888.1084, found 888.1077. Elem. Anal. Calcd. For: $C_{39}H_{33}AuCl_3NO_3$: C, 54.03; H, 3.84; N, 1.62, found: C, 53.63; H, 4.98; N, 1.63.

LaN^C^CAuCl (2a)

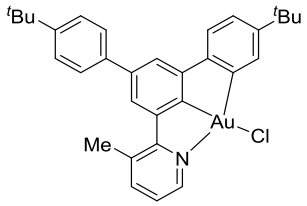

This compound was synthesized by following general procedure **D** using **1a** (200 mg, 0.271 mmol) in acetonitrile:water (6:6 ml) to obtained the product as light yellow solid (129 mg, 72%); m.p. > 350 °C; ^{1}H NMR (500 MHz, CD_2Cl_2): δ 8.84 (d, *J* = 5.0 Hz, 1H), 7.78 (s, 1H), 7.68 (s, 1H), 7.59 (d, *J* = 8.2 Hz, 2H), 7.55 (d, *J* = 7.7 Hz, 1H), 7.52 (d, *J* = 8.2 Hz, 2H), 7.29 (s, 1H), 7.21 – 7.16 (m, 3H), 2.65 (s, 3H), 1.40 (s, 9H), 1.33 (s, 9H); ^{13}C NMR (126 MHz, CD_2Cl_2): δ 165.60, 161.51, 151.73, 151.42, 151.34, 151.26, 150.21, 147.26, 145.12, 142.35, 141.64, 138.91, 134.74, 132.07, 127.49, 126.38, 125.54, 125.12, 124.33, 122.05, 121.81, 35.58, 35.07, 31.70, 31.67, 22.84; IR (film) ν (cm^{-1}) 2958, 2902, 2866, 1589, 1515, 1475, 1460, 1445, 1425, 1388, 1361, 1267, 1250, 1126, 1113, 1006, 868, 824, 783, 765, 757, 550 cm^{-1}; HR-MS (ESI) *m/z* calcd for $C_{32}H_{33}AuClNNa$ [M+Na$^+$] 686.1856, found 686.1859. Elem. Anal. Calcd. For: $C_{32}H_{33}AuClN$: C, 57.88; H, 5.01; N, 2.11, found: C, 57.63; H, 4.98; N, 2.08.

LbN^C^CAuCl (2b)

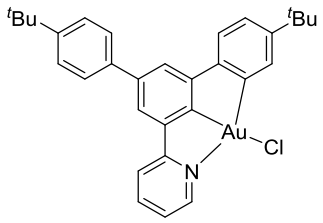

This compound was synthesized by following general procedure **D** using **1b** (200 mg, 0.27 mmol) in acetonitrile:water (6:6 ml) to obtained the product as pale yellow solid (102 mg, 57%); m.p. 269-271 °C; ^{1}H NMR (400 MHz, CD_2Cl_2): δ 8.62 – 8.58 (m, 1H), 7.69 (td, *J* = 7.7, 1.7 Hz, 1H), 7.55 (d, *J* = 2.0 Hz, 1H), 7.54 – 7.45 (m, 5H), 7.15 – 7.04 (m, 4H), 7.00 (d, *J* = 8.0 Hz, 1H), 1.41 (s, 9H), 1.27 (s, 9H); ^{13}C NMR (101 MHz, CD_2Cl_2): δ 165.81, 163.30, 151.39, 151.25, 151.21, 150.97, 149.82, 148.89, 141.62, 141.17, 140.21, 138.36, 131.85, 127.41, 126.25, 125.02, 124.70, 122.39, 122.12, 121.05, 120.83, 35.48, 35.05, 31.74, 31.67; IR (film) ν (cm^{-1}) 2959, 1606, 1589, 1477, 1292, 1265, 1158, 1113, 1018, 1005, 825, 775, 735, 702, 650, 550 cm^{-1}; HR-MS (ESI) *m/z* calcd for $C_{31}H_{31}AuClNNa$ [M+Na^+] 672.1703, found 672.1698. Elem. Anal. Calcd. For: $C_{31}H_{31}AuClN$: C, 57.28; H, 4.81; N, 2.15, found: C, 57.08; H, 4.68; N, 2.03.

LcN^C^CAuCl (2c)

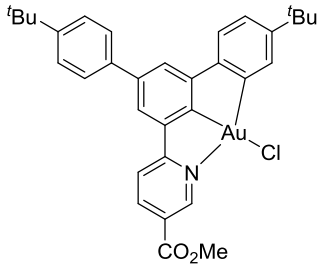

This compound was synthesized by following general procedure **D** using **1c** (50 mg, 0.064 mmol) in acetonitrile:water (4:4 ml) to obtained the product as dark yellow solid (20 mg, 44%); m.p. 339-341 °C; ^{1}H NMR (400 MHz, CD_2Cl_2): δ 8.88 (dd, *J* = 2.0, 0.5 Hz, 1H), 8.09 (dd, *J* = 8.3, 2.0 Hz, 1H), 7.59 (d, *J* = 8.6 Hz, 2H), 7.59 (d, *J* = 8.6 Hz, 2H), 7.50 (d, *J* = 8.5 Hz, 2H), 7.49 – 7.45 (m, 2H), 7.19 (d, *J* = 1.5 Hz, 1H), 7.04 (dd, *J* = 8.0, 2.0 Hz, 1H), 7.01 (d, *J* = 1.5 Hz, 1H), 6.91 (d, *J* = 8.0 Hz, 1H), 3.71 (s, 3H), 1.41 (s, 9H), 1.24 (s, 9H); ^{13}C NMR (101 MHz, CD_2Cl_2): δ 166.53, 166.26, 164.00, 151.90, 151.37, 150.83, 150.71, 149.75, 149.65, 142.12, 141.77, 139.20, 138.15, 131.95, 127.63, 126.73, 126.30, 124.85, 123.38, 122.60, 122.24, 120.57, 53.02, 35.52, 35.09, 31.74, 31.56; IR (film) ν (cm^{-1}) 2952, 1732, 1609, 1435, 1289, 1269, 1125, 1115, 835, 823, 776, 730, 551 cm^{-1}; HR-MS (ESI) *m/z* calcd for $C_{33}H_{33}AuClNNaO_2$ [M+Na^+] 730.1758, found 730.1751. Elem. Anal. Calcd. For: $C_{33}H_{33}AuClNO_2$: C, 55.98; H, 4.70; N, 1.98, found: C, 55.53; H, 4.78; N, 1.80.

LdN^C^CAuCl (2d)

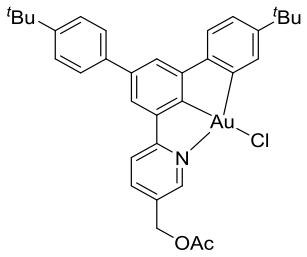

This compound was synthesized by following general procedure **D** using **1d** (100 mg, 0.12 mmol) in acetonitrile:water (4:4 ml) to obtained the product as yellow solid (45 mg, 51%); m.p. 280-282° C; ^{1}H NMR (400 MHz, CD_2Cl_2): δ 8.73 – 8.70 (m, 1H), 7.74 (dd, *J* = 8.2, 2.1 Hz, 1H), 7.65 (d, *J* = 1.9 Hz, 1H), 7.61 – 7.57 (m, 3H), 7.51 (d, *J* = 8.6 Hz, 2H), 7.25 (d, *J* = 1.5 Hz, 1H), 7.18 – 7.14 (m, 2H), 7.09 (d, *J* = 8.0 Hz, 1H), 4.89 (s, 2H), 2.09 (s, 3H), 1.40 (s, 9H), 1.30 (s, 9H); ^{13}C NMR (101 MHz, CD_2Cl_2): δ 170.82, 165.89, 162.98, 151.81, 151.51, 151.23, 150.94, 149.95, 148.51, 141.93, 140.89, 140.03, 138.31, 133.78, 132.05, 127.46, 126.37, 125.06, 122.52, 122.17, 121.30, 120.70, 63.13, 35.58, 35.09, 31.70, 31.65, 21.14; IR (film) ν (cm^{-1}) 2957, 1736, 1615, 1487, 1360, 1234, 1036, 824, 744, 650, 630, 603, 551, 516, 506 cm^{-1}; HR-MS (ESI) *m/z* calcd for $C_{34}H_{35}AuClNNaO_2$ [M+Na^+] 744.1911, found 744.1914. Elem. Anal. Calcd. For: $C_{34}H_{35}AuClNO_2$: C, 56.55; H, 4.99; N, 1.94, found: C, 56.62; H, 4.86; N, 1.94.

LeN^C^CAuCl (2e)

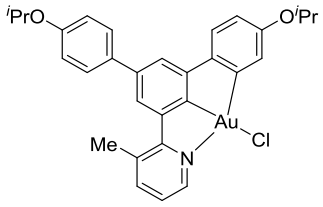

This compound was synthesized by following general procedure **D** using **1e** (200 mg, 0.27 mmol) in acetonitrile:water (6:6 ml) to obtained the product as yellow solid (112 mg, 63%); m.p. 179-181 °C; ^{1}H NMR (400 MHz, CD_2Cl_2): δ 8.44 (dd, *J* = 5.3, 1.5 Hz, 1H), 7.38 (d, *J* = 8.7 Hz, 2H), 7.31 (dd, *J* = 7.7, 0.9 Hz, 1H), 7.26 (d, *J* = 1.3 Hz, 1H), 6.98 (d, *J* = 2.5 Hz, 1H), 6.89 (d, *J* = 8.6 Hz, 4H), 6.80 (d, *J* = 1.4 Hz, 1H), 6.49 (dd, *J* = 8.3, 2.6 Hz, 1H), 4.61 (sept, *J* = 6.0 Hz, 1H), 4.38 (sept, *J* = 6.0 Hz, 1H), 2.43 (s, 3H), 1.39 (d, *J* = 6.0 Hz, 6H), 1.29 (d, *J* = 6.1 Hz, 6H); ^{13}C NMR (101 MHz, CD_2Cl_2): δ 163.93, 161.14, 158.19, 156.83, 152.27, 149.46, 146.94, 146.11, 144.78, 141.81, 140.74, 134.58, 133.79, 128.77, 124.33, 123.93, 122.94, 121.94, 120.64, 116.34, 114.76, 70.44, 70.32, 22.80, 22.48; IR (film) ν (cm^{-1}) 2976, 1585, 1511, 1469, 1425, 1382, 1231, 1184, 1107, 955, 829, 791, 766, 631, 530 cm^{-1}; HR-MS (ESI) *m/z* calcd for $C_{30}H_{29}AuClNNaO2$ [M+Na^+] 690.1445, found 690.1437. Elem. Anal. Caldc. For: $C_{30}H_{29}AuClNO_2$: C, 53.94; H, 4.38; N, 2.10, found: C, 54.19; H, 4.45; N, 2.10.

LfN^C^CAuCl (2f)

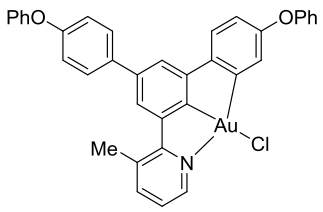

This compound was synthesized by following general procedure **D** using **1f** (100 mg, 0.13 mmol) in acetonitrile:water (4:4 ml) to obtained the product as yellow solid (53 mg, 59%); m.p. 186-188 °C; ^{1}H NMR (400 MHz, CD_2Cl_2): δ 8.54 (dd, *J* = 5.3, 1.5 Hz, 1H), 7.49 (d, *J* = 8.7 Hz, 2H), 7.51 – 7.47 (m, 1H), 7.44 (d, *J* = 1.4 Hz, 1H), 7.40 – 7.33 (m, 4H), 7.20 – 7.10 (m, 3H), 7.09 – 6.96 (m, 9H), 6.65 (dd, *J* = 8.3, 2.6 Hz, 1H), 2.56 (s, 3H); ^{13}C NMR (101 MHz, CD_2Cl_2): δ 164.34, 161.24, 157.75, 157.62, 157.56, 155.95, 152.09, 149.27, 149.07, 147.11, 145.21, 142.13, 140.81, 136.39, 134.86, 130.44, 130.33, 129.10, 125.34, 125.21, 124.25, 124.13, 123.92, 123.15, 121.37, 119.70, 119.44, 119.37, 117.75, 22.86; IR (film) ν (cm^{-1}) 1586, 1557, 1509, 1487, 1472, 1424, 1393, 1226, 1214, 1167, 1130, 896, 870, 834, 790, 749, 691 cm^{-1}; HR-MS (ESI) *m/z* calcd for $C_{36}H_{25}AuClNNaO_2$ [M+Na^+] 758.1132, found 758.1127. Elem. Anal. Calcd. For: $C_{36}H_{25}AuClNO_2$: C, 58.75; H, 3.42; N, 2.40, found: C, 58.81; H, 3.28; N, 1.99.

LgN^C^CAuCl (2g)

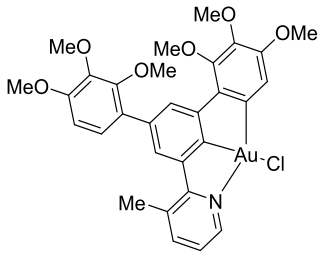

This compound was synthesized by following general procedure **D** using **1g** (100 mg, 0.12 mmol) in acetonitrile:water (4:4 ml) to obtained the product as yellow solid (49 mg, 55%); m.p. 270-272 °C (decomposition); ^{1}H NMR (400 MHz, CD_2Cl_2): δ 9.00 (dd, *J* = 5.3, 1.5 Hz, 1H), 7.81 (d, *J* = 1.5 Hz, 1H), 7.71 (dd, *J* = 7.7, 1.1 Hz, 2H), 7.33 – 7.28 (m, 2H), 7.18 (d, *J* = 8.6 Hz, 1H), 6.80 (d, *J* = 8.7 Hz, 1H), 3.95 (s, 3H), 3.91 (s, 3H), 3.91 (s, 3H), 3.88 (s, 3H), 3.86 (s, 3H), 3.73 (s, 3H), 2.73 (s, 3H); ^{13}C NMR (101 MHz, CD_2Cl_2): δ 163.03, 162.17, 154.12, 152.25, 151.97, 150.73, 149.80, 147.41, 145.32, 145.02, 143.25, 142.81, 141.27, 138.99, 138.90, 134.60, 129.12, 127.62, 126.65, 125.32, 124.22, 114.95, 108.32, 61.54, 61.34, 61.26, 61.04, 56.63, 56.58, 22.90; IR (film) ν (cm^{-1}) 2961, 2934, 1588, 1572, 1556, 1497, 1461, 1397, 1381, 1281, 1260, 1123, 1099, 1090, 1007, 798, 759, 666 cm^{-1}; HR-MS (ESI) *m/z* calcd for $C_{30}H_{29}AuClNNaO_6$ [M+Na^+] 754.1241, found 754.1237. Elem. Anal. Calcd. For: $C_{30}H_{29}AuClNO_6$: C, 49.23; H, 3.99; N, 1.19, found: C, 48.98; H, 3.98; N, 1.81.

LhN^C^CAuCl (2h)

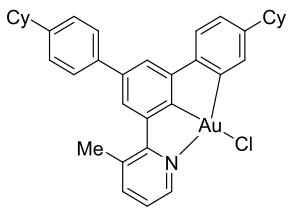

This compound was synthesized by following general procedure **D** using **1h** (100 mg, 0.13 mmol) in acetonitrile:water (6:3 ml) to obtained the product as white solid (42 mg, 47%); m.p. 305-307 °C; ^{1}H NMR (400 MHz, CD_2Cl_2): δ 8.89 (d, *J* = 5.4 Hz, 1H), 7.69 (s, 1H), 7.64 – 7.54 (m, 4H), 7.36 – 7.30 (m, 3H), 7.25 – 7.16 (m, 2H), 7.01 (dd, *J* = 7.8, 1.7 Hz, 1H), 2.68 (s, 3H), 2.64 – 2.57 (m, 1H), 2.53 – 2.42 (m, *J* = 13.2, 6.0 Hz, 1H), 1.96 – 1.74 (m, 9H), 1.53 – 1.40 (m, 9H), 1.38 – 1.26 (m, 2H); IR (film) ν (cm^{-1}) 2923, 2849, 1588, 1394, 1129, 829, 794, 766, 674, 541 cm^{-1}; ^{13}C NMR (101 MHz, CD_2Cl_2): could not get a good spectra due to poor solubility. HR-MS (ESI) *m/z* calcd for $C_{36}H_{37}AuClNNa$ [M+Na^+] 738.2172, found 738.2172. Elem. Anal. Calcd. For: $C_{36}H_{37}AuClN$. 1/2 H_2O: C, 59.63; H, 5.28; N, 1.93, found: C, 59.53; H, 5.09; N, 1.72.

LiN^C^CAuCl (2i)

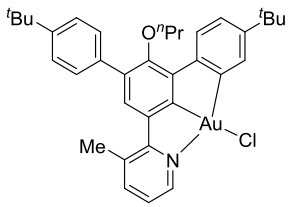

This compound was synthesized by following general procedure **D** using **1i** (100 mg, 0.12 mmol) in acetonitrile:water (4:4 ml) to obtained the product as white solid (36 mg, 40%); m.p. > 350°C; ^{1}H NMR (400 MHz, CD_2Cl_2): δ 8.97 (dd, *J* = 5.3, 1.6 Hz, 1H), 7.89 (d, *J* = 2.1 Hz, 1H), 7.74 (d, *J* = 8.2 Hz, 1H), 7.68 – 7.63 (m, 1H), 7.64 (s, 1H), 7.55 (d, *J* = 8.6 Hz, 2H), 7.48 (d, *J* = 8.6 Hz, 2H), 7.28 (dd, *J* = 7.7, 5.4 Hz, 1H), 7.20 (dd, *J* = 8.2, 2.1 Hz, 1H), 3.44 (t, *J* = 6.5 Hz, 2H), 2.67 (s, 3H), 1.60 – 1.50 (m, 2H), 1.39 (s, 9H), 1.34 (s, 9H), 0.76 (t, *J* = 7.4 Hz, 3H); ^{13}C NMR (101 MHz, CD_2Cl_2): δ 165.78, 161.53, 153.81, 151.44, 151.42, 151.11, 149.94, 147.10, 145.28, 142.58, 137.96, 136.49, 136.27, 134.03, 131.94, 129.57, 129.14, 126.46, 125.77, 125.27, 123.89, 74.77, 35.53, 35.08, 31.71, 31.63, 23.76, 22.74, 10.78; IR (film) ν (cm^{-1}) 2964, 2924, 2901, 2884, 2874, 1588, 1458, 1420, 1382, 1255, 1220, 1124, 1063, 1046, 1042, 1038, 1006, 971, 841, 831, 779, 758, 659, 649, 437 cm^{-1}; HR-MS (ESI) *m/z* calcd for $C_{35}H_{39}AuClNNaO$ [M+Na^+] 744.2278, found 744.2267. Elem. Anal. Calcd. For: $C_{35}H_{39}AuClNO$: C, 58.22; H, 5.44; N, 1.94, found: C, 57.95; H, 5.54; N, 1.76.

LjN^C^CAuCl (2j)

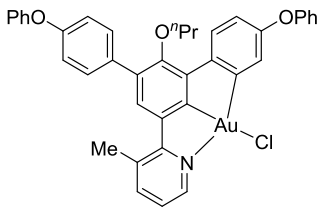

This compound was synthesized by following general procedure **D** using **1j** (100 mg, 0.12 mmol) in acetonitrile:water (4:4 ml) to obtained the product as white solid (36 mg, 40%); m.p. > 350°C; ^{1}H NMR (400 MHz, CD_2Cl_2) δ 8.71 (dd, *J* = 5.4, 1.6 Hz, 1H), 7.71 (d, *J* = 8.5 Hz, 1H), 7.61 – 7.55 (m, 3H), 7.48 (s, 1H), 7.41 – 7.33 (m, 5H), 7.19 – 7.12 (m, 3H), 7.09 – 7.04 (m, 4H), 7.02 – 6.98 (m, 2H), 6.70 (dd, *J* = 8.5, 2.7 Hz, 1H), 3.43 (t, *J* = 6.6 Hz, 2H), 2.60 (s, 3H), 1.63 – 1.48 (m, 2H), 0.80 (t, *J* = 7.4 Hz, 3H); ^{13}C NMR (101 MHz, CD_2Cl_2) δ 164.54, 161.32, 157.83, 157.74, 157.32, 155.50, 153.16, 150.87, 149.21, 147.00, 145.49, 141.73, 137.99, 135.77, 134.32, 134.15, 131.45, 130.39, 130.33, 129.11, 127.62, 125.18, 123.97, 123.87, 119.47, 119.41, 119.15, 117.94, 74.66, 23.81, 22.78, 10.87; IR (film) ν (cm^{-1}) 2987, 2901, 2892, 1587, 1487, 1378, 1253, 1232, 1073, 1056, 898, 798, 744 cm^{-1}; HR-MS (ESI) *m/z* calcd for $C_{39}H_{31}AuClNNaO_3$ [M+Na$^+$] 816.1550, found 816.1538. Elem. Anal. Calcd. For: $C_{39}H_{31}AuClNO_3$: C, 58.99; H, 3.93; N, 1.76, found: C, 58.71; H, 3.88; N, 1.93.

LaN^C^CAuF (3a)

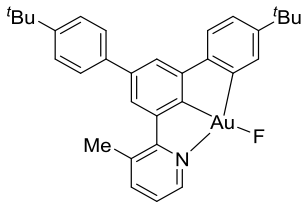

This compound was synthesized by following general procedure **D** in a scintillation vial using **2a** (100 mg, 0.15 mmol), silver fluoride (114 mg, 0.90 mmol) in dry CH_2Cl_2 (4 ml). A yellowish-white solid was isolated in a quantitative yield; m.p. >200 °C (decomposition); ^{1}H NMR (500 MHz, CD_2Cl_2): δ 8.47 (d, *J* = 4.2 Hz, 1H), 7.64 – 7.57 (m, 2H), 7.59 (d, *J* = 8.0 Hz, 2H), 7.52 (d, *J* = 8.0 Hz, 2H), 7.44 (s, 1H), 7.28 –7.23 (m, 2H), 7.20 (d, *J* = 7.9 Hz, 1H), 7.16 (d, *J* = 7.9 Hz, 1H), 2.62 (s, 3H), 1.40 (s, 9H), 1.34 (s, 9H); ^{13}C NMR (126 MHz, CD_2Cl_2): δ 160.53, 151.51, 151.32, 151.19, 150.68, 149.44, 145.67, 145.15, 142.11, 141.83, 139.04, 134.82, 129.11, 127.57, 126.40, 125.26, 125.19, 123.97, 121.97, 121.60, 35.53, 35.08, 31.72, 22.60; ^{19}F NMR (471 MHz, CD_2Cl_2): δ -227.51; IR (film) ν (cm^{-1}) 2951, 2902, 2865, 1589, 1475, 1460, 1426, 1390, 1362, 1250, 1127, 823, 783, 767, 659, 461, 454 cm^{-1}; Elem. Anal. Calcd. For: $C_{32}H_{33}AuFN \cdot 1/2\ H_2O$: C, 58.54; H, 5.22; N, 2.13, found: C, 58.56; H, 5.06; N, 2.04.

LbN^C^CAuF (3b)

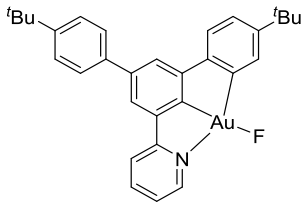

This compound was synthesized by following general procedure **D** using **2b** (60 mg, 0.09 mmol), silver fluoride (70 mg, 0.55 mmol) in dry CH_2Cl_2 (3 ml). A yellowish-white solid was isolated in a quantitative yield; m.p. >200 °C (decomposition); ^{1}H NMR (400 MHz, CD_2Cl_2): δ 8.81 (d, *J* = 4.9 Hz, 1H), 7.85 (td, *J* = 7.8, 1.4 Hz, 1H), 7.69 (d, *J* = 8.2 Hz, 2H), 7.55 (d, *J* = 8.4 Hz, 2H), 7.50 (d, *J* = 8.4 Hz, 2H), 7.33 – 7.24 (m, 3H), 7.17 (dd, *J* = 8.0, 1.7 Hz, 1H), 7.14 (d, *J* = 7.9 Hz, 1H), 1.40 (s, 9H), 1.31 (s, 9H); ^{13}C NMR (101 MHz, CD_2Cl_2): δ 165.84, 163.60, 151.78, 151.43, 151.37, 150.94, 150.21, 149.16, 142.04, 141.49, 140.44, 138.44, 132.04, 127.42, 126.37, 125.21, 124.97, 122.52, 122.28, 121.02, 120.86, 35.58, 35.08, 31.72, 31.67; ^{19}F NMR (376 MHz, CD_2Cl_2): δ -230.15; IR (film) ν (cm^{-1}) 2952, 1589, 1475, 1461, 1426, 1390, 1268, 1250, 1127, 1006, 823, 783, 767, 659, 552, 465 cm^{-1}. HR-MS (EI) *m/z* calcd for $C_{31}H_{31}AuFN$ [M^+] 633.2100, found 633.2096. Elem. Anal. Calcd. For: $C_{31}H_{31}AuFN$: C, 58.77; H, 4.93; N, 2.21; **F, 3.00**, found: C, 58.35; H, 4.90; N, 2.34: **F, 2.69**.

LcN^C^CAuF (3c)

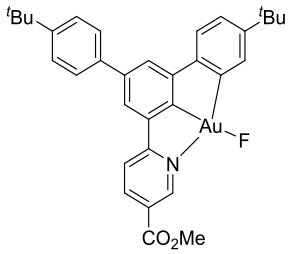

This compound was synthesized by following general procedure **D** using **2c** (15 mg, 0.02 mmol), silver fluoride (16 mg, 0.13 mmol) in dry CH_2Cl_2 (1.5 ml). A yellow solid was isolated in a quantitative yield; m.p. >200 °C (decomposition); ^{1}H NMR (400 MHz, CD_2Cl_2): δ 8.75 (s, 1H), 8.23 – 8.15 (m, 1H), 7.63 – 7.56 (m, 3H), 7.49 (d, *J* = 8.3 Hz, 2H), 7.26 (s, 1H), 7.22 (s, 1H), 7.11 – 7.03 (m, 2H), 6.96 (d, *J* = 7.9 Hz, 1H), 3.83 (s, 3H), 1.40 (s, 9H), 1.26 (s, 9H); ^{13}C NMR (101 MHz, CD_2Cl_2): δ 165.28, 164.03, 151.90, 151.47, 150.49, 150.41, 149.05, 148.70, 142.60, 142.03, 139.17, 138.22, 129.07, 127.62, 126.96, 126.44, 126.39, 125.20, 123.15, 122.24, 121.91, 120.52, 53.18, 35.51, 35.10, 31.74, 31.59; ^{19}F NMR (376 MHz, CD_2Cl_2): δ -231.05; IR (film) ν (cm^{-1}) 2954, 1729, 1609, 1480, 1461, 1434, 1381, 1361, 1289, 1269, 1116, 1035, 822, 777, 732, 551cm^{-1}; Elem. Anal. Calcd. For: $C_{33}H_{33}AuFNO_2 \cdot 1/2\ H_2O$: C, 56.57; H, 4.89; N, 2.00, found: C, 56.38; H, 4.88; N, 1.83.

LdN^C^CAuF (3d)

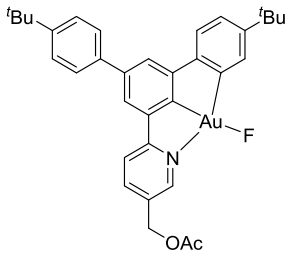

This compound was synthesized by following general procedure **D** using **2d** (15 mg, 0.02 mmol), silver fluoride (16 mg, 0.12 mmol) in dry CH_2Cl_2 (1.5 ml). A yellow solid was isolated in a quantitative yield; m.p. >200 °C (decomposition); ^{1}H NMR (400 MHz, CD_2Cl_2): δ 8.55 (d, *J* = 1.5 Hz, 1H), 7.87 (dd, *J* = 8.3, 2.0 Hz, 1H), 7.71 (d, *J* = 8.2 Hz, 1H), 7.63 (d, *J* = 8.4 Hz, 2H), 7.53 (d, *J* = 8.4 Hz, 2H), 7.42 (d, *J* = 1.8 Hz, 1H), 7.31 (d, *J* = 1.4 Hz, 1H), 7.22 (d, *J* = 1.4 Hz, 1H), 7.20 (dd, *J* = 8.0, 1.9 Hz, 1H), 7.15 (d, *J* = 8.0 Hz, 1H), 4.99 (s, 2H), 2.12 (s, 3H), 1.39 (s, 9H), 1.32 (s, 9H); ^{13}C NMR (101 MHz, CD_2Cl_2): δ 170.84, 162.07, 151.74, 151.53, 150.96, 150.66, 147.68, 142.37, 141.28, 139.90, 138.54, 133.80, 129.14, 127.56, 126.43, 125.33, 122.47, 122.18, 120.93, 120.62, 63.12, 35.54, 35.09, 31.69, 31.65, 21.16; ^{19}F NMR (376 MHz, CD_2Cl_2): δ -231.03; IR (film) ν (cm^{-1}) 2957, 2903, 2866, 1743, 1613, 1590, 1486, 1478, 1458, 1446, 1373, 1361, 1270, 1247, 1214, 1047, 1035, 855, 826, 552, 489 cm^{-1}; Elem. Anal. Calcd. For: $C_{34}H_{35}AuFNO_2$: C, 57.87; H, 5.00; N, 1.98, found: C, 57.65; H, 4.92; N, 1.91.

LeN^C^CAuF (3e)

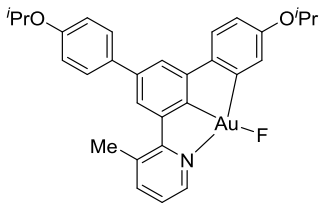

This compound was synthesized by following general procedure **D** using **2e** (20 mg, 0.03 mmol), silver fluoride (22 mg, 0.17 mmol) in dry CH_2Cl_2 (2 ml). A yellow solid was isolated in a quantitative yield; m.p. >200 °C (decomposition); ^{1}H NMR (400 MHz, CD_2Cl_2): δ 8.32 (d, *J* = 4.4 Hz, 1H), 7.52 (d, *J* = 7.5 Hz, 1H), 7.46 (d, *J* = 8.6 Hz, 2H), 7.38 (s, 1H), 7.15 (dd, *J* = 7.6, 5.3 Hz, 1H), 7.03 (d, *J* = 8.3 Hz, 1H), 6.97 – 6.92 (m, 3H), 6.83 (d, *J* = 2.1 Hz, 1H), 6.59 (dd, *J* = 8.3, 2.5 Hz, 1H), 4.62 (sept, *J* = 6.0 Hz, 1H), 4.50 (sept, *J* = 6.0 Hz, 1H), 2.54 (s, 3H), 1.38 (d, *J* = 6.0 Hz, 6H), 1.32 (d, *J* = 6.0 Hz, 6H); ^{13}C NMR (101 MHz, CD_2Cl_2): δ 160.48, 158.33, 157.04, 150.80, 150.37, 145.95, 145.55, 145.06, 141.85, 141.41, 134.74, 134.06, 128.91, 124.01, 123.79, 123.08, 120.62, 119.04, 116.54, 115.66, 70.59, 70.53, 22.59, 22.52, 22.46; ^{19}F NMR (376 MHz, CD_2Cl_2): δ -226.93; IR (film) ν (cm^{-1}) 2974, 1606, 1587, 1556, 1511, 1470, 1426, 1396, 1382, 1372, 1233, 1185, 1107, 954, 864, 830, 795, 766, 631, 532, 473, 464 cm^{-1}. Elem. Anal. Calcd. For: $C_{30}H_{29}AuFNO_2$: C, 55.31; H, 4.49; N, 2.15, found: C, 55.31; H, 4.46; N, 2.11.

LfN^C^CAuF (3f)

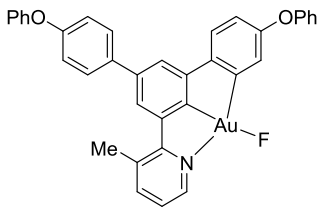

This compound was synthesized by following general procedure **D** using **2f** (20 mg, 0.03 mmol), silver fluoride (20 mg, 0.16 mmol) in dry CH_2Cl_2 (2 ml). A yellow solid was isolated in a quantitative yield; m.p. >200 °C (decomposition); ^{1}H NMR (400 MHz, CD_2Cl_2): δ 8.21 (d, *J* = 4.7 Hz, 1H), 7.54 (d, *J* = 7.3 Hz, 1H), 7.50 (d, *J* = 8.4 Hz, 2H), 7.43 – 7.32 (m, 5H), 7.19 – 7.11 (m, 3H), 7.10 – 6.97 (m, 8H), 6.88 (s, 1H), 6.71 (dd, *J* = 8.2, 2.4 Hz, 1H), 2.53 (s, 3H); ^{13}C NMR (101 MHz, CD_2Cl_2): δ 160.28, 157.77, 157.63, 157.59, 156.08, 150.74, 149.88, 148.71, 145.52, 145.27, 141.98, 141.12, 136.55, 134.96, 130.44, 130.39, 129.18, 124.78, 124.13, 124.03, 123.97, 123.15, 122.28, 121.12, 119.68, 119.60, 119.44, 118.11, 22.56; ^{19}F NMR (376 MHz, CD_2Cl_2): δ -226.98; IR (film) ν (cm^{-1}) 1585, 1486, 1471, 1426, 1224, 1180, 1168, 870, 828, 786, 764, 748, 691, 475 cm^{-1}.

LgN^C^CAuF (3g)

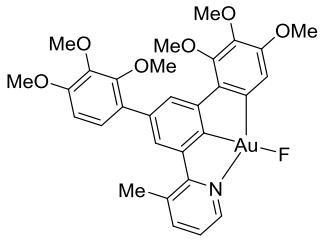

This compound was synthesized by following general procedure **D** using **2g** (35 mg, 0.04 mmol), silver fluoride (37 mg, 0.25 mmol) in dry CH_2Cl_2 (2 ml). A yellow solid was isolated in a quantitative yield; m.p. >200 °C (decomposition); ^{1}H NMR (500 MHz, CD_2Cl_2): δ 8.61 (s, 1H), 7.73 (s, 1H), 7.70 (s, 1H), 7.62 (s, 1H), 7.37 (s, 1H), 7.13 (d, *J* = 6.2 Hz, 1H), 6.93 (s, 1H), 6.76 (d, *J* = 5.8 Hz, 1H), 3.93 (s, 3H), 3.90 (s, 9H), 3.85 (s, 3H), 3.72 (s, 3H), 2.69 (s, 3H); ^{13}C NMR (101 MHz, CD_2Cl_2): δ 161.10, 154.08, 152.29, 151.92, 150.85, 150.05, 145.89, 145.47, 143.68, 143.20, 142.87, 140.97, 138.87, 138.39, 134.72, 129.07, 127.30, 126.19, 125.32, 123.95, 111.77, 108.28, 61.49, 61.31, 61.26, 61.00, 56.78, 56.54, 22.69; ^{19}F NMR (471 MHz, CD_2Cl_2): δ -224.85; IR (film) ν (cm^{-1}) 2962, 2935, 2836, 1589, 1574, 1496, 1462, 1396, 1381, 1303, 1280, 1228, 1124, 1101, 1091, 1055, 1007, 949, 799, 775, 765, 666, 550, 456 cm^{-1}; Elem. Anal. Calcd. For: $C_{30}H_{29}AuFNO_6$: C, 50.36; H, 4.09; N, 1.96, found: C, 50.09; H, 4.18; N, 2.02.

LhN^C^CAuF (3h)

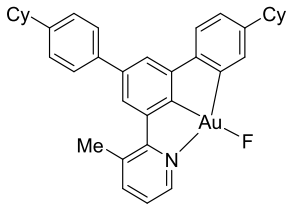

This compound was synthesized by following general procedure **D** using **2h** (10 mg, 0.02 mmol), silver fluoride (14 mg, 0.17 mmol) in dry CH_2Cl_2 (1 ml). A white solid was isolated in a quantitative yield; m.p. >200 °C (decomposition); ^{1}H NMR (400 MHz, CD_2Cl_2): δ 8.53 (d, *J* = 4.5 Hz, 1H), 7.66 (d, *J* = 7.7 Hz, 1H), 7.63 (s, 1H), 7.54 (d, *J* = 7.9 Hz, 2H), 7.35 – 7.27 (m, 5H), 7.20 (d, *J* = 7.9 Hz, 1H), 7.03 (d, *J* = 7.1 Hz, 1H), 2.66 (s, 3H), 2.62 – 2.56 (m, 1H), 2.54 – 2.47 (m, 1H), 1.93 – 1.85 (m, 8H), 1.81 – 1.74 (m, 2H), 1.51 – 1.41 (m, 8H), 1.33 – 1.27 (m, 2H); ^{13}C NMR (101 MHz, CD_2Cl_2): δ 160.56, 151.43, 150.91, 149.54, 148.73, 148.40, 145.79, 145.30, 142.11, 141.98, 139.33, 134.80, 130.81, 127.93, 127.73, 126.79, 124.95, 124.07, 122.32, 121.59, 45.44, 44.87, 35.13, 35.00, 27.52, 26.77, 22.65; ^{19}F NMR (376 MHz, CD_2Cl_2): δ -227.59; IR (film) ν (cm^{-1}) 2921, 2849, 1630, 1588, 1514, 1471, 1446, 1424, 1393, 1127, 1006, 871, 822, 788, 538, 478 cm^{-1}; Elem. Anal. Calcd. For: $C_{36}H_{37}AuFN$: C, 61.80; H, 5.33; N, 2.00, found: C, 61.55; H, 5.30; N, 2.07.

LiN^C^CAuF (3i)

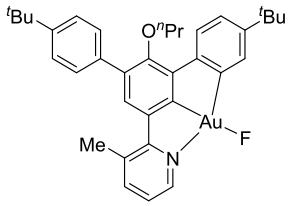

This compound was synthesized by following general procedure **D** using **2i** (15 mg, 0.02 mmol), silver fluoride (27 mg, 0.16 mmol) in dry CH_2Cl_2 (2 ml). A white solid was isolated in a quantitative yield; m.p. >200 °C (decomposition); ^{1}H NMR (400 MHz, CD_2Cl_2): δ 8.63 (d, *J* = 3.8 Hz, 1H), 7.76 (d, *J* = 8.2 Hz, 2H), 7.59 (s, 1H), 7.55 – 7.46 (m, 5H), 7.40 (dd, *J* = 7.6, 5.4 Hz, 1H), 7.23 (dd, *J* = 8.2, 2.0 Hz, 1H), 3.47 (t, *J* = 6.4 Hz, 2H), 2.69 (s, 3H), 1.59 – 1.49 (m, 2H), 1.38 (s, 9H), 1.35 (s, 9H), 0.75 (t, *J* = 7.4 Hz, 3H); ^{13}C NMR (101 MHz, CD_2Cl_2): δ 160.65, 153.67, 151.24, 151.15, 148.14, 145.64, 145.44, 143.12, 137.76, 136.49, 136.30, 134.09, 129.56, 128.80, 128.70, 126.37, 125.79, 125.51, 125.48, 123.65, 74.83, 35.47, 35.09, 31.71, 31.64, 23.77, 22.52, 10.75; ^{19}F NMR (376 MHz, CD_2Cl_2): δ -227.18; IR (film) ν (cm^{-1}) 2962, 2866, 1636, 1588, 1460, 1421, 1380, 1255, 1220, 1124, 1061, 1005, 966, 836, 780, 652, 555, 485, 475 cm^{-1}; Elem. Anal. Calcd. For: $C_{35}H_{39}AuFNO$: C, 59.57; H, 5.57; N, 1.98, found: C, 59.62; H, 5.48; N, 1.94.

LjN^C^CAuF (3j)

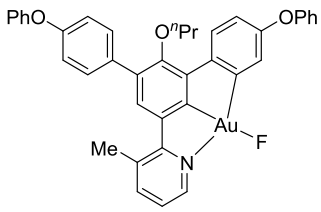

This compound was synthesized by following general procedure **D** using **2j** (20 mg, 0.03 mmol), silver fluoride (19 mg, 0.15 mmol) in dry CH_2Cl_2 (2 ml). A white solid was isolated in a quantitative yield; m.p. >200 °C (decomposition); ^{1}H NMR (400 MHz, CD_2Cl_2) δ 8.38 (s, 1H), 7.66 (d, *J* = 8.5 Hz, 1H), 7.62 (d, *J* = 7.9 Hz, 1H), 7.46 (d, *J* = 8.2 Hz, 2H), 7.38 (s, 1H), 7.31 – 7.28 (m, 2H), 7.27 – 7.22 (m, 3H), 7.09 – 7.02 (m, 2H), 7.00 – 6.93 (m, 7H), 3.38 (t, *J* = 6.2 Hz, 2H), 2.55 (s, 3H), 1.47 (q, *J* = 14.1, 7.2 Hz, 3H), 0.71 (t, *J* = 7.4 Hz, 3H); ^{13}C NMR could not be recorded due to poor solubility of this compound. ^{19}F NMR (376 MHz, CD_2Cl_2) δ -227.04; IR (film) ν (cm^{-1}) 2987, 2901, 2892, 1587, 1487, 1378, 1253, 1232, 1073, 1056, 898, 798, 744 cm^{-1}; Elem. Anal. Calcd. For: $C_{39}H_{31}AuFNO_3 \cdot 1/2\ CH_2Cl_2$: C, 57.85; H, 3.93; N, 1.71, found: C, 58.05; H, 3.90; N, 1.73.

LaN^C^CAuCCOOMe (4a)

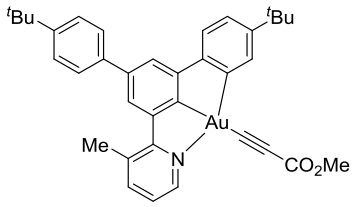

In a J-young tube, a mixture of **3a** (6 mg, 9.20 µmol) and methylpropiolate (1.16 mg, 13.8 µmol) in dichloromethane (1 ml) was stirred at 25 °C for 3 h. Reaction progress was followed by NMR. After completion, the solvent was evaporated and resulted solid was washed with cold pentane to obtained the pure product as a pale brown solid in a quantitative yield or residue could also purified by silica gel chromatography using dichloromethane/hexane as eluent, m.p. >200 °C (decomposition); ^{1}H NMR (400 MHz, CD_2Cl_2): δ 8.80 (d, *J* = 5.1 Hz, 1H), 7.79 (s, 1H), 7.69 (s, 1H), 7.64 (d, *J* = 7.8 Hz, 1H), 7.55 (d, *J* = 8.5 Hz, 2H), 7.49 (d, *J* = 8.5 Hz, 2H), 7.33 (s, 1H), 7.21 – 7.16 (m, 3H), 3.77 (s, 3H), 2.65 (s, 3H), 1.39 (s, 9H), 1.34 (s, 9H); ^{13}C NMR (126 MHz, CD_2Cl_2): δ 172.60, 164.24, 155.47, 153.26, 151.89, 151.81, 151.16, 150.16, 148.19, 145.34, 144.94, 141.33, 139.22, 134.78, 134.39, 133.98, 127.43, 126.33, 125.56, 124.98, 124.73, 122.07, 121.35, 97.84, 52.49, 35.42, 35.05, 31.72, 31.65, 22.88; IR (film) ν (cm^{-1}) 2956, 3131, 1698, 1586, 1476, 1424, 1250, 1215, 1124, 1113, 1007, 863, 830, 811 cm^{-1}; HR-MS (ESI) *m/z* calcd for $C_{36}H_{36}AuNNaO_2$ [M+Na$^+$] 734.2304, found 734.2302. Anal. Calcd. For: $C_{36}H_{36}AuNO_2$: C, 60.76; H, 5.10; N, 1.97, found: C, 60.32; H, 4.98; N, 2.01.

LaN^C^CAuCCPh (5a)

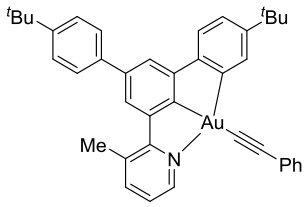

Same procedure like **4a**, **3a** (20 mg, 0.03 mmol), phenyl acetylene (4.6 mg, 0.05 mmol) furnished the compound **5a** as white solid (21 mg, yield 97%), m.p. >200 °C (decomposition); ^{1}H NMR (400 MHz, CD_2Cl_2) δ 8.93 (d, *J* = 4.5 Hz, 1H), 8.02 (s, 1H), 7.73 (s, 1H), 7.60 – 7.48 (m, 5H), 7.39 (d, *J* = 8.4 Hz, 2H), 7.35 – 7.25 (m, 4H), 7.22 – 7.14 (m, 2H), 7.10 (dd, *J* = 7.7, 5.3 Hz, 1H), 2.68 (s, 3H), 1.36 (s, 9H), 1.36 (s, 9H); ^{13}C NMR (126 MHz, CD_2Cl_2) δ 173.83, 164.54, 153.50, 151.89, 151.62, 151.09, 150.07, 148.36, 145.34, 144.68, 141.12, 139.37, 134.60, 132.24, 128.83, 127.43, 126.36, 125.61, 124.86, 124.53, 122.02, 121.21, 35.44, 35.03, 31.74, 31.70, 22.92 (few quaternary carbon are missing due to poor solubility); IR (film) ν (cm^{-1}) 2960, 2903, 2866, 2362, 1588, 1475, 1371, 1275, 1126, 913, 824, 682 cm^{-1}; HR-MS (ESI) *m/z* calcd for $C_{40}H_{38}AuNNa$ [M+Na^+] 752.2562, found 752.2556. Elem. Anal. Calcd. For: $C_{40}H_{38}AuN \cdot 1/2\ H_2O$: C, 65.04; H, 5.32; N, 1.90, found: C, 64.93; H, 5.11; N, 1.70.

LaN^C^CAuCC(4-^{t}Bu-C_6H_4) (6a)

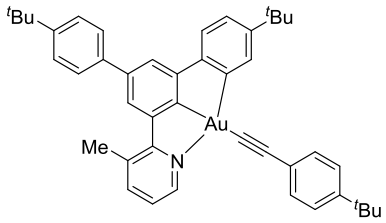

Same procedure like **4a**, **3a** (20 mg, 0.03 mmol), 4-tert butyl phenylacetylene (7.3 mg, 0.05 mmol) furnished the compound **6a** as white solid (20 mg, yield 87%), m.p. >200 °C (decomposition); ^{1}H NMR (400 MHz, CD_2Cl_2) δ 9.03 (dd, *J* = 5.3, 1.5 Hz, 1H), 8.08 (d, *J* = 1.0 Hz, 1H), 7.79 (d, *J* = 1.2 Hz, 1H), 7.62 (d, *J* = 8.5 Hz, 2H), 7.57 (dd, *J* = 7.8, 1.0 Hz, 1H), 7.48 – 7.44 (m, 2H), 7.42 (d, *J* = 8.6 Hz, 2H), 7.39 – 7.34 (m, 3H), 7.25 – 7.20 (m, 2H), 7.14 (dd, *J* = 7.7, 5.3 Hz, 1H), 2.71 (s, 3H), 1.38 (s, 9H), 1.36 (s, 9H), 1.36 (s, 9H); ^{13}C NMR (101 MHz, CD_2Cl_2) δ 174.18, 164.61, 153.62, 151.80, 151.38, 150.84, 150.09, 150.03, 148.37, 145.36, 144.47, 140.97, 139.64, 134.68, 134.55, 131.83, 130.63, 127.56, 126.29, 125.78, 125.69, 124.70, 124.64, 124.36, 121.84, 121.15, 106.57, 35.42, 35.12, 35.01, 31.77, 31.73, 31.64, 22.93; IR (film) ν (cm^{-1}) 2961, 2903, 2866, 2360, 1588, 1488, 1463, 1424, 1381, 1235, 1220, 832, 782, 767 cm^{-1}; HR-MS (ESI) *m/z* calcd for $C_{44}H_{46}AuNNa$ [M+Na^+] 808.3188, found 808.3180. Elem. Anal. Calcd. For: $C_{44}H_{46}AuN \cdot 1/2\ H_2O$: C, 66.49; H, 5.96; N, 1.76, found: C, 66.48; H, 5.81; N, 1.48.

LaN^C^CAuCC(3,5-bistrifluoromethyl-C_6H_4) (7a)

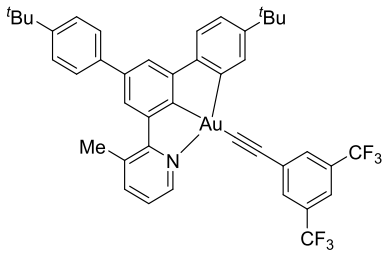

Same procedure like **4a**, **3a** (20 mg, 0.03 mmol), 3,5-bis trifluoromethyl phenylacetylene (10 mg mg, 0.05 mmol) furnished the compound **7a** as white solid (23 mg, yield 95%), m.p. >200 °C (decomposition); ^{1}H NMR (400 MHz, CD_2Cl_2) δ 8.83 (dd, *J* = 5.3, 1.5 Hz, 1H), 7.97 – 7.92 (m, 3H), 7.77 (s, 1H), 7.68 (d, *J* = 1.2 Hz, 1H), 7.55 (d, *J* = 8.5 Hz, 2H), 7.51 (dd, *J* = 7.7, 1.0 Hz, 1H), 7.36 (d, *J* = 8.5 Hz, 2H), 7.28 (d, *J* = 1.2 Hz, 1H), 7.21 (dd, *J* = 8.0, 1.9 Hz, 1H), 7.16 (d, *J* = 8.0 Hz, 1H), 7.06 (dd, *J* = 7.7, 5.3 Hz, 1H), 2.62 (s, 3H), 1.35 (s, 9H), 1.33 (s, 9H); ^{13}C NMR (101 MHz, CD_2Cl_2) δ 173.51, 164.57, 153.49, 151.94, 151.64, 151.13, 150.08, 148.25, 145.41, 144.72, 141.26, 139.35, 137.40, 134.68, 134.33, 132.16, 131.96, 131.83, 129.82, 127.42, 126.28, 125.67, 125.05, 124.55, 122.08, 121.32, 104.08, 35.42, 34.99, 31.65, 31.63, 22.89; ^{19}F NMR (376 MHz, CD_2Cl_2) δ -63.35; IR (film) ν (cm^{-1}) 2961, 2904, 2867, 2355, 2131, 1371, 1275, 1169, 1133, 913, 891, 825, 682 cm^{-1}; HR-MS (ESI) *m/z* calcd for $C_{44}H_{36}AuF_6NNa$ [M+Na^+] 888.2309, found 888.2296. Elem. Anal. Calcd. For: $C_{44}H_{36}F_6AuN$: C, 58.27; H, 4.19; N, 1.62, found: C, 57.87; H, 4.23; N, 1.55.

4. X-Ray Diffraction Analysis data for compounds 1a, 2a, 2d, 3d and 4a

The CCDC numbers contain the supplementary crystallographic data for this paper. These data can be obtained free of charge from the Cambridge Crystallographic Data Centre via www.ccdc.cam.ac.uk/data_request/cif.

Crystallographic Analysis

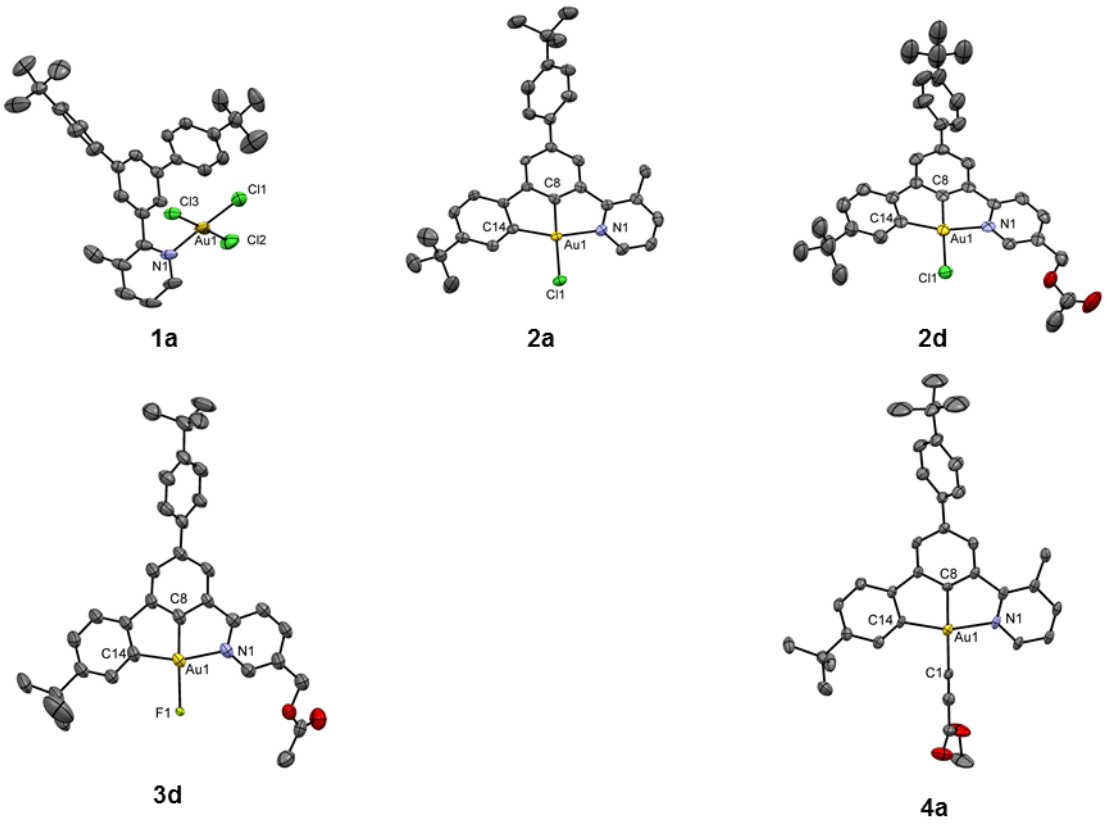

Figure 1: The solid-state molecular structures of **1a** (CCDC-1033830), **2a** (CCDC-1033772, only one of the two symmetry-independent molecules is shown), **2d** (CCDC-1058552), **3d** (CCDC-1033763) and **4a** (CCDC-1033775) with atoms drawn using 50% probability ellipsoids.

Table 1: Selected geometric parameters for complexes **1a**, **2a**, **2d**, **3d** and **4a**.

		1a	**2a** (molecule A)	**2d**	**3d**	**4a**
Bond Lengths (Å)	Au(1)-X(1)[a]	2.2598(14)	2.3654(12)	2.3602(19)	2.264(3)	2.044(6)
	Au(1)-N(1)	2.056(3)	2.136(4)	2.145(6)	2.144(5)	2.127(5)
	Au(1)-C(8)	-	1.978(5)	1.981(7)	1.921(8)	1.961(5)
	Au(1)-C(14)	-	2.024(5)	2.020(7)	2.035(7)	2.019(5)
Bond Angles (°)	N(1)-Au(1)-Cl(1)	177.18(10)	-	-	-	-
	N(1)-Au(1)-C(14)	-	160.60(18)	160.5(3)	160.30(3)	160.1(2)
	C(8)-Au(1)-X(1)	-	178.51(14)	178.68(18)	178.1(2)	179.3(2)

[a] X = Cl in **1a**, **2a** and **2d**; F in **3d**; C in **4a**.

A typical d^8-square planar molecular structure was confirmed by X-Ray diffraction analysis of compound **1a**, with *trans* bond angles N(1)-Au(1)-Cl(1) = 177.18(10)° and Cl(2)-Au(1)-Cl(3) = 177.57(6)°. Bond lengths for Au(1)-Cl(1) = 2.2598(14) Å and N(1)-Au(1) = 2.056(3) Å were measured. The (N^C^C) ligand arrangement is not planar, with all rings inclined to one another, precluding the possibility of π-π stacking interactions.

A distorted square planar geometry was confirmed for biscyclometalated compounds **2a** and **2d** (with two symmetry-independent molecules in the structure of **2a**). The *trans* angles around the Au(III) center deviate significantly from ideal values, as a result of the tethered nature of the pyridine and phenyl substituents with respect to the central aromatic ring. The restricted bite angle translates into N(1)-Au(1)-C(14) = 160.60(18)° and C(8)-Au(1)-Cl(1) = 178.51(14)° values measured for molecule A of **2a** (very similar values also for molecule B) and N(1)-Au(1)-C(14) = 160.5(3)° and C(8)-Au(1)-Cl(1) = 178.68(18)° for complex **2d**. Interestingly, the *cis*-related Au-N and Au-C distances resemble those reported for classical pincer (C^N^C)Au(III)Cl analogues: Au(1)-N(1) = 2.136(4) and 2.145(6) Å and Au(1)-C(8) =1.978(5) and 1.981(7) Å found for **2a** (molecule A) and **2d**, respectively. As expected, the *trans*-effect of the central Csp^2-atom of the ligand results in a much longer and thus weakened Au(1)-Cl(1) bond, with bond lengths of 2.3654(12) and 2.3602(19) Å **2a** (molecule A) and **2d** respectively, compared with 2.282(2) Å found for the analogous (C^N^C)-Au(III)Cl complex.[1]

Au(III)-fluoride complex **3d** showed unique features, albeit disorder in the structure reduces the precision of the geometric parameters. First, although the Au-N bond (2.144(5) Å) is comparable to those found in **2a** and **2d**, the Csp^2-Au bond (Au(1)-C(8) = 1.921(8) Å) is shorter than those in the corresponding chlorides **2a** and **2d**. A remarkably long Au-F distance (2.264(3) Å) is also found in **3d** compared with previously reported examples (e.g. 2.034(3) Å),[2] which explains the enhanced reactivity of the fluoro ligand.

In compound **4a**, the distance between the metal center and the anionic ligand are also unique with Au-Csp (Au(1)-C(1)) = 2.044(6) Å in **4a**, the latter being longer than the 1.945(8)-2.008(11) Å found for the corresponding Au-C bonds in the analogous (C^N^C)-Au(III)Csp complexes.[3] The Au-C bond length involving the central carbon atom of the (N^C^C) ligand is 1.961(5) Å for **4a**.

Crystal packing

Interesting packing motifs are evident in these five structures. The tridentate nature of the (N^C^C) ligand constrains the three coordinating rings to be coplanar, thereby offering the potential for π-π stacking interactions and indeed such interactions are found in each of these five structures with interplanar spacings ranging from 3.30-3.55 Å. In each case, adjacent molecules within the π-π stacks are arranged head-to-tail with the overlay of the rings showing an offset arrangement, often with the pyridyl ring in one molecule lying over a five-membered coordination ring of the neighboring molecule. In **2a**, the two symmetry-independent molecules stack together and this pair then aligns with an adjacent pair across a center of inversion to give a short stack of four molecules. Adjacent stacks are oriented differently, thus precluding an extension of the π-π system. The Au…Au distances within these stacks are 4.2578(8) and 4.8391(7) Å.

In **3d**, the stacking is similar to that in **2a** with molecules related by a center of inversion aligning to give an Au···Au distance of 5.1519(8) Å; here the stacks extend indefinitely parallel to the crystallographic *b*-axis. In **4a**, the arrangement is similar to that in **3d** forming extended π-π stacks parallel to the *a*-axis and alternating Au···Au distances within each stack of 4.3993(4) and 5.3237(4) Å.

4.1 Compound 1a (CCDC 1033830)

Table 1. *Crystallographic Data*

Crystallised from		dichloromethane / hexane
Empirical formula		$C_{32}H_{35}AuCl_3N$
Formula weight [g mol^{-1}]		736.96
Crystal colour, habit		yellow, prism
Crystal dimensions [mm]		0.11 × 0.16 × 0.22
Temperature [K]		160(1)
Crystal system		trigonal
Space group		$R\bar{3}$ (#148)
Z		18
Reflections for cell determination		14735
2□ range for cell determination [°]		4–57
Unit cell parameters	a [Å]	27.4437(4)
	b [Å]	27.4437(4)
	c [Å]	21.4211(4)
	α [°]	90
	β [°]	90
	γ [°]	90
	V [Å^3]	13971.9(4)
F(000)		6552
D_X [g cm^{-3}]		1.576

μ(Mo $K\alpha$) [mm^{-1}]	5.033
Scan type	ω
$2\theta_{(max)}$ [°]	57.0
Transmission factors (min; max)	0.398; 0.604
Total reflections measured	30472
Symmetry independent reflections	6856
R_{int}	0.025
Reflections with $I > 2\sigma(I)$	5506
Reflections used in refinement	6856
Parameters refined; restraints	378; 31
Final $R(F)$ [$I > 2\sigma(I)$ reflections]	0.0286
$wR(F^2)$ (all data)	0.0697
Weights:	$w = [\sigma^2(F_o^2) + (0.0277P)^2 + 51.2809P]^{-1}$ where $P = (F_o^2 + 2F_c^2)/3$
Goodness of fit	1.007
Final Δ_{max}/σ	0.002
$\Delta\rho$ (max; min) [e Å^{-3}]	0.86; -0.79
$\sigma(d_{(C-C)})$ [Å]	0.004 – 0.007

4.2 Compound 2a (CCDC 1033772)

The asymmetric unit contains two crystallographically independent Au molecules and one solvent molecule of dichloromethane (site-occupancy factor of 0.5).

Table 2. *Crystallographic Data*

Identification code	NV1403
Empirical formula	$C_{129}H_{134}Au_4Cl_6N_4$
Formula weight	2740.96
Temperature/K	160(1)
Crystal system	orthorhombic
Space group	Pbca
a/Å	12.02494(11)
b/Å	28.0660(3)
c/Å	33.5034(3)
α/°	90
β/°	90
γ/°	90
Volume/Å^3	11307.15(18)
Z	4
ρ_{calc}mg/mm^3	1.610
m/mm^{-1}	5.367
F(000)	5416.0
Crystal size/mm^3	0.21 × 0.1 × 0.03

Radiation	MoKα (λ = 0.71073)
2Θ range for data collection	4.414 to 52.744°
Index ranges	-15 ≤ h ≤ 15, -35 ≤ k ≤ 35, -41 ≤ l ≤ 41
Reflections collected	89863
Independent reflections	11545 [R_{int} = 0.0409, R_{sigma} = 0.0249]
Data/restraints/parameters	11545/210/722
Goodness-of-fit on F^2	1.105
Final R indexes [I>=2σ (I)]	R_1 = 0.0307, wR_2 = 0.0637
Final R indexes [all data]	R_1 = 0.0466, wR_2 = 0.0721
Largest diff. peak/hole / e $Å^{-3}$	1.70/-1.19

4.3 Compound 2d (CCDC 1058552)

The asymmetric unit contains one molecule of the Au-complex and five solvent molecules presumed to be water. As the solvent molecules could not be modelled adequately, their contribution to the diffraction data was removed by using the *SQUEEZE* procedure.

Table 3. *Crystallographic Data*

Crystallised from	CH_2Cl_2/ MeCN
Empirical formula	$C_{34}H_{35}AuClNO_7$
Formula weight [g mol^{-1}]	812.12
Crystal colour, habit	pale yellow, prism
Crystal dimensions [mm]	0.11 × 0.17 × 0.34

Temperature [K]		160(1)
Crystal system		monoclinic
Space group		$P2_1/c$ (#14)
Z		4
Reflections for cell determination		12509
2□ range for cell determination [°]		5−55
Unit cell parameters	a [Å]	6.93861(14)
	b [Å]	19.3263(4)
	c [Å]	26.4496(6)
	α [°]	90
	β [°]	97.449(2)
	γ [°]	90
	V [Å^3]	3516.90(13)
F(000)		1632
D_X [g cm^{-3}]		1.534
μ(Mo $K\alpha$) [mm^{-1}]		4.304
Scan type		ω
2θ(max) [°]		56.8
Transmission factors (min; max)		0.570; 1.000
Total reflections measured		34283
Symmetry independent reflections		7827
R_{int}		0.039

Reflections with $I > 2\sigma(I)$	6277
Reflections used in refinement	7827
Parameters refined; restraints	421; 258
Final $R(F)$ [$I > 2\sigma(I)$ reflections]	0.0503
$wR(F^2)$ (all data)	0.1215
Weights:	$w = [\sigma^2(F_o^2) + (0.0380P)^2 + 21.3626P]^{-1}$ where $P = (F_o^2 + 2F_c^2)/3$
Goodness of fit	1.122
Final Δ_{max}/σ	0.001
$\Delta\rho$ (max; min) [e Å^{-3}]	1.89; -1.67
$\sigma(d_{(C-C)})$ [Å]	0.007 – 0.015

4.4 Crystal Structure of Compound 3d (CCDC 1033763)

Although fluorides **3** crystallize under standard solvent diffusion, biphasic or slow evaporation conditions, highly disordered and in some cases even intricately twinned crystals were mostly obtained whose structures could not satisfactorily be solved by crystallographic analysis. Finally, suitable, albeit disordered, crystals of compound **3d** could be obtained by slow diffusion of hexane into a concentrated solution of the complex in dichloromethane, enabling the confirmation of both composition and structure.

The molecule of the Au-complex in the structure of $C_{34}H_{35}AuFNO_2 \cdot 0.5C_6H_{14}$ lies across in a mirror plane and some of the peripheral groups are disordered about the mirror. The structure is clearly and unambiguously defined, but the precision of the geometric parameters is poorer than usual. The structure also contains some highly disordered solvent, which is presumed to be hexane. The solvent molecules could not be modelled sufficiently well, so their contribution to the diffraction data was removed by using the *SQUEEZE* procedure.

Table 4. *Crystallographic Data*

Crystallised from	dichloroethane / hexane

Empirical formula		$C_{37}H_{42}AuFNO_2$
Formula weight [g mol^{-1}]		748.71
Crystal colour, habit		colourless, prism
Crystal dimensions [mm]		0.10 × 0.10 × 0.35
Temperature [K]		160(1)
Crystal system		monoclinic
Space group		*I*2/*m* (#12)
Z		4
Reflections for cell determination		8722
2θ range for cell determination [°]		5–55
Unit cell parameters	*a* [Å]	14.9575(4)
	b [Å]	6.75050(10)
	c [Å]	35.2795(6)
	α [°]	90
	β [°]	100.810(2)
	γ [°]	90
	V [Å^3]	3498.98(12)
F(000)		1500
D_X [g cm^{-3}]		1.421
μ(Mo *K*α) [mm^{-1}]		4.255
Scan type		ω
2θ(max) [°]		56.0

Transmission factors (min; max)	0.588; 1.000
Total reflections measured	18284
Symmetry independent reflections	4166
R_{int}	0.034
Reflections with $I > 2\sigma(I)$	3502
Reflections used in refinement	4166
Parameters refined; restraints	296; 36
Final $R(F)$ [$I > 2\sigma(I)$ reflections]	0.0359
$wR(F^2)$ (all data)	0.1044
Weights:	$w = [\sigma^2(F_o^2) + (0.0641P)^2 + 1.4953P]^{-1}$ where $P = (F_o^2 + 2F_c^2)/3$
Goodness of fit	1.116
Final Δ_{max}/σ	0.001
$\Delta\rho$ (max; min) [e Å^{-3}]	1.57; -0.62
$\sigma(d_{(C-C)})$ [Å]	0.008 – 0.018

4.5 Compound 4a (CCDC 1033775)

Table 5. *Crystallographic Data*

Identification code	nv1401
Empirical formula	$C_{36}H_{36}AuNO_2$
Formula weight	711.62
Temperature/K	160(1)

Crystal system	triclinic
Space group	P-1
a/Å	6.80422(19)
b/Å	13.1141(4)
c/Å	16.8248(6)
α/°	88.044(3)
β/°	86.370(3)
γ/°	84.718(2)
Volume/Å^3	1491.31(8)
Z	2
ρ_{calc}mg/mm^3	1.585
m/mm^{-1}	4.965
F(000)	708.0
Crystal size/mm^3	0.16 × 0.06 × 0.03
Radiation	MoKα (λ = 0.71073)
2Θ range for data collection	4.854 to 52.746°
Index ranges	-8 ≤ h ≤ 8, -16 ≤ k ≤ 16, -20 ≤ l ≤ 20
Reflections collected	20399
Independent reflections	6107 [R_{int} = 0.0383, R_{sigma} = 0.0416]
Data/restraints/parameters	6107/156/400

Goodness-of-fit on F^2	1.088
Final R indexes [I>=2σ (I)]	R_1 = 0.0417, wR_2 = 0.0854
Final R indexes [all data]	R_1 = 0.0482, wR_2 = 0.0880
Largest diff. peak/hole / e $Å^{-3}$	4.31/-2.99

References

[1] Li, C. K.-L., Sun, R. W.-Y., Kui, S. C.-F., Zhu, N., Che, C.-M. *Chem. Eur. J.* **2006**, *12*, 5253.

[2] Mankad, N. P., Toste, F. D. *J. Am. Chem. Soc.* **2010**, *132*, 12859.

[3] Wong, K. M.-C., Hung, L.-L., Lam, W. H., Zhu, N., Yam, V. W.-W. *J. Am. Chem. Soc.* **2007**, 129, 4350.

CHAPTER 3

EVIDENCE FOR DIRECT TRANSMETALATION OF Au^{III}-F WITH BORONIC ACIDS

CHAPTER 3

Evidence for Direct Transmetalation of Au^{III}-F with Boronic Acids

Roopender Kumar, Anthony Linden and Cristina Nevado

(*J. Am. Chem. Soc.* **2016**, *138*, 13790-13793)

Transmetalation is a fundamental step in metal catalyzed cross-coupling reactions.[1] The prominent role of Suzuki reactions in modern synthetic chemistry[2a] has fostered efforts towards establishing a detailed mechanistic basis for the interaction of boron reagents with Pd^{II} species.[2b-e] Gold-catalyzed oxidative couplings have recently emerged as powerful complementary tools for the efficient formation of Csp^3-Csp^2, Csp^2-Csp^2 and Csp-Csp^2 bonds.[3] Interestingly, boronic acids are involved as productive reaction partners in many of these transformations.[4] While Au^I-B transmetalation has been studied in detail,[5] examples of Au^{III}/B transmetalation are less abundant. Pioneering studies by Bochmann and co-workers showed that κ^3-[(C^N^C)Au(OX)] complexes react smoothly with aryl boronic acids in the absence of external base to produce the corresponding arylation products [(C^N^C)AuAr].[6] Our group also demonstrated that [$(Ph_3P)Au(C_6F_5)Cl_2$] react with electron deficient aryl boronic acids ($Ar^FB(OH)_2$) under neutral conditions to form stable [$(Ph_3P)Au(C_6F_5)Ar^FCl$] species.[7] These processes showcase the synergistic combination of Au^{III} and B, however, most gold catalyzed oxidative-cross couplings involving boronic acids as reaction partners employ Selectfluor as stoichiometric oxidant and thus Au^{III}-F species have been invoked as the key partners of boron species towards the formation of new C-C bonds.[4b-f] Such putative Au^{III}-F intermediates remain largely elusive due to their intrinsic unstable character[8] and thus the nature of the interaction Au^{III}-F/B is still a matter of intense discussion.

In a seminal contribution towards the understanding of these transformations, Toste *et al.* showed that *in situ* generated *cis*-[(NHC)$AuMeF_2$] species (NHC: *N*-heterocyclic carbene), in equilibrium with the corresponding dimer, rapidly react with aryl boronic acids to produce toluene derivatives (Scheme 1A).[9] Since the electronics on the boronic acid did not affect the reaction outcome, a single step bimolecular reductive elimination (**I**) rather than a conventional two-step transmetalation and reductive elimination pathway was proposed for the Csp^3-Csp^2 bond formation, a hypothesis also supported by DFT calculations.[4f] Recently, You[10] *et al.* managed to establish a catalytic cycle in which 2-(*o*-tolyl)pyridine substrates react with gold in the presence of N-fluorobenzenesulfonimide (NFSI) and aryl boronic acids to produce the corresponding cross-coupling products *via* reductive elimination on biaryl gold(III) intermediate **II** (Scheme 1B).[10] Here, the role of fluorine remains unclear as Csp^2-Au^{III}-F species **III** can be proposed to precede transmetalation, or alternatively, non-coordinated fluoride anions produced *in situ* might be responsible for the C-B cleavage (**IV**).[12] Thus, even if Au^{III} is isoelectronic to Pd^{II}, our understanding of the interaction Au^{III}-F/B and of the specific nature of the individual steps forging the new C-C bonds (direct transmetalation or bimolecular reductive elimination) is still limited and mostly restricted to indirect experimental evidence.

Here we present the synthesis of monomeric, easy to handle Csp^2-Au^{III}-bis and mono-fluorido complexes together with a detailed study on their reactivity with aryl boronic acids. Our results provide experimental evidence for the ability of Au^{III}-F species to undergo "classical" transmetalation with aryl boronic acids by isolation of the corresponding transmetalation products. We also demonstrate that, in contrast to previously studied systems,[9] the product formation is indeed governed by both the electronic and steric features of the organic residue on the boronic acid (Scheme 1C).

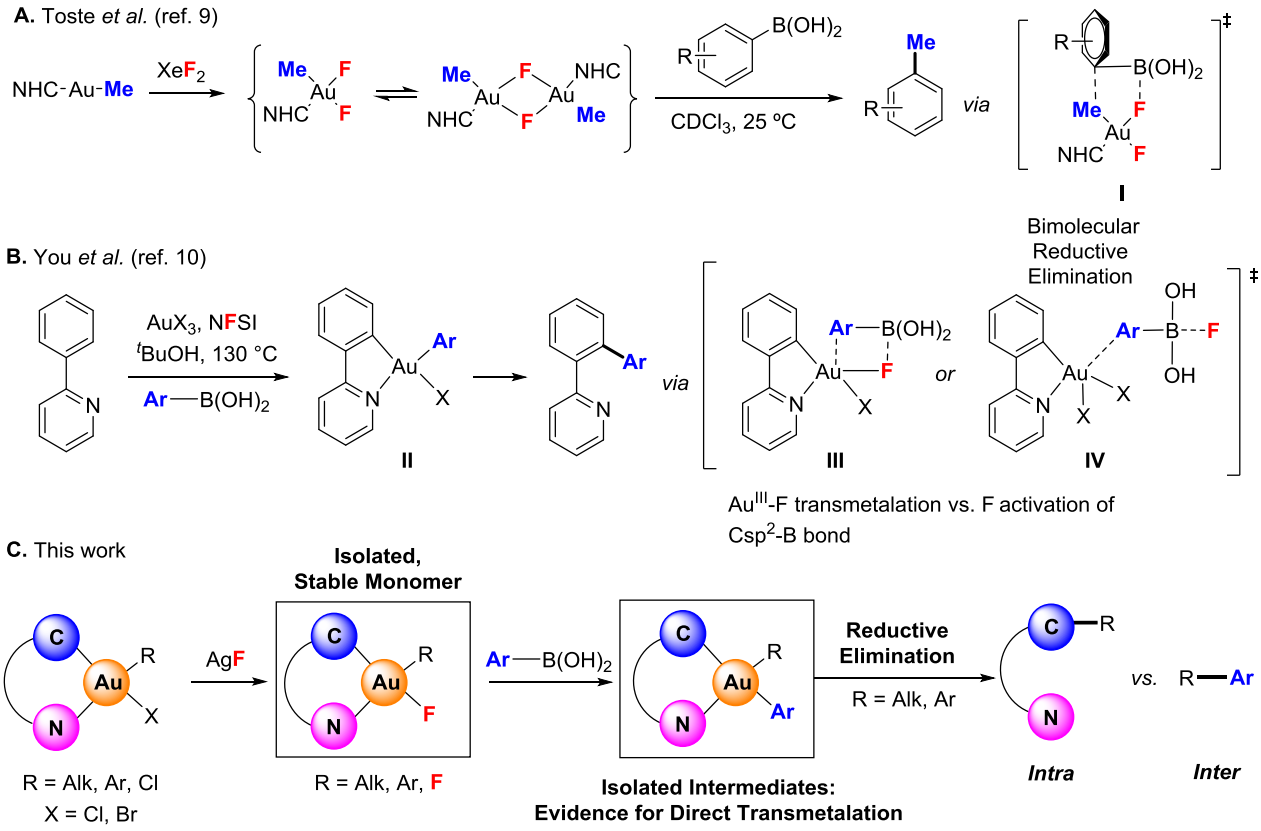

Scheme 1. Synthesis and reactivity of Au^{III}-F with boronic acids.

As seen in Scheme 1, methods to produce Au^{III}-F species *in situ* have mostly relied on the reaction of (NHC)- or (C^N)-stabilized gold(I) complexes with strong oxidants such as XeF_2 or NFSI.[8-10] Recently, our group reported the synthesis of a novel class of pincer κ^3-[(N^C^C)AuCl] complexes in which a facile Cl/F ligand exchange reaction in the presence of AgF successfully yielded the corresponding fluorides κ^3-[(N^C^C)AuF].[13] Aware of the ability of 2-phenylpyridine based ligands (C^N) to stabilize electron deprived gold(III) species,[14] *cis*-dichloro-2-(2-fluorophenyl)- and 2-(3,4,5-trimethoxyphenyl)-3-methylpyridine-gold(III) complexes **1** and **2** were treated with AgF in dichloromethane at room temperature producing the corresponding difluorides **3** and **4** in high yields.[15] Interestingly, [(C^N)AuArBr] **5** and [(C^N)AuMeBr] **6**[16] were also efficiently transformed under similar conditions into the corresponding monofluoride species [(C^N)AuRF] **7** (R = 3,5-$(CF_3)_2$-C_6H_3-) and **8** (R = Me) (Scheme 2).

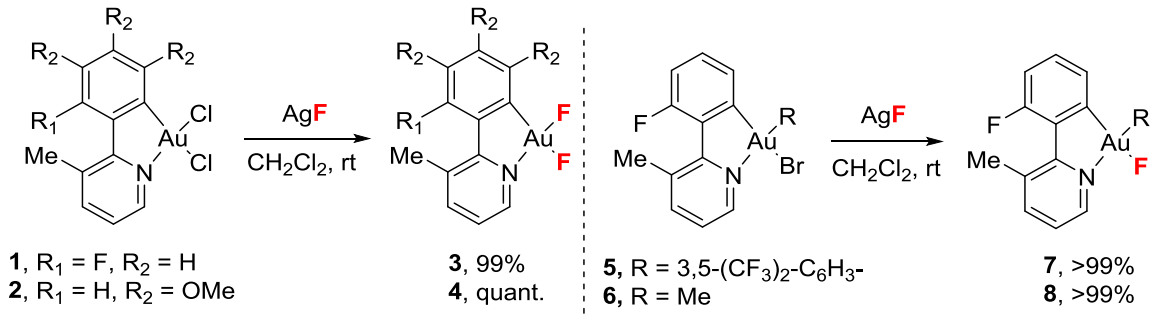

Scheme 2. Synthesis of Csp^2-Au^{III}-bis and monofluorido complexes via halogen/F exchange reactions.

The monomeric structure of Au^{III}-F complexes **3**, **4**, **7** and **8** could be confirmed by ^{19}F NMR as well as by successful X-Ray diffraction analysis of the corresponding crystals.[17] As expected, the Au^{III}-F bond *trans* to the strong σ-donor aryl ligand is substantially elongated compared to the one *trans* to the pyridino moiety, particularly in the case of electron-rich (C^N) precursors. Distorted square planar geometries were observed for all complexes, with a more acute angle observed in compound **7** compared to that measured in the difluoride complexes **3** and **4** (Figure 1). Differences in the ^{19}F NMR of these complexes are also diagnostic, with the signals of F-*trans* to the phenyl ring appearing at higher fields compared to those opposite to the pyridino group (**3**: F(1): -252.4 ppm, F(2): -191.8 ppm. **4**: F(1): -281.2 ppm, F(2): -170.8 ppm. **7**: F(2): -208.5ppm. **8**: F(1): -220.8 ppm).[15]

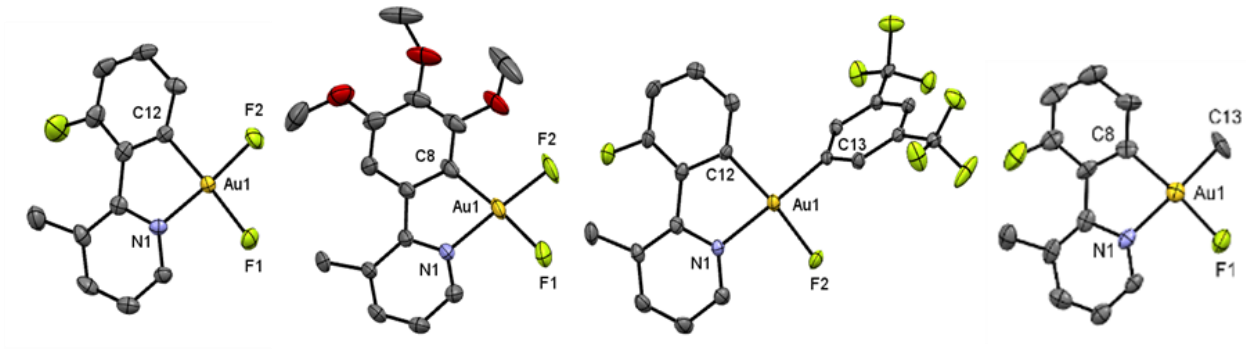

Figure 1. Solid-state molecular structures of (from left to right) [(N^C)AuF_2] complexes **3**, **4** and [(N^C)AuRF] **7** and **8** with atoms drawn using 50% probability ellipsoids and hydrogen atoms have been omitted for clarity. Selected bond lengths [Å]: **3**: Au(1)-F(1) = 2.014(3), Au(1)-F(2) = 1.951(4); **4**: Au(1)-F(1) = 2.025(4), Au(1)-F(2) = 1.940(3); **7**: Au(1)-F(2) = 2.011(4); **8**: Au(1)-F(1) = 2.023(7) and angles [°]: **3**: N(1)-Au(1)-F(1) = 94.80(17); **4**: N(1)-Au(1)-F(1) = 93.98(16); **7**: N(1)-Au(1)-F(2) = 91.6(2); **8**: N(1)-Au(1)-F(1) = 92.5(3).

The reactivity of these discrete Csp^2-Au^{III}-F complexes with different aryl boronic acids was explored next. Interestingly, the reaction of **3** with two equivalents of (pentafluorophenyl)boronic acid furnished the corresponding bis-aryl complexes [(C^N)$Au(C_6F_5)_2$] **9a** in 81% yield, thus demonstrating that Csp^2-Au^{III}-F species can react with boronic acids via a direct transmetalation (Scheme 3).

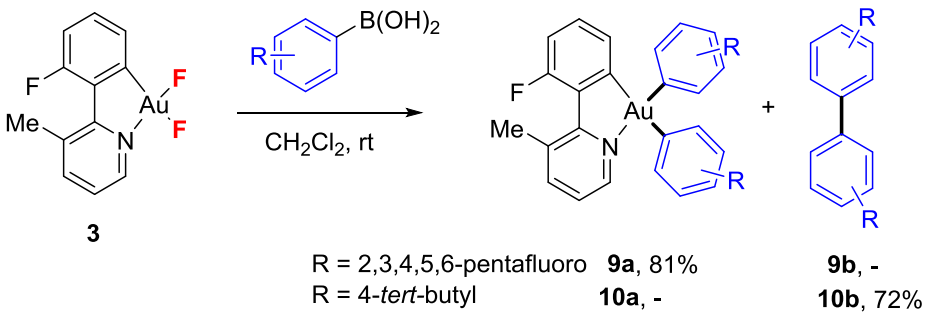

Scheme 3. Reaction of [(C^N)AuF$_2$] 3 with aryl boronic acids.

The reaction with (4-*tert*-butylphenyl)boronic acid yielded homocoupling product **10b** in 72% yield as a result of a facile reductive elimination between the two electron-rich aromatic residues. It is important to note that cross-coupling products stemming from a reductive elimination with the 2-phenyl pyridine ligand were not detected in the reaction mixtures.

The reactivity of monofluorido complexes **7** and **8** was also investigated. As shown in Table 1, a bimolecular reductive elimination pathway would deliver the *intermolecular* cross-coupling products (**12**). If a direct transmetalation were to take place via **11**, both *intra*- and *intermolecular* reductive elimination products (**12** vs. **13**/**14**)[18] could be observed. The reaction of 4-(*tert*butylphenyl)- and 4-(fluorophenyl)boronic acids (**A**, **B**) with **7** in dichloromethane at room temperature produced both *inter*- (**12A** and **12B**) and *intramolecular* (**13**) reductive elimination products in comparable yields (Table 1, entries 1, 2). Monitoring by ^{1}H NMR the reaction of **7** with 4-(*tert*butylphenyl)boronic acid (**A**) at -40ºC enabled us to detect a new species, which was assigned to transmetalation product **11A**. Upon warming to room temperature, reductive elimination products are observed suggesting that the cross-coupling products observed in entries 1 and 2 can stem from the corresponding direct transmetalation intermediates **11** (see SI).[15] Interestingly, the reaction of **7** with (pentafluorophenyl)boronic acid (**C**) produced preferentially product **13** in 81% yield showing that a sterically encumbered, electron deprived intermediates favour the corresponding *intramolecular* reductive elimination process (entry 3). An equally sterically demanding, but less electronically deprived partner, such as (2,4,6-trifluorophenyl)boronic acid (**D**), enabled the isolation of transmetalation product **11D** in 51% yield (entry 4). **11D** undergoes quantitative reductive elimination to **13** upon heating (see SI).[15] The reaction of complex **8** with 4-(*tert*butylphenyl)boronic acid **A** delivered intermolecular reductive elimination **12A'**, together with homocoupling product **10b** (entry 5).[19] In contrast, the reactions with pentafluorophenyl- and 2,3,6-trifluorophenyl boronic acid furnished exclusively *intramolecular* reductive elimination products **14C** and **14E** in high yields (entries 6, 7). As such, the reaction outcome seems to be governed by both the electronic and steric features of the organic residue on the boron counterpart as well as by the electronic nature of the cycloaurated complex, thus hinting towards the involvement of transmetalation intermediates **11** in these transformations, in contrast to a potential bimolecular reductive elimination pathway in which the electronic features of the boron reagent would not be expected to play such an important role.[9] These results highlight

the mechanistic diversity underlying gold-catalyzed oxidative couplings combining Selectfluor and boronic acids. For preliminary results on a catalytic version of these transformations, see experimental section.[15]

Table 1. Reaction of [(N^C)AuRF] **7** and **8** with aryl boronic acids[a]

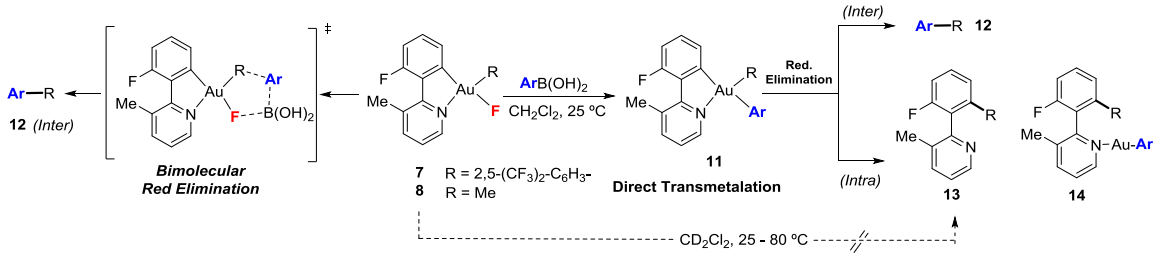

Entry	Starting Material[a]	Ar	Product Distribution[b,c]			
			11	**12**	**13**	**14**
1	**7**, R = 3,5-$(CF_3)_2$-C_6H_3	4-^{t}Bu-C_6H_4- (**A**)	-	**12A**, 57%	40%	-
2	„	4-F-C_6H_4- (**B**)	-	**12B**, 32%	68%	-
3	„	C_6F_5- (**C**)	-	-	81%	-
4	„	2,4,6-$C_6F_3H_2$- (**D**)	**11D**, 51%	-	19%	-
5	**8**, R = Me	4-^{t}Bu-C_6H_4- (**A**)	-	**12A'**, 33%[d,e]	traces	
6	„	C_6F_5- (**C**)	-	-	-	**14C**, 88%
7	„	2,3,6-$C_6F_3H_2$- (**E**)	-	-	-	**14E**, 74%

"-": not observed. [a] No intramolecular reductive elimination was observed in complexes **7** and **8** even after prolonged heating at 80 °C[15] [b] Reaction conditions: $ArB(OH)_2$ (1.2 equiv), CH_2Cl_2, 25 °C, 30 min-1 h. [c] Transmetalation intermediates **11A** (R = 3,5-$(CF_3)_2$-C_6H_3) and **11A'** (R = Me) were observed when the reaction was performed at – 40 °C. Warming up the reaction to 25 °C delivers cross coupling products (see SI). [d] 29% yield of homocoupling product **10b** could be isolated. [e] Reaction with boronic acid **B** showed a similar outcome.

The ability of Csp^2-Au^{III}-F species to undergo direct transmetalation with aryl boronic acids was further confirmed with κ³-[(N^C^C)AuF] species.[13] As shown in Scheme 4, the reaction of **15** with (4-*tert*butylphenyl)boronic acid delivered complex **16a** in 62% yield. Pentafluoro-, 3,5-difluoro- and 2,4,6-trifluorophenyl boronic acids delivered aryl biscyclometalated complexes κ³-[(N^C^C)AuAr] **16b-d** in high yields.

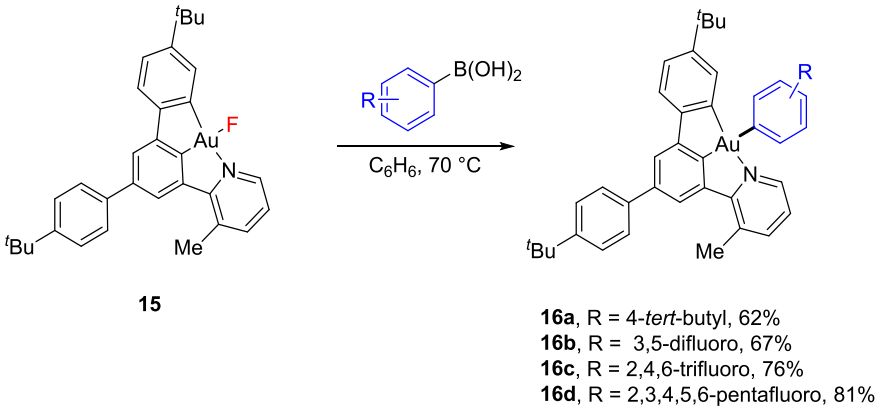

Scheme 4. Reaction of κ^3-[(N^C^C)AuF] 15 with aryl boronic acids.

These tranformations showcase that a direct transmetalation Au^{III}-F/B is indeed possible regardless of the electronic nature of the boronic acid provided enough stabilization is in place to prevent the reductive elimination to give a new Csp^2-Csp^2 bond. The structures of complexes **9a**, **11D**, **14C**, **15, 16a** and **16b** could be unambiguously stablished by X-Ray diffraction analysis.[17]

In conclusion we report here the synthesis, isolation and characterization of four novel, difluoro-[(C^N)AuF_2], arylmonofluoro-[(C^N)AuArF] and alkylmonofluoro-[(C^N)AuAlkF] gold(III) complexes isolated in monomeric form via facile X/F exchange reactions. The underlying reactivity of the Au^{III}-F bond with aryl boronic acids has been studied in detail under neutral reaction conditions. Importantly, we provide the first experimental evidence for a direct Au^{III}-F/B transmetalation preceding the Csp^2-Csp^2 or Csp^2-Csp^3 bond formation. Our results thus showcase that different mechanistic scenarios can operate in gold-catalyzed oxidative couplings involving Selectfluor and boronic acids.

References

[1] Wendt, O. F. *Curr. Org. Chem.* **2007**, *11*, 1417-1433.

[2] (a) Suzuki, A. *Angew. Chem. Int. Ed.* **2011**, *50*, 6722. (b) Carrow, B. P., Hartwig, J. F. *J. Am. Chem. Soc.* **2011**, *133*, 2116. (c) Amatore, C., Jutand, A., Le Duc, G. *Chem. Eur. J.* **2012**, *18*, 6616. (d) Lennox, A. J. J., Lloyd-Jones, G. C. *Angew. Chem. Int. Ed.* **2013**, *52*, 7362. (e) Thomas, A. A., Denmark, S. E. *Science* **2016**, *352*, 329.

[3] For selected examples: (a) Cui, *L.*, Zhang, G., Zhang, L. *Bioorg. Med. Chem. Lett.* **2009**, *19*, 3884. (b) Kar, *A.*, Mangu, N., Kaiser, H. M., Tse, M. K. *J. Organomet. Chem.* **2009**, *694*, 524. *(*c) de Haro, T., Nevado, C. *Angew. Chem. Int. Ed.* **2011**, *50*, 906. (d) Hopkinson, M. N.,Tessier, A. Salisbury, A., Gouverneur, V. *Chem. Eur. J.* **2010**, *16*, 4739. (e) Hashmi, A. S. K., Ramamurthi, T. D., Todd, M. H., Tsang, A. S.-K., Graf, K. *Aust. J. Chem.* **2010**, *63*, 1619. (f) Ball, L. T., Green, M., Lloyd-Jones, G. C., Russell, C. A. *Org. Lett.* **2010**, *12*, 4724. (g) Ball, L. T., Lloyd-Jones, G. C., Russell, C. A. Science ***2012***, *337*, 1644.(h) Serra, J., Whiteoak, C. J., Acuña-Pares, F., Font, M., Luis, J. M., Lloret-Fillol, J.,

Ribas, X. *J. Am. Chem. Soc.* **2015**, *137*, 13389. For selected reviews on this topic: (i) Hopkinson, M. N., Gee, A. D., Gouverneur, V. *Chem. Eur. J.* **2011**, *17*, 8248. (j) Wegner, H. A., Auzias, M. *Angew. Chem. Int. Ed.* **2011**, *50*, 8236. (k) Hopkinson, M. N., Gee, A. D., Gouverneur, V. *Isr. J. Chem.* **2010**, *50*, 675. (l) Boorman, T. C.; Larrosa, I. *Chem. Soc. Rev.* **2011**, *40*, 1910. (m) Nevado, C., de Haro, T. in *New Strategies in Chemical Synthesis and Catalysis*, Wiley-VCH Verlag GmbH & Co. KGaA, **2012**, pp. 247.

[4] (a) Carrettin, S., Guzman, J., Corma, A. *Angew. Chem. Int. Ed.* **2005**, *44*, 2242. (b) Zhang, G.; Peng, Y., Cui, L., Zhang, L. *Angew. Chem. Int. Ed.* **2009**, *48*, 3112. (c) Zhang, G., Cui, L.; Wang, Y.; Zhang, L. *J. Am. Chem. Soc.* **2010**, *132*, 1474. (d) Wang, W., Jasinski, J., Hammond, G. B., Xu, B. *Angew. Chem. Int. Ed.* **2010**, *49*, 7247. (e) Brenzovich, W. E.; Benitez, D.; Lackner, A. D., Shunatona, H. P., Tkatchouk, E., Goddard, W. A., Toste, F. D. *Angew. Chem. Int. Ed.* **2010**, *49*, 5519. (f) Tkatchouk, E., Mankad, N. P., Benitez, D., Goddard, W. A., Toste, F. D. *J. Am. Chem. Soc.* **2011**, *133*, 14293.

[5] (a) Sladek, A., Hofreiter, S., Paul, M., Schmidbaur, H. *J. Organomet. Chem.* **1995**, *501*, 47. (b) Partyka, D. V., Zeller, M., Hunter, A. D., Gray, T. G. *Inorg. Chem.* **2012**, *51*, 8394. (c) Maity, A., Sulicz, A. N., Deligonul, N., Zeller, M., Hunter, A. D., Gray, T. G. *Chem. Sci.* **2015**, *6*, 981. (d) Hashmi, A. S. K., Ramamurthi, T. D., Rominger, F. *J. Organomet. Chem.* **2009**, *694*, 592. (e) Hansmann, M. M., Rominger, F., Boone, M. P., Stephan, D. W., Hashmi, A. S. K. *Organometallics* **2014**, *33*, 4461. (f) Dupuy, S., Crawford, L., Bühl, M., Slawin, A. M. Z., Nolan, S. P. *Adv. Synth. Catal.* **2012**, *354*, 2380. (g) Hirner, J. J., Blum, S. A. *Tetrahedron* **2015**, *71*, 4445.

[6] (a) Rosca, D.-A., Smith, D. A., M. Bochmann, *Chem. Commun.* **2012**, *48*, 7247. (b) Smith, D. A., Roşca, D.-A., Bochmann, M. *Organometallics* **2012**, *31*, 5998.

[7] (a) Hofer, M., Gomez-Bengoa, E., Nevado, C. *Organometallics* **2014**, *33*, 1328. (b) M. Hofer, C. Nevado, *Tetrahedron* **2013**, *69*, 5751.

[8] For transformations invoking Au^{III}-F species see ref. 3a, 3d-f, ref. 4 and also: (*a*) de Haro, T., Nevado, C. *Chem. Commun.* **2011**, *47*, 248. (b) de Haro, T., Nevado, C. *Adv. Synth. Catal.* **2010**, *352*, 2767. (c) Hopkinson, M. N., Ross, J. E., Giuffredi, G. T., Gee, A. D. Gouverneur, V. *Org. Lett.* **2010**, *12*, 4904. (d) Simonneau, A., Garcia, P., Goddard, J-P., Mouriès-Mansuy, V., Malacria, M., Fensterbank, L. *Beilstein J. Org. Chem.* **2011,** *7*, 1379. For recent examples of well characterized Au^{III}-X species: e) Guenther, J., Mallet-Ladeira, S., Estevez, L., Miqueu, K., Amgoune, A., Bourissou, D. *J. Am. Chem. Soc.* **2014**, *136*, 1778. (f) Joost, M., Zeineddine, A., Estevez, L., Mallet-Ladeira, S., Miqueu, K., Amgoune, A., Bourissou, D. *J. Am. Chem. Soc.* **2014**, *136*, 14654. For examples of well characterized Au^{I}-F species: g) Akana, J. A., Bhattacharyya, K. X., Müller, P., Sadighi, J. P. *J. Am. Chem. Soc.* **2007**, *129*, 7736. (h) Nahra, F., Patrick, S. R., Bello, D., Brill, M., Obled, A., Cordes, D. B., Slawin, A. M. Z., O'Hagan, D., Nolan, S. P. *ChemCatChem* **2015**, *7*, 240.

[9] (a) Mankad, N. P., Toste, F. D. *J. Am. Chem. Soc.* **2010**, *132*, 12859. (b) Mankad, N. P., Toste, F. D. *Chem. Sci.* **2012**, *3*, 72-76.

[10] Wu, Q., Du, C., Huang, Y., Liu, X., Long, Z., Song, F., You, J. *Chem. Sci.* **2015**, *6*, 288.

[11] (a) Wolfe, W. J., Winston, M. S., Toste, F. D. *Nat. Chem.* **2014**, *6*, 453.; (b) Winston, M. S., Wolf, W. J., Toste, F. D. *J. Am. Chem. Soc.* **2015**, *137*, 7921. (c) Vicente, J., Dolores Bermudez, M., Escribano, J. *Organometallics* **1991**, *10*, 3380.

[12] Au^{III}-F species do not seem to be necessary for a successful reductive elimination (see equation 5 in ref. 10).

[13] Kumar, R., Linden, C. Nevado, *Angew. Chem. Int. Ed.* **2015**, *54*, 14287. See also ref. 11b.

[14] Henderson, W. in *Advances in Organometallic Chemistry, Vol. 54* (Eds.: W. Robert, F. H. Anthony), Academic Press, **2006**, pp. 207.

[15] For experimental details, see Supporting Information.

[16] (a) Langseth, E., Görbitz, C. H., Heyn, R. H., Tilset, M. *Organometallics* **2012**, *31*, 6567. For other examples of ligand exchange reactions preferably occurring *trans* to the pyridine group, see: (b) Szentkuti, A., Bachmann, M.,. Garg, J. A., Blacque, O., Venkatesan, K. *Chem. Eur. J.* **2014**, *20*, 2585. (c) Venugopal, A., Shaw, A. P., Törnroos, K. W., Heyn, R. H., Tilset, M. *Organometallics* **2011**, *30*, 3250. (d) Langseth, E., Nova, A., Traseth, E. A., Rise, F. Oien, S., W., Heyn, R. H., Tilset, M. *J. Am. Chem. Soc.* **2014**, *136*, 10104.

[17] CCDC-1487417 (**1**), 1487425 (**2**), 1486854 (**3**), 1486862 (**4**), 1487420 (**5**), 1486864 (**7**), 1487498 (**8**), 1486865 (**9a**), 1486866 (**11D**), 1486867 (**14C**), 1486905 (**15**), 1033770 (**16a**) and 1486892 (**16b**) contain the supplementary crystallographic data for this paper. The data can be obtained free of charge from The Cambridge Crystallographic Data Centre via www.ccdc.cam.ac.uk/structures.

[18] Note that compound **13** shown in Table 1 is formed from the corresponding complexes **14** upon purification via column chromatography in silica gel.

[19] For homocoupling products via Au(I)/Au(III) trasmetalation, see: (a)Leyva-Pérez, A.; Doménech, A.; Al-Resayes, S. I.; Corma, A. *ACS Catal*. **2012**, *2*, 121. (b) Hofer, M.; Nevado, C. *Eur. J. Inorg. Chem.* **2012**, *9*, 1338. (c) Hofer, M.; Nevado, C. *Tetrahedron* **2013**, *69*, 5751.

CHAPTER 3

EXPERIMENTAL SECTION

Table of Contents

1. General Information

NMR spectra were recorded on AV2 400 or AV2 500 MHz Bruker spectrometers. Chemical shifts are given in ppm. The spectra were calibrated to the residual ^{1}H and ^{13}C signals of the solvents. Multiplicities are abbreviated as follows: singlet (s), doublet (d), triplet (t), quartet (q), doublet-doublet (dd), quintet (quint), septet (sept), multiplet (m), and broad (b). The compounds were characterized by ^{1}H, ^{13}C, and ^{19}F NMR spectroscopy. Infrared spectra were recorded on a JASCO FT/IR-4100 spectrometer. High-resolution electrospray ionization and electronic impact mass spectrometry was performed on a Finnigan MAT 900 (Thermo Finnigan, San Jose, CA; USA) double focusing magnetic sector mass spectrometer. Ten spectra were acquired. A mass accuracy ≤ 2 ppm was obtained in the peak matching acquisition mode by using a solution containing 2 <l PEG200, 2 <l PPG450, and 1.5 mg NaOAc (all obtained from Sigma-Aldrich, CH-Buchs) dissolved in 100 mL MeOH (HPLC Supra grade, Scharlau, E-Barcelona) as internal standard. GC-MS analysis was done on a Finnigan Voyager GC8000 Top. Elemental microanalysis was carried out with Leco TruSpec Micro-CHNS analyser. Microwave reaction was done in Discover & Explorer SP (CEM). Gold complexes decompose before melting temperature is reached (T^{a} > 200°C).

Materials and Methods:

Unless otherwise stated, starting materials were purchased from Aldrich and/or Fluka. Solvents were purchased in HPLC quality, degassed by purging thoroughly with nitrogen and dried over activated molecular sieves of appropriate size. Alternatively, they were purged with argon and passed through alumina columns in a solvent purification system (Innovative Technology). Conversion was monitored by thin layer chromatography (TLC) using Merck TLC silica gel 60 F254. Compounds were visualized by UV-light at 254 nm and by dipping the plates in an ethanolic vanillin/sulfuric acid solution or an aqueous potassium permanganate solution followed by heating. Flash column chromatography was performed over silica gel (230-400 mesh).

2. Experimental procedures and characterization of starting materials and products

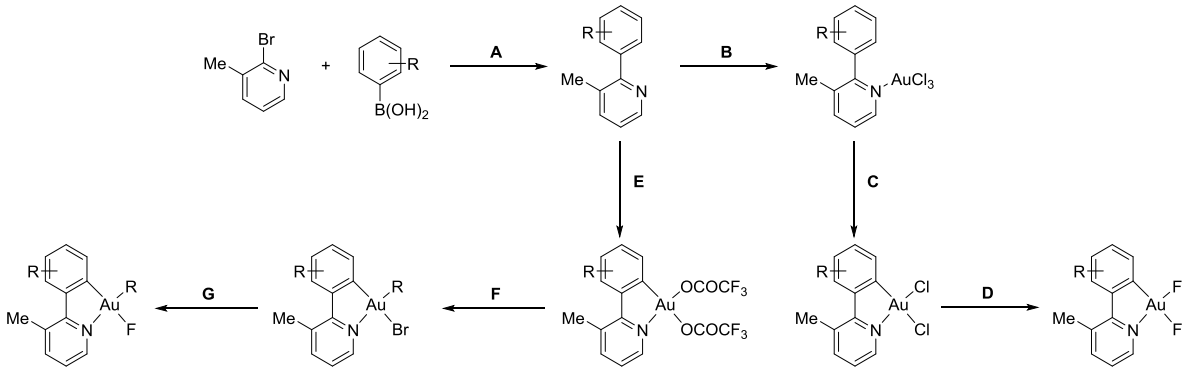

General Procedure A:

In a Schlenk tube, the corresponding bromopyridine (1 equiv), boronic acid (1.3 equiv) and potassium carbonate (3 equiv) were dissolved in a mixture of THF/H_2O (3/1). The reaction mixture was degassed for 20-30 minutes. $Pd(PPh_3)_2Cl_2$ (5 mol%) was added and the reaction mixture was stirred at 80°C for 14 h. Ethyl acetate (20 ml) was added, and the organic layer was washed with distilled water and dried over anhydrous magnesium sulfate. After filtration, the solvent was evaporated under reduced pressure and the reaction crude was purified by silica gel chromatography using EtOAc/Hexane as eluent. Compounds **L1** and **L2** were prepared using general procedure **A**.

2-(2-Fluorophenyl)-3-methylpyridine (L1)

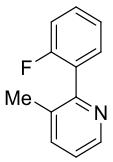

This compound was synthesized following general procedure **A** using 2-bromo-3-methylpyridine (1.00 g, 5.81 mmol), 2-fluoro-phenyl boronic acid (1.06 g, 7.55 mmol), potassium carbonate (2.41 g, 17.4 mmol) and $Pd(PPh_3)_2Cl_2$ (200 mg, 0.29 mmol) in THF:H_2O (30:10 ml). **L1** was isolated as a colorless oil (810 mg, 74%). ^{1}H NMR (500 MHz, CD_2Cl_2) δ 8.50 (d, *J* = 4.6 Hz, 1H), 7.61 (d, *J* = 7.7 Hz, 1H), 7.45 – 7.37 (m, 2H), 7.29 – 7.21 (m, 2H), 7.16 (t, *J* = 9.2 Hz, 1H), 2.22 (s, 3H). ^{13}C NMR (126 MHz, CD_2Cl_2) δ 161.22 (s), 159.27 (s), 154.68 (s), 147.51 (s), 138.22 (s), 133.13 (s), 131.91 (d, *J* = 3.8 Hz), 130.52 (d, *J* = 8.1 Hz), 129.17 (d, *J* = 16.2 Hz), 124.77 (d, *J* = 3.5 Hz), 123.28 (s), 116.03 (d, *J* = 22.2 Hz), 19.18 (d, *J* = 4.0 Hz). ^{19}F NMR (376 MHz, CD_2Cl_2) δ -116.42 (dt, *J* = 11.4, 5.8 Hz). IR (film) ν (cm^{-1}) 2984, 1582, 1491, 1454, 1209, 1101, 1023, 791, 752 cm^{-1}. HR-MS (ESI) *m/z* calcd for $C_{12}H_{11}FN$ [$M+H^+$] 188.0870, found 188.0869.

3-Methyl-2-(3,4,5-trimethoxyphenyl)pyridine (L2)

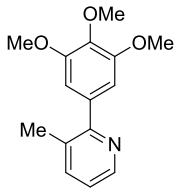

This compound was synthesized following general procedure **A** using 2-bromo-3-methylpyridine (400 mg, 2.32 mmol), 3,4,5-trimethoxy phenyl boronic acid (640 mg, 3.02 mmol), potassium carbonate (963 mg, 6.97 mmol) and $Pd(PPh_3)_2Cl_2$ (81 mg, 0.11 mmol) in THF:H_2O (12:4 ml). **L1** was isolated as a white solid (602 mg, 82%). ^{1}H NMR (400 MHz, CD_2Cl_2) δ 8.46 (dd, *J* = 4.7, 1.1 Hz, 1H), 7.59 (dd, *J* = 7.7, 1.0 Hz, 1H), 7.17 (dd, *J* = 7.7, 4.7 Hz, 1H), 6.73 (s, 2H), 3.86 (s, 6H), 3.83 (s, 3H), 2.36 (s, 3H). ^{13}C NMR (101 MHz, CD_2Cl_2) δ 159.09 (s), 153.57 (s), 147.30 (s), 138.96 (s), 138.50 (s), 136.94 (s), 131.34 (s), 122.59 (s), 106.98 (s), 61.05 (s), 56.66 (s), 20.51 (s). IR (film) ν (cm^{-1}) 2937, 1587, 1559, 1507, 1457, 1416, 1404, 1341, 1232, 1127, 1114, 1005, 841, 799 cm^{-1}. HR-MS (ESI) *m/z* calcd for $C_{15}H_{18}NO_3$ [M+H^+] 260.1281, found 260.1277.

General Procedure B:

A solution of ligand **L1-2** (1 equiv) in acetonitrile was slowly added to a sodium tetrachloroaurate dihydrate (1 equiv) solution in water. Immediate formation of a yellow/brown solid was observed. Reaction was stirred at 25°C for 2 to 3 hour. The resulting solid was filtered, washed with cold distilled water and dried, alternatively, the reaction mixture was diluted with distilled water and the organic compound was extracted with CH_2Cl_2 (15 x 3 ml). The organic phases were combined and dried over anhydrous magnesium sulfate. After evaporation of the solvent under reduced pressure, the product was obtained in reported yields. Compounds **L1-2AuCl$_3$** were prepared using general procedure **B**.

L1AuCl$_3$

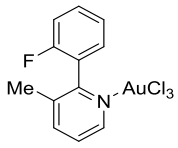

This compound was synthesized following general procedure **B** using **L1** (250 mg, 1.35 mmol) in acetonitrile (10 ml), sodium tetrachloroaurate dihydrate (531 mg, 0.59 mmol) in water (10 ml) to furnish the product as a dark yellow powder (647 mg, 99%). ^{1}H NMR (500 MHz, CD_2Cl_2) δ 8.66 (d, *J* = 5.8 Hz, 1H), 8.06 (d, *J* = 7.9 Hz, 1H), 7.80 – 7.66 (m, 3H), 7.50 (td, *J* = 7.6, 0.9 Hz, 1H), 7.32 (t, *J* = 9.0 Hz, 1H), 2.33 (s, 3H). ^{13}C NMR (101 MHz, CD_2Cl_2) δ 161.19 (s), 158.69 (s), 148.25 (s), 143.88 (s),

141.06 (s), 134.35 (d, *J* = 8.4 Hz), 131.65 (d, *J* = 1.8 Hz), 127.77 (s), 125.75 (d, *J* = 3.7 Hz), 124.67 (d, *J* = 15.6 Hz), 117.17 (d, *J* = 20.9 Hz), 19.88 (d, *J* = 2.7 Hz). ^{19}F NMR (376 MHz, $CDCl_2$) δ -109.83 – -109.93 (dt, *J* = 11.9, 6.4 Hz). IR (film) ν (cm^{-1}) 2987, 2971, 1462, 1393, 1383,1275, 1075, 1066, 764 cm^{-1}. HR-MS (EI) *m/z* calcd for $C_{12}H_{10}AuCl_3FN$ [M^+] 488.9522, found 488.9518. Anal. Calcd. For: $C_{12}H_{10}AuCl_3FN$: C, 29.38; H, 2.05; N, 2.86, found: C, 29.59; H, 2.11; N, 2.85.

L2AuCl$_3$

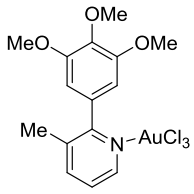

This compound was synthesized following general procedure **B** using **L1** (259 mg, 1.00 mmol) in acetonitrile (8 ml), sodium tetrachloroaurate dihydrate (397 mg, 1.00 mmol) in water (8 ml) to furnish the product as a dark red brown powder (562 mg, Quant.). Note: this compound was directly used in the cyclization step to get compound **2** (no NMR data is given as the compound partially cyclize in dichloromethane at room temperature).

L1Au(OAc^F)$_2$

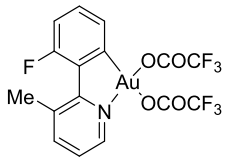

This compound was synthesized using the modified procedure from Tilset *et. al*.[1] In a 35 ml microwave vial, compound **L1** (200 mg, 1.07 mmol), $Au(OAc)_3$ (399 mg, 1.07 mmol) were dissolved in a mixture of TFA/water (5/5 ml). The reaction mixture was refluxed at 125°C for 30 minutes in a microwave oven. The reaction mixture was diluted with dichloromethane and the organic phase was washed with distilled water (10 x 3 ml). The organic phases were separated and dried with anhydrous magnesium sulfate. After evaporation of the solvent under reduced pressure, the residue was purified by a short chromatography column on silica gel to furnish the pure product as a yellowish powder (579 mg, 89%). ^{1}H NMR (400 MHz, CD_2Cl_2) δ 8.57 (dd, *J* = 5.9, 0.9 Hz, 1H), 8.11 (dd, *J* = 7.9, 0.8 Hz, 1H), 7.54 (dd, *J* = 7.9, 5.9 Hz, 1H), 7.40 (td, *J* = 8.2, 5.2 Hz, 1H), 7.25 (ddd, *J* = 12.0, 8.4, 1.0 Hz, 1H), 7.02 (dd, *J* = 8.0, 0.9 Hz, 1H), 2.68 (d, *J* = 11.3 Hz, 3H). ^{13}C NMR (126 MHz, CD_2Cl_2) δ 161.57 (d, *J* = 4.6 Hz), 160.88 (d, *J* = 39.4 Hz), 158.02 (s), 155.93 (s), 148.74 (s), 146.76 (s), 139.25 (d, *J* = 1.8 Hz), 137.65 (s), 133.47 (d, *J* = 9.2 Hz), 130.15 (d, *J* = 11.8 Hz), 125.34 (s), 124.54 (d, *J* = 2.6 Hz), 119.26 (d, *J* = 24.7 Hz), 117.34 (s), 115.05 (s), 23.32 (d, *J* = 23.3 Hz). ^{19}F NMR (376 MHz, CD_2Cl_2) δ -73.59 – -74.28

(m), -74.93 (s), -92.39 – -93.45 (m). IR (film) ν (cm^{-1}) 2973, 2906, 1735, 1703, 1592, 1402, 1167, 1144, 846, 780, 728 cm^{-1}. Anal. Calcd. For: $C_{16}H_9AuF_7NO_4$: C, 31.55; H, 1.49; N, 2.30, found: C, 31.45; H, 1.40; N, 2.33.

General Procedure C:

In a 35 ml microwave vial, compound **L1-2AuCl$_3$** (1 equiv.) was dissolved in a mixture of acetonitrile:water (1:4). The reaction mixture was refluxed at 120-160°C for 60 minutes in a microwave oven. The reaction mixture was diluted with distilled water and the aqueous layer was extracted with CH_2Cl_2 (3 x 15 ml). The organic phases were combined and dried with anhydrous magnesium sulfate. After evaporation of solvent under reduced pressure, the residue was purified by column chromatography on silica gel to furnish the pure product. Compounds **1-2** were prepared using general procedure **C**.

[(C^N)AuCl$_2$] (1)

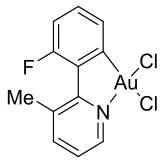

This compound was synthesized following general procedure **C** using **L1AuCl$_3$** (300 mg, 0.61 mmol) in acetonitrile:water (2:8 ml) at 160°C to obtain the product as a yellow solid (205 mg, 77%). ^{1}H NMR (400 MHz, CD_2Cl_2) δ 9.79 (dd, *J* = 5.9, 1.0 Hz, 1H), 8.03 (dd, *J* = 7.9, 0.9 Hz, 1H), 7.95 (dd, *J* = 8.1, 1.0 Hz, 1H), 7.52 (dd, *J* = 7.8, 5.9 Hz, 1H), 7.44 (td, *J* = 8.2, 5.4 Hz, 1H), 7.18 (ddd, *J* = 11.9, 8.3, 1.0 Hz, 1H), 2.61 (d, *J* = 11.3 Hz, 3H). ^{13}C NMR (126 MHz, CD_2Cl_2) δ 161.73 (s), 158.62 (s), 156.54 (s), 149.89 (s), 147.74 (s), 147.08 (s), 136.50 (s), 133.24 (d, *J* = 8.9 Hz), 127.12 (d, *J* = 2.7 Hz), 124.79 (s), 117.66 (d, *J* = 24.2 Hz), 23.08 (d, *J* = 22.6 Hz). ^{19}F NMR (376 MHz, CD_2Cl_2) δ -95.03 (pd, *J* = 11.1, 5.2 Hz). IR (film) ν (cm^{-1}) 2968, 1586, 1560, 1427, 1404, 1228, 1140, 869, 802, 778, 700 cm^{-1}. HR-MS (EI) *m/z* calcd for $C_{12}H_9AuCl_2FN$ [M^+] 452.9756, found 452.9764. Anal. Calcd. For: $C_{12}H_9AuCl_2FN$: C, 31.74; H, 2.00; N, 3.08, found: C, 31.81; H, 2.09; N, 3.02.

[(C^N)AuCl$_2$] (2)

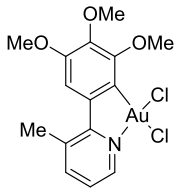

This compound was synthesized following general procedure **C** using **L2AuCl$_3$** (281 mg, 0.50 mmol) in acetonitrile:water (2:8 ml) at 120°C to obtain the product as yellow solid (228 mg, 87%). ^{1}H NMR (500 MHz, CD_2Cl_2) δ 9.75 (dd, *J* = 6.0, 1.2 Hz, 1H), 7.92 (dd, *J* = 7.7, 0.8 Hz, 1H), 7.34 – 7.29 (m, 2H), 3.92 (s, 3H), 3.92 (s, 3H), 3.86 (s, 3H), 2.83 (s, 3H). ^{13}C NMR (126 MHz, CD_2Cl_2) δ 163.68 (s), 154.65 – 154.38 (m), 153.89 (s), 148.10 (s), 147.24 (s), 146.15 (s), 140.20 (s), 139.45 (s), 133.74 (s), 122.99 (s), 109.65 (s), 62.99 (s), 61.45 (s), 56.86 (s), 23.14 (s). IR (film) ν (cm^{-1}) 2900, 1576, 1455, 1445, 1405, 1336, 1274, 1107, 999, 764, 754 cm^{-1}. HR-MS (EI) *m/z* calcd for $C_{15}H_{16}AuCl_2NO_3$ [M$^+$] 525.0167, found 525.0173. Anal. Calcd. For: $C_{15}H_{16}AuCl_2NO_3$: C, 34.24; H, 3.06; N, 2.66, found: C, 34.19; H, 3.07; N, 2.58.

[(C^N)Au(3,5-(CF$_3$)$_2$-C$_6$H$_3$-)Br] (5)

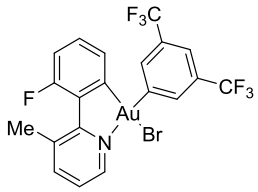

This compound was synthesized using the procedure from Tilset *et al*.[1] **L1Au(OAc^F)$_2$** (200 mg, 0.33 mmol), 3,5-bis(trifluoromethyl)phenylmagnesium bromide (200 mg, 0.66 mmol) in THF (15 ml) at –78°C to rt for 2 h. The compound **5** was obtained as a white solid (146 mg, 66%). ^{1}H NMR (500 MHz, CD_2Cl_2) δ 9.64 (d, *J* = 4.4 Hz, 1H), 7.98 (d, *J* = 6.0 Hz, 3H), 7.75 (s, 1H), 7.54 (dd, *J* = 7.8, 5.4 Hz, 1H), 7.25 (td, *J* = 8.0, 5.3 Hz, 1H), 7.10 (dd, *J* = 11.6, 8.4 Hz, 1H), 6.42 (dd, *J* = 7.7, 0.7 Hz, 1H), 2.57 (d, *J* = 10.6 Hz, 3H). ^{13}C NMR (126 MHz, CD_2Cl_2) δ 160.64 – 159.34 (m), 157.82 (s), 149.74 (s), 148.47 (s), 145.32 (s), 142.63 (s), 135.71 (s), 134.02 (s), 132.99 (d, *J* = 8.6 Hz), 132.18 (d, *J* = 10.0 Hz), 131.65 (q, *J* = 32.7 Hz), 128.85 (d, *J* = 2.7 Hz), 124.82 (s), 122.95 (s), 120.58 – 120.17 (m), 116.61 (d, *J* = 24.2 Hz), 22.37 (d, *J* = 21.2 Hz). IR (film) ν (cm^{-1}) 2968, 2900, 1589, 1465, 1347, 1270, 1116, 1094, 887, 783 cm^{-1}. HR-MS (EI) *m/z* calcd for $C_{20}H_{12}AuBrF_7N$ [M$^+$] 674.9707, found 674.9707. Anal. Calcd. For: $C_{20}H_{12}AuBrF_7N$: C, 35.53; H, 1.79; N, 2.07, found: C, 35.69; H, 1.74; N, 2.06.

[(C^N)Au(Me)Br] (6)

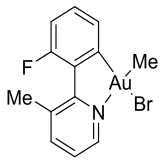

This compound was synthesized using the procedure from Tilset *et al*.[1] **L1Au(OAc^{F})$_2$** (500 mg, 0.82 mmol), methylmagnesium bromide (195 mg, 1.64 mmol) in THF (30 ml) at – 78°C to rt for 2 h. The compound **6** was obtained as a white solid (270 mg, 68%). ^{1}H NMR (500 MHz, CD_2Cl_2) δ 9.49 (d, *J* = 3.4 Hz, 1H), 7.88 (d, *J* = 7.4 Hz, 1H), 7.46 (dd, *J* = 9.2, 3.7 Hz, 2H), 7.37 (d, *J* = 6.9 Hz, 1H), 7.14 – 7.07 (m, 1H), 2.51 (d, *J* = 10.3 Hz, 3H), 1.70 (s, 3H). ^{13}C NMR (126 MHz, CD_2Cl_2) δ 160.41 (s), 158.74 (d, *J* = 3.5 Hz), 158.36 (s), 148.35 (s), 147.61 (s), 144.26 (s), 135.01 (s), 132.39 (d, *J* = 8.5 Hz), 125.22 (d, *J* = 2.6 Hz), 124.63 (s), 115.98 (d, *J* = 24.2 Hz), 22.13 (d, *J* = 20.7 Hz), 8.70 (s). ^{19}F NMR (471 MHz, CD_2Cl_2) δ -99.86 (s). IR (film) ν (cm^{-1}) 2973, 2900, 1580, 1459, 1437, 1231, 1116, 869, 843, 767, 707 cm^{-1}. HR-MS (ESI) *m/z* calcd for $C_{13}H_{12}AuBrFN$ [M$^+$] 476.9797, found 476.9790. Anal. Calcd. For: $C_{13}H_{12}AuBrFN$: C, 32.66; H, 2.53; N, 2.93, found: C, 32.89; H, 2.52; N, 2.86.

General Procedure D:

In a glovebox, a mixture of cyclometalated gold chloride/bromide complex (1 equiv) and silver fluoride (6-8 equiv) was dissolved in dry CH_2Cl_2 in a scintillation vial. The reaction was allowed to settle and the mixture was stirred for 22 h at 25°C and the reaction progress was monitored by NMR. The reaction mixture was allowed to settle and the mixture was filtered over a cotton path so that the corresponding gold fluoride was obtained after evaporation of the solvent under reduced pressure. Compounds **3, 4, 7-8** were prepared using general procedure **D**.

[(C^N)AuF$_2$] (3)

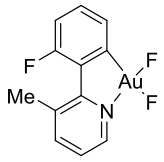

This compound was synthesized following general procedure **D** using **1** (40 mg, 0.09 mmol), silver fluoride (89 mg, 0.70 mmol) in dry CH_2Cl_2 (2 ml) to obtain the product as a white solid (36 mg, 99%).^{1}H NMR (500 MHz, CD_2Cl_2) δ 9.08 (d, *J* = 5.7 Hz, 1H), 8.03 (dd, *J* = 7.9, 0.8 Hz, 1H), 7.47 (dd, *J* = 7.7, 5.9 Hz, 1H), 7.39 – 7.33 (m, 2H), 7.17 (ddd, *J* = 12.5, 8.1, 1.5 Hz, 1H), 2.68 (d, *J* = 11.6 Hz, 3H). ^{13}C NMR (126 MHz, CD_2Cl_2) δ 161.62 (s), 157.81 (s), 155.73 (s), 148.08 (s), 146.86 (s), 136.59 (s), 132.84 (dd, *J* = 9.2, 2.2 Hz), 129.76 (d, *J* = 11.2 Hz), 124.52 (s), 124.44 (d, *J* = 2.9 Hz), 118.18 (dd, *J* = 25.1,

0.9 Hz), 23.39 (d, *J* = 24.0 Hz). ^{19}F NMR (471 MHz, CD_2Cl_2) δ -89.16 – -104.16 (m), -191.79 (d, *J* = 45.9 Hz), -252.42 (d, *J* = 34.9 Hz). IR (film) ν (cm^{-1}) 2987, 2971, 1590, 1406, 1393, 1384, 1275, 1233, 1066, 1055, 881, 702 cm^{-1}. Anal. Calcd. For: $C_{12}H_9AuF_3N$: C, 34.22; H, 2.15; N, 3.33, found: C, 34.22; H, 2.26; N, 3.22.

[(C^N)AuF$_2$] (4)

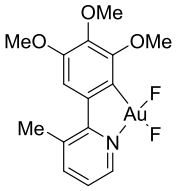

This compound was synthesized following general procedure **D** using **2** (100 mg, 0.19 mmol), silver fluoride (193 mg, 1.52 mmol) in dry CH_2Cl_2 (4 ml) to obtain the product as a yellow solid (93 mg, 99%). ^{1}H NMR (400 MHz, CD_2Cl_2) δ 9.05 (d, *J* = 5.0 Hz, 1H), 7.93 (ddd, *J* = 7.8, 1.4, 0.6 Hz, 1H), 7.29 (dd, *J* = 7.5, 6.2 Hz, 1H), 7.24 (s, 1H), 3.95 (s, 3H), 3.93 (s, 3H), 3.82 (d, *J* = 0.7 Hz, 3H), 2.81 (s, 3H). ^{13}C NMR (126 MHz, CD_2Cl_2) δ 163.20 (s), 155.76 (s), 154.16 (s), 147.72 (s), 146.45 (s), 146.01 (s), 139.30 (s), 133.95 (s), 122.61 (s), 109.54 (s), 63.31 (d, *J* = 5.9 Hz), 61.62 (s), 56.94 (s), 22.35 (s). ^{19}F NMR (376 MHz, CD_2Cl_2) δ -170.80 (d, *J* = 76.8 Hz), -281.22 (d, *J* = 67.6 Hz). IR (film) ν (cm^{-1}) 2947, 1577, 1556, 1447, 1419, 1392, 1336, 1102, 1089, 998 cm^{-1}.

[(C^N)Au(3,5-(CF$_3$)$_2$-C$_6$H$_3$-)F] (7)

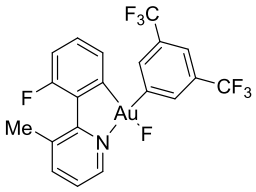

This compound was synthesized following general procedure **D** using **5** (50 mg, 0.07 mmol), silver fluoride (56 mg, 0.44 mmol) in dry CH_2Cl_2 (2 ml) to obtain the product as a white solid (45 mg, >99%). ^{1}H NMR (400 MHz, CD_2Cl_2) δ 8.95 (dd, *J* = 5.3, 1.5 Hz, 1H), 8.08 (s, 2H), 8.00 (dd, *J* = 7.9, 1.5 Hz, 1H), 7.81 (s, 1H), 7.60 (dd, *J* = 7.9, 5.3 Hz, 1H), 7.22 (td, *J* = 8.0, 5.4 Hz, 1H), 7.09 (ddd, *J* = 12.0, 8.4, 1.0 Hz, 1H), 6.70 (dd, *J* = 7.7, 1.0 Hz, 1H), 2.59 (d, *J* = 10.9 Hz, 3H). ^{13}C NMR (126 MHz, CD_2Cl_2) δ 159.55 (s), 158.39 (d, *J* = 3.9 Hz), 157.49 (s), 146.29 (s), 145.14 (s), 144.51 (s), 135.75 (s), 134.05 – 133.90 (m), 133.00 (d, *J* = 9.0 Hz), 131.36 (d, *J* = 32.7 Hz), 130.93 (d, *J* = 2.8 Hz), 125.18 (s), 124.39 (s), 123.01 (s), 121.07 (dd, *J* = 7.9, 3.9 Hz), 116.62 (d, *J* = 24.4 Hz), 22.52 (d, *J* = 22.0 Hz). ^{19}F NMR (376 MHz, CD_2Cl_2) δ -60.07 – -64.83 (m), -94.73 – -100.03 (m), -208.52 (s). IR (film) ν (cm^{-1}) 1587,

1465, 1349, 1272, 1183, 1102, 1091, 880, 784, cm^{-1}. Anal. Calcd. For: $C_{20}H_{12}AuF_8N$: C, 39.04; H, 1.97; N, 2.28, found: C, 39.17; H, 1.05; N, 2.29.

[(C^N)Au(Me)F] (8)

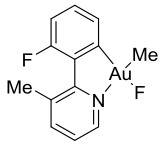

This compound was synthesized following general procedure **D** using **6** (100 mg, 0.21 mmol), silver fluoride (159 mg, 1.25 mmol) in dry CH_2Cl_2 (4 ml) to obtain the product as a white solid (87 mg, 99%). ^{1}H NMR (500 MHz, CD_2Cl_2) δ 8.82 (d, *J* = 4.8 Hz, 1H), 7.90 (d, *J* = 7.8 Hz, 1H), 7.52 (dd, *J* = 7.8, 5.2 Hz, 1H), 7.33 (dd, *J* = 7.9, 5.3 Hz, 1H), 7.28 (d, *J* = 7.4 Hz, 1H), 7.05 (dd, *J* = 11.7, 8.4 Hz, 1H), 2.51 (d, *J* = 10.8 Hz, 4H), 1.46 (s, 3H). ^{13}C NMR (126 MHz, CD_2Cl_2) δ 159.86 (s), 157.82 (s), 157.31 (d, *J* = 3.6 Hz), 145.18 (s), 144.46 (s), 135.08 (s), 132.36 (d, *J* = 8.7 Hz), 127.95 (d, *J* = 2.6 Hz), 124.30 (s), 115.78 (d, *J* = 24.3 Hz), 22.30 (d, *J* = 21.7 Hz).^{19}F NMR (471 MHz, CD_2Cl_2) δ -99.02, -220.85. IR (film) ν (cm^{-1}) 2989, 2916, 1582, 1562, 1464, 1443, 1405, 1232, 1121, 877, 796, 780, 709 cm^{-1}.

[(C^N)Au(C_6F_5)$_2$] (9a)

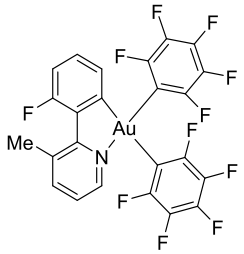

In the glovebox, a scintillation vial was charged with compound **3** (40 mg, 0.09 mmol) and dichloromethane (4 ml) is then added. Pentafluorophenyl boronic acid (44 mg, 0.21 mmol) was added to this solution. Reaction progress was followed by NMR, after 60 min the reaction vial is taken out of glovebox and solvent was evaporated under reduced pressure. The reaction crude was purified by silica gel chromatography to furnish compound **9a** as a white solid (55 mg, 81%). ^{1}H NMR (500 MHz, CD_2Cl_2) δ 8.21 (d, *J* = 4.5 Hz, 1H), 8.01 (dd, *J* = 7.8, 0.9 Hz, 1H), 7.38 – 7.31 (m, 2H), 7.13 – 7.05 (m, 1H), 6.68 (d, *J* = 6.7 Hz, 1H), 2.61 (d, *J* = 10.4 Hz, 3H). ^{13}C NMR (126 MHz, CD_2Cl_2) δ 163.64 (d, *J* = 4.1 Hz), 160.65 (s), 158.58 (s), 158.06 (s), 148.19 (s), 148.15 – 147.91 (m), 146.47 – 146.00 (m), 145.92 (s), 144.75 – 144.08 (m), 141.26 (qd, *J* = 14.1, 9.0 Hz), 139.99 – 139.06 (m), 137.97 – 137.16 (m), 134.13 (d, *J* = 8.1 Hz), 133.78 (d, *J* = 8.3 Hz), 129.75 (d, *J* = 2.7 Hz), 127.82 (t, *J* = 50.7 Hz), 124.86 (s), 116.53 (d, *J* = 24.4 Hz), 108.06 (t, *J* = 39.3 Hz), 22.75 (d, *J* = 21.4 Hz). ^{19}F NMR (376 MHz, CD_2Cl_2) δ -97.65 – -97.99 (m), -121.13 – -121.35 (m), -121.35 – -121.53 (m), -157.48 (t, *J* = 19.7 Hz),

-158.32 (t, *J* = 19.7 Hz), -161.04 – -161.24 (m), -161.86 – -162.05 (m). IR (film) ν (cm^{-1}) 2984, 2900, 1590, 1506, 1476, 1458, 1443, 957, 812, 783 cm^{-1}. HR-MS (EI) *m/z* calcd for $C_{24}H_9AuF_{11}N$ [M^+] 717.0219, found 717.0193.

4,4'-Di-*tert*-butyl-1,1'-biphenyl (10b)

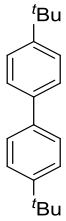

In the glovebox, a scintillation vial was charged with compound **3** (20 mg, 0.05 mmol) and dichloromethane (2 ml) is then added. 4-*tert*-Butylphenyl boronic acid (18.4 mg, 0.10 mmol) was added to this solution. Reaction progress was followed by NMR. After 60 min, the reaction vial is taken out of the glovebox and the solvent was evaporated under reduced pressure. The reaction crude was purified by silica gel chromatography to furnish compound **10b** as a white solid (9 mg, 72%). Spectroscopic data match with those previously reported in the literature.[2]

4'-(*tert*-Butyl)-3,5-bis(trifluoromethyl)-1,1'-biphenyl (12A)

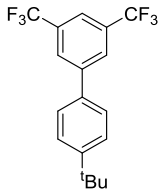

In the glovebox, a scintillation vial was charged with compound **7** (50 mg, 0.08 mmol) and dichloromethane (2 ml) is then added. 4-*tert*-Butylphenyl boronic acid (17.5 mg, 0.10 mmol) was added to this solution. Reaction progress was followed by NMR. After 60 min, the reaction vial is taken out of the glovebox and the solvent was evaporated under reduced pressure. The reaction crude was purified by silica gel chromatography to furnish compound **12A** as a colorless oil (16 mg, 57%). Spectroscopic data match with those previously reported in the literature. [2]

4'-Fluoro-3,5-bis(trifluoromethyl)-1,1'-biphenyl (12B)

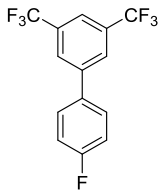

In the glovebox, a scintillation vial was charged with compound **7** (50 mg, 0.08 mmol) and dichloromethane (2 ml) is then added. 4-Fluorophenyl boronic acid (13.6 mg, 0.10 mmol) was added to this solution. Reaction progress was followed by NMR. After 60 min, the reaction vial is taken out of the glovebox and the solvent was evaporated under reduced pressure. The reaction crude was purified by silica gel chromatography to furnish compound **12B** as a colorless oil (8 mg, 32%). Spectroscopic data match with those previously reported in the literature.[3]

2-(3-Fluoro-3',5'-bis(trifluoromethyl)-[1,1'-biphenyl]-2-yl)-3-methylpyridine (13)

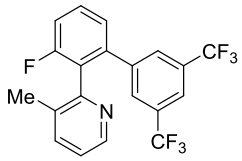

In the glovebox, a scintillation vial was charged with compound **7** (50 mg, 0.08 mmol) and dichloromethane (2 ml) is then added. 4-Fluorophenyl boronic acid (13.6 mg, 0.10 mmol) was added to this solution. Reaction progress was followed by NMR. After 60 min, the reaction vial is taken out of the glovebox and the solvent was evaporated under reduced pressure. The reaction crude was purified by silica gel chromatography to furnish compound **13** a colorless oil (22 mg, 68%). ^{1}H NMR (500 MHz, CD_2Cl_2) δ 8.42 (dd, *J* = 4.8, 1.0 Hz, 1H), 7.70 (s, 1H), 7.61 (s, 2H), 7.59 – 7.53 (m, 1H), 7.46 (dd, *J* = 7.8, 0.8 Hz, 1H), 7.34 (dd, *J* = 7.7, 0.5 Hz, 1H), 7.32 – 7.28 (m, 1H), 7.15 (dd, *J* = 7.8, 4.8 Hz, 1H), 1.95 (s, 3H). ^{13}C NMR (126 MHz, CD_2Cl_2) δ 161.65 (s), 159.70 (s), 153.06 (d, *J* = 0.7 Hz), 147.46 (s), 142.39 (d, *J* = 2.7 Hz), 140.71 (d, *J* = 3.6 Hz), 138.27 (s), 133.53 (s), 131.47 (q, *J* = 33.3 Hz), 130.78 (d, *J* = 9.0 Hz), 130.09 (dd, *J* = 3.6, 1.0 Hz), 128.14 (d, *J* = 18.5 Hz), 125.97 (d, *J* = 3.3 Hz), 123.63 (s), 121.32 (dt, *J* = 7.8, 3.9 Hz), 116.59 (d, *J* = 22.8 Hz), 18.75 (d, *J* = 1.1 Hz). ^{19}F NMR (376 MHz, CD_2Cl_2) δ -63.25 – -63.50 (m), -114.88 (dd, *J* = 9.9, 6.0 Hz). IR (film) ν (cm^{-1}) 1573, 1458, 1378, 1274, 1239, 1168, 1112, 1096, 899, 846, 745 cm^{-1}. HR-MS (ESI) *m/z* calcd for $C_{20}H_{13}AuF_7N$ [M+H$^+$] 400.0930, found 400.0949.

[(C^N)Au(3,5-$(CF_3)_2$-C_6H_3-)(2,4,6-$(F)_3$-C_6H_2-)] (11D)

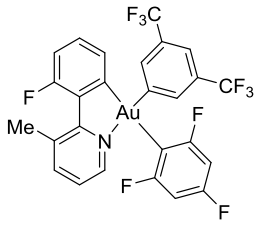

In the glovebox, a scintillation vial was charged with compound **7** (20 mg, 0.03 mmol) and dichloromethane (2 ml) is then added. 2,4,6-Trifluorophenyl boronic acid (6.8 mg, 0.04 mmol) was added to this solution. Reaction progress was followed by NMR. After 60 min, the reaction vial is taken out of the glovebox and the solvent was evaporated under reduced pressure. The reaction crude was purified by silica gel chromatography to furnish compound **11D** as a white solid (12 mg, 51%). ^{1}H NMR (400 MHz, CD_2Cl_2) δ 8.16 (d, *J* = 4.5 Hz, 1H), 7.96 – 7.92 (m, 3H), 7.64 (s, 1H), 7.35 – 7.27 (m, 2H), 7.03 (ddd, *J* = 12.2, 8.2, 1.0 Hz, 1H), 6.67 – 6.61 (m, 2H), 6.59 (d, *J* = 7.2 Hz, 1H), 2.58 (d, *J* = 10.3 Hz, 3H). ^{13}C NMR (101 MHz, CD_2Cl_2) δ 166.73 (dd, *J* = 24.6, 14.8 Hz), 164.64 – 164.16 (m), 163.09 (d, *J* = 4.1 Hz), 161.14 (s), 158.55 (s), 147.97 (s), 144.99 (s), 141.21 (s), 135.97 (d, *J* = 0.8 Hz), 134.24 (d, *J* = 7.3 Hz), 134.24 (d, *J* = 7.3 Hz), 133.40 (d, *J* = 3.3 Hz), 133.25 (d, *J* = 8.0 Hz), 131.52 (q, *J* = 32.6 Hz), 129.99 (d, *J* = 2.8 Hz), 125.48 (s), 124.36 (s), 122.77 (s), 119.72 – 119.13 (m), 115.57 (d, *J* = 24.3 Hz), 100.78 (ddd, *J* = 33.5, 24.6, 4.6 Hz), 22.47 (d, *J* = 20.9 Hz). ^{19}F NMR (376 MHz, CD_2Cl_2) δ -62.92 – -63.09 (m), -93.36 (t, *J* = 6.8 Hz), -99.81 – -100.28 (m), -113.40 – -113.91 (m). IR (film) ν (cm^{-1}) 2973, 2906, 1586, 1349, 1273, 1121, 994, 894, 842, 784 cm^{-1}. HR-MS (EI) *m/z* calcd for $C_{26}H_{14}AuF_{10}N$ [M^+] 727.0626, found 727.0624. Anal. Calcd. For: $C_{26}H_{14}AuF_{10}N$: C, 42.93; H, 1.94; N, 1.93, found: C, 43.06; H, 1.86; N, 1.89.

Complex (14C)

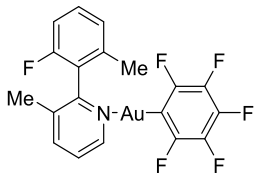

In the glovebox, a scintillation vial was charged with compound **8** (50 mg, 0.12 mmol) and dichloromethane (3 ml) is then added. Pentafluorophenyl boronic acid (30 mg, 0.14 mmol) was added to this solution. Reaction progress was followed by NMR. After 60 min, the reaction vial is taken out of the glovebox and the solvent was evaporated under reduced pressure. The reaction crude was purified by silica gel chromatography to furnish compound **14C** as a white solid (59 mg, 88%). ^{1}H NMR (500 MHz, CD_2Cl_2) δ 8.61 (dd, *J* = 5.5, 0.8 Hz, 1H), 7.98 (ddd, *J* = 7.9, 1.4, 0.7 Hz, 1H), 7.58 (dd, *J* = 7.8, 5.5 Hz, 1H), 7.45 (td, *J* = 8.0, 6.1 Hz, 1H), 7.19 (d, *J* = 7.7 Hz, 1H), 7.08 (dd, *J* = 13.1, 4.4 Hz, 1H),

2.16 (d, *J* = 28.9 Hz, 7H). ^{13}C NMR (126 MHz, CD_2Cl_2) δ 161.08 (s), 159.13 (s), 155.67 (s), 149.73 (s), 141.74 (s), 139.23 (s), 137.68 (s), 131.76 (d, *J* = 8.9 Hz), 126.78 (d, *J* = 3.0 Hz), 125.63 (s), 113.62 (d, *J* = 21.3 Hz), 19.75 (d, *J* = 2.4 Hz), 19.39 (s) (Note: ^{13}C signals for the C_6F_5 moiety are not compiled here due to their low intensity). ^{19}F NMR (471 MHz, CD_2Cl_2) δ -116.33 – -116.57 (m), -161.22 (t, *J* = 20.3 Hz), -163.73 – -164.84 (m). IR (film) ν (cm^{-1}) 2968, 2906, 1499, 1456, 1441, 952, 801, 783 cm^{-1}; HR-MS (EI) *m/z* calcd for $C_{19}H_{12}AuF_6N$ [M^+] 565.0534, found 565.0524. Anal. Calcd. For: $C_{19}H_{12}AuF_6N$: C, 40.37; H, 2.14, N, 2.48, found: C, 40.23; H, 2.12, N, 2.45.

Complex (14E)

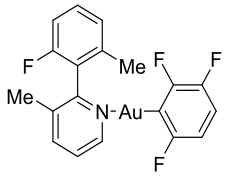

In the glovebox, a scintillation vial was charged with compound **8** (30 mg, 0.07 mmol) and dichloromethane (2 ml) is then added. 2,3,4-Trifluorophenyl boronic acid (15 mg, 0.09 mmol) was added to this solution. Reaction progress was followed by NMR. After 60 min, the reaction vial is taken out of the glovebox and the solvent was evaporated under reduced pressure. The reaction crude was purified by silica gel chromatography to furnish compound **14E** as a white solid (29 mg, 74%). ^{1}H NMR (500 MHz, CD_2Cl_2) δ 8.66 – 8.59 (m, 1H), 7.97 (dd, *J* = 7.9, 0.7 Hz, 1H), 7.56 (dd, *J* = 7.8, 5.5 Hz, 1H), 7.44 (td, *J* = 8.0, 6.0 Hz, 1H), 7.19 (d, *J* = 7.7 Hz, 1H), 7.07 (t, *J* = 8.8 Hz, 1H), 6.75 – 6.67 (m, 1H), 6.61 – 6.54 (m, 1H), 2.18 (s, 3H), 2.15 (s, 3H). ^{13}C NMR (126 MHz, CD_2Cl_2) δ 163.79 (ddd, *J* = 229.2, 19.8, 1.9 Hz), 160.07 (d, *J* = 244.9 Hz), 155.60 (s), 154.91 (ddd, *J* = 231.8, 23.0, 11.1 Hz), 149.71 (s), 147.42 (ddd, *J* = 242.8, 19.6, 4.0 Hz), 141.52 (s), 139.25 (d, *J* = 2.2 Hz), 137.51 (s), 131.61 (d, *J* = 8.9 Hz), 126.72 (d, *J* = 3.0 Hz), 125.85 (d, *J* = 16.2 Hz), 125.51 (s), 121.45 (ddd, *J* = 55.3, 48.6, 2.1 Hz), 113.99 (dd, *J* = 20.4, 9.5 Hz), 113.56 (d, *J* = 21.3 Hz), 109.36 (ddd, *J* = 33.2, 5.9, 3.3 Hz), 19.78 (d, *J* = 2.4 Hz), 19.37 (s). ^{19}F NMR (376 MHz, CD_2Cl_2) δ -93.89 – -94.01 (m), -112.37 (dd, *J* = 29.0, 10.1 Hz), -115.95 – -116.48 (m), -145.73 – -146.09 (m). HR-MS (EI) *m/z* calcd for $C_{19}H_{14}AuF_4N$ [H^+] 529.0728, found 529.0712.

For compounds 16a-d, the following work-up was carried out: after completion of the reaction, the solvent was evaporated under reduced pressure and compounds **16a-d** were purified by silica gel column chromatography using DCM/Hexane as eluent.

[(N^C^C)Au(4-*tert*Bu-C_6H_4-] (16a)

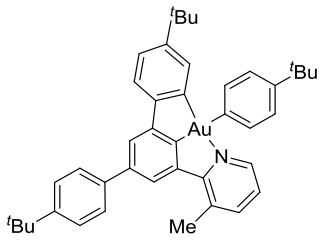

In a J-young tube, a mixture of **15** (50 mg, 0.77 mmol) and *4-tert*-butylphenyl boronic acid (15 mg, 0.08 mmol) in benzene (1 ml) was heated at 70 °C for 2 h. Reaction progress was followed by ^{1}H NMR. Compound **16a** was obtained as a light yellow solid (35 mg, 62% yield). ^{1}H NMR (500 MHz, CD_2Cl_2) δ 8.53 (d, *J* = 5.3 Hz, 1H), 7.91 (s, 1H), 7.74 (d, *J* = 7.7 Hz, 1H), 7.61 (dd, *J* = 8.4, 2.2 Hz, 5H), 7.52 (d, *J* = 8.4 Hz, 2H), 7.39 (d, *J* = 8.1 Hz, 2H), 7.36 (d, *J* = 8.0 Hz, 1H), 7.28 (d, *J* = 2.0 Hz, 1H), 7.22 – 7.17 (m, 2H), 2.83 (s, 3H), 1.40 (s, 9H), 1.38 (s, 9H), 1.19 (s, 9H). ^{13}C NMR (126 MHz, CD_2Cl_2) δ 181.74 (s), 172.08 (s), 166.91 (s), 154.57 (s), 151.71 (s), 151.13 (s), 151.05 (s), 149.51 (s), 147.70 (s), 146.84 (s), 145.39 (s), 144.48 (s), 139.98 (s), 137.25 (s), 134.57 (s), 134.08 (s), 127.48 (s), 126.42 (s), 125.69 (s), 125.40 (s), 124.47 (s), 123.91 (s), 121.96 (s), 121.08 (s), 35.42 (s), 35.09 (s), 34.79 (s), 31.93 (s), 31.78 (s), 31.59 (s), 23.07 (s). IR (film) ν (cm^{-1}) 2957, 2900, 2864, 1587, 1541, 1508, 1473, 1457, 1361, 1253, 1118, 828, 787 cm^{-1}. HR-MS (ESI) *m/z* calcd for $C_{42}H_{46}AuNNa$ [M+Na^+] 784.3188, found 784.3173.

[(N^C^C)Au(3,5-$(F)_2$-C_6H_3-)] (16b)

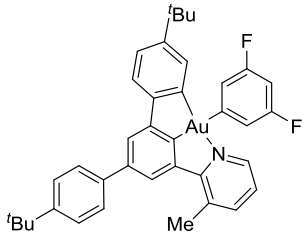

Same procedure as for compound **16a** using a mixture of **15** (20 mg, 0.03 mmol) and 3,5-difluorophenyl boronic acid (5.3 mg, 0.03 mmol). Compound **16b** was obtained as a light yellow solid (15 mg, 67% yield). ^{1}H NMR (400 MHz, CD_2Cl_2) δ 8.34 (dd, *J* = 5.4, 1.4 Hz, 1H), 7.90 (d, *J* = 1.2 Hz, 1H), 7.79 (dd, *J* = 7.8, 1.0 Hz, 1H), 7.62 – 7.60 (m, 2H), 7.59 (t, 1H), 7.53 (t, 1H), 7.51 (t, 1H), 7.38 (d, *J* = 7.8 Hz, 1H), 7.28 (dd, *J* = 2.4, 1.5 Hz, 1H), 7.27 – 7.22 (m, 2H), 7.21 (d, *J* = 2.1 Hz, 1H), 7.19 (dd, *J* = 3.9, 1.9 Hz, 1H), 6.66 (tt, *J* = 9.6, 2.4 Hz, 1H), 2.84 (s, 3H), 1.39 (s, 9H), 1.20 (s, 9H). ^{13}C NMR (101 MHz, CD_2Cl_2) δ 181.19 (s), 178.61 (t, *J* = 2.1 Hz), 166.37 (s), 165.52 (d, *J* = 9.9 Hz), 163.02 (d, *J* = 9.8 Hz), 154.26 (s), 151.71 – 151.10 (m), 149.18 (s), 146.80 (s), 145.24 (s), 144.77 (s), 141.16 (s), 139.67 (s), 134.79 (s), 133.66 (s), 127.42 (s), 126.41 (s), 125.39 (s), 124.73 (s), 124.16 (s), 122.14 (s), 121.28 (s),

118.77 (dd, *J* = 14.3, 3.7 Hz), 99.89 (t, *J* = 25.3 Hz), 35.29 (s), 35.05 (s), 31.70 (s), 31.51 (s), 23.05 (s). ^{19}F NMR (376 MHz, CD_2Cl_2) δ -113.79 – -113.88 (m). IR (film) ν (cm^{-1}) 2958, 1592, 1572, 1471, 1396, 1255, 1103, 968, 826, 791 cm^{-1}. HR-MS (ESI) *m/z* calcd for $C_{38}H_{36}AuF_2NNa$ [M+Na^+] 764.2373, found 764.2373.

[(N^C^C)Au(2,4,6-(F)$_3$-C$_6$H$_2$-)] (16c)

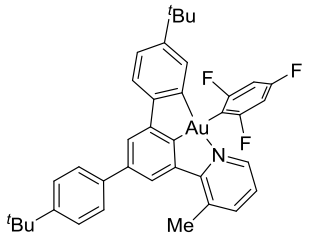

Same procedure as for compound **16a** using a mixture of **15** (20 mg, 0.03 mmol) and 2,4,6-trifluorophenyl boronic acid (5.8 mg, 0.033 mmol). Compound **16c** was obtained as a light yellow solid (17 mg, 76% yield). ^{1}H NMR (500 MHz, CD_2Cl_2) δ 8.38 (dd, *J* = 5.3, 1.2 Hz, 1H), 7.92 (d, *J* = 1.3 Hz, 1H), 7.82 (dd, *J* = 7.8, 0.9 Hz, 1H), 7.62 – 7.60 (m, 3H), 7.52 (d, *J* = 8.5 Hz, 2H), 7.38 (d, *J* = 8.0 Hz, 1H), 7.25 (dd, *J* = 7.7, 5.3 Hz, 1H), 7.21 (dd, *J* = 8.0, 2.0 Hz, 1H), 7.11 (d, *J* = 1.9 Hz, 1H), 6.78 – 6.73 (m, 2H), 2.86 (s, 3H), 1.39 (s, 9H), 1.19 (s, 9H). ^{13}C NMR (101 MHz, CD_2Cl_2) δ 176.63 (s), 168.54 – 167.56 (m), 165.65 (s), 153.79 (s), 151.83 (s), 151.63 (s), 151.21 (s), 149.79 (s), 147.07 (s), 144.98 (s), 144.88 (s), 141.39 (s), 139.53 (s), 134.75 (s), 134.07 (s), 127.41 (s), 126.41 (s), 125.47 (s), 124.79 (s), 124.40 (s), 122.13 (s), 121.50 (s), 101.12 – 97.62 (m), 35.21 (s), 35.05 (s), 31.69 (s), 31.44 (s), 23.01 (s). ^{19}F NMR (376 MHz, CD_2Cl_2) δ -88.24 (t, *J* = 6.1 Hz), -115.27 (dq, *J* = 9.1, 7.1 Hz). IR (film) ν (cm^{-1}) 2952, 1586, 1401, 1101, 991, 831, 787 cm^{-1}. HR-MS (ESI) *m/z* calcd for $C_{38}H_{35}AuF_3NNa$ [M+Na^+] 782.2279, found 782.2278. Anal. Calcd. For: $C_{38}H_{35}AuF_3N$: C, 60.08; H, 4.64; N, 1.84, found: C, 60.07; H, 4.80; N, 1.70.

[(N^C^C)Au(C$_6$F$_5$)] (16d)

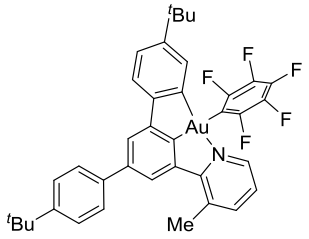

Same procedure as for compound **16a** using a mixture of **15** (20 mg, 0.03 mmol) and pentafluorophenyl boronic acid (7.1 mg, 0.03 mmol). Compound **16d** was obtained as a white solid (20 mg, 81% yield). ^{1}H NMR (500 MHz, CD_2Cl_2) δ 8.31 (d, *J* = 5.4 Hz, 1H), 7.93 (s, 1H), 7.86 (d, *J* = 7.7 Hz, 1H), 7.62 (d,

J = 5.3 Hz, 3H), 7.53 (d, *J* = 8.1 Hz, 2H), 7.39 (d, *J* = 8.1 Hz, 1H), 7.30 – 7.26 (m, 1H), 7.23 (d, *J* = 7.9 Hz, 1H), 7.04 (s, 1H), 2.88 (s, 3H), 1.39 (s, 9H), 1.21 (s, 9H). ^{19}F NMR (471 MHz, CD_2Cl_2) δ -118.81 (dd, *J* = 28.4, 9.1 Hz), -159.36 (t, *J* = 19.8 Hz), -161.18 – -164.17 (m). Note: due to poor solubility ^{13}C NMR could not be recorded. IR (film) ν (cm^{-1}) 2963, 1588, 1500, 1478, 1461, 1449, 1434, 1421, 1393, 1384, 1348, 1254, 1126, 1064, 1056, 1048, 954, 829, 789, 779 cm^{-1}. HR-MS (ESI) *m/z* calcd for $C_{38}H_{34}AuF_5N$ [M+H$^+$] 796.2272, found 796.2253. Anal. Calcd. For: $C_{38}H_{33}AuF_5N$: C, 57.36; H, 4.18; N, 1.76, found: C, 57.38; H, 4.15; N, 1.71.

3. Reductive Elimination on 11D

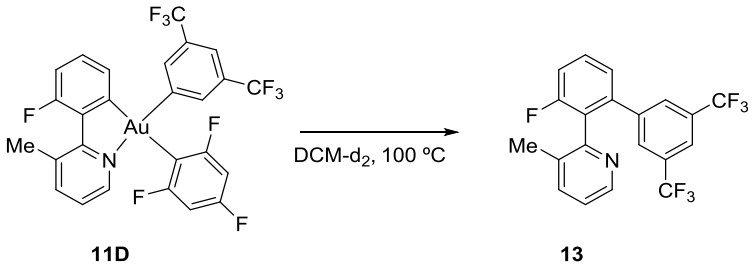

11D **13**

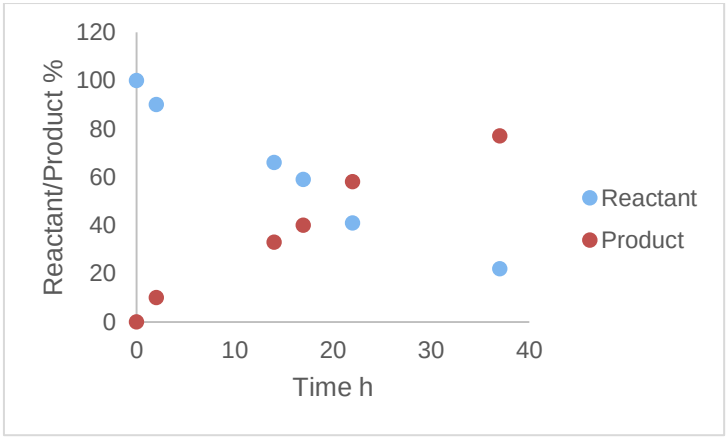

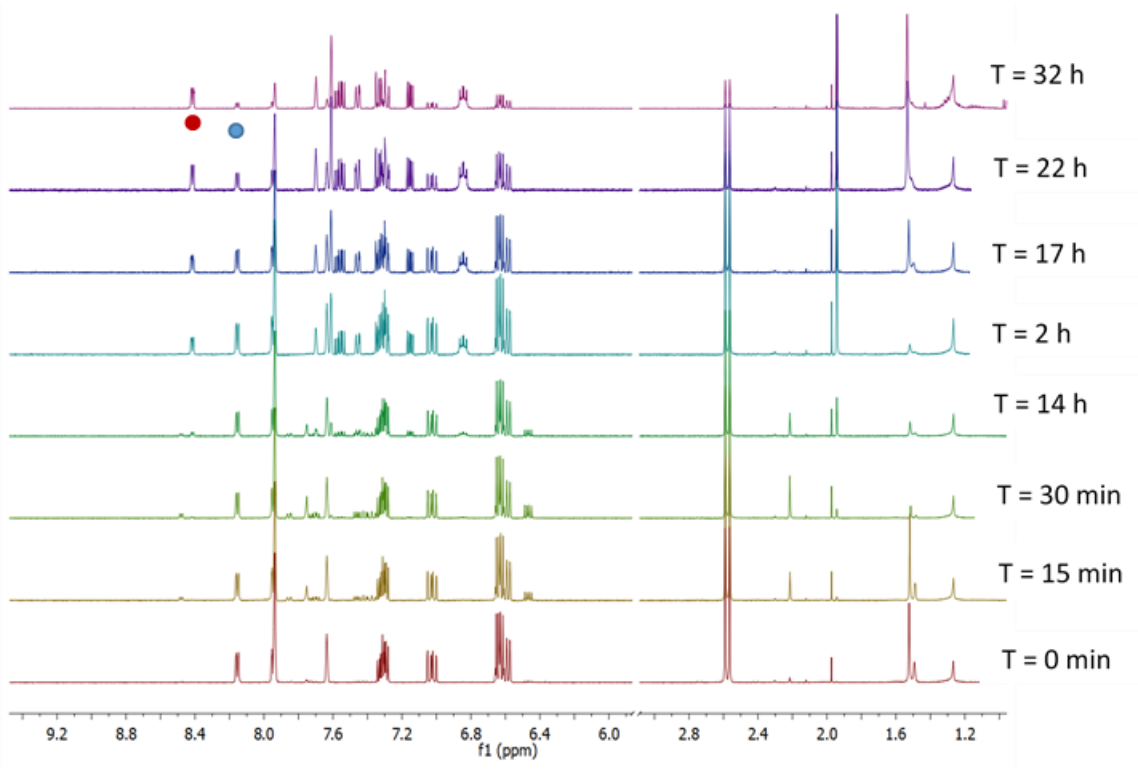

^{1}H NMR traces of reductive elimination on **11D** at 100°C in CD_2Cl_2.

4. Reductive Elimination on 7

For both compounds **7** and **8** no change was observed when heated up in solution up to 80 ºC. Only at 100 ºC, slow conversion to **13** was observed for **7** (**8** remain unreacted under those conditions). These results confirm that intramolecular reductive elimination product **13** observed in the experiments summarized in Table 1 do not stem from reductive elimination on gold(III)-monofluoride complexes **7**, **8**.

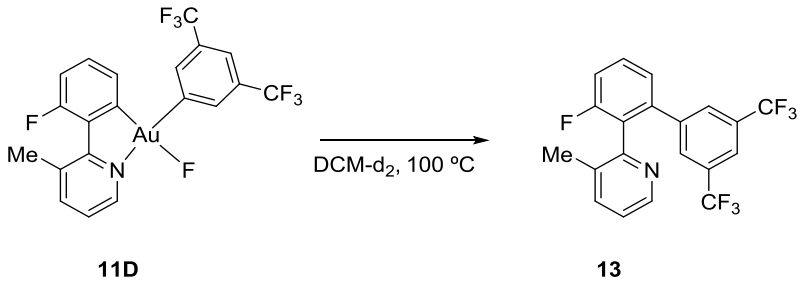

11D **13**

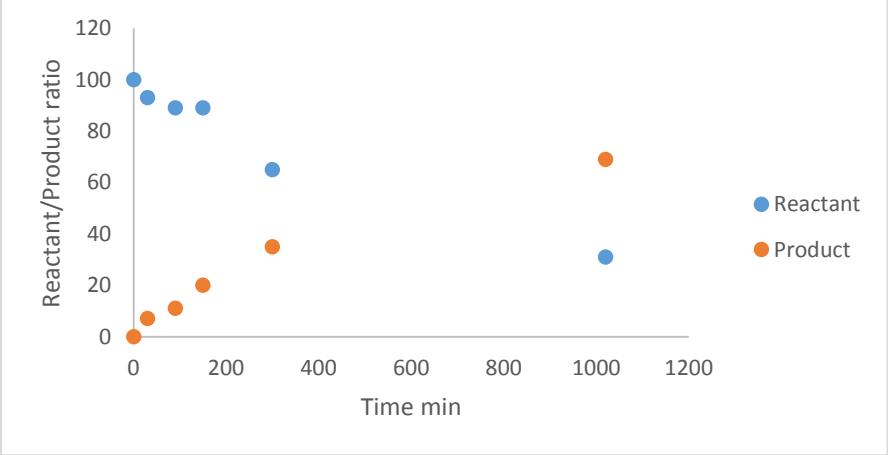

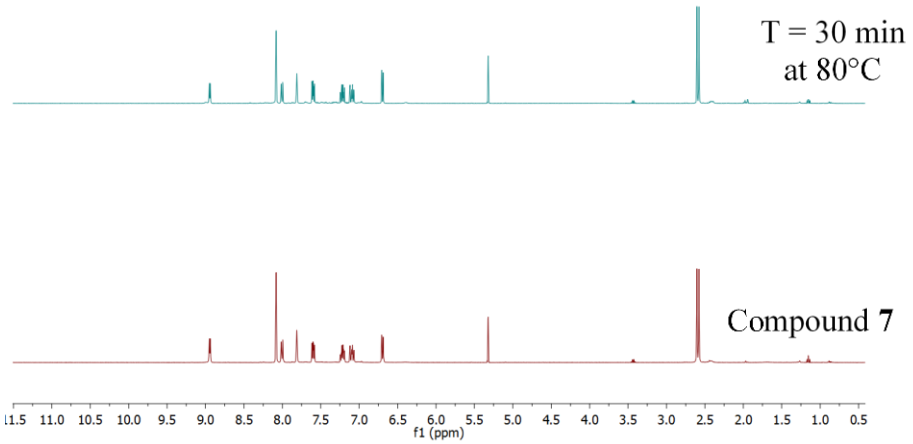

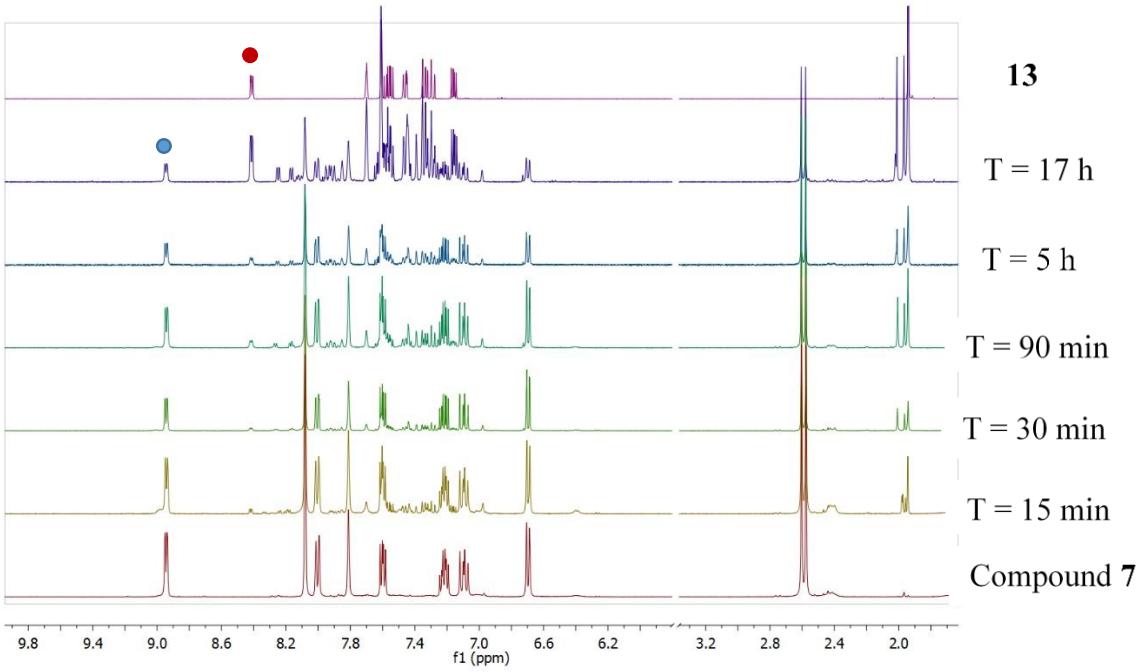

^{1}H NMR traces of reductive elimination on **7** at 100°C in CD_2Cl_2.

5. Reaction of complexes 7 and 8 with boronic acids at low temperature

General procedure:

In the glovebox, a J-young tube was charged with compounds **7** or **8** (0.04 mmol) and dichloromethane-d_2 (1 ml) was then added. The solution was cooled down to -78 °C and boronic acid (0.05 mmol) was added. Reaction progress was followed by ^{1}H NMR (starting from -40 °C to 20 °C) over the indicated period of time. Trimethoxybenzene was used as internal standard (**IS**).

Reaction of complex **7** with (4-*tert*-butylphenyl) boronic acid (**A**) at low temperature in CD_2Cl_2.

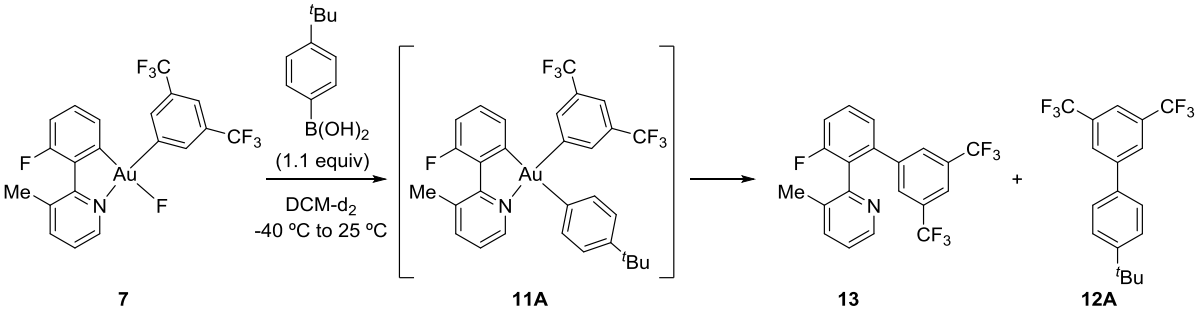

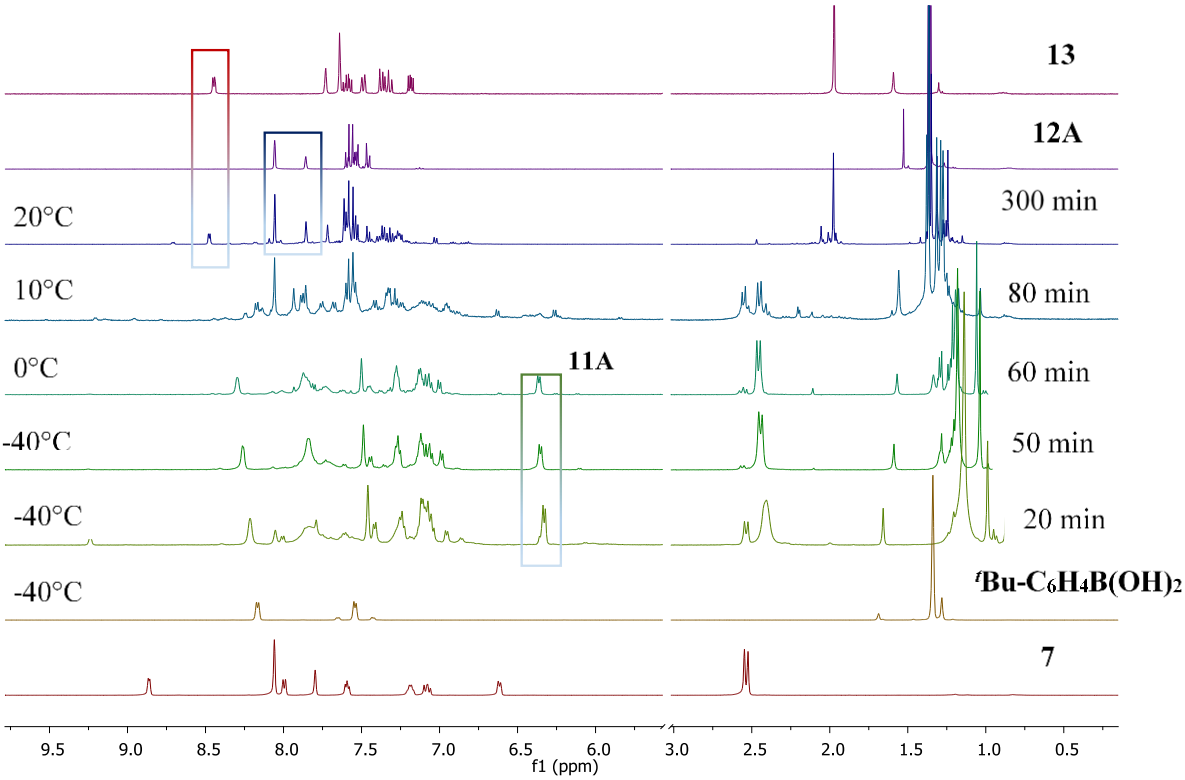

Reaction of complex **8** with boronic acid (**A**)

The signals of compound **12A´** and **10b** detected in the reaction mixture match with those previously reported in the literature.[4] Conversion to the products was determined using trimethoxybenzene as internal standard (**IS**).

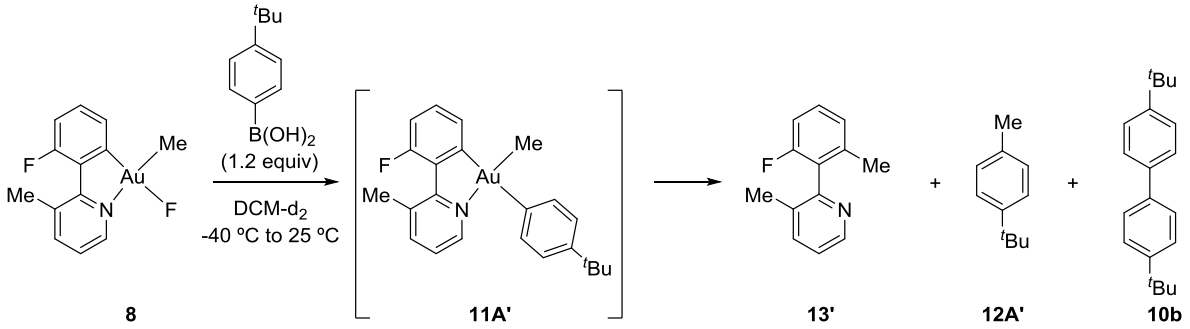

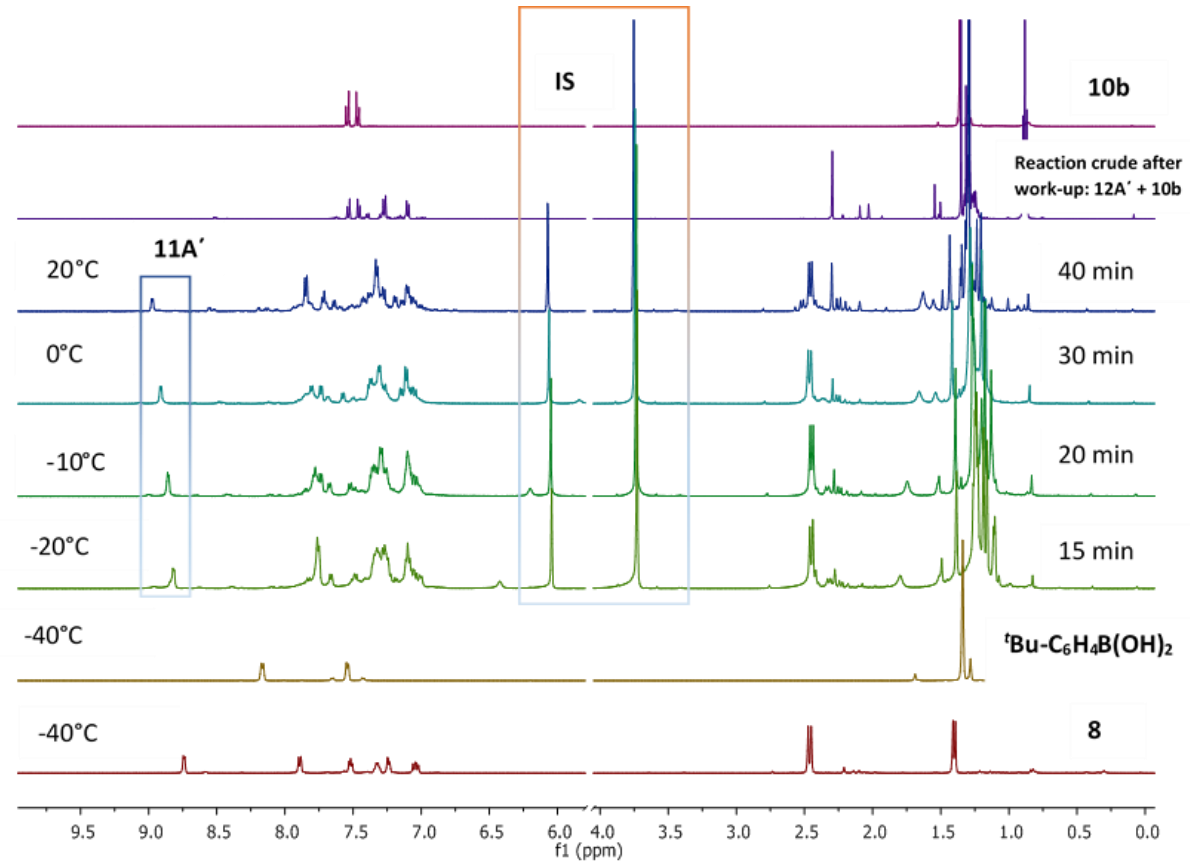

Reaction of complex **8** with boronic acid (**B**) at low temperature

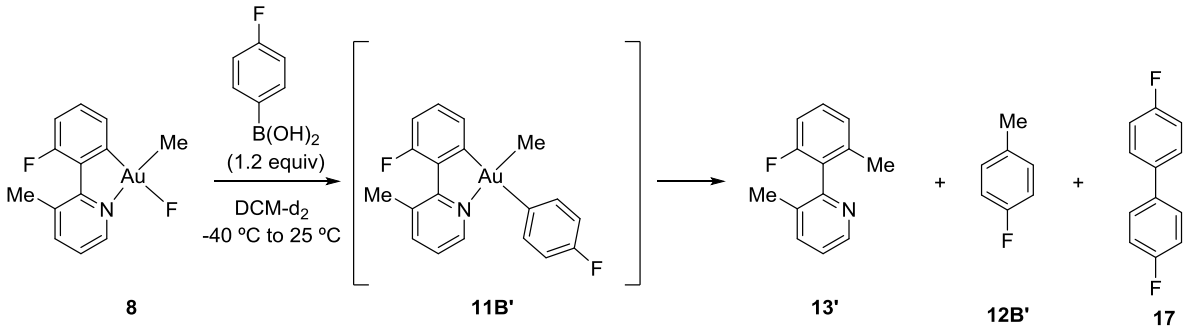

Spectroscopic data of compound **12B´** and **17** match with those reported in the literature.[5],[6]

6. Catalytic Experiments

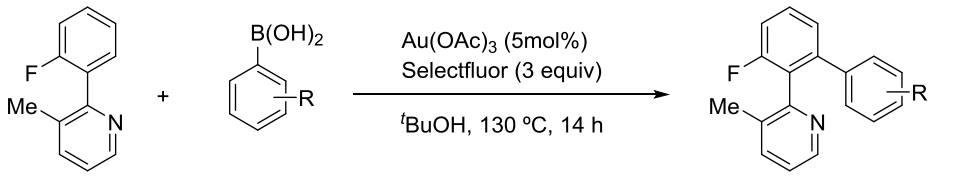

R = 3,5-bis-trifluoromethyl, **13** (53%)
R = 4-fluoro, **18** (37%)
R = 4-*tert*-butyl, **19** (41%)

General procedure (E) for the catalytic arylation of 2-(2-fluorophenyl)-3-methylpyridine

In a 5ml dry schlenk tube, a mixture of 2-(2-fluorophenyl)-3-methylpyridine (0.2 mmol), arylboronic acid (0.6 mmol), Selectfluor (0.6 mmol) and gold triacetate (0.01 mmol) was dissolved in *tert*-butanol (2 ml). The reaction mixture was heated at 130°C for 14 h. The reaction was then cooled down to room temperature and was diluted with distilled water. The organic compound was extracted with CH_2Cl_2 (3 x 10 ml). The organic phases were combined and dried over anhydrous magnesium sulfate and the solvent was evaporated under reduced pressure. The residue was purified by chromatography on silica gel using dichloromethane/acetone (98/2) as eluent. Compounds **13, 18** and **19** were obtained using this general procedure.

2-(3-Fluoro-3',5'-bis(trifluoromethyl)-[1,1'-biphenyl]-2-yl)-3-methylpyridine (13)

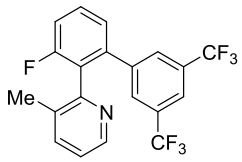

This compound was synthesized following general procedure **E** using 2-(2-fluorophenyl)-3-methylpyridine (37 mg, 0.2 mmol), (3,5-bis(trifluoromethyl)phenyl)boronic acid (155 mg, 0.6 mmol), Selectfluor (213 mg, 0.6 mmol), $Au(OAc)_3$ (3.7 mg, 0.01 mmol) in 2 ml ^{t}BuOH. The product was obtained as a colorless oil (42 mg, 53 %).

2-(3,4'-Difluoro-[1,1'-biphenyl]-2-yl)-3-methylpyridine (18)

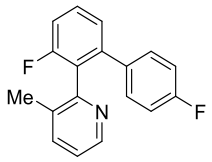

This compound was synthesized following general procedure **E** using 2-(2-fluorophenyl)-3-methylpyridine (37 mg, 0.20 mmol), (4-fluorophenyl)boronic acid (81 mg, 0.60 mmol), selectfluor (213 mg, 0.60 mmol), $Au(OAc)_3$ (3.7 mg, 0.01 mmol) in (2) ml ^{t}BuOH. The product was obtained as a colorless oil (21 mg, 37 %). ^{1}H NMR (500 MHz, CD_2Cl_2) δ 8.42 (d, *J* = 4.4 Hz, 1H), 7.47 (td, *J* = 8.0, 5.8 Hz, 1H), 7.43 (dd, *J* = 7.7, 0.7 Hz, 1H), 7.26 (d, *J* = 7.6 Hz, 1H), 7.19 (t, *J* = 8.8 Hz, 1H), 7.14 (dd, *J* = 7.7, 4.8 Hz, 1H), 7.09 (dd, *J* = 8.8, 5.4 Hz, 2H), 6.86 (t, *J* = 8.8 Hz, 2H), 1.92 (s, 3H). ^{13}C NMR (126 MHz, CD_2Cl_2) δ 163.51 (s), 161.57 (d, *J* = 4.0 Hz), 159.64 (s), 154.04 (s), 147.22 (s), 142.76 (d, *J* = 3.3 Hz), 138.01 (s), 136.52 (t, *J* = 3.0 Hz), 133.41 (s), 131.43 (d, *J* = 8.1 Hz), 130.19 (d, *J* = 9.1 Hz), 127.79 (d, *J* = 17.4 Hz), 126.12 (d, *J* = 3.0 Hz), 123.24 (s), 115.15 (dd, *J* = 22.1, 11.0 Hz), 18.84 (s). ^{19}F NMR (471 MHz, CD_2Cl_2) δ -99.02, -220.85. IR (film) ν (cm^{-1}) 1604, 1571, 1511, 1457, 1232, 1222, 1159, 892, 838, 795 cm^{-1}. HR-MS (ESI) *m/z* calcd for $C_{18}H_{14}F_2N$ [M+H$^+$] 382.1088, found 382.1086.

2-(4'-(*tert*-Butyl)-3-fluoro-[1,1'-biphenyl]-2-yl)-3-methylpyridine (19)

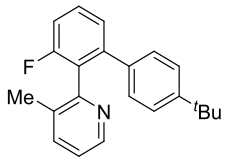

This compound was synthesized following general procedure **E** using 2-(2-fluorophenyl)-3-methylpyridine (37 mg, 0.20 mmol), (4-(*tert*-butyl)phenyl)boronic acid (107 mg, 0.60 mmol), selectfluor (213 mg, 0.60 mmol), $Au(OAc)_3$ (3.7 mg, 0.01 mmol) in (2 ml) ^{t}BuOH. The product was

obtained as a colorless oil (26 mg, 41 %). ^{1}H NMR (500 MHz, CD_2Cl_2) δ 8.43 (d, *J* = 4.7 Hz, 1H), 7.49 – 7.42 (m, 2H), 7.28 (d, *J* = 7.7 Hz, 1H), 7.19 (d, *J* = 8.2 Hz, 2H), 7.14 (dd, *J* = 7.9, 5.1 Hz, 2H), 7.03 (d, *J* = 8.2 Hz, 2H), 1.93 (s, 3H), 1.25 (d, *J* = 0.6 Hz, 9H). ^{13}C NMR (126 MHz, CD_2Cl_2) δ 161.64 (s), 159.70 (s), 154.39 (s), 150.59 (s), 147.14 (s), 143.62 (d, *J* = 3.3 Hz), 137.87 (s), 137.42 (d, *J* = 2.6 Hz), 133.54 (s), 130.07 (d, *J* = 9.2 Hz), 129.29 (s), 126.30 (d, *J* = 3.1 Hz), 125.33 (s), 123.13 (s), 114.66 (d, *J* = 22.8 Hz), 34.84 (s), 31.52 (s), 18.91 (d, *J* = 0.9 Hz). ^{19}F NMR (376 MHz, CD_2Cl_2) δ -116.09 (dd, *J* = 9.3, 5.7 Hz). IR (film) ν (cm^{-1}) 2961, 1612, 1457, 1261, 1235, 884, 837, 791, 750 cm^{-1}. HR-MS (ESI) *m/z* calcd for $C_{22}H_{23}FN$ [$M+H^+$] 320.1809, found 320.1805.

7. X-Ray Diffraction Analysis data for compounds 1-5, 7-8, 9a, 11D, 14C, 15, 16a, and 16b.

The CCDC numbers contain the supplementary crystallographic data for this paper. These data can be obtained free of charge from the Cambridge Crystallographic Data Centre via www.ccdc.cam.ac.uk/data_request/cif.

Crystallographic Analysis

Compound 1 (CCDC 1487417)

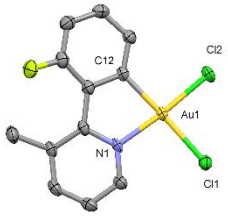

Table 1. *Crystallographic Data*

Crystallised from		CH_2Cl_2 / pentane
Empirical formula		$C_{12}H_9AuCl_2FN$
Formula weight [g mol^{-1}]		454.08
Crystal colour, habit		colourless, needle
Crystal dimensions [mm]		0.05 × 0.10 × 0.35
Temperature [K]		160(1)
Crystal system		orthorhombic
Space group		*Pbca* (#61)
Z		8
Reflections for cell determination		74428
2θ range for cell determination [°]		4–60
Unit cell parameters	*a* [Å]	7.8063(1)
	b [Å]	17.0746(3)

	c [Å]	17.8920(3)
	α [°]	90
	β [°]	90
	γ [°]	90
	V [Å^3]	2384.81(6)
F(000)		1680
D_X [g cm^{-3}]		2.529
μ(Mo $K\alpha$) [mm^{-1}]		12.814
Scan type		ϕ and ω
2θ(max) [°]		60
Transmission factors (min; max)		0.035; 0.484
Total reflections measured		42122
Symmetry independent reflections		3473
R_{int}		0.065
Reflections with $I > 2\sigma(I)$		2872
Reflections used in refinement		3471
Parameters refined		155
Final $R(F)$ [$I > 2\sigma(I)$ reflections]		0.0257
	$wR(F^2)$ (all data)	0.0582
Weights:	$w = [\sigma^2(F_O^2) + (0.0202P)^2 + 8.5508P]^{-1}$ where $P = (F_O^2 + 2F_C^2)/3$	
Goodness of fit		1.075

Final Δ_{max}/σ	0.001
$\Delta\rho$ (max; min) [e Å^{-3}]	1.90; -1.10
$\sigma(d_{(C-C)})$ [Å]	0.005 – 0.007

Compound 2 (CCDC 1487425)

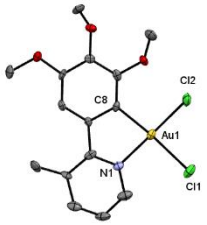

Table 2. *Crystallographic Data*

Crystallised from	CH_2Cl_2 / hexane
Empirical formula	$C_{15}H_{16}AuCl_2NO_3$
Formula weight [g mol^{-1}]	526.17
Crystal colour, habit	yellow, plate
Crystal dimensions [mm]	0.04 × 0.12 × 0.20
Temperature [K]	160(1)
Crystal system	triclinic
Space group	$P\bar{1}$ (#2)
Z	4
Reflections for cell determination	19431
2□ range for cell determination [°]	5–58
Unit cell parameters a [Å]	7.45780(10)

b [Å]	11.0845(2)
c [Å]	19.2172(5)
α [°]	84.5978(18)
β [°]	89.4342(18)
γ [°]	87.8411(14)
V [Å^3]	1580.40(5)
F(000)	1000
D_X [g cm^{-3}]	2.211
μ(Mo $K\alpha$) [mm^{-1}]	9.689
Scan type	ω
2θ(max) [°]	58.4
Transmission factors (min; max)	0.580; 1.000
Total reflections measured	37208
Symmetry independent reflections	17289
R_{int}	0.056
Reflections with $I > 2\sigma(I)$	14884
Reflections used in refinement	17286
Parameters refined	406
Final $R(F)$ [$I > 2\sigma(I)$ reflections]	0.0422
$wR(F^2)$ (all data)	0.1122

Weights: $w = [\sigma^2(F_o^2) + (0.0653P)^2 + 6.5943P]^{-1}$ where $P = (F_o^2 + 2F_c^2)/3$

Goodness of fit	1.066
Final Δ_{max}/σ	0.001
$\Delta\rho$ (max; min) [e Å^{-3}]	1.70; -1.80
$\sigma(d_{(C-C)})$ [Å]	0.013 – 0.017

Compound 3 (CCDC 1486854)

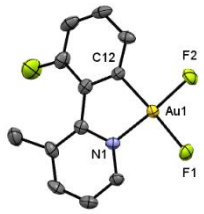

Table 3. *Crystallographic Data*

Crystallised from	CH_2Cl_2/ pentane
Empirical formula	$C_{12}H_9AuF_3N$
Formula weight [g mol^{-1}]	421.17
Crystal colour, habit	colourless, plate
Crystal dimensions [mm]	0.04 × 0.19 × 0.27
Temperature [K]	160(1)
Crystal system	orthorhombic
Space group	*Pbca* (#61)
Z	8
Reflections for cell determination	10144
2θ range for cell determination [°]	6–60

Unit cell parameters	a [Å]	7.45956(14)
	b [Å]	16.6803(2)
	c [Å]	16.8248(4)
	α [°]	90
	β [°]	90
	γ [°]	90
	V [Å^3]	2093.48(7)
F(000)		1552
D_x [g cm^{-3}]		2.673
μ(Mo $K\alpha$) [mm^{-1}]		14.069
Scan type		ω
$2\theta_{(max)}$ [°]		60.9
Transmission factors (min; max)		0.108; 0.628
Total reflections measured		23823
Symmetry independent reflections		2998
R_{int}		0.044
Reflections with $I > 2\sigma(I)$		2330
Reflections used in refinement		2998
Parameters refined		155
Final $R(F)$ [$I > 2\sigma(I)$ reflections]		0.0299
$wR(F^2)$ (all data)		0.0676

Weights:	$w = [\sigma^2(F_o^2) + (0.0199P)^2 + 12.6096P]^{-1}$ where $P = (F_o^2 + 2F_c^2)/3$
Goodness of fit	1.090
Final Δ_{max}/σ	0.001
$\Delta\rho$ (max; min) [e Å^{-3}]	2.15; -1.76
$\sigma(d_{(C-C)})$ [Å]	0.007 – 0.010

Compound 4 (CCDC 1486862)

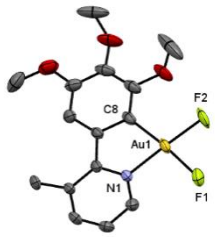

Table 4. *Crystallographic Data*

Crystallised from	CH_2Cl_2 / pentane
Empirical formula	$C_{15.5}H_{17}AuClF_2NO_3$
Formula weight [g mol^{-1}]	535.72
Crystal colour, habit	yellow, prism
Crystal dimensions [mm]	0.15 × 0.17 × 0.21
Temperature [K]	160(1)
Crystal system	monoclinic
Space group	*C*2/*c* (#15)
Z	8
Reflections for cell determination	5785

2□ range for cell determination [°]		4–59
Unit cell parameters	*a* [Å]	13.7561(2)
	b [Å]	16.1000(8)
	c [Å]	14.8396(2)
	α [°]	90
	β [°]	101.2087(15)
	γ [°]	90
	V [Å^3]	3223.86(18)
F(000)		2040
D_X [g cm^{-3}]		2.207
μ(Mo *K*α) [mm^{-1}]		9.327
Scan type		ω
2θ(max) [°]		58.8
Transmission factors (min; max)		0.508; 1.000
Total reflections measured		8280
Symmetry independent reflections		4068
R_{int}		0.018
Reflections with $I > 2\sigma(I)$		3745
Reflections used in refinement		4067
Parameters refined		217
Final	$R(F)$ [$I > 2\sigma(I)$ reflections]	0.0366
	$wR(F^2)$ (all data)	0.0777

Weights:	$w = [\sigma^2(F_o^2) + (0.0206P)^2 + 42.4267P]^{-1}$ where $P = (F_o^2 + 2F_c^2)/3$
Goodness of fit	1.046
Final Δ_{max}/σ	0.002
$\Delta\rho$ (max; min) [e Å^{-3}]	3.06; -3.00
$\sigma(d_{(C-C)})$ [Å]	0.006 – 0.010

Compound 5 (CCDC 1487420)

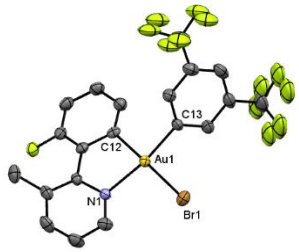

Table 5. *Crystallographic Data*

Crystallised from	CH_2Cl_2 / pentane
Empirical formula	$C_{20}H_{12}AuBrF_7N$
Formula weight [g mol^{-1}]	676.18
Crystal colour, habit	colourless, prism
Crystal dimensions [mm]	0.28 × 0.30 × 0.35
Temperature [K]	160(1)
Crystal system	triclinic
Space group	$P\bar{1}$ (#2)
Z	2

Reflections for cell determination		54208
2θ range for cell determination [°]		4–60
Unit cell parameters	a [Å]	9.0882(1)
	b [Å]	9.6379(1)
	c [Å]	13.1489(2)
	α [°]	76.8345(8)
	β [°]	74.7697(9)
	γ [°]	64.6373(9)
	V [Å^3]	995.35(2)
F(000)		632
D_x [g cm^{-3}]		2.256
μ(Mo $K\alpha$) [mm^{-1}]		9.499
Scan type		ϕ and ω
2θ(max) [°]		60
Transmission factors (min; max)		0.099; 0.215
Total reflections measured		27530
Symmetry independent reflections		5820
R_{int}		0.059
Reflections with $I > 2\sigma(I)$		5454
Reflections used in refinement		5820
Parameters refined; restraints		329; 276
Final $R(F)$ [$I > 2\sigma(I)$ reflections]		0.0331

$wR(F^2)$ (all data)	0.0896
Weights:	$w = [\sigma^2(F_O^2) + (0.0456P)^2 + 3.9518P]^{-1}$ where $P = (F_O^2 + 2F_C^2)/3$
Goodness of fit	1.068
Secondary extinction coefficient	0.0054(5)
Final Δ_{max}/σ	0.001
$\Delta\rho$ (max; min) [e Å^{-3}]	1.82; -1.97
$\sigma(d_{(C-C)})$ [Å]	0.007 – 0.001

Compound 7 (CCDC 1486864)

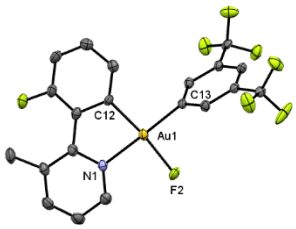

Table 6. *Crystallographic Data*

Crystallised from	dichloromethane / pentane
Empirical formula	$C_{20}H_{12}AuF_8N$
Formula weight [g mol^{-1}]	615.28
Crystal colour, habit	purple, needle
Crystal dimensions [mm]	0.13 × 0.13 × 0.35
Temperature [K]	160(1)
Crystal system	orthorhombic
Space group	*Pna*2$_1$ (#33)

Z		4
Reflections for cell determination		9761
2□ range for cell determination [°]		5−65
Unit cell parameters	a [Å]	15.4933(3)
	b [Å]	26.3923(5)
	c [Å]	4.40199(10)
	α [°]	90
	β [°]	90
	γ [°]	90
	V [Å^3]	1799.99(6)
F(000)		1160
D_X [g cm^{-3}]		2.270
μ(Mo K□) [mm^{-1}]		8.288
Scan type		ω
$2\theta_{(max)}$ [°]		64.4
Transmission factors (min; max)		0.180; 0.652
Total reflections measured		15752
Symmetry independent reflections		5610
R_{int}		0.032
Reflections with $I > 2\sigma(I)$		5123
Reflections used in refinement		5610
Parameters refined; restraints		272; 1

Final $R(F)$ [$I > 2\sigma(I)$ reflections]	0.0339
$wR(F^2)$ (all data)	0.0756
Weights:	$w = [\sigma^2(F_o^2) + (0.0303P)^2 + 4.2752P]^{-1}$ where $P = (F_o^2 + 2F_c^2)/3$
Goodness of fit	1.110
Final Δ_{max}/σ	0.001
$\Delta\rho$ (max; min) [e Å^{-3}]	1.56; -1.94
$\sigma(d_{(C-C)})$ [Å]	0.009 – 0.012

Compound 8 (CCDC 1487498)

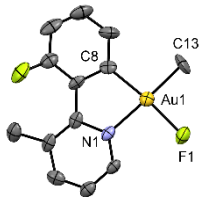

Table 7. *Crystallographic Data*

Crystallised from	CH_2Cl_2 / pentane
Empirical formula	$C_{13}H_{12}AuF_2N$
Formula weight [g mol^{-1}]	417.20
Crystal colour, habit	colourless, plate
Crystal dimensions [mm]	0.03 × 0.09 × 0.19
Temperature [K]	160(1)
Crystal system	monoclinic
Space group	$P2_1/c$ (#14)

Z		8
Reflections for cell determination		7233
2θ range for cell determination [°]		5−54
Unit cell parameters	a [Å]	7.5121(2)
	b [Å]	18.0598(6)
	c [Å]	17.0484(5)
	α [°]	90
	β [°]	99.554(3)
	γ [°]	90
	V [Å^3]	2280.82(12)
F(000)		1552
D_X [g cm^{-3}]		2.430
μ(Mo $K\alpha$) [mm^{-1}]		12.900
Scan type		ω
2θ(max) [°]		56.9
Transmission factors (min; max)		0.230; 0.694
Total reflections measured		22427
Symmetry independent reflections		5092
R_{int}		0.051
Reflections with $I > 2\sigma(I)$		3860
Reflections used in refinement		5092
Parameters refined		311

Final $R(F)$ [$I > 2\sigma(I)$ reflections]	0.0540
$wR(F^2)$ (all data)	0.1339
Weights:	$w = [\sigma^2(F_o^2) + (0.0509P)^2 + 30.8450P]^{-1}$ where $P = (F_o^2 + 2F_c^2)/3$
Goodness of fit	1.076
Final Δ_{max}/σ	0.000
$\Delta\rho$ (max; min) [e Å^{-3}]	4.47; -1.93
$\sigma(d_{(C-C)})$ [Å]	0.014 – 0.02

Compound 9a (CCDC 1486865)

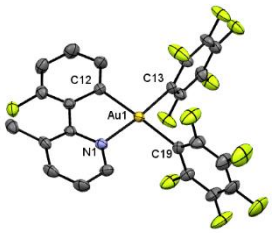

Table 8. *Crystallographic Data*

Crystallised from	dichloromethane / pentane
Empirical formula	$C_{24}H_{15}AuF_{11}NO_3$
Formula weight [g mol^{-1}]	771.34
Crystal colour, habit	colourless, prism
Crystal dimensions [mm]	0.13 × 0.20 × 0.24
Temperature [K]	160(1)
Crystal system	orthorhombic

Space group		$Pna2_1$ (#33)
Z		4
Reflections for cell determination		13319
2θ range for cell determination [°]		5–65
Unit cell parameters	a [Å]	21.1376(3)
	b [Å]	16.4885(2)
	c [Å]	7.53055(8)
	α [°]	90
	β [°]	90
	γ [°]	90
	V [Å^3]	2624.60(6)
F(000)		1472
D_X [g cm^{-3}]		1.952
μ(Mo $K\alpha$) [mm^{-1}]		5.730
Scan type		ω
2θ(max) [°]		64.9
Transmission factors (min; max)		0.298; 0.587
Total reflections measured		22332
Symmetry independent reflections		8226
R_{int}		0.025
Reflections with $I > 2\sigma(I)$		7286
Reflections used in refinement		8226

Parameters refined; restraints	335; 1
Final $R(F)$ [$I > 2\sigma(I)$ reflections]	0.0252
$wR(F^2)$ (all data)	0.0581
Weights:	$w = [\sigma^2(F_O^2) + (0.0245P)^2 + 1.2062P]^{-1}$ where $P = (F_O^2 + 2F_C^2)/3$
Goodness of fit	1.065
Final Δ_{max}/σ	0.001
$\Delta\rho$ (max; min) [e Å^{-3}]	0.68; -0.85
$\sigma(d_{(C-C)})$ [Å]	0.006 – 0.009

Compound 11D (CCDC 1486866)

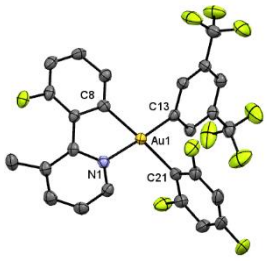

Table 9. *Crystallographic Data*

Crystallised from	CH_2Cl_2 / n-pentane
Empirical formula	$C_{26}H_{14}AuF_{10}N$
Formula weight [g mol^{-1}]	727.35
Crystal colour, habit	colourless, prism
Crystal dimensions [mm]	0.09 × 0.19 × 0.20
Temperature [K]	160(1)

Crystal system		monoclinic
Space group		$P2_1/c$ (#14)
Z		4
Reflections for cell determination		32639
2θ range for cell determination [°]		5–63
Unit cell parameters	a [Å]	7.37190(10)
	b [Å]	18.1864(2)
	c [Å]	17.5332(2)
	α [°]	90
	β [°]	93.3304(12)
	γ [°]	90
	V [Å^3]	2346.67(5)
F(000)		1384
D_X [g cm^{-3}]		2.059
μ(Mo $K\alpha$) [mm^{-1}]		6.365
Scan type		ω
$2\theta_{(max)}$ [°]		63.5
Transmission factors (min; max)		0.041; 0.070
Total reflections measured		70201
Symmetry independent reflections		7728
R_{int}		0.060
Reflections with $I > 2\sigma(I)$		7104

Reflections used in refinement	7721
Parameters refined	344
Final $R(F)$ [$I > 2\sigma(I)$ reflections]	0.0379
$wR(F^2)$ (all data)	0.0869
Weights:	$w = [\sigma^2(F_o^2) + (0.0253P)^2 + 8.5535P]^{-1}$ where $P = (F_o^2 + 2F_c^2)/3$
Goodness of fit	1.193
Final Δ_{max}/σ	0.003
$\Delta\rho$ (max; min) [e Å^{-3}]	2.31; -1.52
$\sigma(d_{(C-C)})$ [Å]	0.006 – 0.008

Compound 14C (CCDC 1486867)

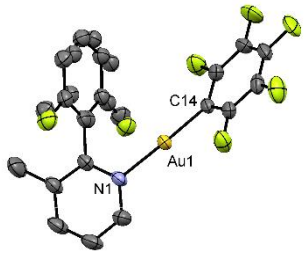

Table 10. *Crystallographic Data*

Crystallised from	CH_2Cl_2 / pentane
Empirical formula	$C_{19}H_{12}AuF_6N$
Formula weight [g mol^{-1}]	565.26
Crystal colour, habit	colourless, prism
Crystal dimensions [mm]	0.10 × 0.17 × 0.20
Temperature [K]	160(1)

Crystal system		monoclinic
Space group		$P2_1/n$ (#14)
Z		4
Reflections for cell determination		8997
2θ range for cell determination [°]		5–60
Unit cell parameters	a [Å]	10.2954(2)
	b [Å]	9.7990(3)
	c [Å]	17.9311(4)
	α [°]	90
	β [°]	104.827(2)
	γ [°]	90
	V [Å^3]	1748.73(7)
F(000)		1064
D_X [g cm^{-3}]		2.147
μ(Mo $K\square$) [mm^{-1}]		8.476
Scan type		ω
$2\theta_{(max)}$ [°]		61.0
Transmission factors (min; max)		0.263; 0.466
Total reflections measured		22421
Symmetry independent reflections		4828
R_{int}		0.030
Reflections with $I > 2\sigma(I)$		4013

Reflections used in refinement	4827
Parameters refined; restraints	320; 265
Final $R(F)$ [$I > 2\sigma(I)$ reflections]	0.0255
$wR(F^2)$ (all data)	0.0551
Weights:	$w = [\sigma^2(F_o^2) + (0.0180P)^2 + 2.4037P]^{-1}$ where $P = (F_o^2 + 2F_c^2)/3$
Goodness of fit	1.092
Final Δ_{max}/σ	0.002
$\Delta\rho$ (max; min) [e Å^{-3}]	1.65; -1.43
$\sigma(d_{(C-C)})$ [Å]	0.005 – 0.011

Compound 15 (CCDC 1486905)

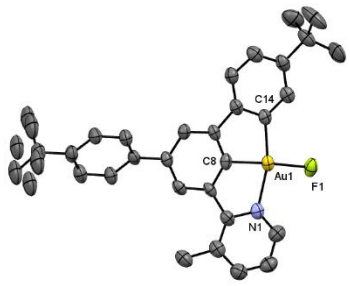

Table 11. *Crystallographic Data*

Crystallised from	CH_2Cl_2 / pentane
Empirical formula	$C_{34.83}H_{39.33}AuCl_{2.33}FN$
Formula weight [g mol^{-1}]	770.69
Crystal colour, habit	colourless, plate
Crystal dimensions [mm]	0.05 × 0.10 × 0.20

Temperature [K]		160(1)
Crystal system		tetragonal
Space group		$I4_1/a$ (#88)
Z		48
Reflections for cell determination		43709
2θ range for cell determination [°]		4–51
Unit cell parameters	a [Å]	31.0475(2)
	b [Å]	31.0475(2)
	c [Å]	41.4313(4)
	α [°]	90
	β [°]	90
	γ [°]	90
	V [Å^3]	39937.5(7)
F(000)		18384
D_x [g cm^{-3}]		1.538
μ(Mo $K\alpha$) [mm^{-1}]		4.637
Scan type		ω
2θ(max) [°]		57.1
Transmission factors (min; max)		0.744; 1.000
Total reflections measured		205574
Symmetry independent reflections		23576
R_{int}		0.076

Reflections with $I > 2\sigma(I)$	15612
Reflections used in refinement	23571
Parameters refined; restraints	1240; 1074
Final $R(F)$ [$I > 2\sigma(I)$ reflections]	0.0463
$wR(F^2)$ (all data)	0.1120
Weights:	$w = [\sigma^2(F_o^2) + (0.0356P)^2 + 391.1380P]^{-1}$ where $P = (F_o^2 + 2F_c^2)/3$
Goodness of fit	1.031
Final Δ_{max}/σ	0.005
$\Delta\rho$ (max; min) [e Å^{-3}]	1.88; -1.51
$\sigma(d_{(C-C)})$ [Å]	0.004 – 0.013

Compound 16a (CCDC 1033770)

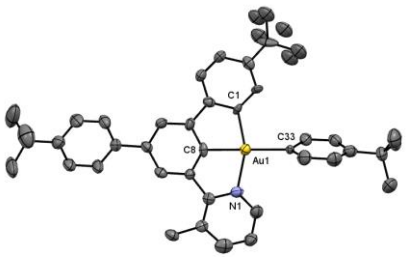

The asymmetric unit contains solvent molecules of pentane together with the main Au molecules in ratio 1:1. The methyl groups of one *tert*-butyl ligand is disordered over two sets of sites with site-occupancy ratios of 0.362(12):0.638(12). Some restraints were used to correct the geometry of the disordered components and the thermal parameters of the corresponding atoms.

Table 12. *Crystallographic Data*

Identification code	RK0503

Empirical formula	$C_{47}H_{58}NAu$
Formula weight	833.91
Temperature/K	160(1)
Crystal system	monoclinic
Space group	$P2_1/a$
a/Å	18.8532(10)
b/Å	10.5063(6)
c/Å	19.8505(14)
α/°	90
β/°	93.844(5)
γ/°	90
Volume/Å^3	3923.1(4)
Z	4
ρ_{calc}mg/mm^3	1.412
m/mm^{-1}	3.782
F(000)	1704.0
Crystal size/mm^3	0.33 × 0.21 × 0.03
Radiation	MoKα (λ = 0.71073)
2Θ range for data collection	4.832 to 50.69°
Index ranges	$-22 \leq h \leq 22$, $-10 \leq k \leq 12$, $-18 \leq l \leq 23$

Reflections collected	27436
Independent reflections	7165 [R_{int} = 0.0934, R_{sigma} = 0.0992]
Data/restraints/parameters	7165/117/486
Goodness-of-fit on F^2	1.025
Final R indexes [I>=2σ (I)]	R_1 = 0.0608, wR_2 = 0.1307
Final R indexes [all data]	R_1 = 0.0996, wR_2 = 0.1529
Largest diff. peak/hole / e $Å^{-3}$	3.04/-1.34

Compound 16b (CCDC 1486892)

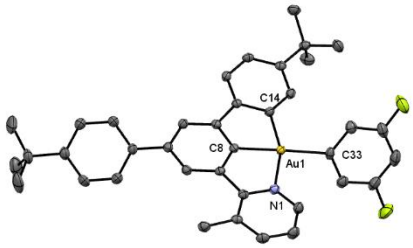

Table 13. *Crystallographic Data*

Crystallised from	CH_2Cl_2
Empirical formula	$C_{38}H_{36}AuF_2N$
Formula weight [g mol^{-1}]	741.64
Crystal colour, habit	pale-yellow, prism
Crystal dimensions [mm]	0.09 × 0.16 × 0.20
Temperature [K]	160(1)
Crystal system	monoclinic
Space group	$P2_1/c$ (#14)

Z		4
Reflections for cell determination		37855
2θ range for cell determination [°]		5−61
Unit cell parameters	a [Å]	17.69275(19)
	b [Å]	12.14541(9)
	c [Å]	15.50402(15)
	α [°]	90
	β [°]	114.0321(12)
	γ [°]	90
	V [Å^3]	3042.80(6)
F(000)		1472
D_X [g cm^{-3}]		1.619
μ(Mo $K\alpha$) [mm^{-1}]		4.875
Scan type		ω
2θ(max) [°]		61.1
Transmission factors (min; max)		0.733; 1.000
Total reflections measured		73914
Symmetry independent reflections		8776
R_{int}		0.044
Reflections with $I > 2\sigma(I)$		7590
Reflections used in refinement		8776
Parameters refined		386

Final	$R(F)$ [$I > 2\sigma(I)$ reflections]	0.0209
	$wR(F^2)$ (all data)	0.0468
Weights:	$w = [\sigma^2(F_o^2) + (0.0157P)^2 + 2.8746P]^{-1}$ where $P = (F_o^2 + 2F_c^2)/3$	
Goodness of fit		1.072
Final Δ_{max}/σ		0.007
$\Delta\rho$ (max; min) [e Å^{-3}]		1.25; -0.75
$\sigma(d_{(C-C)})$ [Å]		0.003 – 0.004

References

[1] E. Langseth, C. H. Görbitz, R. H. Heyn, M. Tilset, *Organometallics* **2012**, *31*, 6567-6571.

[2] Q. Zhou, Y.-N. Wang, X.-Q. Guo, X.-H. Zhu, Z.-M. Li, X.-F. Hou, *Organometallics* **2015**, *34*, 1021-1028.

[3] H. Minami, T. Saito, C. Wang, M. Uchiyama, *Angew. Chem. Int. Ed.* **2015**, *54*, 4665-4668.

[4] N. Barbero, R. Martin, *Org. Lett.* **2012**, *14*, 796-799.

[5] J. S. Ng, J. A. Katzenellenbogen, M. R. Kilbourn, *J.Org. Chem.* **1981**, *46*, 2520-2528.

[6] J. H. Goldstein, A. R. Tarpley, *J. Phy. Chem.* **1971**, *75*, 421-430.

CHAPTER 4

FIRST GOLD(III)-FORMATE: EVIDENCE FOR β-HYDRIDE ELIMINATION

CHAPTER 4

First Gold(III)-Formate: Evidence for β-Hydride Elimination

Roopender Kumar, Jean-Philippe Krieger, Enrique Gómez-Bengoa, Thomas Fox, Anthony Linden and Cristina Nevado

(*Angew. Chem. Int. Ed.* **2017**, *accepted*)

β-Hydride elimination from a metal alkyl or alkoxy complex is an elementary reaction in catalysis that has been harnessed as a productive step in industrially relevant transformations such as olefin polymerization, Mizoroki-Heck coupling or the Wacker process among many others.[1] Metal formates or carboxylates also undergo β-hydride elimination to produce CO_2 and metal hydrides (M-H). This reactivity has been efficiently exploited in several transformations including the Water-Gas Shift Reaction (WGSR) as well as the dehydrogenation of formic acid (FA).[2] Over the past years, in depth mechanistic understanding on β-hydride elimination processes has been stablished for transition metals such as Pd, Ru, Ni, Pt, Ir, etc.[1] In contrast, and despite prominent developments in gold catalysis,[3] β-hydride elimination on gold was long deemed unfeasible[4] and reports on gold complexes undergoing β-hydride elimination are scarce.[5] Pioneer work by Hashmi and co-workers demonstrated that the IPr-gold(I) ethyl complex does not undergo β-hydride elimination even at high temperature (Scheme 1B).[6] In a seminal work towards Csp^3-F bond forming reductive elimination, Toste *et al.* showed that NHC-gold(III) alkyl difluoride complexes form alkenes via β-hydride elimination along with the corresponding alkyl fluorides (Scheme 1C).[7] Recently, Bourissou and co-workers thoroughly investigated β-hydride elimination on low coordinate (P^C) type cyclometalated gold(III) alkyl complexes (Scheme 1D).[8] In 2015, Bochmann's group reported the insertion of CO onto a gold(III) hydroxo complex κ^3-[(C^N^C)Au(OH)].[9] While the corresponding gold(III) carboxylate could not be isolated, its formation was supported by observation of the corresponding Au(III)-H as a result of the β-hydride elimination (Scheme 1E). The stability of this gold(III) hydride proved to be remarkable as it could withstand air, moisture and even acetic acid.[10] Further, these species could hydroaurate alkynes in the presence of a radical initiator *via* homolytic cleavage of the Au-H bond to form the corresponding *trans*-vinylgold(III) complexes.[11] Importantly, gold(III) carboxylates and formates have been proposed as intermediates prone to undergo β-hydride elimination in gold-catalyzed WGSR[12] and dehydrogenation of formic acid,[13] but isolation or direct characterization of these species to substantiate these proposals has proven remarkably challenging. In this context, the resulting gold hydrides have also attracted significant attention[14] although experimental validation for their participation in catalysis remains scarce.

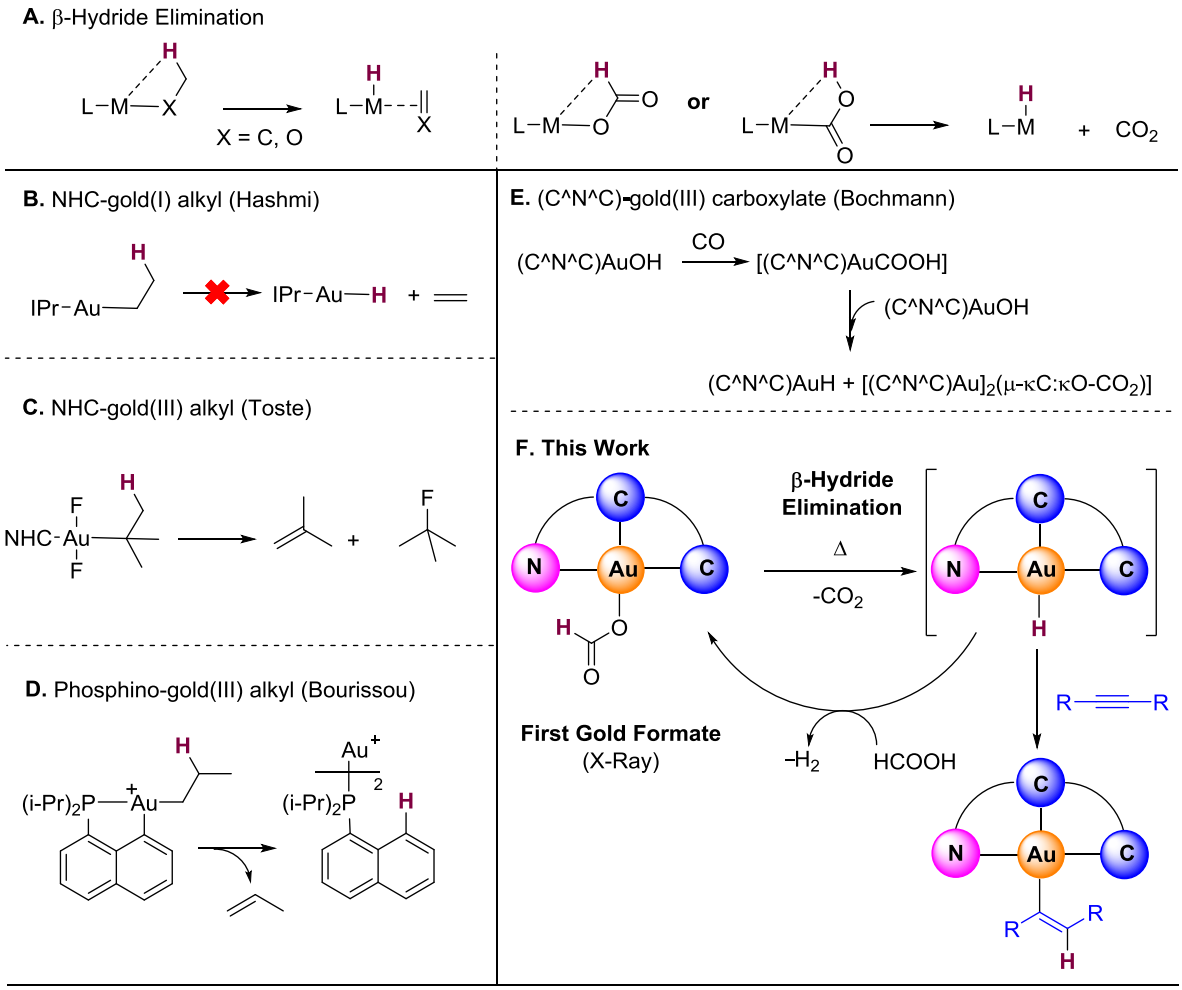

Scheme 1 A. General pathways for M-H formation via β-hydride elimination; **B-D.** Precedents of β-hydride elimination on gold; **E.** β-Hydride elimination on (C^N^C)Au-carboxylate; **F.** Evidence for β-hydride elimination on novel gold(III) formate.

Our group has recently disclosed the synthesis of stable, yet reactive towards nucleophiles (alkynes and boronic acids), (N^C^C)-gold(III) fluoride complexes.[15] We envisioned that the novel κ^3-(N^C^C) pincer template could enable the synthesis of largely elusive gold(III) intermediates. Herein, we present the synthesis of a stable gold(III) formate together with a study of its reactivity towards β-hydride elimination and in the context of a catalytic dehydrogenation of formic acid (Scheme 1F).

Cognizant of the basic nature of [(N^C^C)Au^{III}F] species,[15] we envisioned its potential use as precursors of gold(III) formates. Indeed, after preliminary experiments, the reaction of gold(III) fluoride **1** in the presence of formic acid in CH_2Cl_2 at room temperature furnished the corresponding formate **2** in quantitative yield (Scheme 2).[16] Gold(III) formate **2** is stable under ambient conditions as a solid but decomposes in solution over prolonged periods of time (days). ^{1}H NMR analysis of **2** in CD_2Cl_2 shows a sharp singlet resonance at δ = 9.46 ppm, characteristic of the formate moiety. Furthermore, a

single crystal was grown by slow diffusion of MeOH in a concentrated solution of **2** in CH_2Cl_2 confirming the proposed structure by X-ray diffraction analysis (Figure 1).

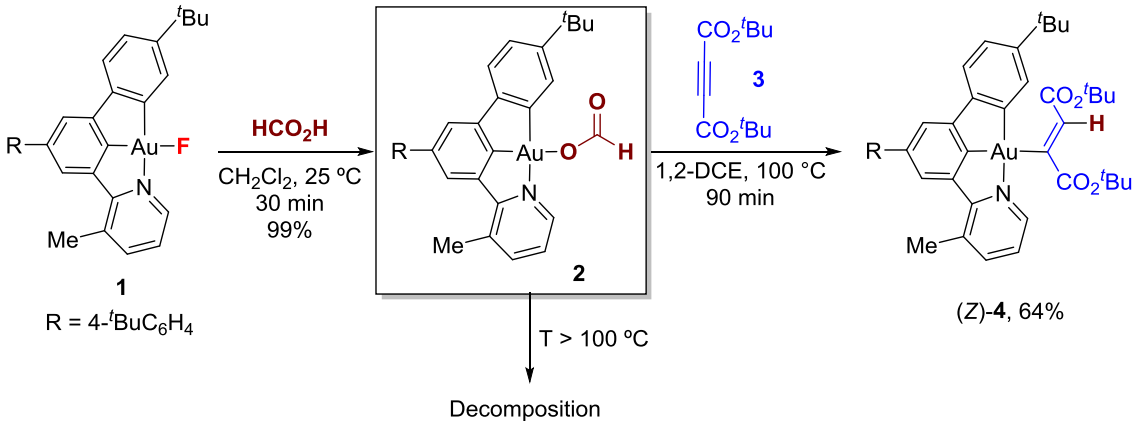

Scheme 2. Synthesis and reactivity of (N^C^C)-gold(III) formate **2**.

Interestingly, the Au-O bond distance [2.102(3) Å] is slightly longer than those previously reported for gold(III)-oxo complexes,[17] most probably due to the strong *trans*-influence of the central Csp^2 carbon of the (N^C^C) ligand. As transition-metal formates are generally known to be precursors of hydrides,[18] we next set out to prove the ability of complex **2** to engage in a β-hydride elimination process. No conversion could be observed by ^1H NMR spectroscopy after stirring **2** in aliphatic chlorinated solvents (CH_2Cl_2, 1,2-DCE) at temperatures up to 60 °C. However, heating **2** at 100 °C resulted in complete conversion and subsequent decomposition of the complex. This result suggested the possible formation of a highly reactive gold(III)-H. Interestingly, the reaction of formate **2** in the presence of di-*tert*-butyl acetylene dicarboxylate (**3**, 5 equiv) in 1,2-DCE at 100 °C afforded (*Z*)-gold(III) vinyl complex **4** in 64% isolated yield (Scheme 2). The reaction was monitored by ^1H NMR and showed a first-order decay in **2** as well as a first-order formation of **4** at comparable rates, thus suggesting a β-hydride elimination process (*cf.* section 3.3 in the SI). In solution, (*Z*)-**4** slowly isomerized to the (*E*)-isomer,[19] which could be characterized by X-Ray diffraction analysis showing an elongated Au(1)-C(33) bond of 2.083(9) Å and a small C(33)-Au(1)-C(13) angle of 95.6º (Figure 1 and ref. 16).

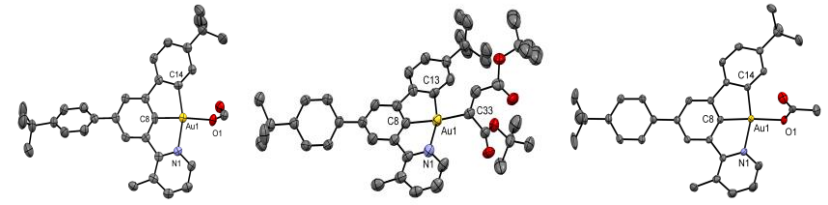

2	4	6

Bond Lengths (A°)	Au(1)-O(1) 2.102(3) Au(1)-C(8) 1.961(4)	Au(1)-C(33) 2.083(9) Au(1)-C(8) 2.004(8)	Au(1)-O(1) 2.0873(17) Au(1)-C(8) 1.952(2)
Bond Angles (°)	O(1)-Au(1)-N(1) 95.25(15) O(1)-Au(1)-C(14) 103.51(17)	C(33)-Au(1)-N(1) 104.5(3) C(33)-Au(1)-C(13) 95.6(3)	O(1)-Au(1)-N(1) 98.87(7) O(1)-Au(1)-C(14) 99.46(8)

Figure 1: The solid-state molecular structures of **2**, **4**, and **6** are shown with atoms drawn using 50% probability ellipsoids and hydrogen atoms have been omitted for clarity.

To support the hypothesis of a putative gold(III) hydride intermediate[20] able to insert the corresponding triple bond, alternative methods for the synthesis of these species were sought (Scheme 3). Treatment of [(N^C^C)Au^{III}Cl] **5** with L-Selectride or $LiHBEt_3$ in dry THF-d_8 at -78 °C followed by addition of di-*tert*-butyl acetylene dicarboxylate furnished the corresponding *trans* addition product (*Z*)-**4** in 55% yield, in line with the results observed in Scheme 2. Interestingly, when the above-mentioned reaction mixture was exposed to formic, acetic and trifluoroacetic acid, the corresponding gold(III) esters **2**, **6** and **7** could be cleanly obtained, all of which were unequivocally characterized by X-Ray diffraction analysis (see Figure 1 and SI).[21]

Having established the reactivity of gold(III) formate **2** towards β-hydride elimination, we envisioned the possibility of designing a homogeneous catalytic system for the dehydrogenation of formic acid. Gold-catalyzed dehydrogenations of FA in heterogeneous fashion have been demonstrated, although typically basic additives or inorganic alkalis are required for efficient performances.[13,22] When complexes **1** or **2** were heated at 100 °C in pure formic acid, a linear production of H_2 versus time and similar moderate catalytic activities (TOF = 3.1 ± 0.3 h^{-1} for **1** and TOF = 3.5 ± 0.3 h^{-1} for **2**) were obtained. Interestingly, neither decomposition nor a decrease in efficiency was noticed for a period of up to 44 h, which translated into TON > 137. An activation energy of the catalytic cycle, E_a = 25.4 ± 1.9 kcal/mol, was calculated using an Arrhenius plot (see SI). [23] These results are also in line with the reactive nature of a putative gold(III) hydride intermediate whose reaction rate with formic acid should be fast at 100 °C compared to the β-hydride elimination of formate **2**. As a result, the mechanism of the dehydrogenation of formic acid can be pictured as a rate-determining β-hydride elimination of

the gold(III) formate **2** upon heating to give a highly reactive hydride, which rapidly reacts with formic acid to release hydrogen and regenerate the formate **2**, thereby closing the catalytic cycle (Scheme 4).

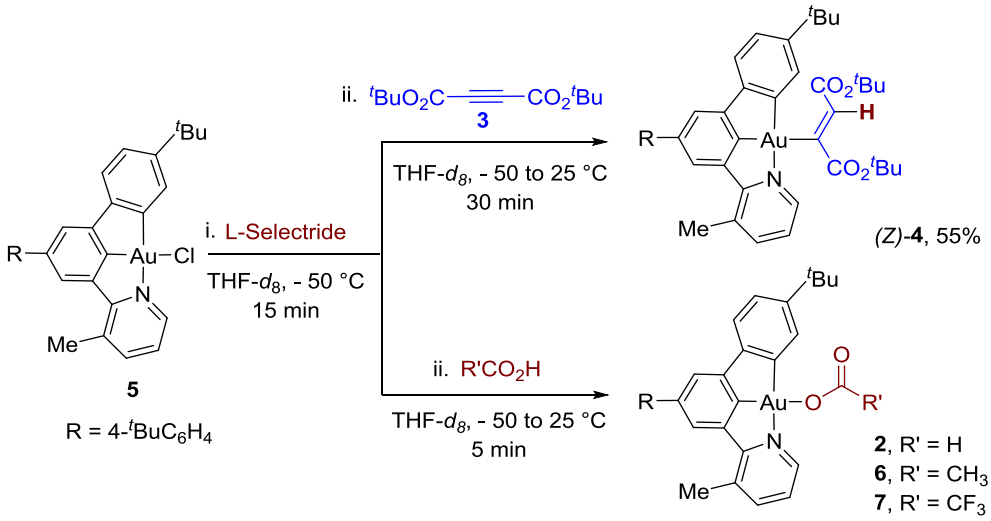

Scheme 3. Synthesis of vinyl gold(III) **4**, and gold(III) esters **2, 6, 7**.

We turned to DFT studies to shed light on the overall reaction energy profile. We were interested in confirming the feasibility of decarboxylation formate-to-hydride and dehydrogenation of FA back from hydride-to-formate. Indeed, the first transition state $\mathbf{TS_{II\text{-}III}}$ was located, corresponding to the *β*-hydride elimination-like decarboxylation step in a 4-membered cyclic structure. The step is exergonic (-3.6 kcal/mol) but needs a relatively high activation energy ($\Delta H^{\ddagger} = 23.8$, $\Delta G^{\ddagger} = 24.2$ kcal/mol), justifying the high temperature required under the experimental conditions (Scheme 4). The high activation energy can be explained by the highly asynchronous and strained TS, showing an initial Au-O bond rupture (2.6 Å) that precedes the formation of the Au-H bond (2.0 Å). The reverse step $\mathbf{TS_{III\text{-}II}}$ was also computed. The gold(III) hydride activates the formic acid molecule in a cyclic 6-membered TS, which seems to be more synchronous than the previous one. Interestingly, the activation energies of $\mathbf{TS_{III\text{-}II}}$ are significantly lower ($\Delta H^{\ddagger} = 11.3$, $\Delta G^{\ddagger} = 22.4$ kcal/mol) than in $\mathbf{TS_{II\text{-}III}}$, and the formation of **II** from **III** is fairly exergonic (-6.7 kcal/mol). Thus, the relative k_1 and k_2 values calculated computationally and the high energy of $\mathbf{TS_{II\text{-}III}}$ are in agreement with the experimental findings indicative of the β-hydride elimination as the rate determining step in this process. Alternative pathways, including the decoordination[24] or protonation of the pyridine ligand preceding the decarboxylation step were also studied. Calculations though showed substantially higher activation energies compared to those reported in Scheme 4 (see section 8 in the SI).

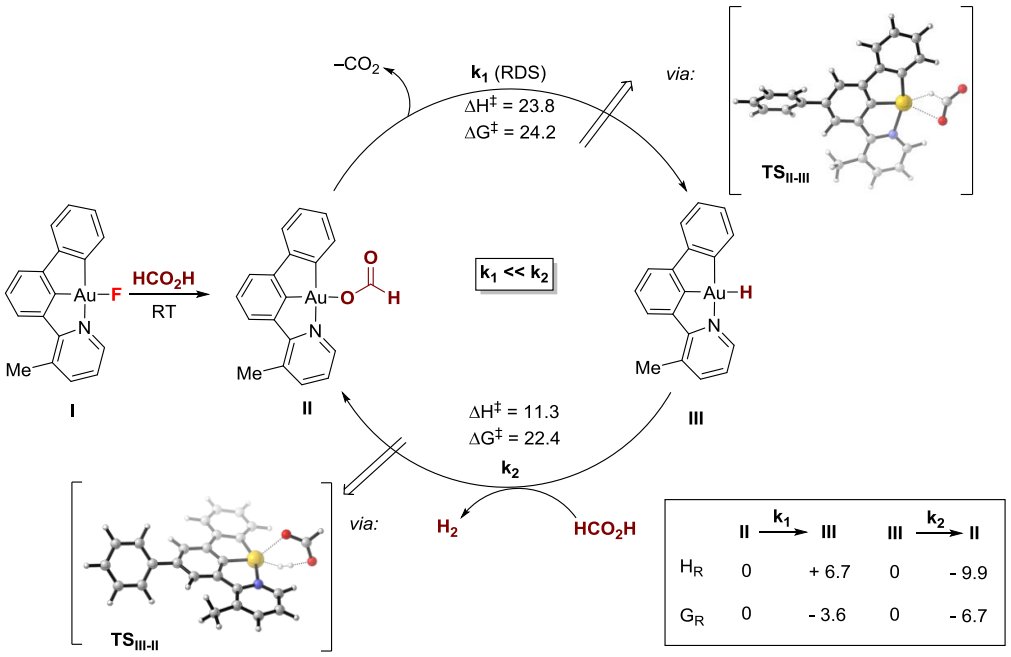

Scheme 4. Proposed catalytic cycle for dehydrogenation of formic acid. Structures and H,G energies (kcal/mol) of the catalytic cycle computed at M06/6-31G**(SDD) level, including solvent effects (IEFPCM, solvent = Formic Acid).

In summary, the synthesis and full characterization of the first gold(III) formate complex, obtained quantitatively from the reaction of a (N^C^C) pincer gold(III) fluoride with formic acid, is described here. This complex undergoes β-hydride elimination upon heating resulting in a catalytic dehydrogenation of pure formic acid. While the efficiency of this catalytic system is far from representing a synthetically useful alternative to existing heterogeneous systems,[13,22] we believe these results provide insightful guidance towards the development of more efficient systems in the near future.

References

[1] (a) R. H. Crabtree, in *The Organometallic Chemistry of the Transition Metals*, John Wiley & Sons, Inc., **2005**, pp. 183-206. (b) J. M. Takacs, X. t. Jiang, *Curr. Org. Chem.* **2003**, *7*, 369-396; (c) M. S. Sigman, E. W. Werner, *Acc. Chem. Res.* **2012**, *45*, 874-884; (d) X. Lu, *Top. Catal.* **2005**, *35*, 73-86; (e) A. K. Rappé, W. M. Skiff, C. J. Casewit, *Chem. Rev.* **2000**, *100*, 1435-1456; f) E. D. Sosa Carrizo , F. M. Bickelhaupt , I. Fernández, *Chem. Eur. J.* **2015**, *21*, 14362-14369.

[2] (a) P. C. Ford, *Acc. Chem. Res.* **1981**, *14*, 31-37; (b) M. Grasemanna, G. Laurenczy, *Energy Environ. Sci.*, **2012**, *5*, 8171-8181; (c) D. Mellmann, P. Sponholz, H. Junge, M. Beller, *Chem. Soc. Rev.* **2016**, *45*, 3954-3988; (d) Ambrosi, S. E. Denmark, *Angew. Chem. Int. Ed.* **2016**, *55*, 12164-12189.

[3] (a) A. S. K. Hashmi, *Angew. Chem. Int. Ed.* **2010**, *49*, 5232-5241; (b) T. C. Boorman, I. Larrosa, *Chem. Soc. Rev.* **2011**, *40*, 1910-1925; (c) T. de Haro, C. Nevado, *Synthesis* **2011**, 2530-2539; (d) H. A. Wegner, M. Auzias, *Angew. Chem. Int. Ed.* **2011**, *50*, 8236-8247; (e) M. Joost, A. Amgoune, D. Bourissou, *Angew. Chem. Int. Ed.* **2015**, *54*, 15022-15045; (f) D.-A. Rosca, J. A. Wright, M. Bochmann, *Dalton Trans.* **2015**, *44*, 20785-20807; (g) R. Kumar, C. Nevado, *Angew. Chem. Int. Ed.* **2017**, *56*, 1994-2015.

[4] (a) A. S. K. Hashmi, L. Schwarz, J.-H. Choi, T. M. Frost, *Angew. Chem. Int. Ed.* **2000**, *39*, 2285-2288; (b) G. Ung, G. Bertrand, *Angew. Chem. Int. Ed.* **2013**, *52*, 11388-11391.

[5] (a) A. Tamaki, S. A. Magennis, J. K. Kochi, *J. Am. Chem. Soc.* **1974**, *96*, 6140-6148; (b) A. Tamaki, J. K. Kochi, *J. Organomet. Chem.* **1973**, *61*, 441-450; (c) C.-M. Ting, Y.-L. Hsu, R.-S. Liu, *Chem. Commun.* **2012**, *48*, 6577-6579; (d) B. Alcaide, P. Almendros, T. M. del Campo, I. Fernandez, *Chem. Commun.* **2011**, *47*, 9054-9056; (e) M. Castiñeira Reis, C. S. López, E. Kraka, D. Cremer, O. N. Faza, *Inorg. Chem.* **2016**, *55*, 8636-8645.

[6] G. Klatt, R. Xu, M. Pernpointner, L. Molinari, T. Quang Hung, F. Rominger, A. S. K. Hashmi, H. Köppel, *Chem. Eur. J.* **2013**, *19*, 3954-3961.

[7] N. P. Mankad, F. D. Toste, *Chem. Sci.* **2012**, *3*, 72-76.

[8] F. Rekhroukh, L. Estevez, S. Mallet-Ladeira, K. Miqueu, A. Amgoune, D. Bourissou, *J. Am. Chem. Soc.* **2016**, *138*, 11920-11929.

[9] D.-A. Roşca, J. Fernandez-Cestau, J. Morris, J. A. Wright, M. Bochmann, *Sci. Adv.* **2015**, 1.

[10] (a) D.-A. Roşca, D. A. Smith, D. L. Hughes, M. Bochmann, *Angew. Chem. Int. Ed.* **2012**, *51*, 10643-10646; (b) A. S. K. Hashmi, *Angew. Chem. Int. Ed.* **2012**, *51*, 12935-12936.

[11] A. Pintus, L. Rocchigiani, J. Fernandez-Cestau, P. H. M. Budzelaar, M. Bochmann, *Angew. Chem. Int. Ed.* **2016**, *55*, 12321-12324.

[12] G. Bond, *Gold Bull.* **2009**, *42*, 337-342.

[13] Q.-Y. Bi, X.-L. Du, Y.-M. Liu, Y. Cao, H.-Y. He, K.-N. Fan, *J. Am. Chem. Soc.* **2012**, *134*, 8926-8933.

[14] (a) H. Ito, T. Yajima, J.-i. Tateiwa, A. Hosomi, *Chem. Commun.* **2000**, 981-982; (b) H. Ito, K. Takagi, T. Miyahara, M. Sawamura, *Org. Lett.* **2005**, *7*, 3001-3004; (c) A. Comas-Vives, C. González-Arellano, A. Corma, M. Iglesias, F. Sánchez, G. Ujaque, *J. Am. Chem. Soc.* **2006**, *128*, 4756-4765; (d) D. Lantos, M. a. Contel, S. Sanz, A. Bodor, I. T. Horváth, *J. Organomet. Chem.* **2007**, *692*, 1799-1805; (e) A. Corma, C. González-Arellano, M. Iglesias, F. Sánchez, *Angew. Chem. Int. Ed.* **2007**, *46*, 7820-7822; (f) H. Ito, T. Saito, T. Miyahara, C. Zhong, M. Sawamura, *Organometallics* **2009**, *28*, 4829-4840; (g) S. Labouille, A. Escalle-Lewis, Y. Jean, N. Mézailles, P. Le Floch, *Chem. Eur. J.* **2011**, *17*, 2256-2265; (h) M. Kidonakis, M. Stratakis, *Org. Lett.* **2015**, *17*, 4538-4541; (i) G. Kleinhans, M. M. Hansmann, G. Guisado-Barrios, D. C. Liles, G. Bertrand, D. I. Bezuidenhou *J. Am. Chem. Soc.*, **2016**, *138*, 15873–15876. For examples of isolated gold(I) hydrides, see: (j) E. Y. Tsui, P. Müller, J. P. Sadighi, *Angew. Chem.*

Int. Ed. **2008**, *47*, 8937-8940; (k) A. Escalle, G. Mora, F. Gagosz, N. Mézailles, X. F. Le Goff, Y. Jean, P. Le Floch, *Inorg. Chem.* **2009**, *48*, 8415-8422.

[15] (a) R. Kumar, A. Linden, C. Nevado, *Angew. Chem. Int. Ed.* **2015**. *54*, 14287-14290; (b) R. Kumar, A. Linden, C. Nevado, *J. Am. Chem. Soc.* **2016**, *138*, 13790-13793.

[16] For additional control experiments, see the Supporting Information. CCDC-1511131 (**2**), 1511132 (**4**), 1511135 (**6**), 1033771(**7**) contain the supplementary crystallographic data for this paper. The data can be obtained free of charge from the Cambridge Crystallographic Data Centre via www.ccdc.cam.ac.uk/structures.

[17] (a) D. A. Smith, D.-A. Roşca, M. Bochmann, *Organometallics* **2012**, *31*, 5998-6000; (b) D.-A. Rosca, D. A. Smith, M. Bochmann, *Chem. Commun.* **2012**, *48*, 7247-7249.

[18] (a) E. A. Bielinski, P. O. Lagaditis, Y. Zhang, B. Q. Mercado, C. Würtele, W. H. Bernskoetter, N. Hazari, S. Schneider, *J. Am. Chem. Soc.* **2014**, *136*, 10234-10237; (b) J. J. A. Celaje, Z. Lu, E. A. Kedzie, N. J. Terrile, J. N. Lo, T. J. Williams, *Nat. Commun.* **2016**, *7*, 11308.

[19] Formation of *trans* addition product (*Z*)-**4** does not seem to be radical mediated (*cf.* section 5.3 and 5.4 in the SI) in contrast to previous observations by Bochmann and co-workers on (C^N^C) complexes (ref. 11). For examples of non-radical *trans*-hydrometalation reactions with Au, see: (a) Q. Wang, S. E. Motika, N. G. Akhmedov, J. L. Petersen, X. Shi, *Angew. Chem. Int. Ed.* **2014**, *53*, 5418-5422; For examples with other metals, see: (b) N. Asao, Y. Yamamoto, *Bull. Chem. Soc. Jpn.* **2000**, *73*, 1071-1087; (c) B. Sundararaju, A. Fürstner, *Angew. Chem. Int. Ed.* **2013**, *52*, 14050-14054; (d) S. M. Rummelt, K. Radkowski, D.-A. Roşca, A. Fürstner, *J. Am. Chem. Soc.* **2015**, *137*, 5506-5519; For a detailed study on alkene insertions onto Au-O complexes, see: (e) E. Langseth, A. Nova, E. A. Tråseth, F. Rise, S. Øien, R. H. Heyn, M. Tilset, *J. Am. Chem. Soc.* **2014**, *136*, 10104-10115.

[20] (a) J. A. Labinger, K. H. Komadina, *J. Organomet. Chem.* **1978**, *155*, C25-C28; (b) P. Hrobárik, V. Hrobáriková, F. Meier, M. Repiský, S. Komorovský, M. Kaupp, *J. Phys. Chem. A.* **2011**, *115*, 5654-5659. (c) A. H. Greif, P. Hrobárik, M. Kaupp, *Chem. Eur. J.* **2017**, 23, 9790-9803.

[21] Note that previously reported gold(III) hydrides were not reactive in the presence of acids. See ref. 10.

[22] (a) Z. Zheng, T. Tachikawa, T. Majima, *J. Am. Chem. Soc.* **2015**, *137*, 948-957; (b) Q. Liu, X. Yang, Y. Huang, S. Xu, X. Su, X. Pan, J. Xu, A. Wang, C. Liang, X. Wang, T. Zhang, *Energy Environ. Sci.* **2015**, *8*, 3204-3207; (c) X. Yang, P. Pachfule, Y. Chen, N. Tsumori, Q. Xu, *Chem. Commun.* **2016**, *52*, 4171-4174.

[23] Control experiments ruled out the potential formation of inhomogeneous gold species being responsible for the observed catalytic activity. When the reaction was stopped after several hours, the gold(III) formate **2** could be recovered from the reaction media. For further details, see ref. 16.

[24] L. Rocchigiani, J. Fernandez-Cestau, P. H. M. Budzelaar, M. Bochmann *Chem. Commun.*, **2017**, *53*, 4358-4361.

CHAPTER 4

EXPERIMENTAL SECTION

Table of Contents

1. General Information

NMR spectra were recorded on AV2 400 or AV2 500 MHz Bruker spectrometers. Chemical shifts are given in ppm. The spectra were calibrated to the residual ^{1}H and ^{13}C signals of the solvents. Multiplicities are abbreviated as follows: singlet (s), doublet (d), triplet (t), quartet (q), doublet-doublet (dd), quintet (quint), septet (sept), multiplet (m), and broad (b). The compounds were characterized by ^{1}H, ^{13}C, and ^{19}F NMR spectroscopy. Infrared spectra were recorded on a JASCO FT/IR-4100 spectrometer. High-resolution electrospray ionization and electronic impact mass spectrometry was performed on a Finnigan MAT 900 (Thermo Finnigan, San Jose, CA; USA) double focusing magnetic sector mass spectrometer. Ten spectra were acquired. A mass accuracy ≤ 2 ppm was obtained in the peak matching acquisition mode by using a solution containing 2 <l PEG200, 2 <l PPG450, and 1.5 mg NaOAc (all obtained from Sigma-Aldrich, CH-Buchs) dissolved in 100 mL MeOH (HPLC Supra grade, Scharlau, E-Barcelona) as internal standard. GC-MS analysis was done on a Finnigan Voyager GC8000 Top. Elemental microanalysis was carried out with Leco TruSpec Micro-CHNS analyser. Microwave reaction was done in Discover & Explorer SP (CEM). Gold complexes decompose before melting temperature is reached (T^{a} > 200 °C).

Materials and Methods:

Unless otherwise stated, starting materials were purchased from Aldrich and/or Fluka. Solvents were purchased in HPLC quality, degassed by purging thoroughly with nitrogen and dried over activated molecular sieves of appropriate size. Alternatively, they were purged with argon and passed through alumina columns in a solvent purification system (Innovative Technology). Conversion was monitored by thin layer chromatography (TLC) using Merck TLC silica gel 60 F254. Compounds were visualized by UV-light at 254 nm and by dipping the plates in an ethanolic vanillin/sulfuric acid solution or an aqueous potassium permanganate solution followed by heating. Flash column chromatography was performed over silica gel (230-400 mesh).

2. Experimental procedures and characterization of starting materials and products

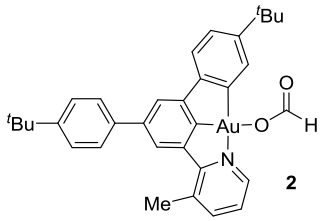

2

To a solution of complex **1** (65 mg, 0.10 mmol) in CH_2Cl_2 (3.0 mL) was added formic acid (46 mg, 1.0 mmol) and the resulting reaction mixture was stirred for 30 minutes. The solvent was evaporated under reduced pressure and the resulting solid was washed with hexanes to yield complex **2** as a yellow solid (67 mg, 100%). ^{1}H NMR (400 MHz, CD_2Cl_2) δ 9.43 (s, 1H), 8.12 (s, 1H), 7.61 (d, J = 6.9 Hz, 1H), 7.50 – 7.43 (m, 5H), 7.29 (d, J = 1.9 Hz, 1H), 7.20 (s, 1H), 7.16 (dd, J = 8.0, 1.9 Hz, 1H), 7.11 (dd, J = 7.6, 5.3 Hz, 1H), 7.04 (d, J = 7.7 Hz, 1H), 2.55 (s, 3H), 1.39 (s, 9H), 1.33 (s, 9H). ^{13}C NMR (101 MHz, CD_2Cl_2) δ 167.48, 160.33, 151.90, 151.64, 150.80, 150.42, 150.00, 146.91, 145.17, 142.20, 141.87, 138.28, 134.75, 129.79, 127.27, 126.48, 125.54, 124.90, 124.34, 122.30, 121.45, 31.68, 31.62, 22.67. IR (film) ν (cm^{-1}) 2958, 1634, 1588, 1473, 1421, 1389, 1275, 1249, 827 cm^{-1}.

[(N^C^C)Au-OCOH] (2-d$_1$)

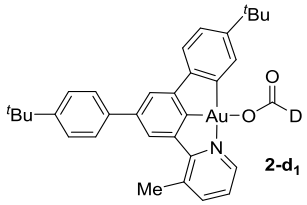

2-d$_1$

To a solution of complex **1** (65 mg, 0.10 mmol) in CH_2Cl_2 (3.0 mL) was added formic acid-d (47 mg, 1.0 mmol) and the resulting reaction mixture was stirred for 30 minutes. The solvent was evaporated under reduced pressure and the resulting solid was washed with hexanes to yield complex **2-d$_1$** as a yellow solid (67 mg, 100%). ^{1}H NMR (400 MHz, CD_2Cl_2) δ 7.99 (s, 1H), 7.57 (d, J = 7.4 Hz, 1H), 7.45 – 7.36 (m, 5H), 7.26 (d, J = 1.6 Hz, 1H), 7.15 – 7.09 (m, 2H), 7.08 – 7.02 (m, 1H), 6.93 (d, J = 7.9 Hz, 1H), 2.47 (s, 3H), 1.38 (s, 9H), 1.31 (s, 9H). ^{13}C NMR (126 MHz, CD_2Cl_2) δ 167.42, 160.18, 152.00, 151.71, 150.73, 150.32, 149.97, 146.85, 145.18, 142.15, 141.84, 138.11, 134.73, 129.93, 127.22, 126.51, 125.59, 124.83, 124.42, 122.38, 121.39, 35.09, 31.68, 31.60, 22.64. IR (film) ν (cm^{-1}) 2957, 1619, 1589, 1264, 1128, 1005, 826, 765 cm^{-1}.

(*Z*)-[(N^C^C)Au-vinyl] (4)

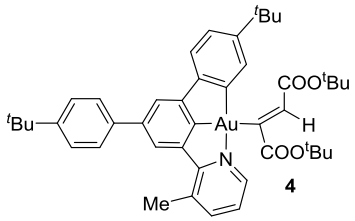

4

In a glovebox, a J-young tube was charged with complex **2** (33.5 mg, 50 µmol), di-*tert*-butyl acetylenedicarboxylate (**3**, 55 mg, 250 µmol) and CD_2Cl_2 (2.5 mL). The J-young tube was sealed, taken out of the glovebox and the reaction mixture was heated at 100 °C for 4 hours. Reaction progress was followed by ^{1}H NMR. After completion of the reaction, the solvent was evaporated and the crude mixture was purified by silica gel chromatography using DCM:hexane as eluent to yield complex **4** (28 mg, 64%) as a yellowish solid. 24% yield of gold(III) chloro complex **5** was also isolated in this reaction. ^{1}H NMR (400 MHz, CD_2Cl_2) δ 8.72 (dd, J = 5.3, 1.6 Hz, 1H), 7.89 (d, J = 1.2 Hz, 1H), 7.82 (dd, J = 7.8, 1.0 Hz, 1H), 7.63 – 7.58 (m, 3H), 7.55 – 7.50 (m, 3H), 7.42 (s, 1H), 7.37 (d, J = 8.0 Hz, 1H), 7.30 (dd, J = 7.7, 5.4 Hz, 1H), 7.21 (dd, J = 8.0, 2.0 Hz, 1H), 2.86 (s, 3H), 1.46 (s, 9H), 1.39 (s, 9H), 1.32 (s, 9H), 1.25 (s, 9H). ^{13}C NMR (101 MHz, CD_2Cl_2) δ 190.31, 176.48, 174.82, 170.79, 165.45, 153.70, 151.76, 151.55, 151.09, 149.84, 146.91, 144.90, 144.55, 141.14, 139.69, 134.57, 133.70, 129.62, 127.42, 126.38, 125.28, 124.46, 124.26, 121.99, 121.35, 60.99, 60.66, 35.42, 35.04, 31.69, 31.63, 23.00, 14.87, 14.56. IR (film) ν (cm^{-1}) 2963, 1712, 1692, 1588, 1364, 1235, 1153, 1135, 825 cm^{-1}. HR-MS (ESI) *m/z* calcd for $C_{44}H_{52}AuNO_4Na$ [M+Na$^+$] 878.3454, found 878.3453.

(*Z*)-[(N^C^C)Au-vinyl-d] (4-d$_1$)

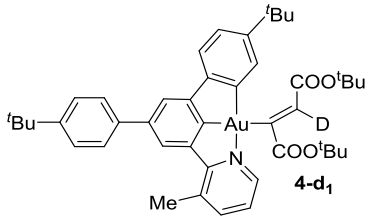

4-d$_1$

In a glovebox, a J-young tube was charged with complex **2-d$_1$** (10 mg, 15 µmol), di-*tert*-butyl acetylenedicarboxylate (**3**, 20 mg, 90 µmol) in 1,2-DCE (1.5 mL). The J-young tube was sealed, taken out of the glovebox and the reaction mixture was heated at 100 °C for 90 minutes. Reaction progress was followed by ^{1}H NMR. After completion of the reaction, the solvent was evaporated and the crude mixture was purified by silica gel chromatography using DCM/hexane as eluent to yield complex **4-d$_1$** (6.8 mg, 53% yield) as a yellowish solid. ^{1}H NMR (400 MHz, CD_2Cl_2) δ 8.72 (dd, J = 5.4, 1.3 Hz, 1H), 7.89 (d, J = 1.3 Hz, 1H), 7.82 (ddd, J = 7.8, 1.7, 0.7 Hz, 1H), 7.62 – 7.59 (m, 3H), 7.54 – 7.50 (m, 3H), 7.37 (d, J = 8.0 Hz, 1H), 7.30 (dd, J = 7.7, 5.4 Hz, 1H), 7.21 (dd, J = 8.0, 2.0 Hz, 1H), 2.86 (s, 3H), 1.46

(s, 9H), 1.39 (s, 9H), 1.32 (s, 9H), 1.25 (s, 9H). ^{13}C NMR (101 MHz, CD_2Cl_2) δ 189.41, 176.25, 175.48, 170.22, 165.56, 153.65, 151.82, 151.49, 151.05, 150.08, 147.04, 144.87, 144.50, 141.02, 139.75, 134.46, 133.72, 127.41, 126.38, 125.21, 124.30, 124.09, 121.88, 121.26, 80.57, 80.38, 35.41, 35.04, 31.70, 28.71, 28.47, 23.01. IR (film) ν (cm^{-1}) 2963, 1713, 1695, 1588, 1389, 1364, 1234, 1153, 1134, 826 cm^{-1}. HR-MS (ESI) *m/z* calcd for $C_{44}H_{51}DAuNO_4Na$ [M+Na^+] 879.3516, found 879.3515.

[(N^C^C)Au-OCOMe] (6)

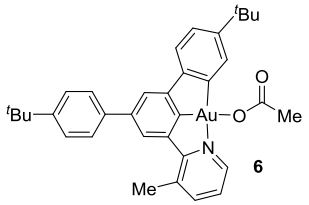

^{1}H NMR (500 MHz, CD_2Cl_2) δ 8.50 (d, *J* = 4.2 Hz, 1H), 7.78 – 7.74 (m, 2H), 7.60 (d, *J* = 8.4 Hz, 2H), 7.53 (s, 2H), 7.44 (dd, *J* = 6.8, 1.6 Hz, 2H), 7.38 (dd, *J* = 7.8, 5.3 Hz, 1H), 7.30 (d, *J* = 8.0 Hz, 1H), 7.25 (dd, *J* = 8.0, 1.9 Hz, 1H), 2.78 (s, 3H), 2.18 (s, 3H), 1.39 (s, 9H), 1.35 (s, 9H). ^{13}C NMR (126 MHz, CD_2Cl_2) δ 176.79, 161.41, 158.63, 151.64, 151.44, 151.33, 151.13, 149.57, 147.50, 145.26, 142.66, 141.96, 138.98, 134.75, 129.64, 127.43, 126.45, 125.46, 125.02, 124.33, 122.10, 121.70, 35.49, 35.08, 31.68, 31.62, 24.97, 22.82. IR (film) ν (cm^{-1}) 2961, 1632, 1589, 1424, 1368, 1313, 1132, 1008, 837, 793 cm^{-1}. HR-MS (EI) *m/z* calcd for $C_{34}H_{36}AuNO_2$ [M^+] 687.2406, found 687.2401.

[(N^C^C)Au-OCOCF$_3$] (7)

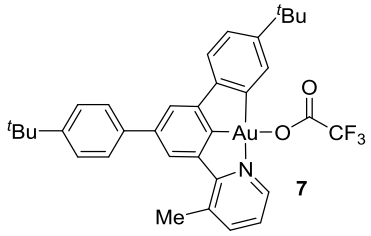

^{1}H NMR (400 MHz, CD_2Cl_2) δ 8.40 (d, *J* = 4.2 Hz, 1H), 7.78 (d, *J* = 7.5 Hz, 1H), 7.72 (s, 1H), 7.57 (d, *J* = 8.6 Hz, 2H), 7.52 (d, *J* = 8.7 Hz, 2H), 7.41 – 7.36 (m, 2H), 7.30 (d, *J* = 1.6 Hz, 1H), 7.27 – 7.22 (m, 2H), 2.74 (s, 3H), 1.39 (s, 9H), 1.31 (s, 9H). Note: ^{13}C NMR could not be recorded due to the poor solubility of complex **7** in common organic solvents. ^{19}F NMR (376 MHz, CD_2Cl_2) δ -74.64. IR (film) ν (cm^{-1}) 2960, 1699, 1588, 1472, 1408, 1212, 1188, 1149, 837, 793 cm^{-1}. HR-MS (EI) *m/z* calcd for $C_{34}H_{33}AuF_3NO_2$ [M^+] 741.2123, found 741.2121.

3. Synthesis of vinyl gold(III) complex 4 and esters 2, 6 and 7 (Scheme 3 of the manuscript)

3.1 Synthesis of vinyl gold(III) complex 4 from complex 5

In a glovebox, a J-young NMR tube was charged with complex **5**[1] (6.6 mg, 10 µmol) and THF-d_8 (1.2 ml). The J-young NMR tube was sealed, taken out of the glovebox and heated to 80 °C in an oil bath to dissolve complex **5**. The J-young NMR tube was cooled down to -78 °C and L-selectride (14 µmol, 1M in THF) was added. di-*tert*-butylacetylenedicarboxylate (**3**, 11 mg, 50 µmol) was added at -50 °C and the reaction with the triple bond was monitored by ^{1}H NMR while increasing the temperature in a controlled manner. No conversion could be detected at temperatures up to -20 °C whereas formation of gold vinyl complex (*Z*)-**4** was observed at -10 °C showing full conversion at room temperature. After completion of the reaction, the solvent was evaporated and the crude mixture was purified by silica gel chromatography using DCM/hexane as eluent to yield complex (*Z*)-**4** (55%).

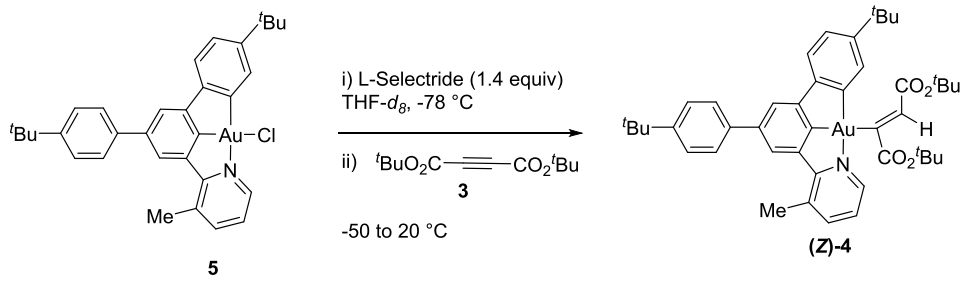

3.2 Synthesis of esters 2, 6, and 7 from complex 5

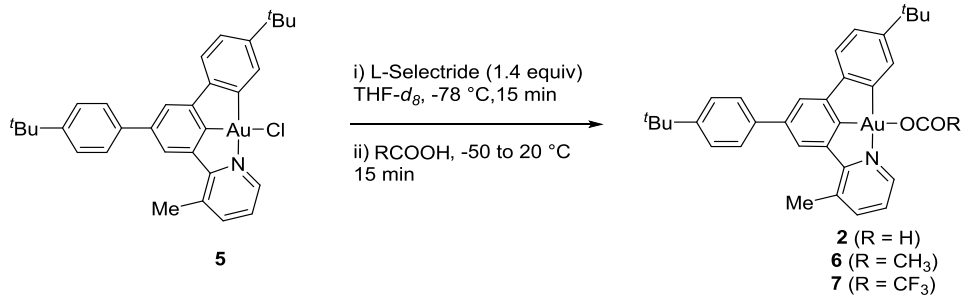

In a glovebox, a J-young NMR tube was charged with gold chloride complex **5**[1] (6.6 mg, 10 µmol) and THF-d_8 (1.2 ml). The J-young NMR tube was sealed, taken out of the glovebox and heated to 80 °C in an oil bath to dissolve complex **5**. The J-young NMR tube was cooled down to -78 °C and L-selectride (14 µmol, 1M in THF) was added. The reaction temperature was raised to -50 °C and after complete conversion of gold chloride **5**, 50 µmol of carboxylic acid (formic acid, acetic acid and trifluoroacetic acid) was added to the reaction mixture. The formation of corresponding esters (**2**, **6** and **7**) was detected by ^{1}H NMR. Complexes **6** and **7** could also be prepared from gold fluoride **1** in an analogous manner to that described in section 2 for the preparation of **2**.

3.3 Synthesis of vinyl gold(III) complex 4 upon heating complex 2

In a J-young NMR tube, a mixture of complex **2** (6.7 mg, 10 µmol), di-*tert*-butylacetylenedicarboxylate (**3**, 11 mg, 50 µmol) and 1,3,5-trimethoxybenzene (1.7 mg, 10 µmol, internal standard IS) in CD_2Cl_2 (1.0 mL) was heated at 100 °C in an oil bath. At the indicated times, the reaction mixture was cooled quickly to 0 °C with an ice/water bath and a ^{1}H NMR spectrum was then recorded. This process was repeated with the same sample to gather all the measurements to monitor the formation of vinyl gold complex (*Z*)-**4**.

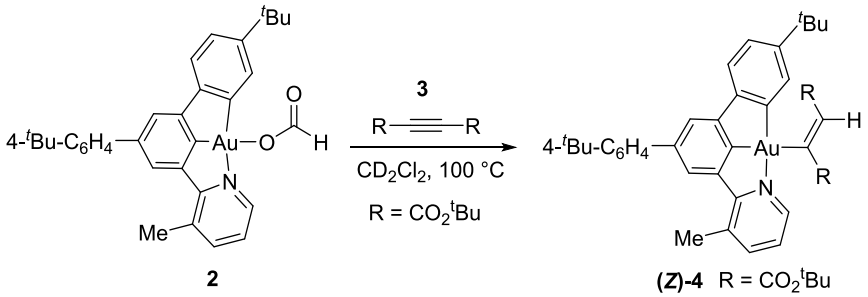

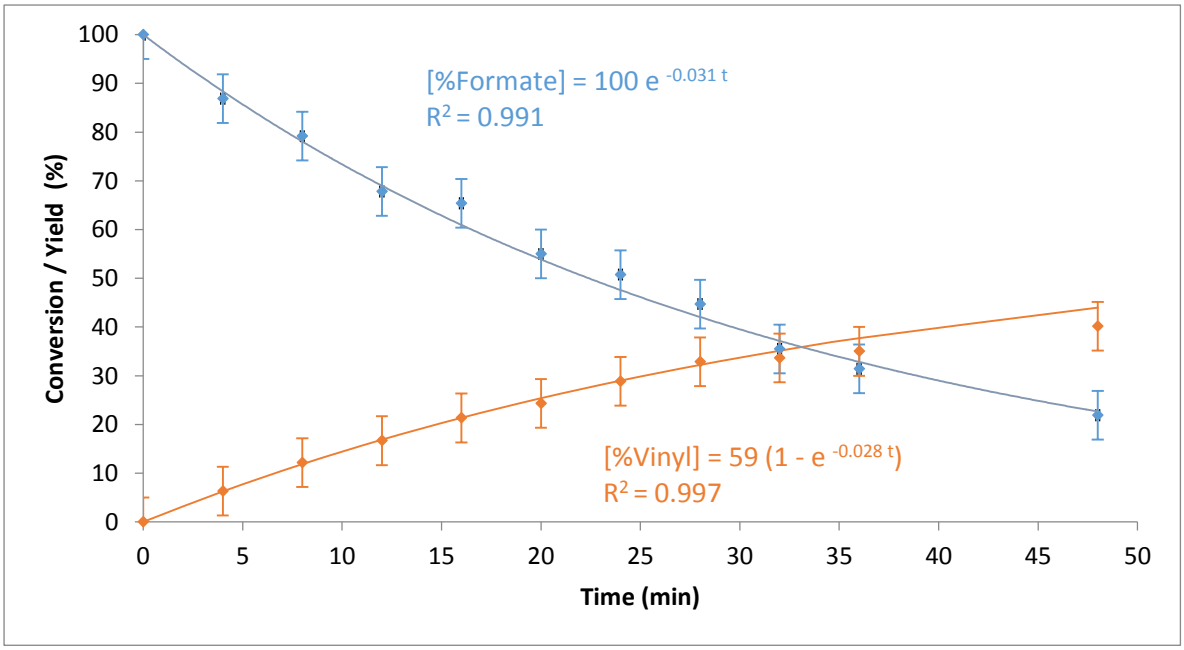

In a J-young NMR tube, a mixture of complex **2-d$_1$** (6.7 mg, 10 µmol), di-*tert*-butylacetylenedicarboxylate (**3**, 11 mg, 50 µmol) and 1,3,5-trimethoxybenzene (1.7 mg, 10 µmol, internal standard IS) in CD_2Cl_2 (1.0 mL) was heated at 100 °C in an oil bath. At the indicated times, the reaction mixture was cooled quickly to 0 °C with an ice/water bath and a ^{1}H NMR spectrum was then

recorded. This process was repeated with the same sample to monitor formation of vinyl gold complex (*Z*)-**4-d$_1$.**

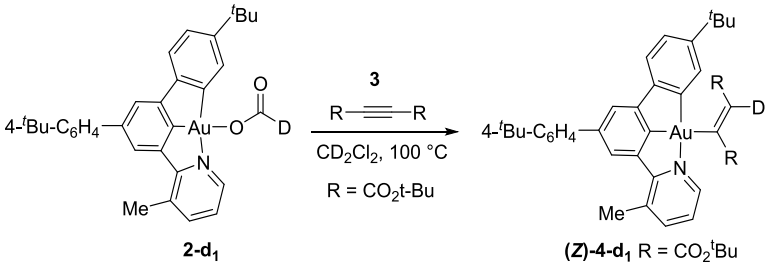

2-d$_1$ **(*Z*)-4-d$_1$** R = $CO_2{}^t$Bu

1. Kinetic study of FA dehydrogenation by GC

4.1 Materials for the dehydrogenation of formic acid

Catalytic dehydrogenation of formic acid experiments were performed in gas-tight vials (Biotage Microwave Process Vial 10 - 20 mL) equipped with gas-tight pierceable caps. Quantification of the gaseous content of the headspace was achieved by gas chromatography using a Varian Chrompack CP-3800 coupled to a thermal conductivity detector (TCD). Depending on the experiment, two different columns were used for the characterization of the gas mixture:

Column 1: detection of H_2, D_2 and N_2.	
Inner Diameter x Length	2 mm x 3 m
Stationary Phase:	Molecular sieves 13X 80-100
Carrier Gas/Flow:	Argon, 20 mL/min
Injection:	Manual, 100 ± 5 µL
Temperature Program:	Isotherm 100 °C
TCD/Filament temperature	150 °C / 170 °C
Limit of detection H_2/D_2 (ppm)	2000/1500

Column 2: detection of H_2, D_2, N_2 and CO_2.	
Inner Diameter x Length	2 mm x 3 m
Stationary Phase:	Carboxen 1000
Carrier Gas/Flow:	Argon, 20 mL/min
Injection:	Manual, 100 ± 5 µL
Temperature Program:	Isotherm 100 °C
TCD*/Filament temperature	150 °C / 170 °C

*Signal amplification of the detector ~10x	
Limit of detection $H_2/D_2/CO_2$ (ppm)	200/150/5000

Injection of the sample (100 µL) was performed with a gas-tight Hamilton syringe. A relative uncertainty of 10% was taken into account due to the precision of the injection. Good separation of The response of the GC detector was calibrated for each relevant gas that could be detected (H_2, D_2, N_2 and CO_2).

Experimental procedure

The measurements were performed on a 100 µL sample of the gas mixture from the headspace of the vial, thereby allowing determination of the molar fraction of H_2 or D_2 produced. All gases used were obtained from certified commercially available gas mixtures. The amount of H_2 or D_2 ($\boldsymbol{n_{H_2/D_2}}$) produced was then calculated with the formula (4), derived from relations (1), (2) and (3):

$$n_{H_2/D_2} = x_{H_2/D_2} \cdot n_{Total} \quad (1)$$

$$n_{Tot} = n_{H_2/D_2} + n_{CO_2} + n_{N_2} \quad (2)$$

$$n_{H_2/D_2} = n_{CO_2} \quad (3)$$

$$\boldsymbol{n_{H_2/D_2} = \frac{x_{H_2/D_2} \cdot n_{N_2}}{1 - 2x_{H_2/D_2}}} \quad (4)$$

$\boldsymbol{n_{H_2/D_2}}$: Moles of H_2 or D_2

$\boldsymbol{n_{CO_2}}$: Moles of CO_2

$\boldsymbol{n_{N_2}}$: Moles of N_2

$\boldsymbol{x_{H_2/D_2}}$: Molar fraction of H_2 or D_2

$\boldsymbol{n_{Total}}$: Total number of moles of gas

The number of moles of N_2 was considered to be the same for each experiment and equal to 1.2 mmol (P = 10^5 bars, V = 31.0 mL, T = 300 K, ideal gas). CO_2 was detected when the GC analyses were performed on column 2. When TONs reached values greater than 50, the measured amount of CO_2 was the same as that of H_2 within a +/-10% margin of error. Control experiments in the absence of gold revealed no decarboxylation of FA under the standard conditions and a trace production (< 5%) of CO due to the thermal decarbonylation of formic acid so that the pressure of CO could be neglected for the calculation of the amount of H_2. Data reported represents the average of two independent runs. A representative GC trace is shown below demonstrating that the gaseous products observed under the reaction conditions could be well resolved.

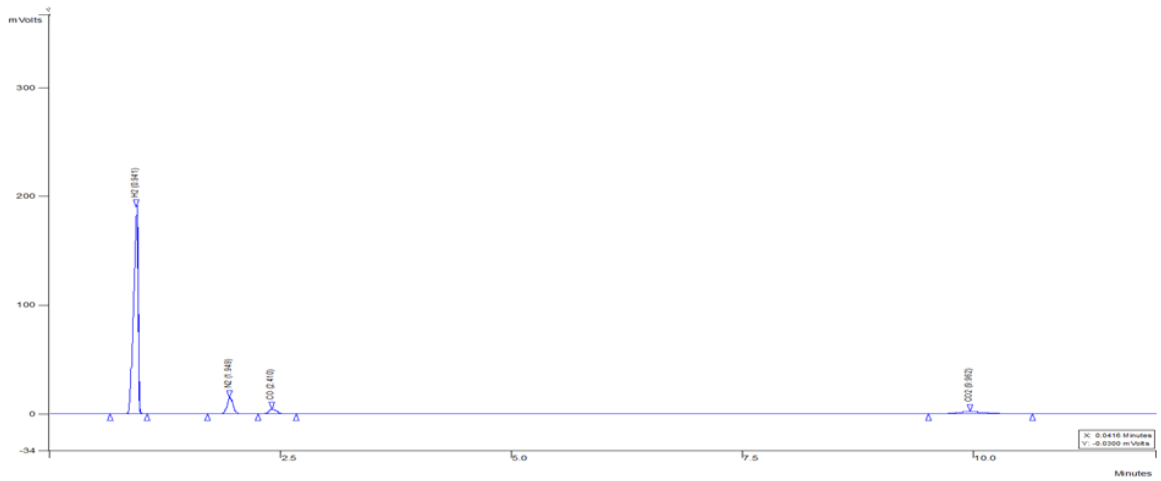

4.2 Results

4.2.1 TOF and TON at 100 °C

Sample preparation & procedure: A vial (Biotage Microwave Process Vial 10 - 20 mL) was charged with a stirring bar and gold(III) fluoride **1** (6.5 mg, 10 µmol) or the gold(III) formate **2** (6.7 mg, 10 µmol). The vial was sealed, evacuated and backfilled with 1 atm of N_2. Freshly distilled formic acid (3.0 mL) was added and the resulting solution was stirred at 100 °C in an oil bath. After the indicated time, the reaction was stopped by plunging the vial into an ice bath and the vial was allowed to reach RT. A 100 µL aliquot of the headspace volume of the vial was taken with a gas-tight Hamilton syringe and manually injected in the GC. The vial was heated further until catalyst decomposition. Two experiments were run in parallel for both the gold fluoride **1** and formate **2**. The measurements were performed with column 1 in the case of the fluoride **1** (**Figure 1**) and with column 2 in the case of the formate **2** (**Figure 2**).

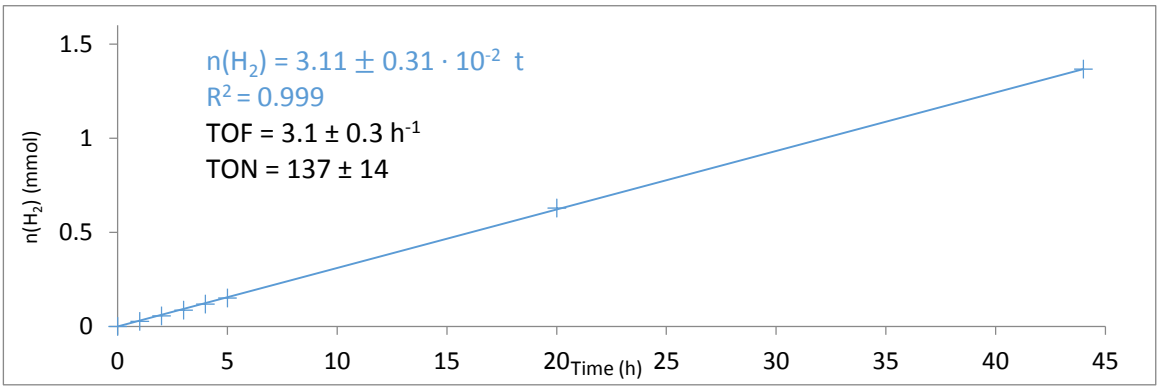

Figure 1. H_2 (mmol) vs. time (h) to determine TOF and TON for gold fluoride 1 in formic acid at 100 °C

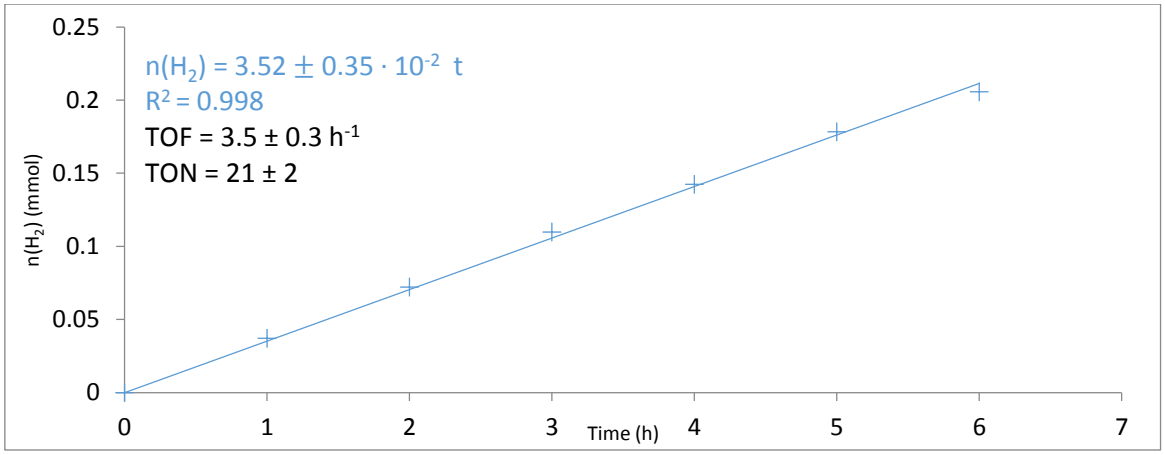

Figure 2. H_2 (mmol) vs. time (h) to determine TOF and TON for gold formate 2 in formic acid at 100 °C

4.2.2 Temperature-dependence study and Arrhenius plot analysis

Sample preparation & procedure: A vial (Biotage Microwave Process Vial 10 - 20 mL) was charged with a stirring bar and gold(III) fluoride **1** (6.5 mg, 10 µmol). The vial was sealed, evacuated and backfilled with 1 atm of N_2. Freshly distilled formic acid (3.0 mL) was added and the resulting solution was stirred at the indicated temperature in a stirred oil bath. After the indicated time, the reaction was stopped by plunging the vial into an ice bath and the vial was then allowed to reach RT. A 100 µL aliquot of the headspace volume of the vial was taken with a gas-tight Hamilton syringe and manually injected in the GC. The vial was then heated further. The measurements were performed with column 2.

Temperature (ºC)	k (s^{-1})	TOF (h^{-1})
90	$(3.78 \pm 0.39) \cdot 10^{-4}$	1.36 ± 0.14
100	$(8.89 \pm 0.89) \cdot 10^{-4}$	3.20 ± 0.32
110	$(2.08 \pm 0.21) \cdot 10^{-3}$	7.47 ± 0.75
120	$(5.72 \pm 0.58) \cdot 10^{-3}$	20.6 ± 2.1

From these experiments, the Arrhenius plot could be obtained, using relations (1) and (2) (**Figure 3**):

$$\boldsymbol{ln(k) = -\frac{E_a}{R}\frac{1}{T} + ln\, A} \qquad \textbf{(1)}$$

$\boldsymbol{k}$: Reaction rate constant (s^{-1})

$\boldsymbol{T}$: Temperature (K)

$$n_{H_2}(t) = k \cdot n_{catalyst} \cdot t \qquad (2)$$

$\boldsymbol{R}$: Gas constant (8.31 J K^{-1} mol^{-1})

$\boldsymbol{A}$: Pre-exponential factor

$\Delta \boldsymbol{E_a}$: Energy of activation (J mol^{-1})

$\boldsymbol{n_{H_2}}$: Moles of H_2 produced (mol)

$\boldsymbol{n_{catalyst}}$: Moles of catalyst (mol)

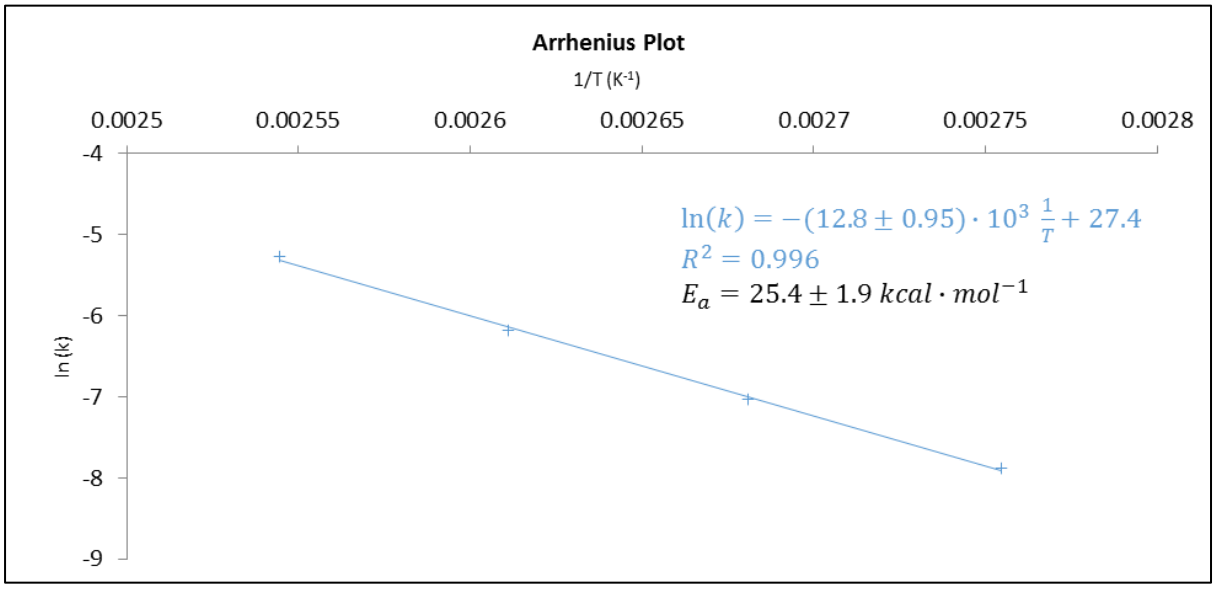

Figure 3. Arrhenius plot for the dehydrogenation of formic acid by gold(III) fluoride 1.

5 Control Experiments

5.1 Light induced isomerization of vinyl gold complex 4

When a dichloromethane solution of (*Z*)-vinyl gold complex **4** was exposed to blue LED light for 2 hours, an isomerization from exclusively (*Z*)-vinyl gold (93:7) to *(E)*-vinyl gold (29:71) was observed.

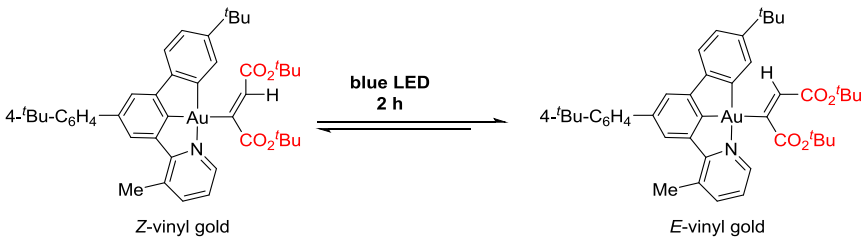

Z-vinyl gold | *E*-vinyl gold

Before blue light	**93**	**7**
After blue light	**29**	**71**

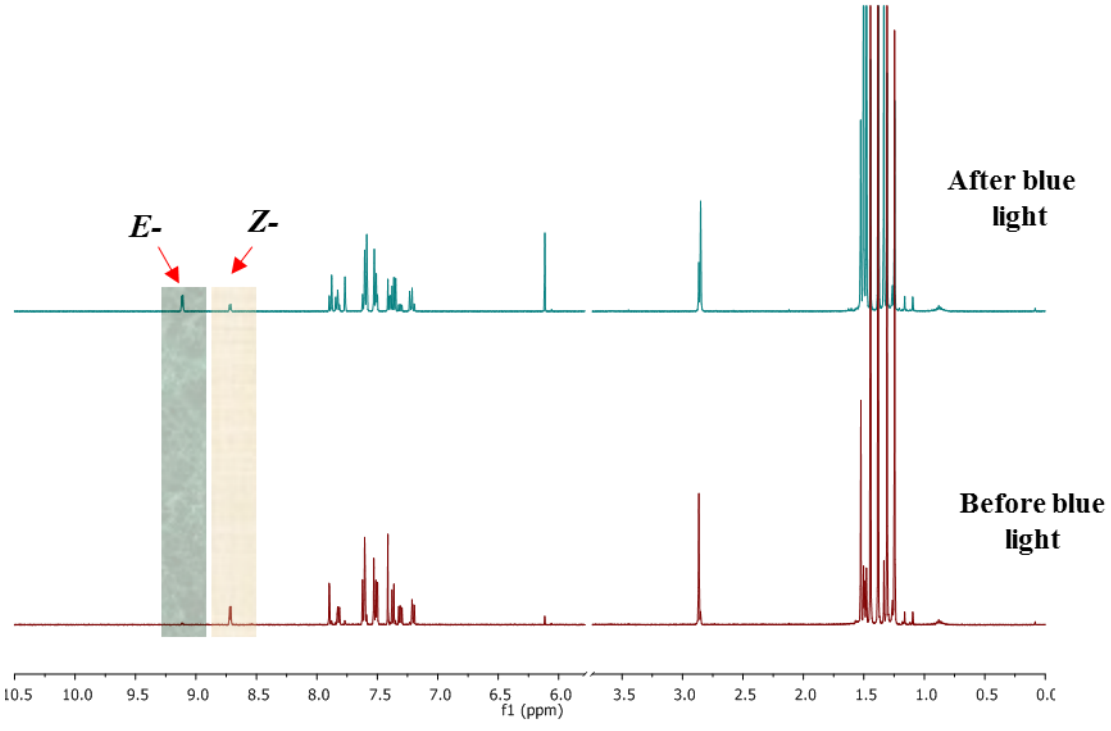

5.2 Confirmation of configuration of *E*-vinyl gold complex (obtained after exposure of (*Z*)-4 to blue-light) by 1D-selective nOe

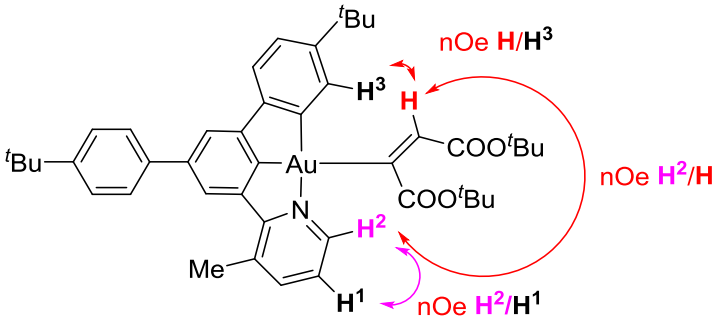

***cis*-vinyl gold**

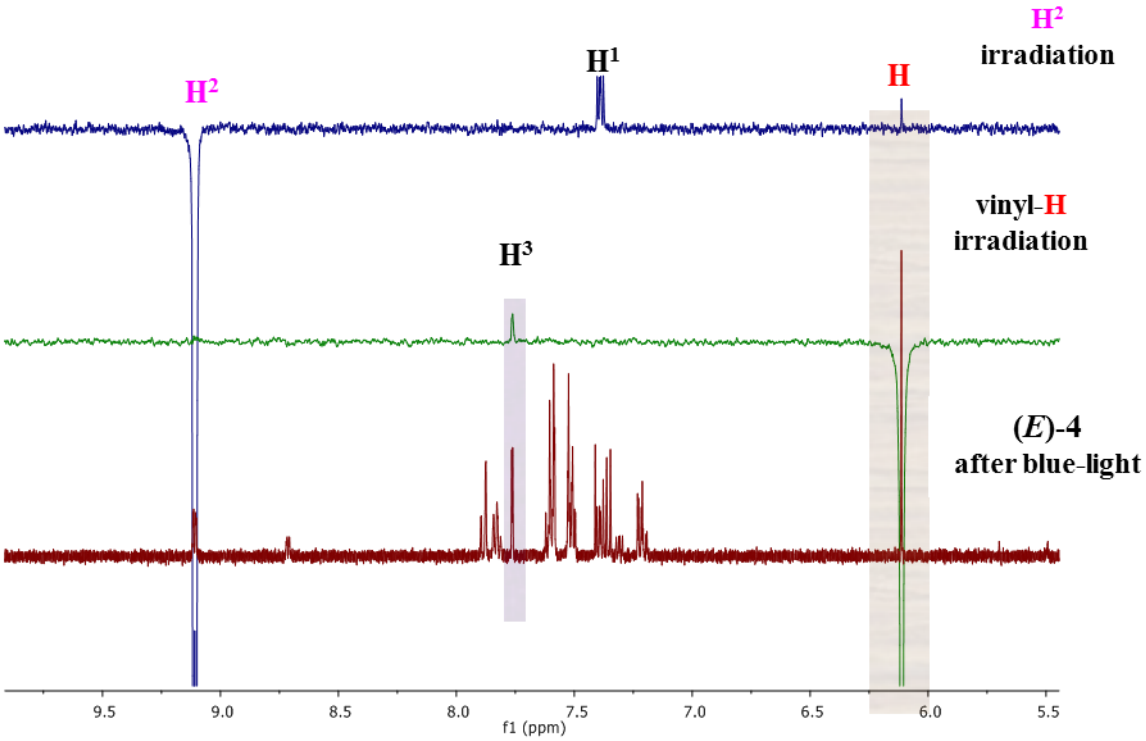

5.3 Formation of vinyl gold complex (*Z*)-4 in the presence of TEMPO

In a J-young NMR tube, a mixture of complex **2** (6.7 mg, 10 µmol), di-*tert*-butylacteylene dicarboxylate (**3**, 11 mg, 50 µmol) and TEMPO (4.6 mg, 30 µmol) in CD_2Cl_2 (1 ml) was heated at 100 °C for 90 minutes. A clean formation of vinyl gold complex (*Z*)-**4** was observed, the reaction mixture was purified by silica gel chromatography using DCM/hexane as eluent to give (*Z*)-**4** as a yellowish solid (4.2 mg, 53% yield). No TEMPO adduct was observed.

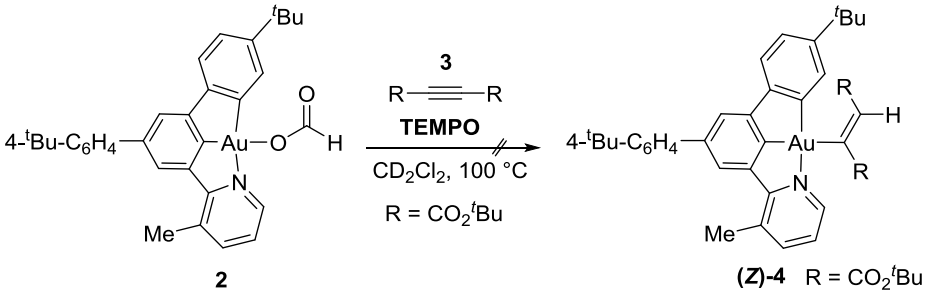

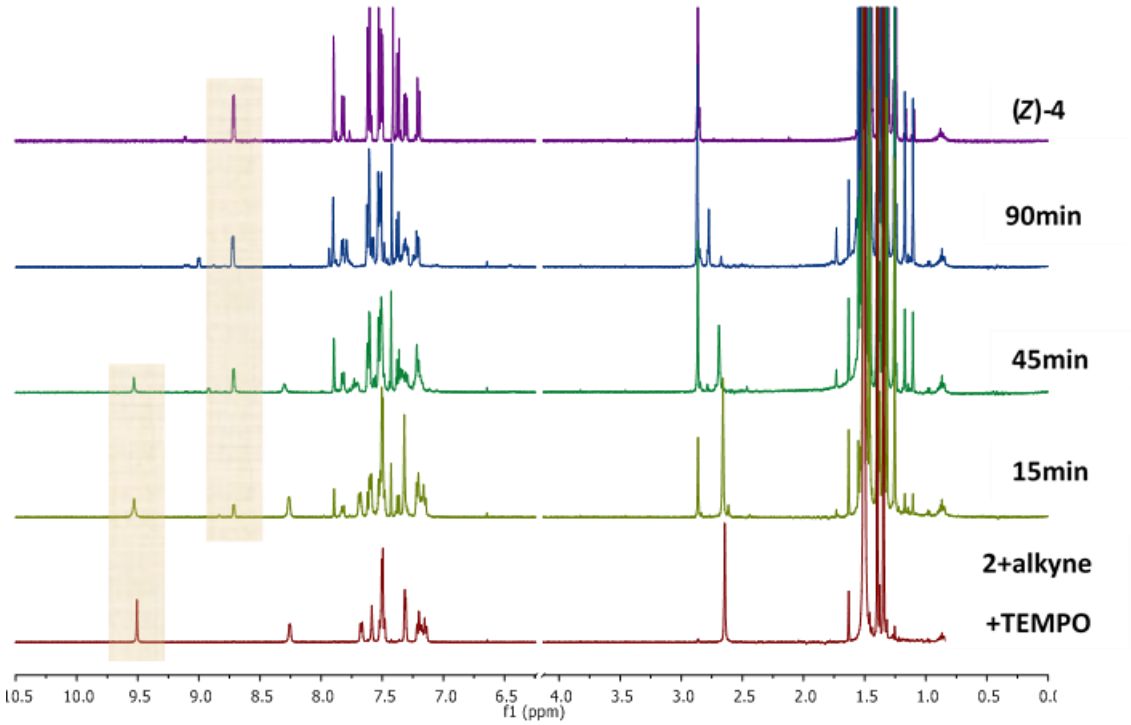

5.4 Radical clock experiment

In a J-young NMR tube, a mixture of complex **2** (6.7 mg, 10 µmol) and diallyl but-2-ynedioate (9.7 mg, 50 µmol) in CD_2Cl_2 (1.0 mL) was heated at 100 °C for 60 minutes and the reaction was monitored by ^1H NMR. The reaction mixture was purified by silica gel chromatography using DCM/hexane as eluent to give complex **8** as a yellowish solid (4.5 mg, 54% yield). No cyclized product **9** was observed.

^1H NMR (400 MHz, CD_2Cl_2) δ 8.64 (dd, J = 5.3, 1.5 Hz, 1H), 7.90 (d, J = 1.2 Hz, 1H), 7.82 (d, J = 7.9 Hz, 1H), 7.64 (s, 1H), 7.63 – 7.58 (m, 3H), 7.52 (d, J = 8.5 Hz, 2H), 7.48 (d, J = 2.0 Hz, 1H), 7.37 (d, J = 8.0 Hz, 1H), 7.30 (dd, J = 7.7, 5.4 Hz, 1H), 7.21 (dd, J = 8.0, 2.0 Hz, 1H), 5.99 – 5.87 (m, 1H), 5.85 – 5.75 (m, 1H), 5.31 – 5.21 (m, 2H), 5.17 – 5.06 (m, 2H), 4.69 – 4.60 (m, 2H), 4.50 (dt, J = 5.6, 1.4 Hz, 2H), 2.86 (s, 3H), 1.38 (s, 9H), 1.29 (s, 9H). ^{13}C NMR (101 MHz, CD_2Cl_2) δ 190.70, 176.00, 174.62, 170.39, 165.42, 153.67, 151.74, 151.60, 151.10, 149.74, 146.88, 144.89, 144.58, 141.18, 139.67, 134.62, 133.66, 133.40, 133.10, 129.57, 127.41, 126.38, 125.29, 124.53, 124.31, 122.02, 121.39, 117.93, 117.68, 65.59, 65.42, 35.42, 35.03, 31.67, 31.61, 23.00. IR (film) ν (cm^{-1}) 2960, 2900, 1700, 1588, 1421, 1253, 1199, 1172, 1008, 990, 926, 828 cm^{-1}. HR-MS (ESI) *m/z* calcd for $C_{42}H_{44}AuNO_4Na$ [M+Na^+] 846.2828, found 846.2837.

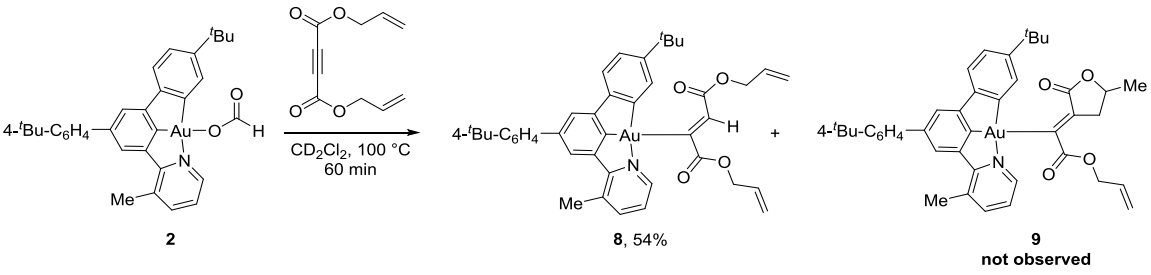

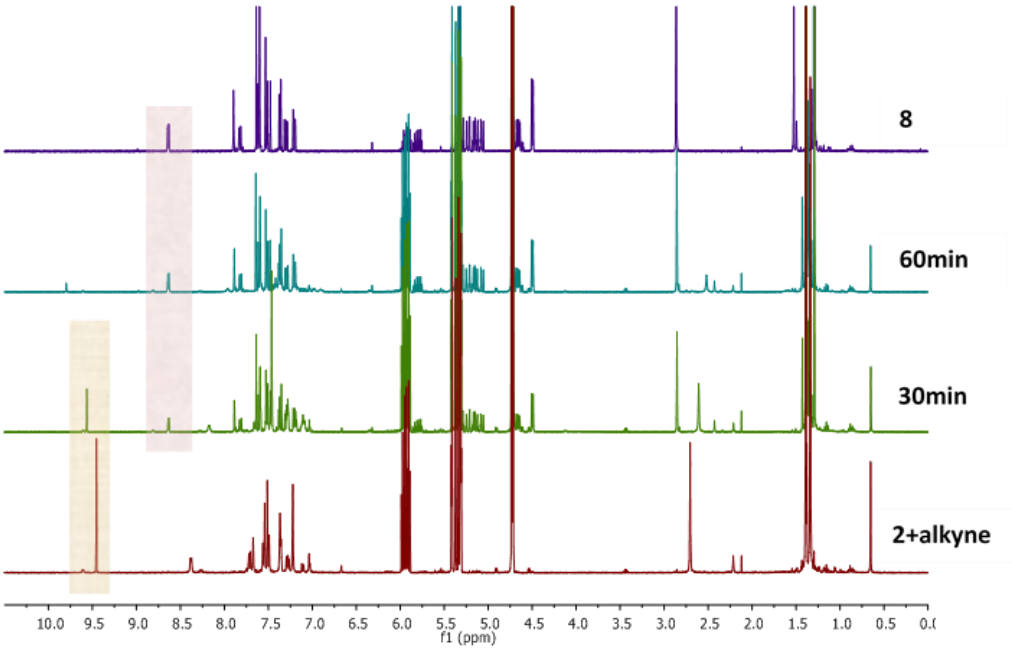

5.5 Dehydrogenation of FA in the presence of mercury (w Hg)

A vial (Biotage Microwave Process Vial 10 - 20 mL) was charged with a stirring bar and the gold(III) fluoride **1** (6.5 mg, 10 µmol). The vial was sealed, evacuated and backfilled with 1 atm of N_2. Dry formic acid (3.0 mL) was added, followed by 0.5 mL Hg (6.77 g, 33.8 mmol, $3.4 \cdot 10^3$ equiv with respect to the catalyst) and the resulting solution was stirred at the indicated temperature in a stirred oil bath. After the indicated time, the reaction was stopped by plunging the vial into an ice bath and the vial was then allowed to reach RT. A 100 µL aliquot of the headspace volume of the vial was taken with a gas-tight Hamilton syringe and manually injected in the GC. The vial was then heated further (**Figure 4**). An experiment without mercury (w/o Hg) was performed in parallel using the same conditions as well as the same batches of formic acid and catalyst.

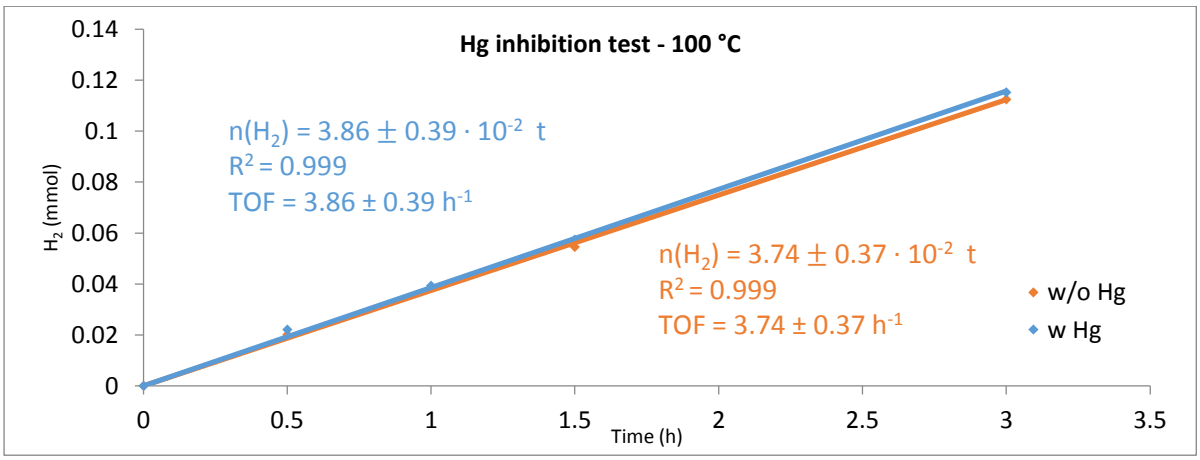

Figure 4. H_2 (mmol) vs. time (h) from gold fluoride 1 in formic acid at 100 °C with or without Hg (500 µL).

6. X-Ray diffraction analysis for compounds 2, 4, 6 and 7

[(N^C^C)Au-OCOH] (2) (CCDC 1511131)

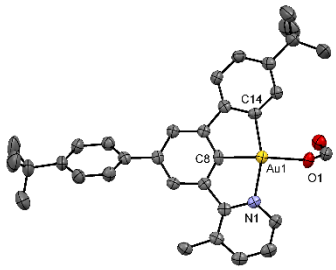

Crystallised from		CH_2Cl_2 / MeOH
Empirical formula		$C_{35}H_{43}AuNO_{4.5}$
Formula weight [g mol^{-1}]		746.67
Crystal colour, habit		colourless, prism
Crystal dimensions [mm]		0.03 × 0.08 × 0.10
Temperature [K]		160(1)
Crystal system		monoclinic
Space group		$P2_1/n$ (#14)
Z		4
Reflections for cell determination		17258
2θ range for cell determination [°]		5−149
Unit cell parameters	a [Å]	6.85898(10)
	b [Å]	25.4870(3)
	c [Å]	18.9537(3)
	α [°]	90
	β [°]	96.6323(15)

γ [°]	90
V [Å^3]	3291.23(8)
F(000)	1500
D_X [g cm^{-3}]	1.507
μ(Cu $K\alpha$) [mm^{-1}]	8.704
Scan type	ω
2θ(max) [°]	148.4
Transmission factors (min; max)	0.587; 1.000
Total reflections measured	31340
Symmetry independent reflections	6622
R_{int}	0.033
Reflections with $I > 2\sigma(I)$	6241
Reflections used in refinement	6619
Parameters refined; restraints	361; 18
Final $R(F)$ [$I > 2\sigma(I)$ reflections]	0.0373
$wR(F^2)$ (all data)	0.0809
Weights:	$w = [\sigma^2(F_O^2) + (0.0173P)^2 + 12.8705P]^{-1}$ where $P = (F_O^2 + 2F_C^2)/3$
Goodness of fit	1.211
Final Δ_{max}/σ	0.002
$\Delta\rho$ (max; min) [e Å^{-3}]	1.04; -0.82
$\sigma(d_{(C-C)})$ [Å]	0.006 – 0.011

[(N^C^C)Au-vinyl] (4) (CCDC 1511132)

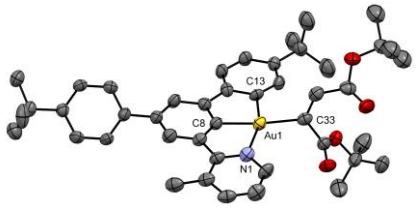

Identification code	NV1613
Empirical formula	$C_{48.6}H_{62.42}AuNO_{4.39}$
Formula weight	927.96
Temperature/K	160(1)
Crystal system	monoclinic
Space group	$P2_1/c$
a/Å	10.61692(17)
b/Å	12.2622(3)
c/Å	34.4571(7)
α/°	90
β/°	92.3794(16)
γ/°	90
Volume/Å^3	4481.99(17)
Z	4
ρ_{calc}g/cm^3	1.375
μ/mm^{-1}	6.499
F(000)	1901.0

Crystal size/mm^3	0.21 × 0.11 × 0.02
Radiation	CuKα (λ = 1.54184)
2Θ range for data collection/°	5.134 to 136.494
Index ranges	-12 ≤ h ≤ 12, -14 ≤ k ≤ 13, -41 ≤ l ≤ 41
Reflections collected	48491
Independent reflections	8173 [R_{int} = 0.0563, R_{sigma} = 0.0344]
Data/restraints/parameters	8173/41/501
Goodness-of-fit on F^2	1.130
Final R indexes [I>=2σ (I)]	R_1 = 0.0672, wR_2 = 0.1486
Final R indexes [all data]	R_1 = 0.0748, wR_2 = 0.1522
Largest diff. peak/hole / e Å^{-3}	3.13/-1.90

[(N^C^C)Au-OCOMe] (6) (CCDC 1511135)

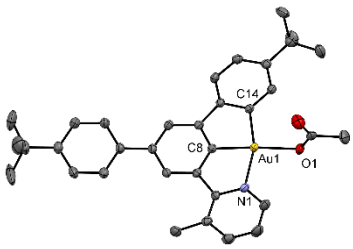

Crystallised from	dichloromethane / hexane
Empirical formula	$C_{34}H_{36}AuNO_2$
Formula weight [g mol^{-1}]	687.63
Crystal colour, habit	colourless, plate
Crystal dimensions [mm]	0.05 × 0.10 × 0.14

Temperature [K]		160(1)
Crystal system		monoclinic
Space group		$P2_1/c$ (#14)
Z		4
Reflections for cell determination		16426
2θ range for cell determination [°]		5–57
Unit cell parameters	a [Å]	16.25560(17)
	b [Å]	9.60195(9)
	c [Å]	18.62443(18)
	α [°]	90
	β [°]	95.6428(9)
	γ [°]	90
	V [Å^3]	2892.92(5)
F(000)		1368
D_x [g cm^{-3}]		1.579
μ(Mo $K\alpha$) [mm^{-1}]		5.133
Scan type		ω
$2\theta_{(max)}$ [°]		56.7
Transmission factors (min; max)		0.762; 1.000
Total reflections measured		29207
Symmetry independent reflections		6560
R_{int}		0.027

Reflections with $I > 2\sigma(I)$	5769
Reflections used in refinement	6560
Parameters refined	351
Final $R(F)$ [$I > 2\sigma(I)$ reflections]	0.0196
$wR(F^2)$ (all data)	0.0420
Weights:	$w = [\sigma^2(F_o^2) + (0.0174P)^2 + 1.8823P]^{-1}$ where $P = (F_o^2 + 2F_c^2)/3$
Goodness of fit	1.039
Final Δ_{max}/σ	0.004
$\Delta\rho$ (max; min) [e Å^{-3}]	0.65; -0.52
$\sigma(d_{(C-C)})$ [Å]	0.003 – 0.005

[(N^C^C)Au-OCOCF$_3$] (7) (CCDC 1033771)

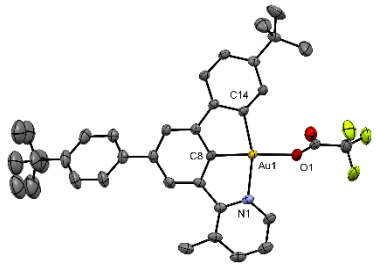

Crystallised from	CH_2Cl_2/ hexane
Empirical formula	$C_{34}H_{33}AuF_3NO_2$
Formula weight [g mol^{-1}]	741.58
Crystal colour, habit	colourless, plate
Crystal dimensions [mm]	0.04 × 0.14 × 0.17

Temperature [K]		160(1)
Crystal system		monoclinic
Space group		$P2_1/c$ (#14)
Z		4
Reflections for cell determination		11531
2θ range for cell determination [°]		5–58
Unit cell parameters	a [Å]	16.6602(3)
	b [Å]	9.69622(17)
	c [Å]	18.8796(3)
	α [°]	90
	β [°]	95.967(2)
	γ [°]	90
	V [Å^3]	3033.31(10)
F(000)		1464
D_X [g cm^{-3}]		1.624
μ(Mo $K\alpha$) [mm^{-1}]		4.899
Scan type		ω
2θ(max) [°]		58.4
Transmission factors (min; max)		0.447; 1.000
Total reflections measured		32054
Symmetry independent reflections		7353
R_{int}		0.053

Reflections with $I > 2\sigma(I)$	6194
Reflections used in refinement	7353
Parameters refined; restraints	402; 102
Final $R(F)$ [$I > 2\sigma(I)$ reflections]	0.0361
$wR(F^2)$ (all data)	0.0968
Weights:	$w = [\sigma^2(F_o^2) + (0.0479P)^2 + 5.2551P]^{-1}$ where $P = (F_o^2 + 2F_c^2)/3$
Goodness of fit	1.081
Final Δ_{max}/σ	0.001
$\Delta\rho$ (max; min) [e Å^{-3}]	1.89; -3.25
$\sigma(d_{(C-C)})$ [Å]	0.006 – 0.009

7. Computational results

The structures were optimized at DFT level by using the M06[1] functional as implemented in Gaussian 09.[2] Calculations were carried out by using the 6-31G(d,p) basis set for C, H, O and N and the Stuttgart/Dresden (SDD) [3] effective core potential (ECP) basis set for Au. Solvent effects were taken into account at the same levels of theory by applying the conductor-like polarizable continuum model (IEFPCM), [4] using Formic Acid as solvent, as in the experimental conditions. The solute cavity was constructed using radii from the UFF force field. The critical stationary points were characterized by frequency calculations in order to verify that they have the right number of imaginary frequencies, and the intrinsic reaction coordinates (IRC) [5] were followed to verify the energy profiles connecting the key transition structures to the correct associated local minima.

8.1 Energies of the structures in Scheme 4 of the manuscript

Table S1.

	E (hartrees)	H (hartress)	G (hartress)	Frequency
II	-1303.667242	-1303.281068	-1303.361682	
TS_{II-III}	-1303.626666	-1303.243123	-1303.323044	-201.6
III	-1115.146890	-1114.781110	-1114.853355	
CO_2	-188.504667	-188.489221	-188.514147	
Formic Acid	-189.678426	-189.640283	-189.668468	
H_2	-1.169430	-1.156050	-1.170838	
TS_{III-II}	-1304.804192	-1304.403352	-1304.486061	-151.0

Cartesian Coordinates

II

Standard orientation:

Center Number	Atomic Number	Atomic Type	Coordinates (Angstroms) X	Y	Z
1	6	0	0.205956	-0.169886	-0.085653
2	6	0	2.949701	-0.270442	0.021548
3	6	0	0.889876	1.046891	-0.054044
4	6	0	0.822221	-1.421982	-0.081418
5	6	0	2.213290	-1.461715	-0.033702
6	6	0	2.289160	0.965657	0.014632
7	1	0	2.739088	-2.415764	-0.056535
8	1	0	2.898089	1.855828	0.099320
9	79	0	-1.776312	-0.142019	-0.122171
10	6	0	-0.125664	-2.541458	-0.137749
11	6	0	0.202328	-3.894852	-0.159666
12	6	0	-1.490625	-2.164291	-0.172860
13	6	0	-0.805502	-4.856781	-0.217148
14	1	0	1.246353	-4.203841	-0.133434
15	6	0	-2.490383	-3.120286	-0.229693
16	6	0	-2.142382	-4.475757	-0.251933
17	1	0	-0.541359	-5.911399	-0.234313
18	1	0	-3.535496	-2.819239	-0.255333
19	1	0	-2.923245	-5.231607	-0.296837
20	6	0	0.046533	2.265643	-0.075171

21	6	0	0.485704	3.601877	-0.117650
22	7	0	-1.294311	2.002869	-0.059767
23	6	0	-0.488895	4.603840	-0.118854
24	6	0	-2.206888	2.974418	-0.055351
25	6	0	-1.840877	4.309060	-0.080581
26	1	0	-0.164248	5.641851	-0.150680
27	1	0	-3.245258	2.657250	-0.016011
28	1	0	-2.595705	5.087923	-0.075409
29	6	0	4.426160	-0.310595	0.094277
30	6	0	5.207440	0.638494	-0.576917
31	6	0	5.076116	-1.301116	0.841258
32	6	0	6.594922	0.600277	-0.499962
33	1	0	4.722879	1.400548	-1.185814
34	6	0	6.463413	-1.340541	0.916730
35	1	0	4.486055	-2.032264	1.390850
36	6	0	7.228380	-0.389551	0.247020
37	1	0	7.184018	1.342235	-1.033943
38	1	0	6.948813	-2.112980	1.508668
39	1	0	8.313591	-0.419688	0.306543
40	6	0	1.923286	4.020387	-0.172798
41	1	0	2.461769	3.761323	0.746179
42	1	0	2.453465	3.560143	-1.014313
43	1	0	1.991958	5.104703	-0.293962

44	8	0	-3.927934	-0.175818	-0.273503
45	6	0	-4.502446	0.359804	0.745282
46	8	0	-3.950244	0.876329	1.714133
47	1	0	-5.611458	0.327723	0.682293

TS_{II-III}

Standard orientation:

Center Number	Atomic Number	Atomic Type	Coordinates (Angstroms) X	Y	Z
1	6	0	0.254912	-0.133747	-0.038164
2	6	0	2.971106	-0.363298	0.020969
3	6	0	0.978077	1.057524	-0.018776
4	6	0	0.790393	-1.418496	-0.051076
5	6	0	2.179702	-1.518919	-0.023213
6	6	0	2.372875	0.904842	0.024644
7	1	0	2.658047	-2.496708	-0.059220
8	1	0	3.024029	1.766966	0.095651
9	79	0	-1.728256	-0.002460	-0.075691
10	6	0	-0.212546	-2.486508	-0.108384
11	6	0	0.047713	-3.853912	-0.135510

12	6	0	-1.555122	-2.040128	-0.141191
13	6	0	-1.008847	-4.761651	-0.193855
14	1	0	1.074840	-4.214655	-0.111071
15	6	0	-2.605460	-2.940889	-0.200579
16	6	0	-2.324239	-4.312133	-0.225341
17	1	0	-0.800196	-5.828376	-0.214530
18	1	0	-3.637704	-2.591309	-0.223896
19	1	0	-3.142705	-5.026872	-0.270135
20	6	0	0.188497	2.310774	-0.021082
21	6	0	0.681595	3.626397	-0.051804
22	7	0	-1.160705	2.102710	0.007553
23	6	0	-0.253774	4.666012	-0.025498
24	6	0	-2.037607	3.106016	0.044757
25	6	0	-1.615769	4.424765	0.032320
26	1	0	0.111563	5.690529	-0.048783
27	1	0	-3.085290	2.818110	0.101392
28	1	0	-2.337326	5.233972	0.061978
29	6	0	4.444889	-0.476899	0.063076
30	6	0	5.255782	0.422293	-0.640393
31	6	0	5.060136	-1.490824	0.807637
32	6	0	6.640793	0.310933	-0.599293
33	1	0	4.795479	1.200829	-1.247132
34	6	0	6.444912	-1.601973	0.848378

35	1	0	4.446562	-2.182431	1.382179
36	6	0	7.240422	-0.701790	0.144765
37	1	0	7.254115	1.012632	-1.159603
38	1	0	6.904707	-2.390924	1.438859
39	1	0	8.323677	-0.789174	0.176111
40	6	0	2.134751	3.982193	-0.118296
41	1	0	2.670918	3.685209	0.790630
42	1	0	2.633850	3.511669	-0.973023
43	1	0	2.250027	5.063993	-0.224520
44	1	0	-3.674229	0.044814	-0.745097
45	6	0	-4.393763	0.033249	0.204262
46	8	0	-3.990972	0.752217	1.145279
47	8	0	-5.370248	-0.689202	0.050571

III

Standard orientation:

Center Number	Atomic Number	Atomic Type	Coordinates (Angstroms) X	Y	Z
1	6	0	-0.157293	-0.118396	-0.018224
2	6	0	2.586106	-0.335462	-0.005550

3	6	0	0.583987	1.062602	0.013040
4	6	0	0.409115	-1.392140	-0.049051
5	6	0	1.798063	-1.495913	-0.050502
6	6	0	1.982638	0.929800	0.030939
7	1	0	2.287809	-2.468158	-0.104869
8	1	0	2.637091	1.789297	0.106659
9	79	0	-2.183305	-0.018204	0.019429
10	1	0	-3.859513	0.029116	0.059407
11	6	0	-0.594004	-2.470005	-0.079828
12	6	0	-0.306432	-3.833007	-0.123320
13	6	0	-1.953873	-2.050757	-0.060071
14	6	0	-1.336136	-4.772552	-0.150489
15	1	0	0.730106	-4.167974	-0.136354
16	6	0	-2.971387	-2.994028	-0.088588
17	6	0	-2.662256	-4.357915	-0.134408
18	1	0	-1.097051	-5.832921	-0.184292
19	1	0	-4.011041	-2.674827	-0.074284
20	1	0	-3.464708	-5.092025	-0.156301
21	6	0	-0.223614	2.308459	0.040981
22	6	0	0.261877	3.630244	0.010385
23	7	0	-1.577155	2.097002	0.087793
24	6	0	-0.669307	4.670731	0.053505
25	6	0	-2.446994	3.109413	0.126387

26	6	0	-2.030846	4.428756	0.118085
27	1	0	-0.303248	5.695240	0.032516
28	1	0	-3.498402	2.838168	0.162236
29	1	0	-2.754952	5.235579	0.153080
30	6	0	4.061475	-0.443065	0.007916
31	6	0	4.858388	0.467865	-0.697336
32	6	0	4.696810	-1.463197	0.727534
33	6	0	6.244605	0.363054	-0.681935
34	1	0	4.383545	1.252885	-1.284389
35	6	0	6.082603	-1.569631	0.741779
36	1	0	4.096304	-2.165458	1.303151
37	6	0	6.862671	-0.656796	0.037069
38	1	0	6.844571	1.075766	-1.243216
39	1	0	6.555990	-2.365040	1.312905
40	1	0	7.946759	-0.739742	0.047782
41	6	0	1.713381	3.991519	-0.076121
42	1	0	2.266781	3.685132	0.819188
43	1	0	2.200081	3.531568	-0.943791
44	1	0	1.823608	5.075060	-0.172025

CO_2

Standard orientation:

Center Number	Atomic Number	Atomic Type	Coordinates (Angstroms) X	Y	Z
1	6	0	0.000000	0.000000	-0.000004
2	8	0	0.000000	0.000000	1.163981
3	8	0	0.000000	0.000000	-1.163978

Formic Acid

Standard orientation:

Center Number	Atomic Number	Atomic Type	Coordinates (Angstroms) X	Y	Z
1	8	0	-1.111263	-0.092509	0.000075
2	1	0	-1.044475	-1.063016	-0.000106
3	6	0	0.127384	0.398674	0.000055
4	8	0	1.135242	-0.260935	-0.000129
5	1	0	0.088338	1.498529	0.000203

H_2

Standard orientation:

Center Number	Atomic Number	Atomic Type	Coordinates (Angstroms) X	Y	Z
1	1	0	0.000000	0.000000	0.370613
2	1	0	0.000000	0.000000	-0.370613

TS_{III-II}

Standard orientation:

Center Number	Atomic Number	Atomic Type	Coordinates (Angstroms) X	Y	Z
1	6	0	-0.244312	0.196168	-0.122799
2	6	0	-2.979469	0.195288	0.043450
3	6	0	-0.874823	-1.049179	-0.093435
4	6	0	-0.898402	1.426624	-0.097305
5	6	0	-2.288620	1.412472	-0.014614
6	6	0	-2.274502	-1.015155	0.005757
7	1	0	-2.847440	2.347523	-0.018106

8	1	0	-2.847805	-1.928975	0.087399
9	79	0	1.740079	0.231469	-0.251110
10	6	0	0.001964	2.578655	-0.180429
11	6	0	-0.377554	3.918663	-0.165496
12	6	0	1.375013	2.251317	-0.282387
13	6	0	0.589986	4.918038	-0.247151
14	1	0	-1.429981	4.187307	-0.088198
15	6	0	2.336399	3.246124	-0.357519
16	6	0	1.937664	4.587550	-0.339257
17	1	0	0.287565	5.962218	-0.236296
18	1	0	3.393454	2.995413	-0.429958
19	1	0	2.688895	5.371545	-0.400276
20	6	0	0.007840	-2.235832	-0.149261
21	6	0	-0.380884	-3.587722	-0.166235
22	7	0	1.336366	-1.922204	-0.188061
23	6	0	0.632830	-4.549983	-0.199949
24	6	0	2.290893	-2.854357	-0.203962
25	6	0	1.972586	-4.202065	-0.209161
26	1	0	0.348484	-5.600144	-0.214684
27	1	0	3.317378	-2.487570	-0.189911
28	1	0	2.755855	-4.952287	-0.224313
29	6	0	-4.454314	0.181625	0.148554
30	6	0	-5.215907	-0.785815	-0.518568

31	6	0	-5.120989	1.139397	0.922683
32	6	0	-6.601930	-0.796450	-0.411921
33	1	0	-4.718727	-1.522435	-1.148090
34	6	0	-6.506877	1.129519	1.028127
35	1	0	-4.544592	1.883609	1.469193
36	6	0	-7.252616	0.161208	0.361654
37	1	0	-7.176504	-1.551575	-0.943173
38	1	0	-7.005615	1.876660	1.640962
39	1	0	-8.336674	0.152622	0.444392
40	6	0	-1.802064	-4.061645	-0.159184
41	1	0	-2.318072	-3.799442	0.771697
42	1	0	-2.378254	-3.644556	-0.992911
43	1	0	-1.832572	-5.150436	-0.251525
44	1	0	3.494143	0.468630	-1.093228
45	8	0	4.811712	-0.972039	0.561292
46	1	0	3.852521	-0.029410	-0.548286
47	6	0	4.339865	-0.590428	1.660816
48	8	0	3.214398	-0.074501	1.869819
49	1	0	4.997621	-0.721076	2.556087

7.2 Additional computational studies

Alternative mechanisms for the reaction summarized in Scheme 4 of the manuscript were explored. All attempts to locate an intermediate with a free vacant in the gold(III) coordination sphere met with failure (Figure 5). When the pyridine is decoordinated on the outset of the calculation, it consistently returned to its original position at the very early stage during the minimization. In addition, when the complexes are forced to have the Py decoordinated ("freezing" the N-Au in a distant position), coordination of the formate via the two oxygen atoms is observed (**II'**) with a TS more than 10 kcal/mol higher in energy than the originally calculated one ($\Delta G^{\neq}$ ca 35 kcal/mol). When the pyridine is protonated in the presence of acid (**II''**) or a second molecule of formic acid is coordinated to gold (**II'''**), much higher energies are obtained for the corresponding intermediates, thus disfavoring their participation in the reaction. Finally, when both substituents are "frozen" (Py not coordinated, formate monocoordinated), the corresponding complex could not be obtained (**II^{IV}**, non existant). These results seem to support the reaction pathway proposed in Scheme 4.

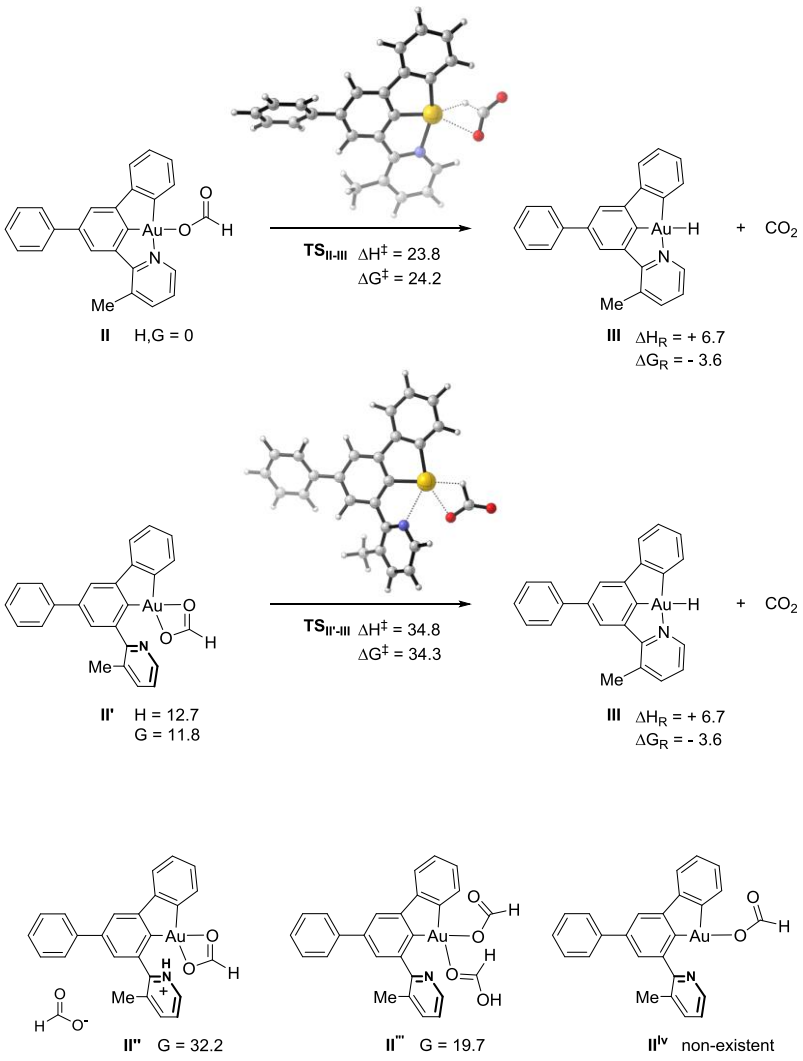

Figure 5: Alternative mechanism for decarboxylation of gold(III) formate.

Table S2.

	E (hartrees)	H (hartress)	G (hartress)	Frequency
II'	-1303.649423	-1303.263744	-1303.344416	
$TS_{II'-III}$	-1303.608569	-1303.225642	-1303.306943	-62.3
II''	-1304.296863	-1303.915358	-1303.995458	
II'''	-1493.333398	-1492.908851	-1492.998811	

II'

Standard orientation:

Center Number	Atomic Number	Atomic Type	Coordinates (Angstroms) X	Y	Z
1	6	0	-0.228217	-0.168653	0.096919
2	6	0	-2.962537	-0.226827	-0.059361
3	6	0	-0.884124	1.027847	-0.157623
4	6	0	-0.856165	-1.402754	0.237036
5	6	0	-2.249548	-1.414536	0.182244
6	6	0	-2.279661	0.990380	-0.212386
7	1	0	-2.800935	-2.344436	0.317360
8	1	0	-2.846493	1.898865	-0.406390
9	79	0	1.729530	-0.149434	-0.299676
10	6	0	0.106557	-2.500832	0.377888

11	6	0	-0.173321	-3.834464	0.664604
12	6	0	1.458291	-2.115875	0.196758
13	6	0	0.865714	-4.758099	0.776433
14	1	0	-1.204145	-4.154721	0.808173
15	6	0	2.491162	-3.028309	0.302419
16	6	0	2.186678	-4.362271	0.599399
17	1	0	0.638282	-5.796154	1.006260
18	1	0	3.522533	-2.715552	0.153649
19	1	0	2.990487	-5.089007	0.691002
20	6	0	-0.002941	2.207172	-0.023738
21	6	0	-0.322219	3.394761	0.643840
22	7	0	1.164693	2.070339	-0.712816
23	6	0	0.621856	4.424556	0.584421
24	6	0	2.058565	3.062049	-0.734126
25	6	0	1.808363	4.279949	-0.119677
26	1	0	0.410034	5.357122	1.104584
27	1	0	2.986164	2.863462	-1.266724
28	1	0	2.536735	5.082359	-0.172688
29	6	0	-4.439138	-0.248995	-0.132924
30	6	0	-5.196443	0.795843	0.411690
31	6	0	-5.111999	-1.311049	-0.749084
32	6	0	-6.584381	0.781602	0.337438
33	1	0	-4.691495	1.615799	0.921273

34	6	0	-6.499999	-1.325221	-0.823306
35	1	0	-4.539288	-2.120867	-1.197893
36	6	0	-7.241304	-0.278509	-0.281494
37	1	0	-7.155254	1.598232	0.773153
38	1	0	-7.004493	-2.153646	-1.315193
39	1	0	-8.326897	-0.289576	-0.340415
40	6	0	-1.590233	3.582731	1.419244
41	1	0	-2.407421	3.934302	0.777183
42	1	0	-1.923048	2.651448	1.889285
43	1	0	-1.448280	4.334280	2.201699
44	8	0	4.170764	0.766241	1.109526
45	6	0	4.542967	0.333438	0.020905
46	8	0	3.797868	-0.156911	-0.906789
47	1	0	5.621205	0.342741	-0.247200

$TS_{II'-III}$

Standard orientation:

Center Number	Atomic Number	Atomic Type	Coordinates (Angstroms) X	Y	Z
1	6	0	-0.178091	0.219836	0.048288

2	6	0	-2.948694	0.230753	0.020381
3	6	0	-0.833737	-1.004612	0.141828
4	6	0	-0.851113	1.444872	-0.015151
5	6	0	-2.243084	1.436916	-0.046324
6	6	0	-2.234407	-0.965909	0.133117
7	1	0	-2.785126	2.377382	-0.135376
8	1	0	-2.784973	-1.891606	0.276541
9	79	0	1.861140	0.320418	-0.018313
10	6	0	0.023248	2.610377	-0.003735
11	6	0	-0.351673	3.952162	-0.012178
12	6	0	1.389521	2.296430	0.069647
13	6	0	0.622463	4.945635	0.054449
14	1	0	-1.404169	4.224976	-0.064206
15	6	0	2.369203	3.270612	0.142664
16	6	0	1.970667	4.612501	0.133947
17	1	0	0.324618	5.990896	0.047725
18	1	0	3.424570	3.013109	0.201133
19	1	0	2.725629	5.392815	0.188917
20	6	0	-0.065089	-2.250571	0.351879
21	6	0	-0.443815	-3.513091	-0.139830
22	7	0	1.065888	-2.066346	1.060161
23	6	0	0.379486	-4.588559	0.201818
24	6	0	1.836107	-3.108666	1.357378

25	6	0	1.517891	-4.404033	0.971060
26	1	0	0.119662	-5.582440	-0.159117
27	1	0	2.744811	-2.895246	1.918445
28	1	0	2.156651	-5.238301	1.244576
29	6	0	-4.425248	0.212486	-0.016509
30	6	0	-5.105628	-0.823815	-0.668304
31	6	0	-5.175173	1.228764	0.587493
32	6	0	-6.494580	-0.842544	-0.715299
33	1	0	-4.539135	-1.609117	-1.167512
34	6	0	-6.564167	1.210373	0.539410
35	1	0	-4.665628	2.028800	1.121504
36	6	0	-7.228900	0.174978	-0.112311
37	1	0	-7.005101	-1.650922	-1.233431
38	1	0	-7.129592	2.004689	1.020957
39	1	0	-8.315363	0.161313	-0.150331
40	6	0	-1.628515	-3.760376	-1.027223
41	1	0	-1.835002	-2.915308	-1.692182
42	1	0	-1.450623	-4.644565	-1.647352
43	1	0	-2.541924	-3.955783	-0.450701
44	1	0	3.949391	0.394421	-0.160014
45	6	0	4.231608	-0.654394	-0.634518
46	8	0	3.219911	-1.389807	-0.826979
47	8	0	5.418887	-0.814499	-0.836246

II''

Standard orientation:

Center Number	Atomic Number	Atomic Type	Coordinates (Angstroms) X	Y	Z
1	6	0	0.236959	0.190279	-0.048487
2	6	0	3.017649	0.047648	-0.081458
3	6	0	0.846190	-1.041960	-0.144043
4	6	0	0.983711	1.366603	0.012176
5	6	0	2.365640	1.284149	-0.001656
6	6	0	2.245453	-1.110682	-0.155820
7	1	0	2.954726	2.195053	0.073729
8	1	0	2.717244	-2.082631	-0.242939
9	79	0	-1.794051	0.393824	0.048088
10	6	0	0.180708	2.576625	0.072664
11	6	0	0.615651	3.898682	0.108552
12	6	0	-1.190578	2.352361	0.054818
13	6	0	-0.304981	4.936553	0.120843
14	1	0	1.681193	4.119521	0.123975
15	6	0	-2.132420	3.358596	0.053792
16	6	0	-1.663993	4.676187	0.094290
17	1	0	0.047235	5.962928	0.148287

18	1	0	-3.195705	3.161028	0.028689
19	1	0	-2.382058	5.490476	0.103860
20	6	0	0.036913	-2.279818	-0.222746
21	6	0	-0.302740	-3.054545	0.887636
22	7	0	-0.424895	-2.624808	-1.437706
23	6	0	-1.102412	-4.167591	0.667473
24	6	0	-1.197799	-3.699673	-1.664351
25	6	0	-1.552121	-4.497435	-0.604571
26	1	0	-1.386038	-4.787898	1.512516
27	1	0	-1.499692	-3.873821	-2.690374
28	1	0	-2.178496	-5.363362	-0.772561
29	6	0	4.490624	-0.035201	-0.086972
30	6	0	5.144731	-1.072964	0.578097
31	6	0	5.259631	0.923780	-0.753629
32	6	0	6.528739	-1.152811	0.578710
33	1	0	4.565459	-1.810296	1.125605
34	6	0	6.643653	0.839933	-0.755974
35	1	0	4.771070	1.725930	-1.297993
36	6	0	7.282667	-0.197643	-0.089157
37	1	0	7.021622	-1.962667	1.108097
38	1	0	7.226986	1.585547	-1.285830
39	1	0	8.366579	-0.261399	-0.089422
40	6	0	0.170982	-2.682973	2.253503

41	1	0	1.262680	-2.719474	2.315830
42	1	0	-0.137082	-1.664732	2.513891
43	1	0	-0.233285	-3.367788	3.004358
44	1	0	-3.860381	0.600907	0.146342
45	6	0	-4.393938	-0.441281	-0.058521
46	8	0	-3.689761	-1.478432	-0.063191
47	8	0	-5.575690	-0.240301	-0.215392
48	1	0	-0.167627	-2.036771	-2.223433

II'''

Standard orientation:

Center Number	Atomic Number	Atomic Type	Coordinates (Angstroms) X	Y	Z
1	6	0	-0.407301	-0.214546	-0.006722
2	6	0	-3.224569	-0.112648	-0.109608
3	6	0	-1.052422	1.015425	-0.117774
4	6	0	-1.173771	-1.398251	0.048497
5	6	0	-2.562107	-1.340395	-0.004723
6	6	0	-2.452129	1.048179	-0.164721
7	1	0	-3.145407	-2.257828	0.063631
8	1	0	-2.939232	2.017433	-0.274377

9	79	0	1.626401	-0.522000	0.080627
10	6	0	-0.392459	-2.625307	0.181476
11	6	0	-0.883330	-3.927774	0.270494
12	6	0	0.996549	-2.433872	0.232131
13	6	0	-0.004103	-4.998793	0.410077
14	1	0	-1.955900	-4.110111	0.233528
15	6	0	1.883983	-3.485907	0.378308
16	6	0	1.368710	-4.783075	0.466797
17	1	0	-0.397189	-6.010065	0.478735
18	1	0	2.954939	-3.309583	0.430924
19	1	0	2.050869	-5.622129	0.580317
20	6	0	-0.346827	2.325380	-0.211765
21	6	0	-0.091773	3.074610	0.949826
22	7	0	-0.027358	2.734059	-1.443349
23	6	0	0.535329	4.305506	0.781004
24	6	0	0.586332	3.912229	-1.574519
25	6	0	0.891257	4.735942	-0.495517
26	1	0	0.752009	4.922688	1.651784
27	1	0	0.841506	4.217523	-2.589134
28	1	0	1.367315	5.700770	-0.653268
29	6	0	-4.699076	-0.041965	-0.158062
30	6	0	-5.385310	1.010362	0.461148
31	6	0	-5.443702	-1.023556	-0.823198

32	6	0	-6.772665	1.080314	0.414204
33	1	0	-4.825736	1.768566	1.006215
34	6	0	-6.831392	-0.954250	-0.869432
35	1	0	-4.927349	-1.835698	-1.332011
36	6	0	-7.501355	0.098100	-0.251158
37	1	0	-7.287226	1.901606	0.907794
38	1	0	-7.391268	-1.722055	-1.398311
39	1	0	-8.586637	0.153065	-0.287956
40	6	0	-0.450561	2.557220	2.307818
41	1	0	-1.523899	2.349540	2.392514
42	1	0	0.070780	1.614424	2.519771
43	1	0	-0.179972	3.277456	3.085734
44	8	0	3.730269	-1.033083	-1.982599
45	6	0	4.280889	-1.127813	-0.890231
46	8	0	3.728610	-0.983554	0.267075
47	1	0	5.365334	-1.358464	-0.823058
48	8	0	2.357473	1.592513	-0.083324
49	6	0	3.435110	2.020940	0.313022
50	1	0	4.231386	1.387269	0.720460
51	8	0	3.738518	3.289738	0.282491
52	1	0	2.972682	3.793935	-0.072710

References

[1] Zhao, Y.; Truhlar, D. G.; *Theor. Chem. Acc.* **2008**, *120*, 215-241.

[2] Gaussian 09, Revision D.01; M. J. Frisch, G. W. Trucks, H. B. Schlegel, G. E. Scuseria, M. A. Robb, J. R. Cheeseman, G. Scalmani, V. Barone, B. Mennucci, G. A. Petersson, H. Nakatsuji, M. Caricato, X. Li, H. P. Hratchian, A. F. Izmaylov, J. Bloino, G. Zheng, J. L. Sonnenberg, M. Hada, M. Ehara, K. Toyota, R. Fukuda, J. Hasegawa, M. Ishida, T. Nakajima, Y. Honda, O. Kitao, H. Nakai, T. Vreven, J. A. Montgomery, Jr., J. E. Peralta, F. Ogliaro, M. Bearpark, J. J. Heyd, E. Brothers, K. N. Kudin, V. N. Staroverov, T. Keith, R. Kobayashi, J. Normand, K. Raghavachari, A. Rendell, J. C. Burant, S. S. Iyengar, J. Tomasi, M. Cossi, N. Rega, J. M. Millam, M. Klene, J. E. Knox, J. B. Cross, V. Bakken, C. Adamo, J. Jaramillo, R. Gomperts, R. E. Stratmann, O. Yazyev, A. J. Austin, R. Cammi, C. Pomelli, J. W. Ochterski, R. L. Martin, K. Morokuma, V. G. Zakrzewski, G. A. Voth, P. Salvador, J. J. Dannenberg, S. Dapprich, A. D. Daniels, O. Farkas, J. B. Foresman, J. V. Ortiz, J. Cioslowski, and D. J. Fox, Gaussian, Inc., Wallingford CT, **2013**.

[3] Fuentealba, P.; Preuss, H.; Stoll, H.; Szentpály, L. v., *Chem. Phys. Lett.* **1982**, *89*, 418-422.

[4] (a) Cancès, E.; Mennucci, B.; Tomasi, J. *J. Chem. Phys*. **1997**, *107*, 3032–3047. (b) Cossi, M.; Barone, V.;Mennuci, B.; Tomasi, J. *Chem. Phys. Lett.* **1998**, *286*, 253–260. (c) Tomasi, J.; Mennucci, B.; Cancès, E. *J. Mol. Struct. (Theochem)*, **1999**, *464*, 211–226

[5] Gonzalez, C.; Schlegel, H. B. *J. Phys. Chem.* **1990**, *94*, 5523–5527.

CHAPTER 5

ALKYNE HYDROMETALLATION BY (N^C^C)-GOLD(III) COMPLEXES: A DETAILED MECHANISTIC INVESTIGATION

CHAPTER 5

Alkyne Hydrometallation by (N^C^C)-Gold(III) Complexes: A Detailed Mechanistic Investigation

Roopender Kumar, Estibaliz Merino, Enrique Gómez -Bengoa, Laura Gómez Martín, Xavi Ribas, and Cristina Nevado

(*Manuscript for Publication*)

Vinyl metal species play a key role in a wide variety of transformations in organic chemistry.[1] Streamlined access to these enabling reaction intermediates can be attained by hydrometallation of a triple bond (Scheme 1A). Despite the plethora of examples available in past and recent literature,[2-4] mechanistic understanding of this fundamental process has substantially laid behind synthetic developments. *Syn*-addition products, stemming from the suprafacial insertion of M-H into the C≡C bond are predominant in this context.[5-7] However, *anti*-additions have also been observed as result of a careful selection of the reaction conditions including the electronic nature of the alkyne and the combination of specific ancillary ligands and metals, thus further expanding the synthetic utility of these transformations.[3d, 3e, 8, 9]

While gold vinyl complexes have been profusely proposed and in certain cases isolated as intermediates in catalytic reactions,[10] examples of alkyne hydroauration processes are extremely scarce. In 2008, Sadighi and co-workers demonstrated the *anti*- insertion of (NHC)Au^{I}-H onto dimethyl acetylenedicarboxylate (DMAD) to form a (*Z*)-vinyl gold(I) complex, although the mechanism behind the observed stereochemical outcome remains obscure (Scheme 1B). [11] Bochmann and co-workers reported that the first isolated gold(III) hydride [(C^N^C)Au^{III}-H], did not react with DMAD but could undergo slow insertion onto other alkynes leading to (*Z*)-vinyl gold(III) complexes. In the presence of a radical initiator (AIBN), the reaction was accelerated, thus suggesting a radical mechanism, which was also confirmed by DFT calculations (Scheme 1C). [12] Our group has recently reported the efficient formation of novel (N^C^C) pincer ligand templates [13] able to stabilize (*Z*)-gold(III) vinyl complexes produced by a *β*-hydride elimination process on the corresponding (N^C^C)Au^{III}-formate precursors in the presence of *tert*-butyl acetylenedicarboxylate (Scheme 1D). [14] Preliminary control experiments ruled out the participation of radical intermediates in this transformation but did not suffice to underpin the actual mechanism behind the alkyne hydroauration reaction. As a result, we decided to investigate the potential underlying pathways in the hydroauration of triple bonds with (N^C^C)-stabilized gold complexes by a combination of stoichiometric experiments, NMR and cryo-MS analysis as well as DFT calculations. The results of this in depth study showcased the likelihood of a neutral pathway governing the formation of (*Z*)-(N^C^C)-gold(III) vinyl species as a result of the concerted but highly

asynchronous addition of both Au and H across the di-*tert*-butyl acetylenedicarboxylate. Further, an alternative method to produce alkyne hydroaurated species has been developed by reaction of the corresponding (N^C^C)-Au^{III}-F with silanes. In this case, in addition to the neutral pathway and based on both computationally and experimental evidence, the involvement of cationic species and a bimetallic *trans*-insertion process can be proposed. All these findings reveal a highly diverse mechanistic scenario governing the formation of (N^C^C)-vinyl gold(III) complexes via *anti*-addition pathways across the π-system and showcase the importance of both, the ancillary ligand template and the substituents on the substrate in producing distinctive reaction intermediates that might hold potential in future applications of these complexes in catalysis.

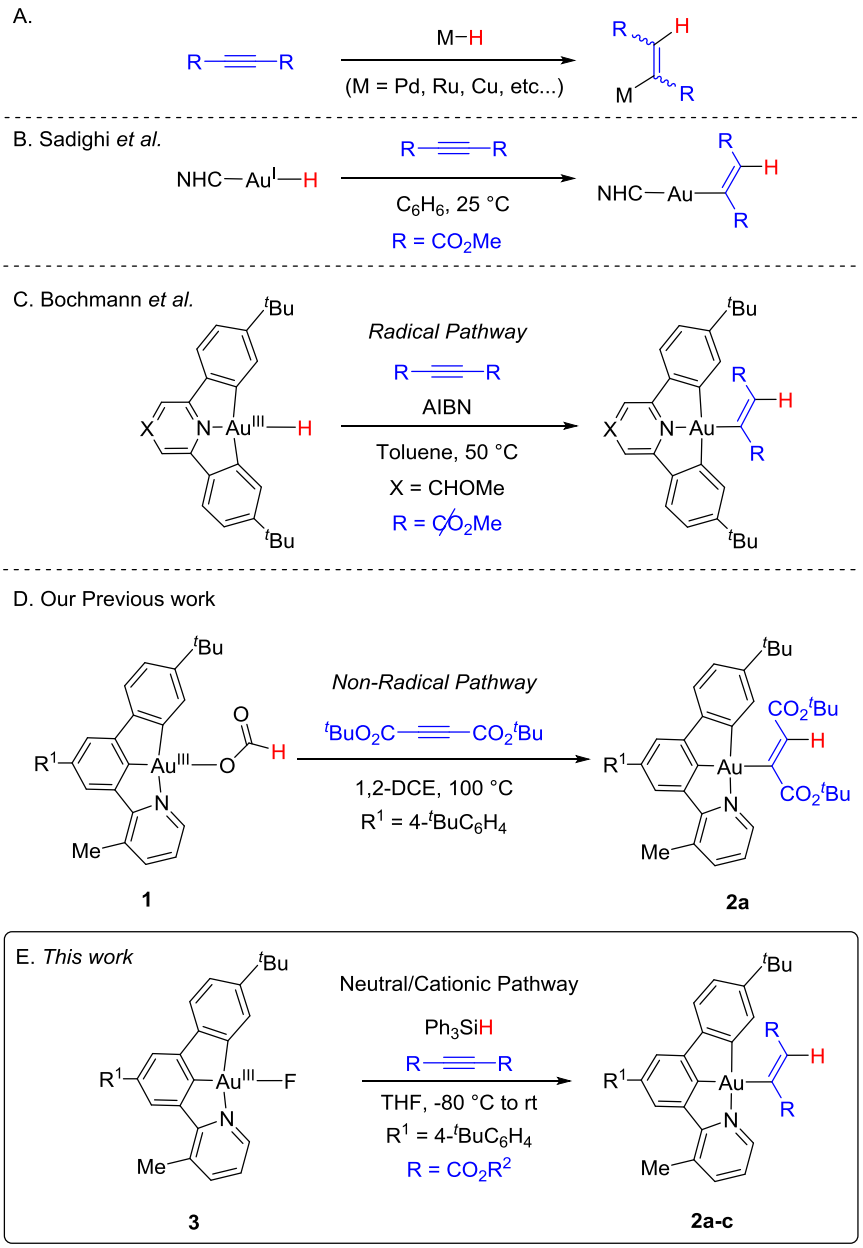

Scheme 1. Gold-mediated hydrometallation of alkynes

Results

(*Z*)-(N^C^C)-Vinyl Gold(III) Species from the corresponding formates via neutral pathway

In our previous study,[14] (N^C^C)Au^{III}-formate **1** reacted with di-*tert*-butyl acetylenedicarboxylate at 100°C to furnish the corresponding (*Z*)-*anti* addition product **2a** in 65% yield (Table 1, entry 1). Based on control experiments and supported by DFT calculations, we proposed that β-hydride elimination takes place on **1** to produce a putative, highly reactive, gold(III) hydride intermediate, which subsequently inserts onto the alkyne to deliver (*Z*)-vinyl complex **2a**. In the presence of light, (*Z*)-**2a** isomerized to the thermodynamically more stable (*E*)-isomer, whose structure could be confirmed by X-Ray diffraction analysis. Reactions in the presence of TEMPO furnished a similar outcome, thus suggesting a non-radical pathway for this transformation. We thus set out to explore potential mechanisms for the formation of **2a** as well as its isomerization. First, DFT calculations were carried out taking neutral (N^C^C)Au^{III}-H **I** as starting point in the presence of di-*tert*-butyl acetylenedicarboxylate (Figure 1). A non-classical, very asynchronous alkyne insertion process leading to (Z)-vinyl complex **II** could be found. Formally, this step consists of a nucleophilic hydride delivery from the gold center onto the alkyne, during which the alkyne gets reduced (and slightly negative) whilst gold becomes positively charged.

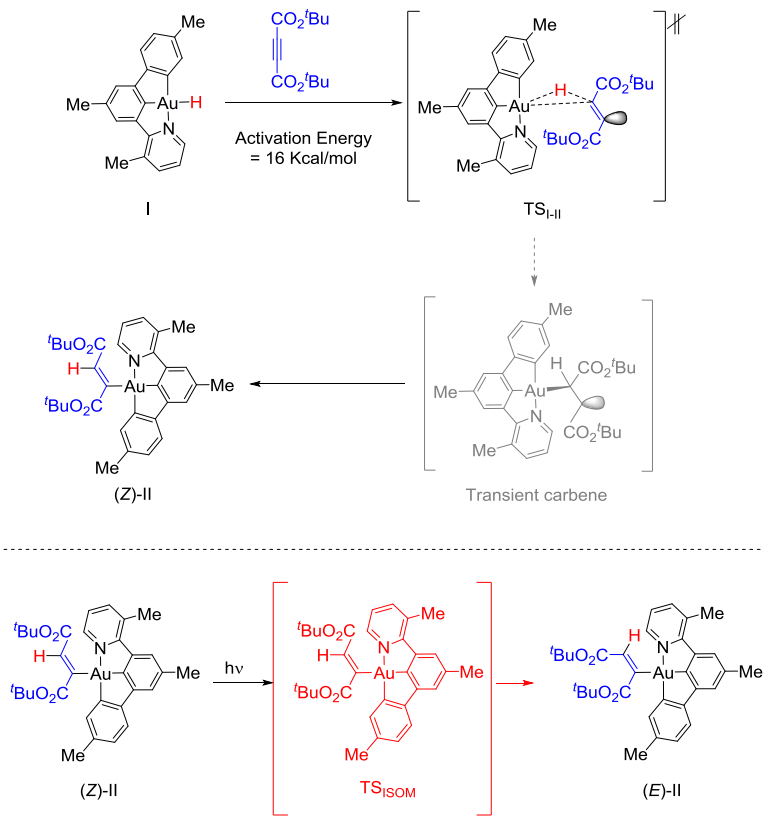

Figure 1. Neutral mechanism for alkyne hydrometallation by (N^C^C)Au^{III}-H complex. Energy calculations were performed at the M06/6-311G** (C, H, N, O), SDD (Au) level.

The so formed alkene adopts a *trans* configuration, and the gold atom slides through it to finally form a Au^{III}-C bond, consistent with the observed insertion product **II**. An activation energy of 16 Kcal/mol calculated by DFT (M06) indicates the compatibility of Au^{III}-H insertion and (*Z*)-alkene formation, devoid of any subsequent equilibration (Figure 1). Interestingly, throughout the calculation, no decoordination of the pyridine ligand with gold could be observed.[15] Alternatively, the structure of the transition state $\mathbf{TS_{I\text{-}II}}$ can be viewed as a 1,2-insertion with formation of a transient carbene, which is not a local minimum in the potential energy surface and directly evolves to the final product **II**. An independent IRC calculation starting from the transition state $\mathbf{TS_{I\text{-}II}}$ allowed us to unequivocally confirm the connection between this transition state and the final product **II**.

Alternative synthesis of (*Z*)-(C^C^N)-gold(III) vinyl species: a mechanistic study

In order to gain additional insights on the hydrometallation process operating on the (N^C^C)-templated gold(III) species, we set out to identify an alternative set of reaction conditions to produce the observed vinyl gold complexes. Previously, we could demonstrate the ability of (C^C^N)Au^{III}F complex **3**, to undergo transmetalation with boron reagents as result of a favorable B-F interaction.[13a, 13c] Silanes have demonstrated to be suitable reagents in alkyne hydrometallation reactions with other metals.[1c, 3b] Here, we envisioned that **3** could become a suitable partner for silanes given the thermodynamically favorable formation of a strong Si-F bond. To our delight, the reaction of (C^C^N)Au^{III}F **3** with Ph_3SiH in the presence of di-*tert*-butyl acetylenedicarboxylate in benzene at room temperature furnished **2a** in 76% yield (Table 1, entry 2). Similar outcomes were obtained when the reactions were carried out in dichloromethane and THF, respectively (see SI). Further, the reaction also worked efficiently with dimethyl-, and diethyl acetylenedicarboxylate delivering hydroauration products **2b** and **2c** in 58 and 69% yields, respectively (Table 1, entries 3-4). When the reaction was carried out with 1,2-diphenylethyne (**4**), methyl but-2-ynoate (**5**) and dimethyl-4,4'-(ethyne-1,2-diyl)dibenzoate (**6**), no conversion to the corresponding gold(III)-vinyl species was observed. Interestingly, DFT calculations performed with these substrates could not locate the corresponding transition states analogous to $\mathbf{TS_{I\text{-}II}}$ shown in Figure 1.

Next, the reaction of a simplified model of gold(III)-fluorido complex **III** with Ph_3SiH in the presence of di-*tert*-butyl acetylenedicarboxylate was analyzed by DFT calculations (Figure 2). Formation of a putative gold(III)-hydride **II** and fluorotriphenylsilane on the outset of the reaction appeared to be a feasible process. As shown in Figure 1, this intermediate can insert the alkyne in a concerted manner via $\mathbf{TS_{I\text{-}II}}$ with an activation energy of ca. 16 kcal/mol (see also Figure 2 left, blue pathway). Interestingly, calculations suggested that this intermediate could react with another molecule of gold(III)-fluoride **III** to produce a cationic di-gold(III)-hydride (**IV**, $d_{Au\text{-}H}$ = 1.79 Å) and $Ph_3SiF_2^-$. Although this step is endergonic (+ 4.2 Kcal/mol), the formation of the dimer **IV** is overall, a highly exothermic process ($\Delta G^{\ddagger}$ = -13.3 Kcal/mol).

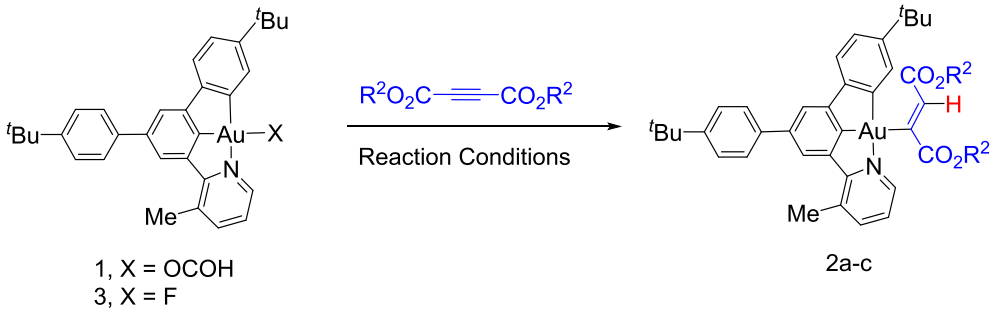

Entry	Au-X	X	Reaction Conditions	R^2	2 (%, Yield)
1	**1**	OCOH	1,2-DCE, 100°C, 60 min	^{t}Bu	**2a** (65)
2	**3**	F	Ph_3SiH, C_6H_6, 25°C, 3 h	^{t}Bu	**2a** (76)
3	**3**	F	Ph_3SiH, C_6H_6, 25°C, 3 h	Me	**2b** (58)
4	**3**	F	Ph_3SiH, C_6H_6, 25°C, 3 h	Et	**2c** (69)

Table 1. Synthesis of gold(III)- vinyl complexes **2a-c**.

The interaction of **IV** with di-*tert*-butyl acetylenedicarboxylate resulted in four possible intermediates (**V-VIII**). The lowest energy one (**V**, + 17.9 kcal/mol) involves the disociation of the dimeric gold(III) hydride to produce **I** and a monomeric cationic complex that immediately coordinates to the carbonyl group of the ester substituent on the alkyne (d_{Au-O} = 2.26 Å). Analogously, this monomeric cationic gold(III) species can coordinate to the triple bond itself as shown in **VI** with an overall energy of 21.1 kcal/mol, i.e. ca. 3.2 kcal/mol higher in energy with respect to **V**. Alternatively, the dimeric gold(III) cationic complex **IV** can coordinate the carbonyl group of the alkyne producing an intermediate **VII** which appears to be higher in energy (23.6 kcal/mol). Finally, intermediate **VIII** stems from the simultaneous coordination of two different gold complexes to both carbonyl groups present in the terminal positions of the alkyne. Interestingly, one of the gold atoms has decoordinated the pyridine ring to offer a vacant in the metal coordination sphere, which is then occupied by the O-atom donor. This intermediate is highly disfavored with an estimated energy > 36 kcal/mol. The transition state ($\mathbf{TS_{VIII-IX}}$) connecting **VIII** with the corresponding hydrometallated complex **IX** (in which the product **II** is still coordinated to a (N^C^C)-gold(III) cation via the ester moiety) could be located but the overall high energy content for this pathway (27.5 kcal/mol) led us to rule out the participation of intermediate **VIII** in the reaction. Transition states connecting **V**, **VI** and **VII** with **IX** ($\mathbf{TS_{V-IX}}$, $\mathbf{TS_{VI-IX}}$, $\mathbf{TS_{VII-IX}}$) could not be found although preliminary results show $\mathbf{TS_{V-IX}}$ to be the one lower in energy among them.

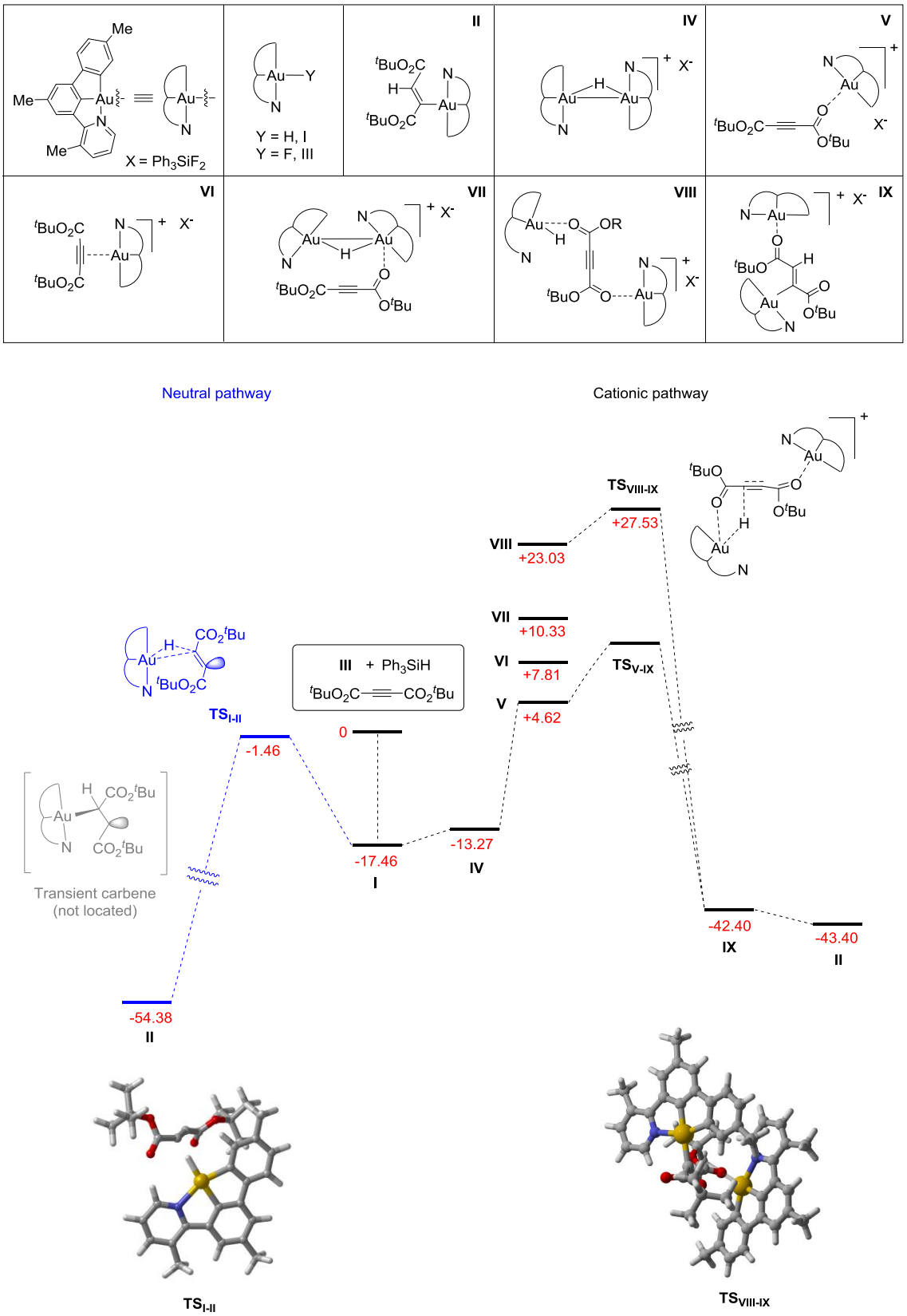

Figure 2. Reaction coordinate diagram for the reaction involving neutral (left side, blue) and cationic (right side, black) intermediates. Energy calculations were performed at the M06/6-311G** (C, H, N, O), SDD (Au) level.

The difference in energy between intermediates **V** and **VI** points towards a highly favorable interaction of the oxygen atom with the highly electrophilic gold(III) center compared to that of the alkyne π-system, thus confirming the previously reported oxophilic character for gold(III) species.[16] Further, these numbers are in line with the lack of reactivity observed for alkynes **4**, **5** and **6** devoid of ester groups directly conjugated with the triple bond. From intermediate **IX**, an almost thermoneutral pathway is observed for the ligand exchange reaction between the cationic gold(III) center and a new molecule of alkyne to regenerate intermediate **V**. As a result, the insertion of the cationic digold-hydride **IV** on the alkyne appear to be the more demanding step in this process.[17]

Cryo-MS Experiments

With the results of the DFT calculations in hand, we set out to acquire experimental evidence that would support the involvement of cationic species analogous to those depicted in Figure 2 (**V-IX**) in the present alkyne hydroauration process. First, the reaction between gold(III)-fluorido complex **3** and Ph_3SiH was monitored by ^1H NMR at -50 °C. New species could be detected by ^1H NMR, which could not be categorically assigned to an specific product, although resulted in a productive reaction outcome upon addition of alkyne to give (*Z*)-vinyl gold(III) complex **2a**. Next, we decided to turn to Cryo-MS analysis to follow the reaction progress and to explore the presence of putative cationic intermediates in this transformation. To this end, and to ensure a better ionization of the in situ produced gold(III) species, the reaction was repeated in mixture of THF:MeCN (10:1) leading to a similar outcome, which provided us with the suitable conditions for monitorization experiments. Thus, in a scintillation vial, (N^C^C)Au^{III}-F **3** was treated with Ph_3SiH in a mixture of THF:MeCN (10:1) at -50°C and after 5 min, a new peak (M^+=1257.4635) was found. Next, addition of di-*tert*-butyl acetylenedicarboxylate and cooling down to -80°C, in order to stabilize putative cationic gold(III) intermediates, furnished two new peaks (M^+=1483.5840 and M^+=854.3484).

The peak with M^+=1257.4635 could be assigned to a dimeric cationic gold(III) complex analogous to **IV**, formed by reaction of two molecules of (N^C^C)Au^{III}F with Ph_3SiH and whose calculated mass is 1257.4630 (Figure 3). The peak with the higher mass (M^+=1483.5840) could correspond to both intermediates similar to **VII** and **VIII** as well as the product immediate precursor **IX**. The energies obtained by DFT calculations suggest the latter hypothesis as the most likely one under the present set up. Finally, the peak with M^+=854.3484 could be correlated with intermediate **V**, which is not only the most stable intermediate after **IV**, but also is regenerated in the reaction upon de-coordination of the product from **IX**. Deuterium labeling experiments strongly support the scenario proposed above as they confirmed the intermediacy of species analogous to **V**-d_1 and **IX**-d_1 in the reaction when Ph_3SiD was used as reagent in this transformation.

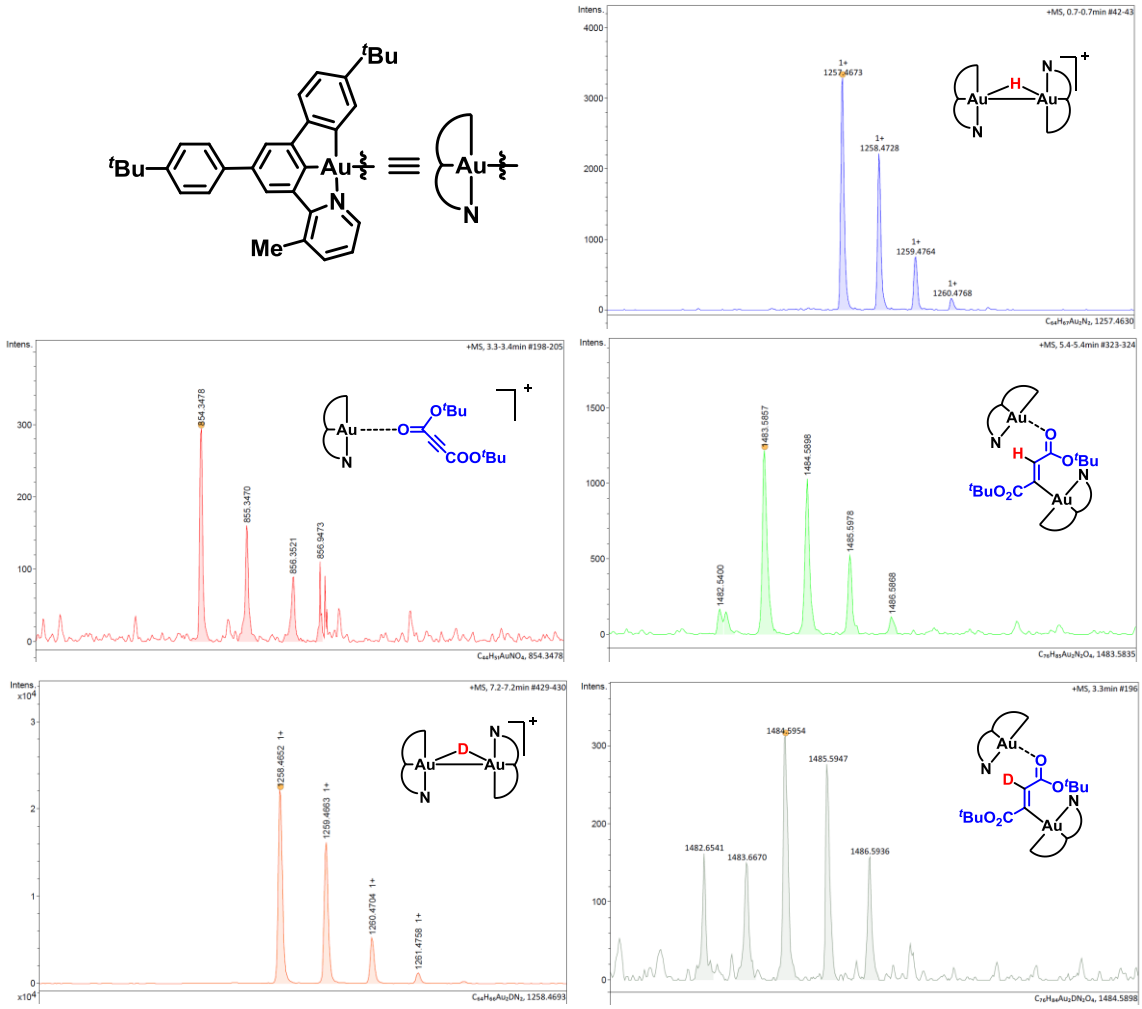

Figure 3. Putative cationic gold (III)-intermediates analogous to **IV-V, IX** detected by Cryo-MS.

Conclusions

A neutral pathway for the formation of (*Z*)-(N^C^C)-vinyl gold(III) complexes **2** has been found involving a concerted but asynchronous addition of the corresponding Au-H bond onto the corresponding di-alkyl acetylenedicarboxylates. Further, the isomerization pathway to the corresponding (*E*)-vinyl species detected after exposure to light has also been computationally characterized. In addition, an alternative method to produce alkyne hydroaurated species has been developed starting from gold(III) fluorides in the presence of silanes. The underlying mechanism in this transformation has been investigated in depth by experimental means as well as by DFT calculations. In addition to a neutral pathway analogous to the one observed for Au-H species, involvement of cationic intermediates seems to be highly likely in these transformations. Further, formation of cationic dimeric gold(III) complexes could be confirmed by cryo-MS experiments, which also confirmed the oxophilic nature of the electrophilic gold(III) center. All these findings reveal the multiple reaction pathways yielding *anti*- addition vinyl gold(III) complexes.

References

[1] (a) F. Alonso, I. P. Beletskaya, M. Yus, *Chem. Rev.* **2004**, *104*, 3079-3160; (b) M. Zaidlewicz, A. Wolan, M. Budny, in *Comprehensive Organic Synthesis II (Second Edition)*, Elsevier, Amsterdam, **2014**, pp. 877-963; (c) B. M. Trost, Z. T. Ball, *Synthesis* **2005**, *2005*, 853-887; (d) U. M. Dzhemilev, A. G. Ibragimov, in *Modern Reduction Methods*, Wiley-VCH Verlag GmbH & Co. KGaA, **2008**, pp. 447-489; (e) A. P. Dobbs, F. K. I. Chio, in *Comprehensive Organic Synthesis II (Second Edition)*, Elsevier, Amsterdam, **2014**, pp. 964-998; (f) R. Barbeyron, E. Benedetti, J. Cossy, J.-J. Vasseur, S. Arseniyadis, M. Smietana, *Tetrahedron* **2014**, *70*, 8431-8452.

[2] (a) R. Shen, T. Chen, Y. Zhao, R. Qiu, Y. Zhou, S. Yin, X. Wang, M. Goto, L.-B. Han, *J. Am. Chem. Soc.* **2011**, *133*, 17037-17044; (b) C. Jahier, O. V. Zatolochnaya, N. V. Zvyagintsev, V. P. Ananikov, V. Gevorgyan, *Org. Lett.* **2012**, *14*, 2846-2849; (c) A. Adhikary, J. R. Schwartz, L. M. Meadows, J. A. Krause, H. Guan, *Inorg. Chem. Front.* **2014**, *1*, 71-82; (d) C. Martin, S. Mallet-Ladeira, K. Miqueu, G. Bouhadir, D. Bourissou, *Organometallics* **2014**, *33*, 571-577; (e) H. Makabe, E.-i. Negishi, in *Handbook of Organopalladium Chemistry for Organic Synthesis*, John Wiley & Sons, Inc., **2003**, pp. 2789-2823.

[3] (a) C. S. Yi, *J. Organomet. Chem.* **2011**, *696*, 76-80; (b) S. Ding, L.-J. Song, L. W. Chung, X. Zhang, J. Sun, Y.-D. Wu, *J. Am. Chem. Soc.* **2013**, *135*, 13835-13842; (c) M. Leutzsch, L. M. Wolf, P. Gupta, M. Fuchs, W. Thiel, C. Farès, A. Fürstner, *Angew. Chem. Int. Ed.* **2015**, *54*, 12431-12436; (d) S. M. Rummelt, K. Radkowski, D.-A. Roşca, A. Fürstner, *J. Am. Chem. Soc.* **2015**, *137*, 5506-5519; (e) D.-A. Roşca, K. Radkowski, L. M. Wolf, M. Wagh, R. Goddard, W. Thiel, A. Fürstner, *J. Am. Chem. Soc.* **2017**.

[4] T. G. Frihed, A. Fürstner, *Bull. Chem. Soc. Jpn.* **2016**, *89*, 135–160.

[5] (a) X. Li, T. Vogel, C. D. Incarvito, R. H. Crabtree, *Organometallics* **2005**, *24*, 62-76; (b) J. J. Pérez-Torrente, D. H. Nguyen, M. V. Jiménez, F. J. Modrego, R. Puerta-Oteo, D. Gómez-Bautista, M. Iglesias, L. A. Oro, *Organometallics* **2016**, *35*, 2410-2422; (c) L.-J. Song, S. Ding, Y. Wang, X. Zhang, Y.-D. Wu, J. Sun, *J. Org.Chem.* **2016**, *81*, 6157-6164.

[6] (a) N. P. Mankad, D. S. Laitar, J. P. Sadighi, *Organometallics* **2004**, *23*, 3369-3371; (b) K. Semba, T. Fujihara, T. Xu, J. Terao, Y. Tsuji, *Adv. Synth. Catal.* **2012**, *354*, 1542-1550; (c) L. R. Collins, I. M. Riddlestone, M. F. Mahon, M. K. Whittlesey, *Chem. Eur. J.* **2015**, *21*, 14075-14084; (d) A. M. Suess, M. R. Uehling, W. Kaminsky, G. Lalic, *J. Am. Chem. Soc.* **2015**, *137*, 7747-7753.

[7] (a) X. Wang, M. Nakajima, R. Martin, *J. Am. Chem. Soc.* **2015**, *137*, 8924-8927; (b) X. Wang, M. Nakajima, E. Serrano, R. Martin, *J. Am. Chem. Soc.* **2016**, *138*, 15531-15534.

[8] (a) L. N. Lewis, K. G. Sy, G. L. Bryant, P. E. Donahue, *Organometallics* **1991**, *10*, 3750-3759; (b) K. Itami, K. Mitsudo, A. Nishino, J.-i. Yoshida, *J. Org. Chem.* **2002**, *67*, 2645-2652.

[9] F. Ye, J. Chen, T. Ritter, *J. Am. Chem. Soc.* **2017**, *139*, 7184-7187.

[10] (a) A. Furstner, *Chem. Soc. Rev.* **2009**, *38*, 3208-3221; (b) A. S. K. Hashmi, A. M. Schuster, F. Rominger, *Angew. Chem., Int. Ed.* **2009**, *48*, 8247-8249; (c) T. J. Brown, D. Weber, M. R. Gagné, R. A. Widenhoefer, *J. Am. Chem. Soc.* **2012**, *134*, 9134-9137; (d) W. Yang, A. S. K. Hashmi, *Chem. Soc. Rev.* **2014**, *43*, 2941-2955; e) M. Wieteck, M. H. Larsen née Vilhelmsen, P. Nösel, J. Schulmeister, F. Rominger, M. Rudolph, M. Pernpointner, A. S. K. Hashmi, *Adv. Synth. Catal.* **2016**, *358*, 1449-1462.

[11] E. Y. Tsui, P. Müller, J. P. Sadighi, *Angew. Chem., Int. Ed.* **2008**, *47*, 8937-8940.

[12] (a) A. Pintus, L. Rocchigiani, J. Fernandez-Cestau, P. H. M. Budzelaar, M. Bochmann, *Angew. Chem., Int. Ed.* **2016**, *55*, 12321-12324; (b) D.-A. Roşca, D. A. Smith, D. L. Hughes, M. Bochmann, *Angew. Chem., Int. Ed.* **2012**, *51*, 10643-10646.

[13] (a) R. Kumar, A. Linden, C. Nevado, *Angew. Chem., Int. Ed.* **2015**, *54*, 14287-14290; (b) R. Kumar, A. Linden, C. Nevado, *J. Am. Chem. Soc.* **2016**, *138*, 13790-13793; (c) R. Kumar, C. Nevado, *Angew. Chem., Int. Ed.* **2017**,*56*, 1994-2015.

[14] R. Kumar, J.-P. Krieger, E. Gómez-Bengoa, T. Fox, A. Linden, C. Nevado, *Angew. Chem., Int. Ed.* **2017**, *accepted*.

[15] L. Rocchigiani, J. Fernandez-Cestau, P. H. M. Budzelaar, M. Bochmann, *Chem. Commun.* **2017**, *53*, 4358-4361.

[16] (a) A. W. Sromek, M. Rubina, V. Gevorgyan, *J. Am. Chem. Soc.* **2005**, *127*, 10500-10501; (b) A. Arcadi, M. Alfonsi, G. Bianchi, G. D'Anniballe, F. Marinelli, *Adv. Synth. Catal.* **2006**, *348*, 331-338; (c) A. S. Dudnik, A. W. Sromek, M. Rubina, J. T. Kim, A. V. Kel'i, V. Gevorgyan, *J. Am. Chem. Soc.* **2008**, *130*, 1440-1452; (d) F. Mo, J. M. Yan, D. Qiu, F. Li, Y. Zhang, J. Wang, *Angew. Chem., Int. Ed.* **2010**, *49*, 2028-2032.

[17] "For mechanistic studies of alkene and alkyne trans insertion reactions on (N^C)Au(OTFA)$_2$ complexes, see: (a) E. Langseth, A. Nova, E. A. Tråseth, F. Rise, S. Øien, R. H. Heyn, M. Tilset, *J. Am. Chem. Soc.* **2014**, *136*, 10104-10115; (b) M. S. M. Holmsen, A. Nova, D. Balcells,

E. Langseth, S. Øien-Ødegaard, R. H. Heyn, M. Tilset, G. Laurenczy, *ACS Catal.* **2017**, 5023-5034.

CHAPTER 5

EXPERIMENTAL SECTION

Table of Contents

1. General Information

NMR spectra were recorded on AV2 400 or AV2 500 MHz Bruker spectrometers. Chemical shifts are given in ppm. The spectra were calibrated to the residual ^{1}H and ^{13}C signals of the solvents. Multiplicities are abbreviated as follows: singlet (s), doublet (d), triplet (t), quartet (q), doublet-doublet (dd), quintet (quint), septet (sept), multiplet (m), and broad (b). The compounds were characterized by ^{1}H, ^{13}C, and ^{19}F NMR spectroscopy. Infrared spectra were recorded on a JASCO FT/IR-4100 spectrometer. High-resolution electrospray ionization and electronic impact mass spectrometry was performed on a Finnigan MAT 900 (Thermo Finnigan, San Jose, CA; USA) double focusing magnetic sector mass spectrometer. Ten spectra were acquired. A mass accuracy ≤ 2 ppm was obtained in the peak matching acquisition mode by using a solution containing 2 <l PEG200, 2 <l PPG450, and 1.5 mg NaOAc (all obtained from Sigma-Aldrich, CH-Buchs) dissolved in 100 mL MeOH (HPLC Supra grade, Scharlau, E-Barcelona) as internal standard. GC-MS analysis was done on a Finnigan Voyager GC8000 Top. Elemental microanalysis was carried out with Leco TruSpec Micro-CHNS analyser. Microwave reaction was done in Discover & Explorer SP (CEM). Gold complexes decompose before melting temperature is reached (T^{a} > 200 °C).

Materials and Methods:

Unless otherwise stated, starting materials were purchased from Aldrich and/or Fluka. Solvents were purchased in HPLC quality, degassed by purging thoroughly with nitrogen and dried over activated molecular sieves of appropriate size. Alternatively, they were purged with argon and passed through alumina columns in a solvent purification system (Innovative Technology). Conversion was monitored by thin layer chromatography (TLC) using Merck TLC silica gel 60 F254. Compounds were visualized by UV-light at 254 nm and by dipping the plates in an ethanolic vanillin/sulfuric acid solution or an aqueous potassium permanganate solution followed by heating. Flash column chromatography was performed over silica gel (230-400 mesh).

2. Experimental procedures and characterization of complexes 2a-c

(*Z*)-[(N^C^C)Au-vinyl] (2a)

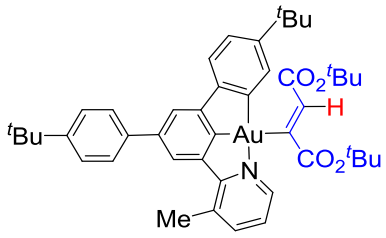

In a glovebox, a scintillation vial was charged with complex **3** (50 mg, 77 µmol) and di-*tert*-butyl acetylenedicarboxylate (87 mg, 386 µmol). The mixture was dissolved in benzene (2 ml), and triphenylsilane (40 mg, 154 µmol) was added. The reaction mixture was stirred for 2 hours at room temperature. After completion of the reaction, the reaction vial was taken out of the glovebox and solvent was evaporated and the crude mixture was purified by silica gel chromatography using DCM:hexane as eluent to yield complex **2a** (50 mg, 76%) as a yellowish solid. ^{1}H NMR (400 MHz, CD_2Cl_2) δ 8.72 (dd, J = 5.3, 1.6 Hz, 1H), 7.89 (d, J = 1.2 Hz, 1H), 7.82 (dd, J = 7.8, 1.0 Hz, 1H), 7.63 – 7.58 (m, 3H), 7.55 – 7.50 (m, 3H), 7.42 (s, 1H), 7.37 (d, J = 8.0 Hz, 1H), 7.30 (dd, J = 7.7, 5.4 Hz, 1H), 7.21 (dd, J = 8.0, 2.0 Hz, 1H), 2.86 (s, 3H), 1.46 (s, 9H), 1.39 (s, 9H), 1.32 (s, 9H), 1.25 (s, 9H). ^{13}C NMR (101 MHz, CD_2Cl_2) δ 190.31, 176.48, 174.82, 170.79, 165.45, 153.70, 151.76, 151.55, 151.09, 149.84, 146.91, 144.90, 144.55, 141.14, 139.69, 134.57, 133.70, 129.62, 127.42, 126.38, 125.28, 124.46, 124.26, 121.99, 121.35, 60.99, 60.66, 35.42, 35.04, 31.69, 31.63, 23.00, 14.87, 14.56. IR (film) ν (cm^{-1}) 2963, 1712, 1692, 1588, 1364, 1235, 1153, 1135, 825 cm^{-1}. HR-MS (ESI) *m/z* calcd for $C_{44}H_{52}AuNO_4Na$ [M+Na$^+$] 878.3454, found 878.3453. Anal. Calcd. For: $C_{44}H_{52}AuNO_4$: C, 61.75; H, 6.12; N, 1.64, found: C, 62.27; H, 6.42; N, 1.57.

(*Z*)-[(N^C^C)Au-vinyl-d] (2a-d_1)

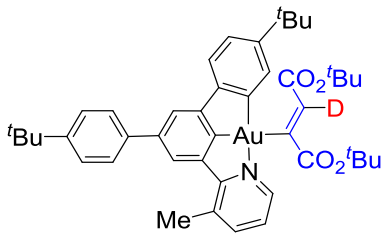

In a glovebox, a scintillation vial was charged with complex **3-d_1** (50 mg, 77 µmol) and di-*tert*-butyl acetylenedicarboxylate (87 mg, 386 µmol). The mixture was dissolved in benzene (2 ml), and triphenylsilane (40 mg, 154 µmol) was added. The reaction mixture was stirred for 2 hours at room temperature. After completion of the reaction, the reaction vial was taken out of the glovebox and solvent was evaporated and the crude mixture was purified by silica gel chromatography using

DCM:hexane as eluent to yield complex **2a-d$_1$** (47 mg, 72%) as a yellowish solid. ^{1}H NMR (400 MHz, CD_2Cl_2) δ 8.72 (dd, J = 5.4, 1.3 Hz, 1H), 7.89 (d, J = 1.3 Hz, 1H), 7.82 (ddd, J = 7.8, 1.7, 0.7 Hz, 1H), 7.62 – 7.59 (m, 3H), 7.54 – 7.50 (m, 3H), 7.37 (d, J = 8.0 Hz, 1H), 7.30 (dd, J = 7.7, 5.4 Hz, 1H), 7.21 (dd, J = 8.0, 2.0 Hz, 1H), 2.86 (s, 3H), 1.46 (s, 9H), 1.39 (s, 9H), 1.32 (s, 9H), 1.25 (s, 9H). ^{13}C NMR (101 MHz, CD_2Cl_2) δ 189.41, 176.25, 175.48, 170.22, 165.56, 153.65, 151.82, 151.49, 151.05, 150.08, 147.04, 144.87, 144.50, 141.02, 139.75, 134.46, 133.72, 127.41, 126.38, 125.21, 124.30, 124.09, 121.88, 121.26, 80.57, 80.38, 35.41, 35.04, 31.70, 28.71, 28.47, 23.01. IR (film) ν (cm^{-1}) 2963, 1713, 1695, 1588, 1389, 1364, 1234, 1153, 1134, 826 cm^{-1}. HR-MS (ESI) *m/z* calcd for $C_{44}H_{51}DAuNO_4Na$ [M+Na$^+$] 879.3516, found 879.3515. Anal. Calcd. For: $C_{44}H_{51}DAuNO_4 \cdot C_6H_6$: C, 64.23; H, 6.36; N, 1.50, found: C, 64.10; H, 6.23; N, 1.61.

(*Z*)-[(N^C^C)Au-vinyl] (2b)

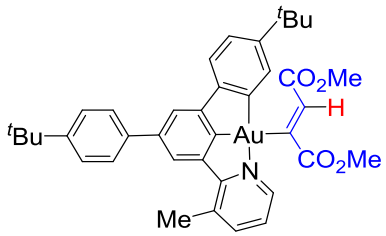

In a glovebox, a scintillation vial was charged with complex **3** (50 mg, 77 µmol) and di-methyl acetylenedicarboxylate (55 mg, 386 µmol). The mixture was dissolved in benzene (2 ml), and triphenylsilane (40 mg, 154 µmol) was added. The reaction mixture was stirred for 2 hours at room temperature. After completion of the reaction, the reaction vial was taken out of the glovebox and solvent was evaporated and the crude mixture was purified by silica gel chromatography using DCM:hexane as eluent to yield complex **2b** (34 mg, 58%) as a yellowish solid. ^{1}H NMR (400 MHz, CD_2Cl_2) δ 8.61 (d, J = 4.7 Hz, 1H), 7.90 (s, 1H), 7.83 (d, J = 7.7 Hz, 1H), 7.63 – 7.59 (m, 4H), 7.52 (d, J = 7.7 Hz, 2H), 7.47 (s, 1H), 7.37 (d, J = 8.8 Hz, 1H), 7.30 (t, J = 6.1 Hz, 1H), 7.21 (d, J = 8.3 Hz, 1H), 3.73 (s, 3H), 3.59 (s, 3H), 2.86 (s, 3H), 1.39 (s, 9H), 1.30 (s, 9H). ^{13}C NMR (101 MHz, CD_2Cl_2) δ 190.65, 176.82, 174.65, 171.30, 165.44, 153.72, 151.73, 151.60, 151.12, 149.67, 146.82, 144.93, 144.57, 141.20, 139.69, 134.63, 133.68, 129.48, 127.42, 126.39, 125.32, 124.50, 124.34, 122.03, 121.40, 52.18, 51.83, 35.42, 35.04, 31.69, 31.59, 23.01. HR-MS (ESI) *m/z* calcd for $C_{38}H_{40}AuNO_4Na$ [M+Na$^+$] 794.2515, found 794.2503. Anal. Calcd. For: $C_{15}H_{16}AuCl_2NO_3$: C, 59.14; H, 5.22; N, 1.82, found: C, 59.26; H, 5.17; N, 1.91.

(*Z*)-[(N^C^C)Au-vinyl] (2c)

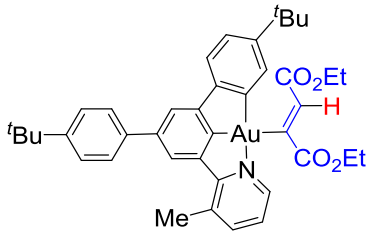

In a glovebox, a scintillation vial was charged with complex **3** (50 mg, 77 µmol) and di-methyl acetylenedicarboxylate (66 mg, 386 µmol). The mixture was dissolved in benzene (2 ml), and triphenylsilane (40 mg, 154 µmol) was added. The reaction mixture was stirred for 2 hours at room temperature. After completion of the reaction, the reaction vial was taken out of the glovebox and solvent was evaporated and the crude mixture was purified by silica gel chromatography using DCM:hexane as eluent to yield complex **2c** (42 mg, 69%) as a yellowish solid. ^{1}H NMR (400 MHz, CD_2Cl_2) δ 8.66 (dd, *J* = 5.4, 1.5 Hz, 1H), 7.89 (d, *J* = 1.2 Hz, 1H), 7.82 (dd, *J* = 7.8, 1.0 Hz, 1H), 7.63 – 7.59 (m, 3H), 7.58 (s, 1H), 7.52 (d, *J* = 8.5 Hz, 2H), 7.49 (d, *J* = 2.0 Hz, 1H), 7.37 (d, *J* = 8.0 Hz, 1H), 7.30 (dd, *J* = 7.7, 5.4 Hz, 1H), 7.21 (dd, *J* = 8.0, 2.0 Hz, 1H), 4.24 – 4.14 (m, 2H), 4.03 (qd, *J* = 7.1, 3.1 Hz, 2H), 2.86 (s, 3H), 1.39 (s, 9H), 1.31 (s, 9H), 1.25 (t, *J* = 7.1 Hz, 3H), 1.09 (t, *J* = 7.1 Hz, 3H). ^{13}C NMR (101 MHz, CD_2Cl_2) δ 190.31, 176.48, 174.82, 170.79, 165.45, 153.70, 151.76, 151.55, 151.09, 149.84, 146.91, 144.90, 144.55, 141.14, 139.69, 134.57, 133.70, 129.62, 127.42, 126.38, 125.28, 124.46, 124.26, 121.99, 121.35, 60.99, 60.66, 35.42, 35.04, 31.69, 31.63, 23.00, 14.87, 14.56. HR-MS (ESI) *m/z* calcd for $C_{40}H_{44}AuNO_4Na$ [M+Na$^+$] 822.2828, found 822.2828. Anal. Calcd. For: $C_{15}H_{16}AuCl_2NO_3$: C, 60.07; H, 5.55; N, 1.75, found: C, 60.79; H, 5.69; N, 1.72.

3. Cryo-MS experiments detection of intermediates analougous to IV-V, IX

In a glovebox, a scintillation vial was charged with complex **3** (5 mg, 8 µmol) and a mixture of THF:MeCN (1:0.1ml) was added, the vial was taken out of glove-box and cooled to -50 °C and a solution of triphenylsilane (4 mg, 15 µmol) in THF (0.5 ml) was added. The reaction mixture was stirred for 5 minutes at -50 °C and a sample was taken for Cryo-MS. A peak at M$^+$=1257.4635 was found which correspond to the gold(III)-hydride dimer **IV^i**. After 20 minutes, a solution of di-*tert*-butyl acetylenedicarboxylate (6 mg, 39 µmol) in THF (0.5 ml) was added and the reaction vial was further cooled to -80 °C, after stirring the reaction mixture for 5 minutes at -80 °C, a sample was taken for Cryo-MS. Two new peaks at M$^+$=1483.5840 and M$^+$=854.3484 were detected which corresponds to intermediates **IX^i**and **V^i** respectively.

Acquisition Parameter

Source Type	ESI	Ion Polarity	Positive	Set Nebulizer	0.0 Bar
Focus	Not active	Set Capillary	4500 V	Set Dry Heater	0 °C
Scan Begin	50 m/z	Set End Plate Offset	-500 V	Set Dry Gas	0.0 l/min
Scan End	3000 m/z	Set Collision Cell RF	700.0 Vpp	Set Divert Valve	Waste

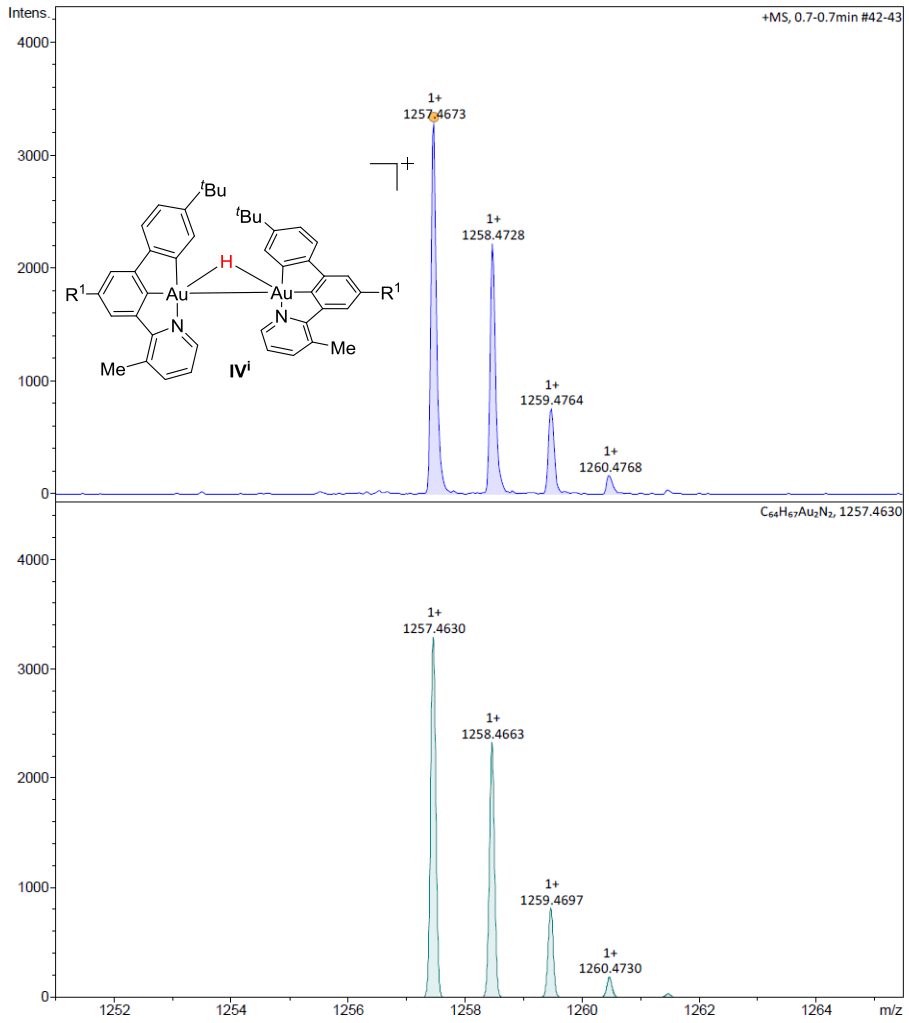

Intermediate IX^{i}

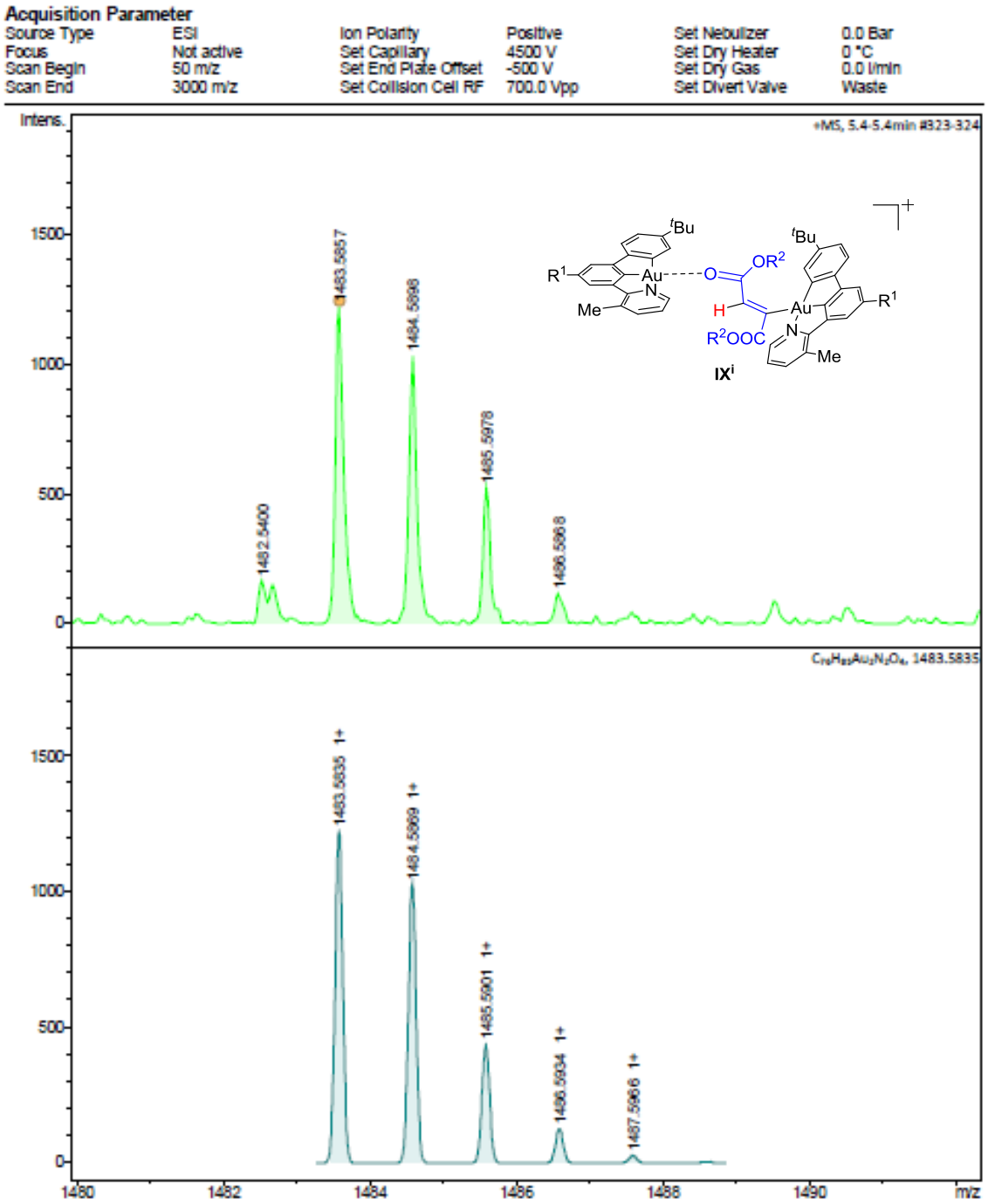

Deuterium Labeling

In a glove-box, a scintillation vial was charged with complex **1c** (5 mg, 8 µmol) and a mixture of THF:MeCN (1:0.1ml) was added, the vial was taken out of glove-box and cooled to -50°C and a solution of triphenylsilane-D (4 mg, 15 µmol) in THF (0.5 ml) was added. The reaction mixture was stirred for 5 minutes at -50°C and a sample was taken for Cryo-MS. A peak at M^+=1258.4652 was found which correspond to the gold(III)-hydride dimer **IV^i-d**. After 20 minutes, a solution of di-*tert*-butyl acetylenedicarboxylate (6 mg, 39 µmol) in THF (0.5 ml) was added and the reaction vial was further cooled to -80°C, after stirring the reaction mixture for 5 minutes at -80°C, a sample was taken for Cryo-MS. Two new peaks at M^+=1484.5954 and M^+=854.3484 were detected which corresponds to intermediates **IX^i-d** and **V^i-d** respectively.

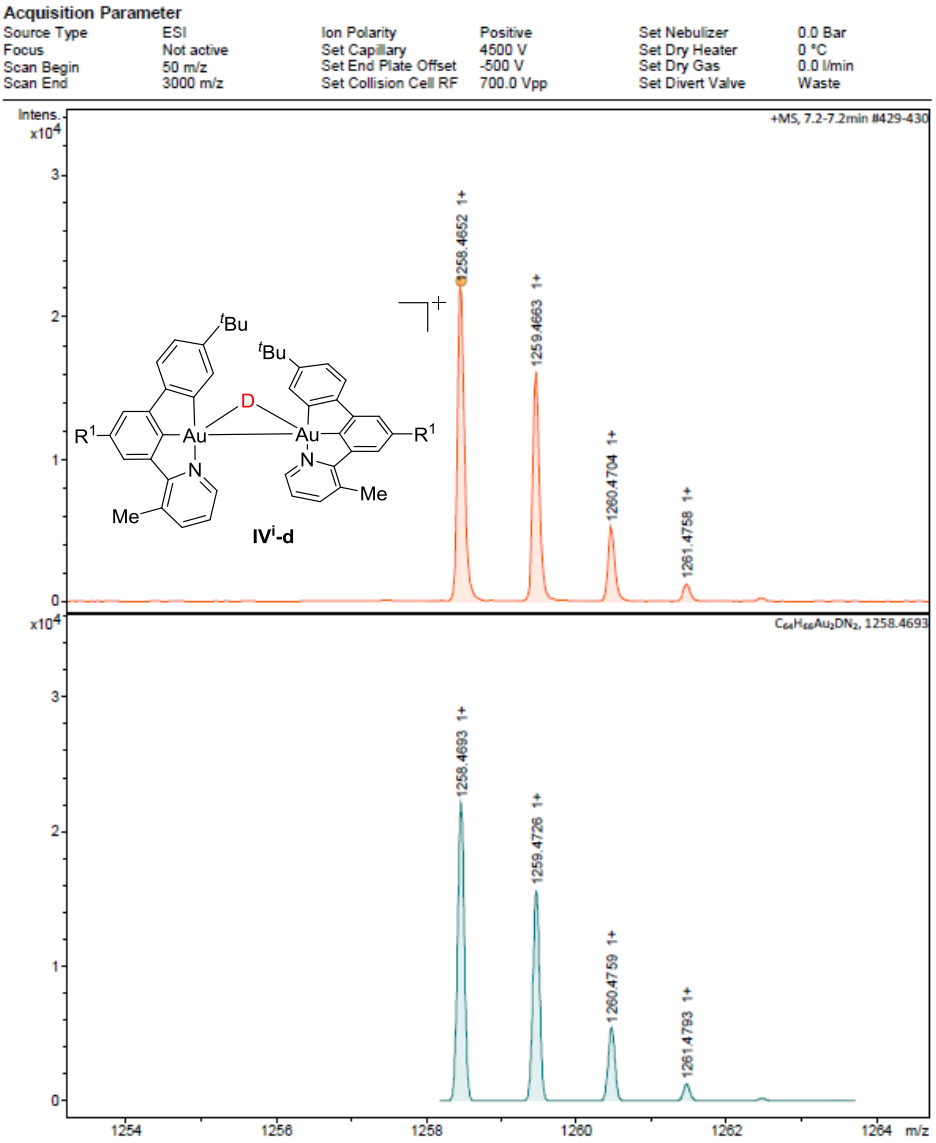

Intermediate IX^{i}-d

Acquisition Parameter

Source Type	ESI	Ion Polarity	Positive	Set Nebulizer	0.0 Bar
Focus	Not active	Set Capillary	4500 V	Set Dry Heater	0 °C
Scan Begin	50 m/z	Set End Plate Offset	-500 V	Set Dry Gas	0.0 l/min
Scan End	3000 m/z	Set Collision Cell RF	700.0 Vpp	Set Divert Valve	Waste

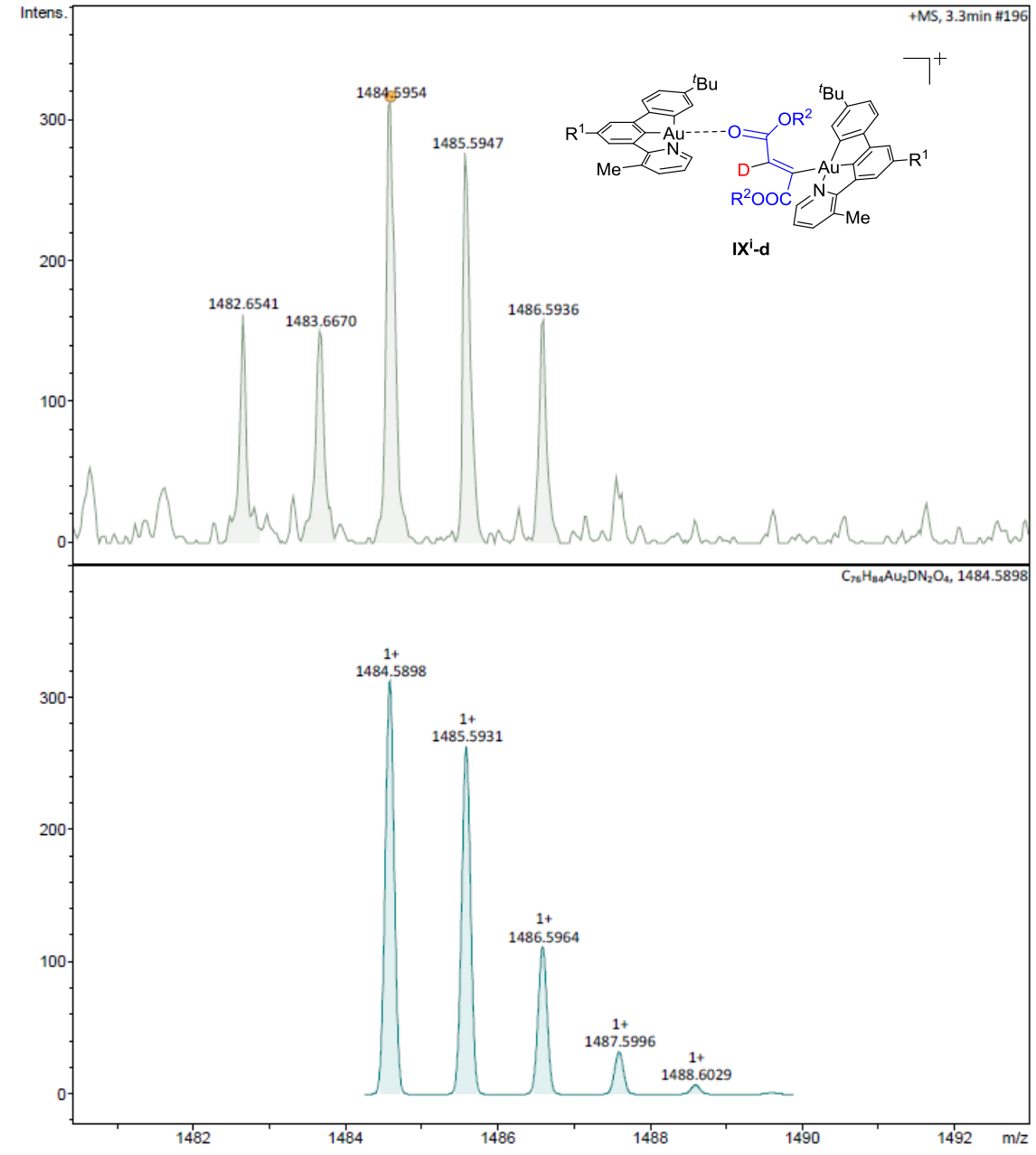

Intermediate V^{i}

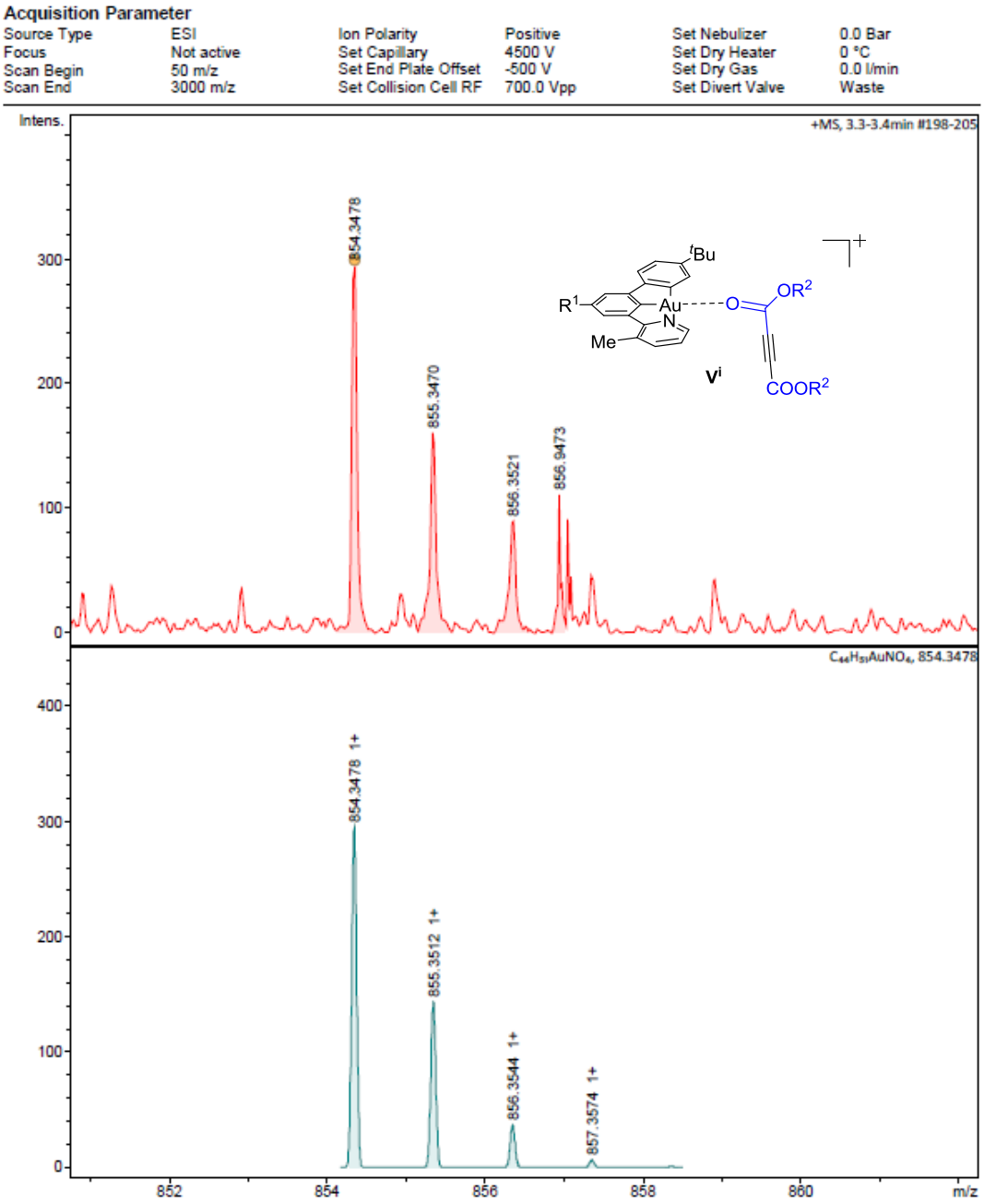

6 Computational results

The structures were optimized at DFT level by using the M06[1] functional as implemented in Gaussian 09.[2] Calculations were carried out by using the 6-311G(d,p) basis set for C, H, O and N and Stuttgart/Dresden (SDD)[3] effective core potential (ECP) basis set for Au. Solvent effects were taken into account at the same levels of theory by applying the conductor-like polarizable continuum model (IEFPCM),[4] using tetrahydrofuran as solvent, as in the experimental conditions. The solute cavity was constructed using radii from the UFF force field. The critical stationary points were characterized by frequency calculations in order to verify that they have the right number of imaginary frequencies, and the intrinsic reaction coordinates (IRC)[5] were followed to verify the energy profiles connecting the key transition structures to the correct associated local minima.

Figure S1. Computed structures and their energies in the neutral mechanism.

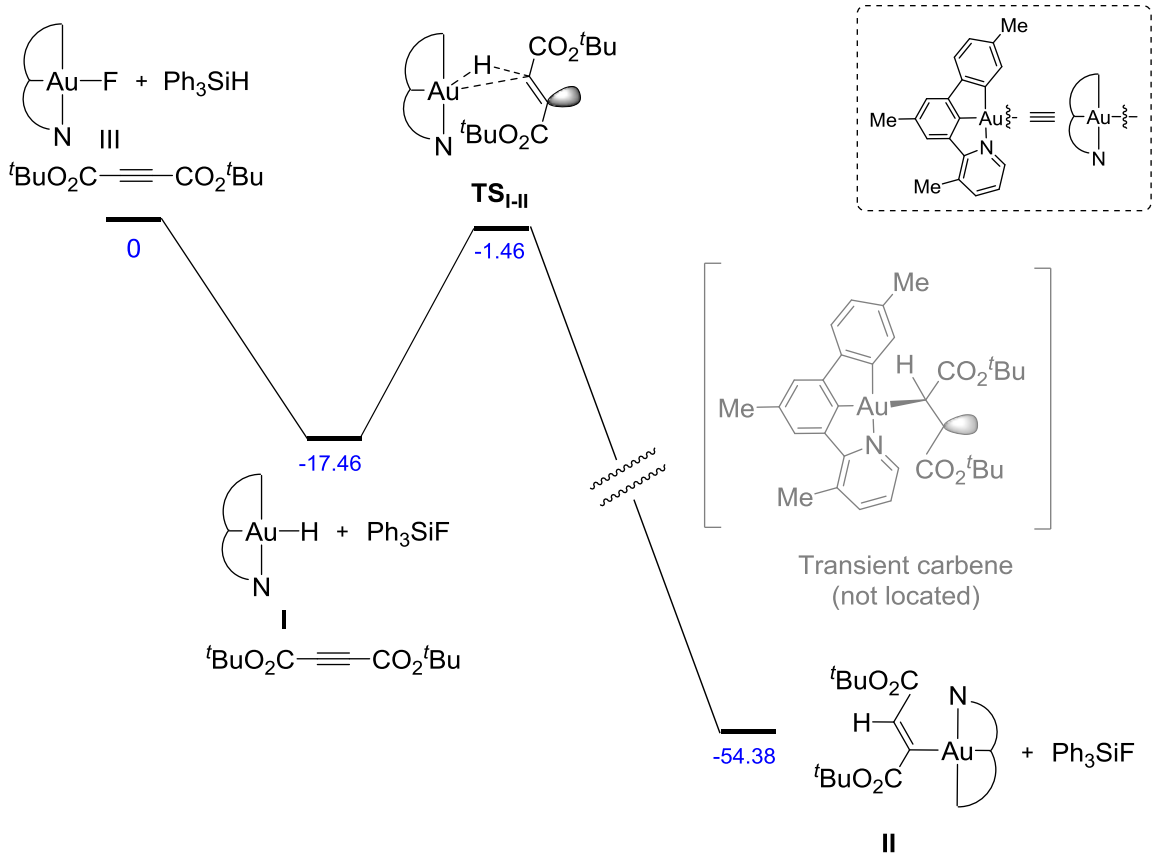

	E (M06) Absolute Hartrees
III	-1062.033185
Ph_3SiH	-984.430442
$^tBuO_2C{-}{\equiv}{-}CO_2{}^tBu$	-768.457694
I	-962.743827
Ph_3SiF	-1083.747628
$TS_{I\text{-}II}$	-1731.160028 (in gas phase)
II	-1731.26035

Figure S2. Computed structures and their energies in the cationic mechanism.

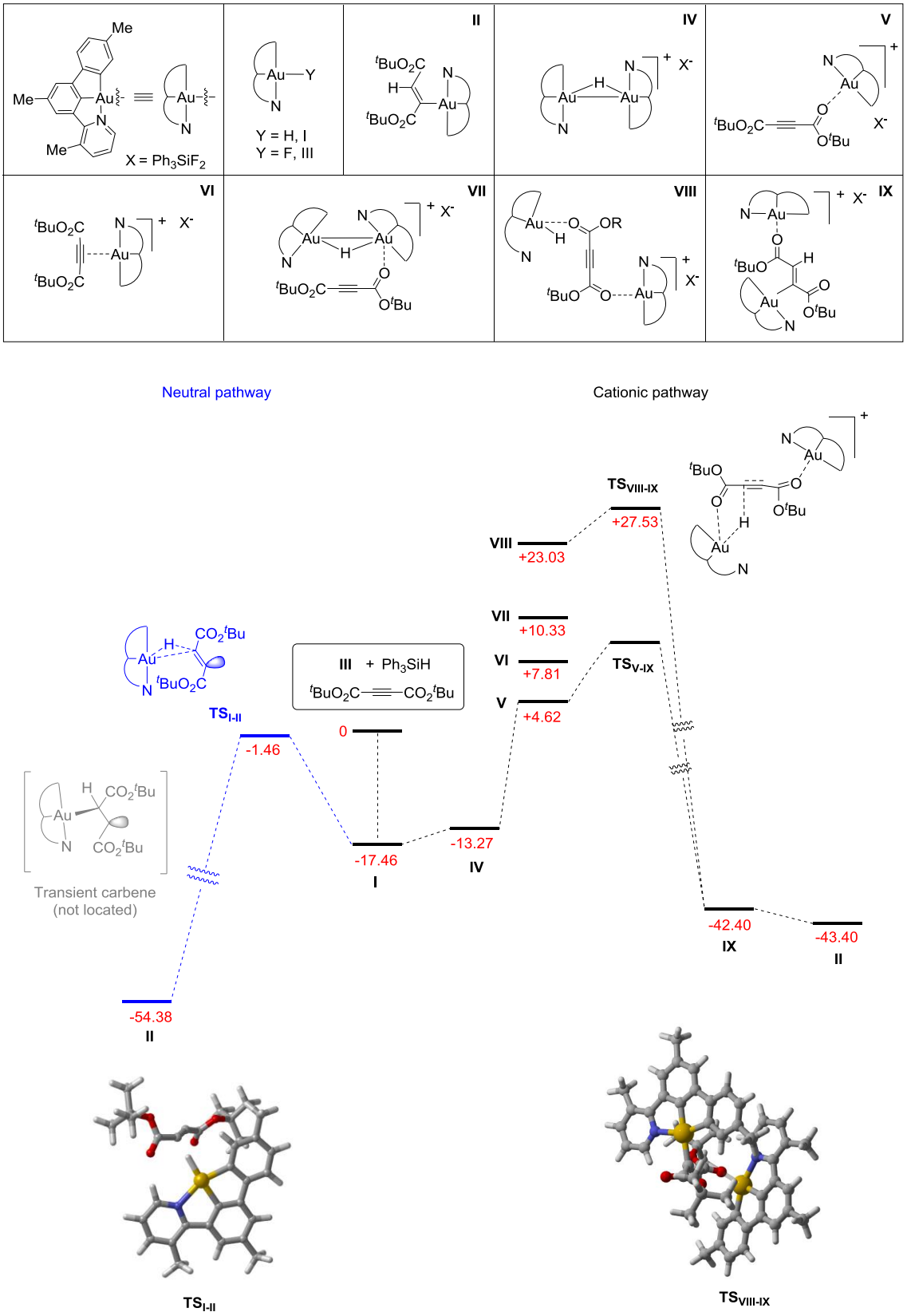

	E (M06) Absolute Hartrees
III	-1062.033185
Ph_3SiH	-984.430442
$^tBuO_2C{-}{\equiv}{-}CO_2{}^tBu$	-768.457694
I	-962.743827
X^-	-1183.746294
IV	-1924.771665
V	-1730.457018
VI	-1730.451969
VII	-2693.191739
VIII	-2693.171528
$TS_{VIII-IX}$	-2693.164343
IX	-2693.275147
	-1194.267993
THF	-232.250966

Cartesian coordinates of the structures involved in the computational study

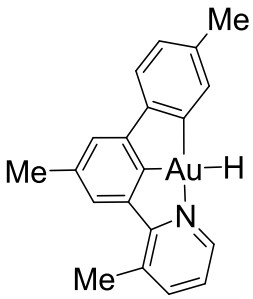

I

Standard orientation:

Center Number	Atomic Number	Atomic Type	Coordinates (Angstroms) X	Y	Z
1	6	C	2.087927	1.143861	0.000033
2	6	C	2.148155	-0.271989	-0.000051
3	6	C	3.373665	-0.915263	-0.000147
4	6	C	4.569102	-0.189534	-0.000155
5	6	C	5.895481	-0.885790	-0.000220
6	6	C	4.502026	1.200818	-0.000068
7	1	H	5.425260	1.776449	-0.000082
8	6	C	3.281029	1.859929	0.000027
9	1	H	3.258644	2.947306	0.000083
10	6	C	0.740881	1.734476	0.000103
11	6	C	-0.274983	0.781800	0.000036

12	79	Au	0.307679	-1.167629	-0.000026
13	6	C	-1.629535	1.091545	0.000088
14	6	C	-1.962768	2.458892	0.000225
15	1	H	-2.988893	2.800635	0.000301
16	6	C	-0.971469	3.437627	0.000295
17	6	C	-1.343395	4.890768	0.000507
18	6	C	0.379575	3.075933	0.000224
19	1	H	1.132881	3.863052	0.000273
20	6	C	-2.537647	-0.082121	0.000004
21	6	C	-3.944421	-0.061413	-0.000084
22	6	C	-4.616948	-1.280981	-0.000144
23	6	C	-3.940757	-2.484736	-0.000132
24	6	C	-2.562299	-2.441148	-0.000069
25	1	H	-5.703288	-1.272420	-0.000210
26	7	N	-1.894549	-1.289242	-0.000003
27	6	C	-4.768402	1.188147	-0.000131
28	1	H	-4.461642	-3.434287	-0.000178
29	1	H	-1.960556	-3.343663	-0.000068
30	1	H	-4.575994	1.804206	0.883686
31	1	H	-5.829972	0.932400	-0.000316
32	1	H	-4.575712	1.804330	-0.883799
33	1	H	-2.427673	5.028887	-0.000034
34	1	H	-0.938849	5.403401	-0.879154

35	1	H	-0.939806	5.402891	0.880910
36	1	H	0.820614	-2.754124	-0.000436
37	1	H	5.777762	-1.972453	-0.000755
38	1	H	6.487625	-0.611794	0.880089
39	1	H	6.487988	-0.610949	-0.880018
40	1	H	3.415541	-2.001376	-0.000219

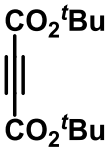

Standard orientation:

Center Number	Atomic Number	Atomic Type	Coordinates (Angstroms) X	Y	Z
1	6	C	-0.589436	-0.521803	0.117910
2	6	C	0.589423	-0.521590	-0.118198
3	6	C	-1.995099	-0.567275	0.479318
4	6	C	1.995031	-0.566631	-0.479876
5	8	O	2.398706	-1.240466	-1.390765
6	8	O	2.693974	0.216776	0.322209
7	8	O	-2.398921	-1.242257	1.389292
8	8	O	-2.693914	0.217166	-0.321867

9	6	C	-4.156783	0.374542	-0.169900
10	6	C	-4.841247	-0.962210	-0.372939
11	6	C	-4.500835	1.330618	-1.292188
12	6	C	-4.460917	0.993248	1.179780
13	6	C	4.156834	0.374293	0.170288
14	6	C	4.841326	-0.962661	0.371904
15	6	C	4.500971	1.329224	1.293524
16	6	C	4.460859	0.994377	-1.178783
17	1	H	-4.237781	0.897032	-2.261537
18	1	H	-3.962603	2.275577	-1.173127
19	1	H	-5.574905	1.538568	-1.283650
20	1	H	-4.527238	-1.409411	-1.321549
21	1	H	-5.923351	-0.801706	-0.415757
22	1	H	-4.625880	-1.658571	0.438596
23	1	H	-4.220140	0.316700	2.001522
24	1	H	-5.528464	1.230893	1.228291
25	1	H	-3.899898	1.924723	1.306281
26	1	H	4.237996	0.894647	2.262450
27	1	H	3.962724	2.274301	1.175469
28	1	H	5.575040	1.537189	1.285112
29	1	H	4.220048	0.318654	-2.001193
30	1	H	5.528396	1.232101	-1.227123
31	1	H	3.899805	1.925964	-1.304307

32	1	H	4.527412	-1.410831	1.320087
33	1	H	5.923433	-0.802190	0.414782
34	1	H	4.625892	-1.658196	-0.440320

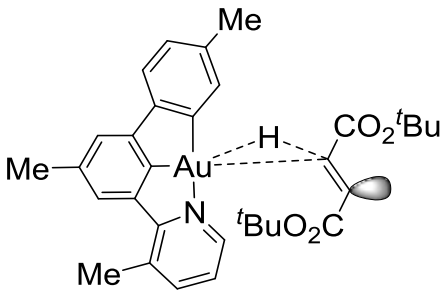

TS_{I-II}

(in gas phase)

Standard orientation:

Center Number	Atomic Number	Atomic Type	Coordinates (Angstroms) X	Y	Z

1	79	Au	-0.55837100	-0.46080200	-0.48716500
2	6	C	-2.54803800	-0.12325700	-0.28916000
3	6	C	-3.36455600	-1.14620000	0.16930300
4	6	C	-4.72960100	-0.83283300	0.30971500
5	6	C	-5.20695100	0.43846000	0.00136100
6	6	C	-4.33562200	1.43184300	-0.45587800

7	6	C	-2.98250100	1.15986100	-0.60705600
8	6	C	-1.90558700	2.04779100	-1.07023300
9	6	C	-6.66318100	0.75991100	0.16216500
10	1	H	-4.73750300	2.41801400	-0.68747200
11	6	C	-2.66821000	-2.42614800	0.45036700
12	1	H	-5.45160200	-1.55780000	0.66154100
13	7	N	-1.32139000	-2.39682800	0.22152900
14	6	C	-0.54043400	-3.45728200	0.41388300
15	6	C	-1.05723700	-4.65525400	0.86775300
16	6	C	-2.41429700	-4.71709900	1.11185900
17	6	C	-3.24911200	-3.62093700	0.91095000
18	1	H	-0.40914500	-5.50955500	1.02133900
19	1	H	-2.85692300	-5.64364600	1.46914200
20	6	C	-4.70876700	-3.78856400	1.19802800
21	6	C	-2.05628300	3.36801100	-1.47296800
22	6	C	-0.96272400	4.10041200	-1.92276300
23	6	C	-0.60771200	1.48005500	-1.10928700
24	6	C	0.47097600	2.21481600	-1.55141400
25	6	C	0.30636800	3.53656500	-1.98286300
26	1	H	1.46322400	1.76916300	-1.56939900
27	1	H	-3.03850100	3.83471500	-1.44379700
28	6	C	1.48014100	4.29162800	-2.52527600
29	1	H	-1.10152000	5.13116100	-2.24170300

30	1	H	0.51516400	-3.32023100	0.18631900
31	1	H	-4.90910400	-4.81013100	1.52988600
32	1	H	-5.32425400	-3.60160000	0.31236400
33	1	H	-5.04909400	-3.11190100	1.98831900
34	1	H	-7.23800200	-0.11341900	0.48194600
35	1	H	-7.09665500	1.11929600	-0.77764500
36	1	H	-6.81494300	1.54907100	0.90718900
37	1	H	1.67481000	4.01466700	-3.56832500
38	1	H	2.38840300	4.06636500	-1.95564200
39	1	H	1.31453600	5.37336000	-2.49873000
40	1	H	1.14302900	-0.59832900	-0.61353100
41	6	C	2.05398700	1.66506300	1.70236100
42	8	O	1.46693700	1.42904000	2.73255700
43	8	O	2.26410200	2.88012400	1.17805800
44	6	C	1.72780700	4.06839900	1.84704800
45	6	C	0.21147700	4.00566000	1.90375900
46	1	H	-0.13728300	3.21443300	2.56884600
47	1	H	-0.17170200	4.96562900	2.26827000
48	1	H	-0.19688600	3.83413500	0.90167900
49	6	C	2.16905400	5.20186900	0.94247600
50	1	H	1.89005200	6.16226700	1.38800300
51	1	H	3.25483000	5.18302500	0.80493900
52	1	H	1.68813200	5.12273400	-0.03658100

53	6	C	2.35679800	4.22280800	3.22065100
54	1	H	3.44900500	4.21482000	3.13880400
55	1	H	2.05433400	5.18532800	3.64748800
56	1	H	2.04604300	3.42660400	3.89770400
57	6	C	2.62188400	0.61992100	0.90601700
58	6	C	2.51606700	-0.36862400	0.16657300
59	6	C	3.12721400	-1.64155600	-0.23487900
60	8	O	2.51426600	-2.64622300	-0.50062800
61	8	O	4.45002400	-1.51760000	-0.22826200
62	6	C	5.32846000	-2.65979500	-0.49815700
63	6	C	5.11385300	-3.16358400	-1.91307300
64	1	H	5.87708900	-3.91404600	-2.14607700
65	1	H	4.12925800	-3.61665400	-2.03611400
66	1	H	5.21757400	-2.34059400	-2.62765700
67	6	C	6.70842300	-2.05009700	-0.35247700
68	1	H	6.84428300	-1.64615700	0.65498900
69	1	H	7.47546100	-2.80983100	-0.53341700
70	1	H	6.84477300	-1.23609800	-1.07047300
71	6	C	5.11422700	-3.74311300	0.54226900
72	1	H	4.13576900	-4.21432300	0.43996000
73	1	H	5.88587300	-4.51142600	0.42373000
74	1	H	5.20433900	-3.32295900	1.54930300

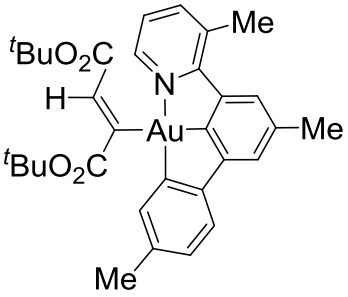

(*Z*)-II

Standard orientation:

Center Number	Atomic Number	Atomic Type	Coordinates (Angstroms) X	Y	Z
1	6	C	0.310355	-2.725188	-1.385054
2	6	C	-0.539440	-1.594378	-1.294602
3	6	C	-1.766550	-1.589927	-1.924991
4	6	C	-2.196431	-2.700643	-2.665306
5	6	C	-3.532084	-2.674930	-3.341700
6	6	C	-1.359644	-3.805941	-2.751716
7	1	H	-1.681447	-4.672795	-3.323986
8	6	C	-0.120546	-3.821262	-2.120306
9	1	H	0.513027	-4.701216	-2.203922
10	6	C	1.589195	-2.619666	-0.672103
11	6	C	1.754565	-1.405318	-0.010453
12	79	Au	0.248546	-0.073679	-0.163055
13	6	C	2.879597	-1.073314	0.736734

14	6	C	3.895229	-2.044863	0.804402
15	1	H	4.807825	-1.879079	1.360141
16	6	C	3.764411	-3.268932	0.152565
17	6	C	4.858882	-4.290916	0.234298
18	6	C	2.612100	-3.555416	-0.584114
19	1	H	2.533186	-4.520418	-1.083382
20	6	C	2.851249	0.273147	1.355797
21	6	C	3.842085	0.855239	2.166620
22	6	C	3.622103	2.147462	2.638421
23	6	C	2.472832	2.848964	2.332968
24	6	C	1.531914	2.221902	1.542118
25	1	H	4.383766	2.605954	3.263013
26	7	N	1.720689	0.988851	1.079138
27	6	C	5.116505	0.175367	2.559014
28	1	H	2.303078	3.855606	2.695632
29	1	H	0.607094	2.709066	1.248075
30	1	H	4.930132	-0.752521	3.108485
31	1	H	5.702671	0.830526	3.206827
32	1	H	5.735038	-0.069239	1.689909
33	1	H	5.684421	-3.948482	0.863435
34	1	H	5.264391	-4.516182	-0.758226
35	1	H	4.488556	-5.234773	0.648835
36	6	C	-1.337750	1.340061	-0.371115

37	6	C	-1.093841	2.314662	-1.445431
38	8	O	-1.604339	2.274397	-2.540482
39	8	O	-0.164819	3.200057	-1.054773
40	6	C	0.483865	4.121050	-1.991626
41	6	C	1.171287	3.329530	-3.087981
42	6	C	1.510595	4.817503	-1.120181
43	6	C	-0.523293	5.116824	-2.533643
44	1	H	1.826186	2.567586	-2.648811
45	1	H	1.789423	4.004884	-3.688822
46	1	H	0.450406	2.839731	-3.744611
47	1	H	2.232806	4.095716	-0.722973
48	1	H	1.023391	5.320625	-0.278031
49	1	H	2.053578	5.566084	-1.705567
50	1	H	-1.271627	4.627993	-3.159436
51	1	H	-0.001470	5.869893	-3.133919
52	1	H	-1.029694	5.630024	-1.709398
53	6	C	-2.481766	1.376023	0.316569
54	6	C	-2.799510	0.375047	1.351326
55	1	H	-3.259360	2.115636	0.119504
56	8	O	-2.014279	-0.407116	1.839951
57	8	O	-4.097010	0.450236	1.674179
58	6	C	-4.714952	-0.479254	2.621368
59	6	C	-4.605650	-1.900711	2.100507

60	6	C	-6.163379	-0.031640	2.633460
61	6	C	-4.099922	-0.316799	3.998843
62	1	H	-5.000568	-1.960928	1.080564
63	1	H	-5.201854	-2.563323	2.736733
64	1	H	-3.573070	-2.252917	2.099441
65	1	H	-3.061143	-0.648843	4.018068
66	1	H	-4.671859	-0.911252	4.719320
67	1	H	-4.144548	0.731654	4.312000
68	1	H	-6.598953	-0.110384	1.632569
69	1	H	-6.242034	1.008267	2.965369
70	1	H	-6.743763	-0.659941	3.316229
71	1	H	-2.412673	-0.716688	-1.859866
72	1	H	-3.595872	-1.850700	-4.060656
73	1	H	-4.339873	-2.526218	-2.616311
74	1	H	-3.727616	-3.607346	-3.878008

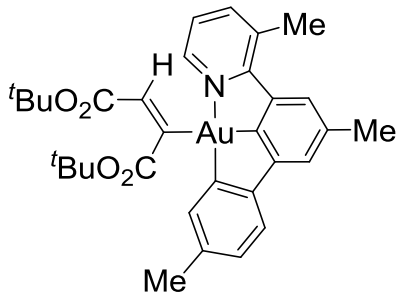

(*E*)-II

Standard orientation:

Center Number	Atomic Number	Atomic Type	Coordinates (Angstroms) X	Y	Z
1	6	C	2.272673	2.636894	0.263417
2	6	C	0.918202	2.250836	0.096204
3	6	C	-0.094140	3.181950	0.195918
4	6	C	0.195633	4.528009	0.462121
5	6	C	-0.917180	5.523250	0.574753
6	6	C	1.523432	4.902809	0.622096
7	1	H	1.760153	5.943918	0.828018
8	6	C	2.551659	3.971208	0.525520
9	1	H	3.581774	4.294220	0.657452
10	6	C	3.263399	1.559767	0.142314
11	6	C	2.697335	0.315366	-0.121448
12	79	Au	0.686776	0.248810	-0.287907
13	6	C	3.430040	-0.855955	-0.281552
14	6	C	4.826407	-0.742293	-0.158144
15	1	H	5.480578	-1.596348	-0.265702
16	6	C	5.427236	0.486222	0.106946
17	6	C	6.917507	0.585378	0.242173
18	6	C	4.646279	1.635489	0.256107
19	1	H	5.140489	2.584421	0.460716
20	6	C	2.627774	-2.068364	-0.573177

21	6	C	3.107641	-3.373748	-0.779603
22	6	C	2.177588	-4.374247	-1.054732
23	6	C	0.824403	-4.111491	-1.128378
24	6	C	0.413018	-2.811949	-0.911907
25	1	H	2.539767	-5.386112	-1.214320
26	7	N	1.282485	-1.840936	-0.644839
27	6	C	4.551873	-3.761835	-0.719317
28	1	H	0.100518	-4.888527	-1.342170
29	1	H	-0.633737	-2.525120	-0.934962
30	1	H	5.147888	-3.240207	-1.474647
31	1	H	4.655523	-4.833657	-0.900013
32	1	H	4.991099	-3.547207	0.259726
33	1	H	7.407741	-0.362345	0.005141
34	1	H	7.203682	0.864019	1.262547
35	1	H	7.325280	1.352822	-0.424130
36	6	C	-1.440810	0.191253	-0.477486
37	6	C	-2.061377	-0.209714	0.796056
38	8	O	-2.440137	0.571285	1.637696
39	8	O	-1.982587	-1.541796	0.958065
40	6	C	-1.964825	-2.159221	2.288480
41	6	C	-0.834581	-1.558796	3.104823
42	6	C	-1.680653	-3.616856	1.983198
43	6	C	-3.306934	-2.018543	2.978962

44	1	H	0.107467	-1.607077	2.545146
45	1	H	-0.710727	-2.132107	4.029530
46	1	H	-1.035470	-0.518682	3.369198
47	1	H	-0.702941	-3.731686	1.503252
48	1	H	-2.446930	-4.024359	1.315702
49	1	H	-1.682187	-4.199498	2.909799
50	1	H	-3.546159	-0.972588	3.176459
51	1	H	-3.277587	-2.559053	3.931592
52	1	H	-4.099922	-2.457091	2.365566
53	6	C	-2.092239	0.533121	-1.591982
54	1	H	-1.131636	2.878356	0.075146
55	1	H	-1.579435	5.280954	1.413384
56	1	H	-1.537794	5.527865	-0.327925
57	1	H	-0.534808	6.535743	0.728789
58	6	C	-3.555981	0.552011	-1.773793
59	8	O	-4.187128	-0.128028	-0.812891
60	8	O	-4.098134	1.130812	-2.687362
61	6	C	-5.633939	-0.049856	-0.623299
62	6	C	-5.844692	-0.882515	0.624547
63	1	H	-6.906401	-0.908172	0.888922
64	1	H	-5.498878	-1.908110	0.456963
65	1	H	-5.278915	-0.459758	1.461169
66	6	C	-6.360922	-0.664641	-1.804145

67	1	H	-7.429637	-0.731109	-1.572831
68	1	H	-6.234697	-0.069097	-2.708895
69	1	H	-5.990324	-1.678180	-1.990426
70	6	C	-6.041743	1.389713	-0.371513
71	1	H	-5.927619	2.004452	-1.265742
72	1	H	-7.090895	1.418819	-0.059566
73	1	H	-5.431862	1.813682	0.433747
74	1	H	-1.554678	0.909663	-2.461092

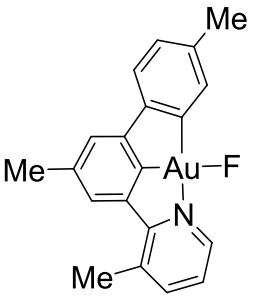

III

Standard orientation:

Center Number	Atomic Number	Atomic Type	Coordinates (Angstroms) X	Y	Z

1	6	C	2.042614	1.310578	0.000115
2	6	C	2.118336	-0.097727	-0.000046
3	6	C	3.335822	-0.747372	-0.000150

4	6	C	4.525839	-0.012323	-0.000089
5	6	C	5.857257	-0.698087	-0.000157
6	6	C	4.450034	1.379387	0.000081
7	1	H	5.371449	1.957657	0.000114
8	6	C	3.228003	2.037857	0.000187
9	1	H	3.199924	3.124975	0.000302
10	6	C	0.681785	1.856701	0.000179
11	6	C	-0.308501	0.875517	0.000090
12	79	Au	0.294511	-1.004001	-0.000066
13	6	C	-1.676232	1.133324	0.000081
14	6	C	-2.045533	2.489354	0.000169
15	1	H	-3.083390	2.791220	0.000174
16	6	C	-1.088648	3.501345	0.000271
17	6	C	-1.508131	4.940637	0.000445
18	6	C	0.271992	3.183662	0.000266
19	1	H	1.004017	3.989956	0.000323
20	6	C	-2.557328	-0.058795	-0.000023
21	6	C	-3.961849	-0.083165	-0.000008
22	6	C	-4.586341	-1.329796	-0.000076
23	6	C	-3.867787	-2.509486	-0.000156
24	6	C	-2.490532	-2.418950	-0.000170
25	1	H	-5.672211	-1.362469	-0.000067
26	7	N	-1.878169	-1.240083	-0.000103

27	6	C	-4.827748	1.137206	0.000071
28	1	H	-4.357171	-3.475583	-0.000206
29	1	H	-1.841593	-3.290226	-0.000237
30	1	H	-4.655604	1.758718	0.884263
31	1	H	-5.880132	0.846774	0.000079
32	1	H	-4.655643	1.758803	-0.884066
33	1	H	-2.595974	5.044082	-0.000160
34	1	H	-1.119134	5.464605	-0.879207
35	1	H	-1.120180	5.464079	0.880876
36	1	H	5.747593	-1.785383	-0.000832
37	1	H	6.446525	-0.418761	0.880288
38	1	H	6.446993	-0.417693	-0.879945
39	1	H	3.367673	-1.834329	-0.000292
40	9	F	0.857705	-2.995441	-0.000221

Ph_3SiH

Standard orientation:

Center Number	Atomic Number	Atomic Type	Coordinates (Angstroms) X	Y	Z

1	14	Si	-1.07084562	-0.17075032	1.05799421

2	6	C	-1.97504813	1.31450581	0.34140545
3	6	C	-1.34577509	2.56200804	0.26430711
4	6	C	-3.29806505	1.21828742	-0.09810786
5	6	C	-2.0127390265	3.6723071887	-0.2328602836
6	1	H	-0.3138565585	2.6695237522	0.5941343312
7	6	C	-3.9701720483	2.3268872586	-0.5971110627
8	1	H	-3.8118259619	0.2598371627	-0.0553335848
9	6	C	-3.3275830299	3.5552012513	-0.6655566576
10	1	H	-1.5061935287	4.6315120153	-0.2857853587
11	1	H	-4.9975761365	2.2308890474,	-0.9358788563
12	1	H	-3.8506723362	4.4223960551	-1.0575842916
13	6	C	-1.9575760826	-1.7511239725	0.5668211299
14	6	C	-2.5082106276	-2.6022114113	1.5271324066
15	6	C	-2.0674249759	-2.1168980588	-0.7794136399
16	6	C	-3.1486713218	-3.7794338936	1.1587079576
17	1	H	-2.43701965	-2.3437688483	2.5817348045
18	6	C	-2.7063998903	-3.2894260489	-1.1528864314
19	1	H	-1.6475313154	-1.473258786	-1.5514450564
20	6	C	-3.2473916594	-4.1237504819	-0.1816638098
21	1	H	-3.5706905715	-4.4289745375	1.9199097595
22	1	H	-2.7817207203	-3.5569962903	-2.2026842972
23	1	H	-3.7464728636	-5.0434694472	-0.4720087869
24	6	C	0.7078176515	-0.1856521878	0.4528716347

25	6	C	1.7345078518	-0.6054463052	1.3035136147
26	6	C	1.0424485237	0.1567345249	-0.861432901
27	6	C	3.048329636	-0.6816089633	0.8602380522
28	1	H	1.505820221	-0.8750733816	2.3329255752
29	6	C	2.3534885509	0.0798334326	-1.3103553805
30	1	H	0.2698000131	0.4990074437	-1.5480051717
31	6	C	3.3588526068	-0.3399650707	-0.4488328614
32	1	H	3.8320804747	-1.0059879508	1.5384808552
33	1	H	2.5929942682	0.3510635733	-2.3343285776
34	1	H	4.3856501841	-0.3970014606	-0.7974417791
35	1	H	-1.0404287384	-0.1259500633	2.5445569907

Ph_3SiF

Standard orientation:

Center Number	Atomic Number	Atomic Type	Coordinates (Angstroms) X	Y	Z
1	14	Si	-1.084686042	-0.1618363264	0.9575632597
2	6	C	-1.9827002036	1.3259877855	0.2860216451
3	6	C	-1.3301987918	2.5591442218	0.1745988718
4	6	C	-3.3326693327	1.255540208	-0.0711609736

5	6	C	-2.0040684237	3.6843265866	-0.2763277231
6	1	H	-0.2786729851	2.6425968203	0.442019874
7	6	C	-4.0098794703	2.3791927875	-0.524496138
8	1	H	-3.860799418	0.3072444588	0.0033089258
9	6	C	-3.3451910988	3.5939590839	-0.62665111
10	1	H	-1.4838616579	4.6339238502	-0.3567449624
11	1	H	-5.0576955395	2.307717752	-0.7998052983
12	1	H	-3.8736356891	4.4733874046	-0.9823625918
13	6	C	-1.9679878448	-1.7501792377	0.5392528626
14	6	C	-2.3804494786	-2.6420078244	1.5317119879
15	6	C	-2.1930416631	-2.0924158311	-0.7985008206
16	6	C	-3.0030232816	-3.8380640922	1.198167747
17	1	H	-2.2148885138	-2.3991948051	2.5781039334
18	6	C	-2.8140130208	-3.2857556784	-1.1349048591
19	1	H	-1.8847823188	-1.4141503256	-1.5935332165
20	6	C	-3.2199407995	-4.1603138297	-0.1340231956
21	1	H	-3.3197271095	-4.5206813412	1.9810543796
22	1	H	-2.9826320754	-3.5360686504	-2.1779032257
23	1	H	-3.7061665433	-5.0955410905	-0.3949471819
24	6	C	0.7037676721	-0.184029172	0.4264950606
25	6	C	1.7022143776	-0.611354483	1.3066467876
26	6	C	1.0711537737	0.1514058081	-0.8805465796
27	6	C	3.0258270785	-0.69352426150.8968350773	

28	1	H	1.4436620632	-0.8781457853	2.3283612851
29	6	C	2.3929598654	0.065500258	-1.2947803164
30	1	H	0.3172945083	0.4920263366	-1.5882830776
31	6	C	3.3718789906	-0.3564704747	-0.4047839106
32	1	H	3.7898775169	-1.0214197678	1.5952919547
33	1	H	2.6608217745	0.3316729304	-2.312804467
34	1	H	4.4071937162	-0.420086444	-0.7257192414
35	9	F	-1.0635706854	-0.0888686414	2.5888619471

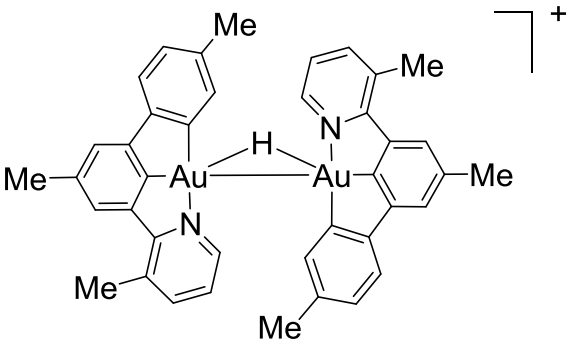

IV

Standard orientation:

Center Number	Atomic Number	Atomic Type	Coordinates (Angstroms) X	Y	Z
1	6	C	-2.395790	2.177783	1.797741
2	6	C	-1.243303	1.892787	1.032760
3	6	C	-0.072425	2.594156	1.237251

4	6	C	-0.001841	3.600087	2.208913
5	6	C	1.280683	4.338313	2.436043
6	6	C	-1.138662	3.876573	2.961572
7	1	H	-1.099072	4.658707	3.715756
8	6	C	-2.321103	3.175886	2.761903
9	1	H	-3.195507	3.417217	3.361198
10	6	C	-3.580604	1.379920	1.473715
11	6	C	-3.376593	0.468567	0.443696
12	79	Au	-1.536774	0.401710	-0.358480
13	6	C	-4.342042	-0.398824	-0.055888
14	6	C	-5.602722	-0.328993	0.562171
15	1	H	-6.417760	-0.969595	0.256338
16	6	C	-5.852393	0.566521	1.599447
17	6	C	-7.206860	0.627523	2.237686
18	6	C	-4.843916	1.420781	2.050691
19	1	H	-5.062667	2.114373	2.860584
20	6	C	-3.914829	-1.280380	-1.166257
21	6	C	-4.706702	-2.204261	-1.870285
22	6	C	-4.098855	-2.937091	-2.887879
23	6	C	-2.766309	-2.773919	-3.210975
24	6	C	-2.044745	-1.845701	-2.491180
25	1	H	-4.701399	-3.653885	-3.438111
26	7	N	-2.602602	-1.134301	-1.512631

27	6	C	-6.158688	-2.448266	-1.605741
28	1	H	-2.295576	-3.344425	-4.001611
29	1	H	-0.994160	-1.655937	-2.688808
30	1	H	-6.328966	-2.842953	-0.599428
31	1	H	-6.546789	-3.180696	-2.316063
32	1	H	-6.751796	-1.535437	-1.714181
33	1	H	-7.880691	-0.129873	1.830523
34	1	H	-7.669353	1.608171	2.082004
35	1	H	-7.139085	0.474957	3.319753
36	1	H	1.938229	4.272690	1.563281
37	1	H	1.828000	3.921118	3.289368
38	1	H	1.100665	5.395281	2.653703
39	1	H	0.813397	2.383139	0.644087
40	79	Au	1.504647	-0.215638	-0.481141
41	6	C	3.358995	-0.703783	0.124345
42	6	C	3.547872	-1.900439	0.804756
43	6	C	4.873342	-2.195905	1.166896
44	6	C	5.920284	-1.329261	0.862973
45	6	C	5.667137	-0.134299	0.187850
46	6	C	4.372384	0.195735	-0.192786
47	6	C	3.908765	1.386034	-0.907454
48	6	C	7.324539	-1.668971	1.260339
49	1	H	6.497838	0.531011	-0.040448

50	6	C	2.334131	-2.710656	1.048223
51	1	H	5.125304	-3.108823	1.686933
52	7	N	1.196022	-2.177625	0.514063
53	6	C	0.019758	-2.791708	0.629788
54	6	C	-0.117398	-3.989785	1.297746
55	6	C	1.014952	-4.539112	1.863394
56	6	C	2.259754	-3.922387	1.757970
57	1	H	-1.086303	-4.466713	1.376880
58	1	H	0.945060	-5.475129	2.409930
59	6	C	3.422749	-4.592495	2.419831
60	6	C	4.695832	2.453829	-1.316534
61	6	C	4.127624	3.530273	-1.987890
62	6	C	2.524267	1.425815	-1.186496
63	6	C	1.966958	2.494143	-1.857013
64	6	C	2.767615	3.569077	-2.270171
65	1	H	0.899272	2.522566	-2.065853
66	1	H	5.762986	2.452974	-1.109457
67	6	C	2.149854	4.720636	-2.999771
68	1	H	4.756733	4.359975	-2.299448
69	1	H	-0.835737	-2.299715	0.176532
70	1	H	3.080410	-5.475534	2.962414
71	1	H	3.919348	-3.933924	3.138240
72	1	H	4.171356	-4.924092	1.693573

73	1	H	7.385651	-2.657168	1.722248
74	1	H	7.717922	-0.938337	1.975317
75	1	H	7.992335	-1.658275	0.392746
76	1	H	1.329676	5.160406	-2.422420
77	1	H	1.728188	4.398792	-3.958416
78	1	H	2.882789	5.505640	-3.201595
79	1	H	0.003470	0.368055	-1.263772

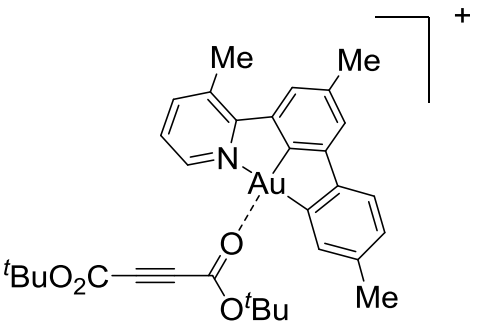

V

Standard orientation:

Center Number	Atomic Number	Atomic Type	Coordinates (Angstroms) X	Y	Z

1	6	C	1.646316	1.484407	0.462521
2	6	C	0.883766	2.527803	0.972554
3	6	C	1.471527	3.786764	0.987671
4	6	C	2.766227	3.967533	0.499715

5	6	C	3.483212	2.885195	-0.007287
6	6	C	2.937052	1.591674	-0.042697
7	1	H	0.925740	4.642926	1.379431
8	1	H	4.480453	3.080564	-0.375149
9	6	C	-0.450268	2.130697	1.421767
10	6	C	-1.422796	2.967293	1.950243
11	6	C	-0.741570	0.756330	1.280181
12	6	C	-2.658176	2.451405	2.329128
13	1	H	-1.223960	4.029751	2.066256
14	6	C	-1.963485	0.251768	1.664423
15	6	C	-2.947206	1.098569	2.195091
16	1	H	-3.415242	3.116927	2.736733
17	1	H	-2.195212	-0.806455	1.557363
18	6	C	3.555194	0.348333	-0.554237
19	6	C	4.837062	0.201752	-1.107003
20	6	C	5.210414	-1.069158	-1.542726
21	6	C	3.121023	-1.946783	-0.880909
22	6	C	4.364245	-2.154997	-1.441591
23	1	H	6.199114	-1.196734	-1.973564
24	1	H	2.401330	-2.750934	-0.761937
25	1	H	4.656264	-3.139991	-1.783459
26	6	C	5.828017	1.312016	-1.256473
27	1	H	5.460946	2.099880	-1.921593

28	1	H	6.073883	1.769730	-0.293769
29	1	H	6.754995	0.926343	-1.684586
30	6	C	-4.277698	0.534260	2.581717
31	1	H	-4.763397	0.063285	1.718391
32	1	H	-4.172817	-0.237110	3.352180
33	1	H	-4.947055	1.308415	2.966441
34	6	C	3.374662	5.336239	0.513296
35	1	H	4.425853	5.313773	0.217645
36	1	H	2.846103	6.004852	-0.174682
37	1	H	3.310171	5.785253	1.509352
38	7	N	2.744506	-0.743669	-0.458345
39	79	Au	0.804711	-0.308003	0.444714
40	6	C	-2.295809	-0.922785	-1.538203
41	6	C	-1.720447	-1.846605	-1.028207
42	6	C	-0.964419	-2.793386	-0.259105
43	8	O	-0.002981	-2.419127	0.417678
44	8	O	-1.402017	-4.004246	-0.335870
45	6	C	-0.828512	-5.144678	0.462277
46	6	C	-1.065514	-4.863184	1.928751
47	1	H	-0.746344	-5.737364	2.504466
48	1	H	-0.496134	-3.999262	2.277331
49	1	H	-2.129758	-4.699487	2.122662
50	6	C	0.633121	-5.324115	0.114547

51	1	H	1.259774	-4.546429	0.554169
52	1	H	0.962881	-6.290158	0.508945
53	1	H	0.773250	-5.340501	-0.971042
54	6	C	-1.658337	-6.310490	-0.022672
55	1	H	-1.359179	-7.214232	0.515474
56	1	H	-2.721182	-6.132065	0.161902
57	1	H	-1.507582	-6.476984	-1.092942
58	6	C	-2.845089	0.281986	-2.143702
59	8	O	-3.806887	0.762785	-1.386112
60	8	O	-2.400627	0.722421	-3.169831
61	6	C	-4.429182	2.082105	-1.673108
62	6	C	-5.411362	2.239495	-0.533952
63	1	H	-5.956019	3.181123	-0.649501
64	1	H	-6.134084	1.417951	-0.528072
65	1	H	-4.885060	2.256208	0.425478
66	6	C	-3.359866	3.154262	-1.613137
67	1	H	-2.650837	3.075571	-2.439102
68	1	H	-3.842458	4.135398	-1.666071
69	1	H	-2.816239	3.094038	-0.663011
70	6	C	-5.145300	2.026160	-3.006190
71	1	H	-4.449555	1.907088	-3.838120
72	1	H	-5.865337	1.201874	-3.018549
73	1	H	-5.697768	2.960814	-3.146063

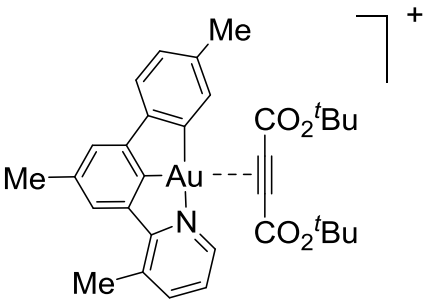

VI

Standard orientation:

Center Number	Atomic Number	Atomic Type	Coordinates (Angstroms) X	Y	Z
1	79	Au	0.180777	0.172951	0.028130
2	6	C	2.018357	0.226549	-0.739585
3	6	C	2.844729	1.272458	-0.349245
4	6	C	4.139328	1.236620	-0.891423
5	6	C	4.541229	0.219024	-1.755921
6	6	C	3.655475	-0.801618	-2.102129
7	6	C	2.362527	-0.814572	-1.591257
8	6	C	1.295282	-1.788255	-1.816191
9	6	C	5.924764	0.223404	-2.329549
10	1	H	3.988515	-1.590160	-2.774108
11	6	C	2.270574	2.260019	0.590553

12	1	H	4.867856	1.996541	-0.645820
13	7	N	1.004330	1.958024	0.996411
14	6	C	0.338500	2.722517	1.856632
15	6	C	0.893196	3.872277	2.379433
16	6	C	2.165666	4.212834	1.969445
17	6	C	2.886491	3.425125	1.072275
18	1	H	0.336106	4.481739	3.079611
19	1	H	2.629039	5.118991	2.348654
20	6	C	4.255596	3.884445	0.682136
21	6	C	1.382631	-2.939552	-2.585297
22	6	C	0.290978	-3.793153	-2.694969
23	6	C	0.080690	-1.510536	-1.154202
24	6	C	-1.001548	-2.353209	-1.273771
25	6	C	-0.909907	-3.517616	-2.051605
26	1	H	-1.941756	-2.136618	-0.768679
27	1	H	2.308659	-3.181180	-3.100411
28	6	C	-2.091925	-4.426434	-2.176631
29	1	H	0.373614	-4.693962	-3.296974
30	1	H	-0.661409	2.400600	2.129079
31	1	H	4.463434	4.854032	1.138103
32	1	H	4.355084	3.999541	-0.401084
33	1	H	5.031537	3.191155	1.021769
34	1	H	6.573148	0.935633	-1.814231

35	1	H	5.904289	0.497192	-3.390110
36	1	H	6.383016	-0.767840	-2.262736
37	1	H	-2.476360	-4.716279	-1.192408
38	1	H	-1.839351	-5.337135	-2.724939
39	1	H	-2.913894	-3.931785	-2.705932
40	6	C	-1.853619	-0.377002	1.411357
41	6	C	-2.238479	0.503782	0.668082
42	6	C	-1.613898	-1.535612	2.290181
43	6	C	-2.776933	1.620088	-0.128452
44	8	O	-2.119441	2.601978	-0.346083
45	8	O	-3.995724	1.333735	-0.500409
46	6	C	-4.799791	2.267552	-1.348959
47	6	C	-6.108810	1.525270	-1.490698
48	6	C	-4.107179	2.429399	-2.684576
49	6	C	-4.988431	3.578129	-0.615792
50	1	H	-3.936515	1.453646	-3.150050
51	1	H	-3.154796	2.954482	-2.589519
52	1	H	-4.756036	3.012149	-3.345639
53	1	H	-5.953865	0.551630	-1.964075
54	1	H	-6.791765	2.109593	-2.113946
55	1	H	-6.575416	1.372511	-0.513319
56	1	H	-5.401448	3.404811	0.382720
57	1	H	-5.704414	4.187386	-1.176220

58	1	H	-4.056325	4.138568	-0.528649
59	8	O	-2.447978	-1.906325	3.064950
60	8	O	-0.426825	-2.029828	2.034644
61	6	C	0.040311	-3.340055	2.563344
62	6	C	0.175422	-3.247583	4.067355
63	1	H	-0.793924	-3.120857	4.553783
64	1	H	0.629636	-4.171789	4.438044
65	1	H	0.828556	-2.413996	4.343352
66	6	C	1.384997	-3.493231	1.886137
67	1	H	1.857541	-4.421316	2.220465
68	1	H	1.269476	-3.531149	0.797240
69	1	H	2.043317	-2.656046	2.139797
70	6	C	-0.925455	-4.417172	2.116282
71	1	H	-1.049481	-4.389519	1.027902
72	1	H	-0.510237	-5.393238	2.385177
73	1	H	-1.902403	-4.316429	2.593449

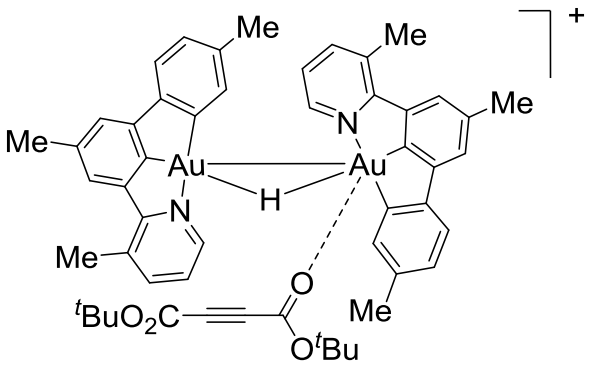

VII

Standard orientation:

Center Number	Atomic Number	Atomic Type	Coordinates (Angstroms) X	Y	Z
1	6	C	-3.251728	0.774166	2.313123
2	6	C	-1.878276	0.845731	1.985125
3	6	C	-0.953791	1.315663	2.891748
4	6	C	-1.364817	1.758281	4.157549
5	6	C	-0.352508	2.303978	5.115118
6	6	C	-2.715404	1.692946	4.477352
7	1	H	-3.045876	2.039242	5.453254
8	6	C	-3.650911	1.203427	3.570699
9	1	H	-4.702169	1.172516	3.846391
10	6	C	-4.128643	0.281690	1.246496
11	6	C	-3.471036	0.043060	0.044663
12	79	Au	-1.479777	0.287000	0.050288

13	6	C	-4.068306	-0.443355	-1.112333
14	6	C	-5.444225	-0.708822	-1.020027
15	1	H	-6.000597	-1.103681	-1.858631
16	6	C	-6.148637	-0.481919	0.162537
17	6	C	-7.620298	-0.756865	0.225273
18	6	C	-5.491784	0.013633	1.291143
19	1	H	-6.057969	0.174511	2.207043
20	6	C	-3.165827	-0.654845	-2.267185
21	6	C	-3.521564	-1.091529	-3.553304
22	6	C	-2.500236	-1.253210	-4.489384
23	6	C	-1.180427	-0.995067	-4.179559
24	6	C	-0.893539	-0.550898	-2.903364
25	1	H	-2.763013	-1.594221	-5.486823
26	7	N	-1.855060	-0.385562	-1.997495
27	6	C	-4.921468	-1.398961	-3.982692
28	1	H	-0.385742	-1.125927	-4.903630
29	1	H	0.123424	-0.313427	-2.599517
30	1	H	-5.333590	-2.257699	-3.441766
31	1	H	-4.937995	-1.644631	-5.046081
32	1	H	-5.594268	-0.550634	-3.827234
33	1	H	-7.958574	-1.339981	-0.634611
34	1	H	-8.191696	0.178018	0.238939
35	1	H	-7.882247	-1.305636	1.135044

36	1	H	0.227133	3.109831	4.650279
37	1	H	0.363010	1.531684	5.418450
38	1	H	-0.825195	2.699654	6.017425
39	1	H	0.100206	1.382190	2.629779
40	79	Au	1.138126	-0.941726	0.427288
41	6	C	2.118203	-2.714692	0.708517
42	6	C	1.465761	-3.882124	0.387819
43	6	C	2.172660	-5.080603	0.527360
44	6	C	3.484333	-5.092044	0.991808
45	6	C	4.111837	-3.882334	1.310652
46	6	C	3.437817	-2.679317	1.164543
47	6	C	3.900427	-1.325665	1.432927
48	6	C	4.232509	-6.379611	1.149883
49	1	H	5.139325	-3.896642	1.670076
50	6	C	0.071210	-3.814193	-0.138519
51	1	H	1.683584	-6.016197	0.262582
52	7	N	-0.064110	-4.064850	-1.445219
53	6	C	-1.277802	-3.990277	-1.981543
54	6	C	-2.410067	-3.654855	-1.252116
55	6	C	-2.265645	-3.402341	0.099467
56	6	C	-1.008795	-3.481099	0.698629
57	1	H	-3.383577	-3.609371	-1.731353
58	1	H	-3.132672	-3.156420	0.709881

59	6	C	-0.856942	-3.275515	2.176281
60	6	C	5.134199	-0.894422	1.913037
61	6	C	5.370244	0.454825	2.140146
62	6	C	2.957911	-0.325258	1.187014
63	6	C	3.148391	1.012879	1.412818
64	6	C	4.394601	1.422343	1.909460
65	1	H	2.375734	1.755666	1.223683
66	1	H	5.913692	-1.624137	2.115871
67	6	C	4.648314	2.870061	2.193704
68	1	H	6.340293	0.768669	2.517401
69	1	H	-1.352476	-4.210664	-3.045036
70	1	H	-1.827915	-3.348805	2.673329
71	1	H	-0.441182	-2.290021	2.418779
72	1	H	-0.185140	-4.019186	2.615442
73	1	H	3.620754	-7.237538	0.861548
74	1	H	4.551174	-6.524174	2.187711
75	1	H	5.137852	-6.386630	0.533756
76	1	H	4.692269	3.053158	3.273185
77	1	H	3.855052	3.500961	1.781779
78	1	H	5.605810	3.195006	1.773252
79	1	H	0.282174	0.618759	0.082069
80	6	C	2.833374	1.076676	-2.589196
81	8	O	2.336732	-0.013810	-2.754453

82	8	O	4.029810	1.350323	-3.057274
83	6	C	4.801158	2.603024	-2.857283
84	6	C	4.083220	3.762010	-3.516905
85	1	H	3.151230	4.025575	-3.011943
86	1	H	4.734962	4.640848	-3.491194
87	1	H	3.867074	3.529072	-4.563959
88	6	C	6.093564	2.295419	-3.583352
89	1	H	6.763530	3.157946	-3.522908
90	1	H	6.592252	1.432580	-3.132992
91	1	H	5.899353	2.077830	-4.637336
92	6	C	5.058182	2.813228	-1.379008
93	1	H	5.480285	1.905863	-0.932913
94	1	H	5.782865	3.624578	-1.256664
95	1	H	4.155466	3.088160	-0.826794
96	6	C	2.079960	2.071511	-1.850595
97	6	C	1.348259	2.750489	-1.178239
98	6	C	0.571826	3.525370	-0.227115
99	8	O	0.899067	3.586480	0.933075
100	8	O	-0.464772	4.086868	-0.810107
101	6	C	-1.377746	5.006521	-0.078865
102	6	C	-0.584820	6.169687	0.481047
103	1	H	-1.286785	6.917539	0.862742
104	1	H	0.070723	5.864643	1.298051

105	1	H	0.014687	6.639482	-0.305343
106	6	C	-2.316209	5.468658	-1.172062
107	1	H	-2.841551	4.618329	-1.616607
108	1	H	-3.059021	6.152597	-0.751036
109	1	H	-1.766782	5.993821	-1.958752
110	6	C	-2.124501	4.234385	0.987655
111	1	H	-1.459299	3.859346	1.769097
112	1	H	-2.863600	4.897758	1.448685
113	1	H	-2.659106	3.388056	0.542498

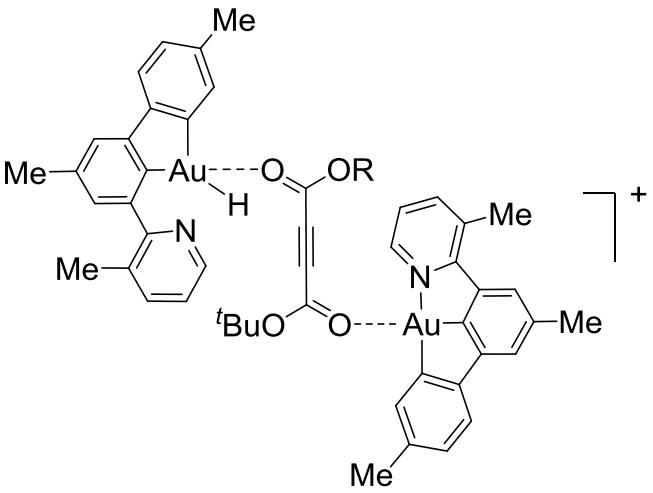

VIII

Standard orientation:

Center Number	Atomic Number	Atomic Type	Coordinates (Angstroms) X	Y	Z

1	6	C	-3.655237	0.629450	-1.505323
2	6	C	-3.289084	0.226227	-2.784768
3	6	C	-3.421454	1.168188	-3.797088
4	6	C	-3.890178	2.453604	-3.513564
5	6	C	-4.251985	2.798003	-2.212620
6	6	C	-4.152689	1.876962	-1.156180
7	1	H	-3.150085	0.915187	-4.820198
8	1	H	-4.598681	3.808076	-2.039062
9	6	C	-2.832200	-1.162239	-2.863130
10	6	C	-2.505562	-1.867421	-4.015139
11	6	C	-2.792660	-1.841683	-1.630592
12	6	C	-2.177996	-3.214754	-3.939241
13	1	H	-2.524255	-1.370811	-4.981916
14	6	C	-2.488355	-3.183877	-1.559680
15	6	C	-2.175435	-3.896200	-2.723557
16	1	H	-1.932419	-3.758188	-4.848273
17	1	H	-2.496637	-3.699718	-0.601485
18	6	C	-4.476728	2.084628	0.272083
19	6	C	-5.170849	3.169132	0.829963
20	6	C	-5.338808	3.184027	2.214153
21	6	C	-4.226284	1.108793	2.399767
22	6	C	-4.855725	2.170428	3.017561

23	1	H	-5.871428	4.018139	2.661771
24	1	H	-3.861231	0.256430	2.965021
25	1	H	-4.981765	2.184668	4.092718
26	6	C	-5.753412	4.297214	0.038360
27	1	H	-4.979707	4.975767	-0.338182
28	1	H	-6.333555	3.941562	-0.817194
29	1	H	-6.418356	4.887993	0.671270
30	6	C	-1.822810	-5.349799	-2.659510
31	1	H	-0.744825	-5.499709	-2.797213
32	1	H	-2.097666	-5.787200	-1.694752
33	1	H	-2.327489	-5.916703	-3.447582
34	6	C	-4.004280	3.455896	-4.620778
35	1	H	-4.352092	4.424417	-4.254542
36	1	H	-3.038939	3.605385	-5.115031
37	1	H	-4.706639	3.112395	-5.387449
38	7	N	-4.054881	1.072621	1.081839
39	79	Au	-3.296557	-0.655446	-0.042172
40	6	C	5.665691	1.674256	-0.291015
41	6	C	4.418277	2.132585	0.168813
42	6	C	4.261771	3.470515	0.485449
43	6	C	5.316891	4.382716	0.354885
44	6	C	6.544493	3.909372	-0.097067
45	6	C	6.723247	2.568780	-0.417757

46	1	H	3.300085	3.836043	0.849625
47	1	H	7.376817	4.602280	-0.198197
48	1	H	7.697252	2.231873	-0.765745
49	6	C	5.716359	0.245302	-0.618599
50	6	C	6.828519	-0.416311	-1.125851
51	6	C	4.526455	-0.489021	-0.431126
52	6	C	6.786558	-1.768415	-1.460358
53	1	H	7.757192	0.131813	-1.277020
54	6	C	4.447886	-1.825872	-0.790574
55	6	C	5.591135	-2.454203	-1.295678
56	1	H	5.529689	-3.504849	-1.575200
57	6	C	3.183485	-2.603253	-0.698226
58	6	C	2.931306	-3.424881	0.408955
59	6	C	1.150208	-3.057968	-1.638170
60	6	C	1.699492	-4.063054	0.447044
61	6	C	0.787552	-3.874506	-0.579360
62	1	H	0.457089	-2.887284	-2.463209
63	1	H	1.459737	-4.708112	1.290397
64	1	H	-0.184500	-4.358324	-0.570200
65	79	Au	2.996926	0.585980	0.355748
66	7	N	2.327417	-2.441417	-1.707005
67	6	C	5.113660	5.831255	0.677889
68	1	H	4.545718	6.337538	-0.111997

69	1	H	4.548067	5.956760	1.607325
70	1	H	6.066783	6.356613	0.785404
71	6	C	8.008103	-2.454156	-1.989368
72	1	H	8.449353	-1.893627	-2.819916
73	1	H	8.778815	-2.536718	-1.214677
74	1	H	7.780376	-3.463120	-2.342515
75	6	C	3.915877	-3.559345	1.525750
76	1	H	4.869020	-3.973189	1.180393
77	1	H	4.139082	-2.581830	1.969204
78	1	H	3.526792	-4.210693	2.313094
79	8	O	-2.606951	-2.094437	1.579334
80	1	H	1.997910	-0.710003	0.505697
81	8	O	1.360123	1.965734	1.089863
82	8	O	-0.787448	2.577827	1.260052
83	6	C	-0.570391	4.019808	0.891624
84	6	C	-1.984203	4.552302	0.889953
85	1	H	-1.968740	5.628898	0.698005
86	1	H	-2.568908	4.067090	0.102548
87	1	H	-2.469514	4.373975	1.854894
88	6	C	0.039307	4.096887	-0.491990
89	1	H	1.083516	3.778721	-0.513070
90	1	H	-0.538069	3.488970	-1.197776
91	1	H	-0.009251	5.137300	-0.828300

92	6	C	0.264591	4.678144	1.966349
93	1	H	0.329285	5.748401	1.746727
94	1	H	-0.207321	4.560844	2.946468
95	1	H	1.277760	4.276099	2.005869
96	8	O	-0.898397	-2.718587	2.899452
97	6	C	-1.496512	-4.016531	3.379290
98	6	C	-1.755626	-4.923076	2.196033
99	1	H	-2.017751	-5.914778	2.577237
100	1	H	-2.579291	-4.570703	1.572315
101	1	H	-0.853886	-5.029143	1.584287
102	6	C	-2.741409	-3.702919	4.178817
103	1	H	-3.091702	-4.628060	4.646522
104	1	H	-2.517131	-2.987181	4.975427
105	1	H	-3.547770	-3.312669	3.555208
106	6	C	-0.395054	-4.557696	4.260624
107	1	H	-0.715142	-5.509808	4.692675
108	1	H	0.519564	-4.727540	3.685310
109	1	H	-0.174446	-3.862510	5.075031
110	6	C	-0.789245	-0.680306	1.865040
111	6	C	-0.315995	0.392655	1.606289
112	6	C	0.182476	1.715761	1.290750
113	6	C	-1.507541	-1.908026	2.104922

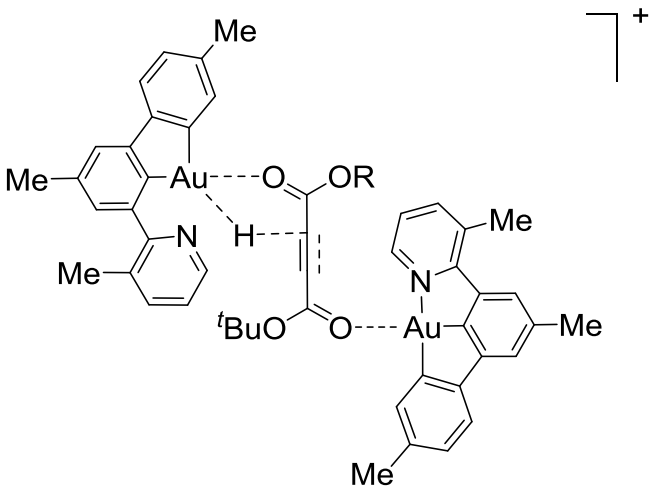

$TS_{VIII-IX}$

Standard orientation:

Center Number	Atomic Number	Atomic Type	Coordinates (Angstroms) X	Y	Z
1	6	C	3.778348	0.801787	1.341755
2	6	C	3.395349	0.936509	2.671367
3	6	C	3.767701	2.109188	3.316648
4	6	C	4.483657	3.096671	2.635791
5	6	C	4.856215	2.902118	1.307141
6	6	C	4.520559	1.725250	0.617324
7	1	H	3.494408	2.273193	4.357343
8	1	H	5.398995	3.699084	0.817290
9	6	C	2.663774	-0.216876	3.194753
10	6	C	2.263612	-0.410707	4.511088

11	6	C	2.413247	-1.238553	2.258055
12	6	C	1.661615	-1.602368	4.887189
13	1	H	2.440818	0.363431	5.253346
14	6	C	1.822592	-2.426198	2.636441
15	6	C	1.448454	-2.629910	3.970645
16	1	H	1.365046	-1.750313	5.922733
17	1	H	1.662976	-3.219968	1.909175
18	6	C	4.822698	1.374719	-0.787303
19	6	C	5.686106	2.053662	-1.661792
20	6	C	5.782862	1.580072	-2.969449
21	6	C	4.268330	-0.164416	-2.478826
22	6	C	5.068090	0.480051	-3.400553
23	1	H	6.444171	2.096596	-3.658980
24	1	H	3.702286	-1.054734	-2.735504
25	1	H	5.138109	0.116475	-4.417962
26	6	C	6.500055	3.250220	-1.284871
27	1	H	5.873980	4.141642	-1.163376
28	1	H	7.052317	3.097300	-0.353974
29	1	H	7.223950	3.468722	-2.072122
30	6	C	0.855993	-3.930071	4.419294
31	1	H	-0.120581	-3.782022	4.893925
32	1	H	0.730120	-4.628618	3.587044
33	1	H	1.498223	-4.414002	5.163108

34	6	C	4.845618	4.363923	3.347596
35	1	H	3.948683	4.890388	3.690193
36	1	H	5.451476	4.154337	4.235185
37	1	H	5.411696	5.042020	2.705069
38	7	N	4.162579	0.267468	-1.226469
39	79	Au	3.089998	-0.785020	0.377768
40	6	C	-5.767305	1.792799	0.045645
41	6	C	-4.463490	2.270932	-0.143872
42	6	C	-4.222754	3.614283	-0.349096
43	6	C	-5.284011	4.530391	-0.368121
44	6	C	-6.576515	4.048562	-0.184184
45	6	C	-6.823157	2.696637	0.021977
46	1	H	-3.205748	3.977981	-0.501112
47	1	H	-7.408698	4.748242	-0.203780
48	1	H	-7.846603	2.355896	0.160053
49	6	C	-5.856955	0.348597	0.252366
50	6	C	-7.024573	-0.365686	0.482180
51	6	C	-4.631153	-0.345728	0.223407
52	6	C	-7.002510	-1.744065	0.692011
53	1	H	-7.980491	0.155075	0.504982
54	6	C	-4.580117	-1.709751	0.445696
55	6	C	-5.778221	-2.397315	0.673776
56	1	H	-5.736760	-3.471202	0.848411

57	6	C	-3.309087	-2.481041	0.486436
58	6	C	-2.775251	-3.044045	-0.679744
59	6	C	-1.618628	-3.303615	1.787019
60	6	C	-1.610350	-3.784564	-0.538464
61	6	C	-1.011531	-3.916896	0.703675
62	1	H	-1.180746	-3.377609	2.781188
63	1	H	-1.169746	-4.244602	-1.418223
64	1	H	-0.099064	-4.493481	0.830220
65	79	Au	-2.993640	0.792594	-0.169438
66	7	N	-2.751722	-2.612355	1.689809
67	6	C	-5.020184	5.991401	-0.563217
68	1	H	-4.277154	6.161869	-1.348956
69	1	H	-5.932418	6.530561	-0.832775
70	1	H	-4.626799	6.446505	0.353517
71	6	C	-8.276001	-2.488316	0.949319
72	1	H	-8.735050	-2.166246	1.890483
73	1	H	-9.009204	-2.303946	0.157098
74	1	H	-8.105759	-3.566013	1.010947
75	6	C	-3.406200	-2.840786	-2.019471
76	1	H	-4.441837	-3.196943	-2.038107
77	1	H	-3.433619	-1.776997	-2.284069
78	1	H	-2.846009	-3.368618	-2.796876
79	6	C	-0.169792	-0.063703	-1.104225

80	6	C	0.464867	-1.075806	-1.377204
81	6	C	1.226070	-2.257235	-1.543933
82	8	O	2.228727	-2.474923	-0.841686
83	8	O	0.808644	-3.048668	-2.490370
84	6	C	1.560941	-4.264673	-2.937102
85	6	C	1.632981	-5.274273	-1.810978
86	1	H	2.097779	-6.185909	-2.199806
87	1	H	2.233842	-4.915013	-0.973883
88	1	H	0.634406	-5.542363	-1.452329
89	6	C	2.928687	-3.849433	-3.435718
90	1	H	3.584343	-3.530638	-2.622900
91	1	H	3.394593	-4.708873	-3.927214
92	1	H	2.841519	-3.047922	-4.176851
93	6	C	0.696977	-4.766674	-4.072698
94	1	H	1.142950	-5.671163	-4.496093
95	1	H	-0.309510	-5.012368	-3.720798
96	1	H	0.618720	-4.014516	-4.862597
97	6	C	-0.238393	1.396966	-1.066764
98	8	O	0.863675	1.938637	-1.485013
99	8	O	-1.217211	2.027077	-0.678232
100	6	C	1.056970	3.429509	-1.517553
101	6	C	2.419572	3.554836	-2.157320
102	1	H	2.683666	4.612492	-2.246963

103	1	H	3.173444	3.061187	-1.539896
104	1	H	2.426532	3.106038	-3.155405
105	6	C	-0.003608	4.075183	-2.383897
106	1	H	-0.986886	4.082620	-1.912795
107	1	H	0.296432	5.111168	-2.569987
108	1	H	-0.069879	3.567935	-3.351587
109	6	C	1.072167	3.937797	-0.092118
110	1	H	0.093514	3.857620	0.384710
111	1	H	1.812496	3.390928	0.504241
112	1	H	1.359600	4.993976	-0.102544
113	1	H	-1.753397	-0.396490	-0.262528

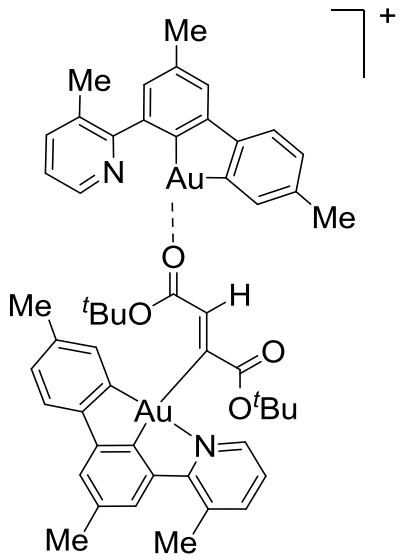

IX

Standard orientation:

Center Number	Atomic Number	Atomic Type	Coordinates (Angstroms) X	Y	Z
1	6	C	-3.517703	-2.535643	0.841363
2	6	C	-2.523362	-1.566168	1.097845
3	6	C	-1.268610	-1.933708	1.525857
4	6	C	-0.963323	-3.283122	1.756991
5	6	C	0.391062	-3.659309	2.268500
6	6	C	-1.946569	-4.235010	1.512699
7	1	H	-1.718297	-5.285136	1.678484
8	6	C	-3.208511	-3.871868	1.052666
9	1	H	-3.953357	-4.640506	0.862303
10	6	C	-4.795576	-1.998574	0.369995
11	6	C	-4.824659	-0.611861	0.269299
12	79	Au	-3.182761	0.351626	0.810132
13	6	C	-5.912363	0.147361	-0.146591
14	6	C	-7.062123	-0.586478	-0.482261
15	1	H	-7.966387	-0.091841	-0.807864
16	6	C	-7.087014	-1.977192	-0.400947
17	6	C	-8.327495	-2.734354	-0.765520
18	6	C	-5.956433	-2.678477	0.022455
19	1	H	-5.996347	-3.764559	0.080177
20	6	C	-5.721016	1.614976	-0.166404

21	6	C	-6.634938	2.589167	-0.598509
22	6	C	-6.238739	3.924262	-0.523574
23	6	C	-4.996528	4.294996	-0.048033
24	6	C	-4.140420	3.289570	0.350975
25	1	H	-6.936235	4.687927	-0.855293
26	7	N	-4.499296	2.011016	0.289007
27	6	C	-7.995490	2.289864	-1.142728
28	1	H	-4.693575	5.332880	0.007824
29	1	H	-3.143147	3.491272	0.731125
30	1	H	-7.949470	1.623166	-2.008964
31	1	H	-8.479445	3.214703	-1.461830
32	1	H	-8.641540	1.822823	-0.392741
33	1	H	-9.134013	-2.064680	-1.072671
34	1	H	-8.685619	-3.330727	0.080102
35	1	H	-8.133951	-3.430308	-1.588435
36	1	H	1.179600	-3.129617	1.719595
37	1	H	0.572151	-4.733472	2.173437
38	1	H	0.494816	-3.393398	3.327585
39	1	H	-0.490535	-1.188587	1.680221
40	79	Au	2.615692	0.067828	-0.402501
41	6	C	4.355124	-0.702021	0.260159
42	6	C	5.372572	0.163722	0.648685
43	6	C	6.574809	-0.432968	1.067787

44	6	C	6.722133	-1.818486	1.088457
45	6	C	5.671768	-2.644493	0.680023
46	6	C	4.470862	-2.089427	0.255472
47	6	C	3.268559	-2.773372	-0.235871
48	6	C	8.006215	-2.434559	1.556697
49	1	H	5.813860	-3.724266	0.692763
50	6	C	5.050346	1.606428	0.541546
51	7	N	3.808964	1.860460	0.033706
52	6	C	3.357462	3.098492	-0.146753
53	6	C	4.120013	4.201307	0.177732
54	6	C	5.374775	3.976101	0.710457
55	6	C	5.870750	2.689047	0.906794
56	1	H	3.737351	5.202135	0.020070
57	1	H	6.001259	4.819682	0.986607
58	6	C	7.239875	2.548410	1.494095
59	6	C	3.110197	-4.147116	-0.367012
60	6	C	1.919788	-4.678142	-0.851704
61	6	C	2.192516	-1.931365	-0.612262
62	6	C	1.015802	-2.469138	-1.093197
63	6	C	0.861521	-3.856512	-1.220003
64	1	H	0.183688	-1.827141	-1.377010
65	6	C	-0.419419	-4.417898	-1.753880
66	1	H	2.356774	3.189686	-0.558533

67	1	H	7.643655	3.533915	1.734265
68	1	H	7.934967	2.069611	0.797403
69	1	H	7.231622	1.959788	2.416397
70	1	H	8.786184	-1.682308	1.698874
71	1	H	8.375174	-3.175376	0.840025
72	1	H	7.867180	-2.955025	2.511000
73	1	H	-1.282017	-3.856692	-1.378125
74	1	H	-0.545383	-5.467344	-1.471314
75	1	H	-0.447353	-4.363142	-2.848762
76	6	C	-0.257217	1.354148	-0.483493
77	6	C	0.775901	0.834772	-1.158610
78	6	C	-0.315770	1.489518	0.969274
79	6	C	0.578671	0.650923	-2.619360
80	8	O	-0.389859	0.123198	-3.114425
81	8	O	1.641718	1.105104	-3.283952
82	8	O	-1.388597	1.423234	1.591448
83	8	O	0.827727	1.691335	1.563018
84	6	C	1.814672	0.884897	-4.727392
85	6	C	3.175969	1.494113	-4.994085
86	6	C	0.736562	1.615031	-5.503917
87	6	C	1.832273	-0.605347	-5.010400
88	1	H	0.719026	2.674101	-5.226477
89	1	H	-0.249963	1.183698	-5.326833

90	1	H	0.959725	1.548747	-6.573945
91	1	H	3.179392	2.558389	-4.739060
92	1	H	3.430240	1.390542	-6.053236
93	1	H	3.944869	0.989725	-4.400287
94	1	H	2.565291	-1.104406	-4.366427
95	1	H	2.126428	-0.768803	-6.052357
96	1	H	0.852978	-1.059698	-4.849679
97	6	C	0.999789	1.763623	3.040717
98	6	C	2.495920	1.949035	3.183261
99	6	C	0.252447	2.967646	3.574380
100	6	C	0.564692	0.460614	3.677890
101	1	H	-0.515191	0.309037	3.624881
102	1	H	0.856238	0.477701	4.732782
103	1	H	1.076535	-0.386540	3.205175
104	1	H	2.827576	2.852568	2.661317
105	1	H	3.033496	1.087427	2.774497
106	1	H	2.750016	2.045696	4.242666
107	1	H	-0.828939	2.844783	3.500896
108	1	H	0.551013	3.871528	3.033876
109	1	H	0.514097	3.103139	4.628598
110	1	H	1.811162	-5.756429	-0.941842
111	1	H	3.921282	-4.815350	-0.087044
112	1	H	7.426089	0.157014	1.378447

113	1	H	-1.188737	1.621021	-0.990561

$Ph_3SiF_2^-$

Standard orientation:

Center Number	Atomic Number	Atomic Type	Coordinates (Angstroms) X	Y	Z
1	14	Si	-1.0882409521	-0.2355730337	0.0122340477
2	6	C	-2.0385300918	1.4214480217	0.0231950721
3	6	C	-1.6782124631	2.4671917423	-0.8315804071
4	6	C	-3.1249289961	1.6388652873	0.8753336284
5	6	C	-2.3562589454	3.6796448691	-0.8268578349
6	1	H	-0.8473437146	2.3234057659	-1.5185060563
7	6	C	-3.8332066386	2.8343318872	0.8635501361
8	1	H	-3.4210198894	0.8507021372	1.5639652043
9	12	C	-3.4447433313	3.8640079148	0.0161901159
10	1	H	-2.0422068024	4.4815570056	-1.4906455809
11	1	H	-4.6864338582	2.9676727718	1.5241740952
12	1	H	-3.9877400848	4.8054003049	0.0126232352
13	6	C	-2.0311477217	-1.9037290119	-0.0572594899
14	6	C	-2.7981900898	-2.3679146516	1.0183932058

15	6	C	-1.9736476055	-2.7230024307	-1.1909390041
16	6	C	-3.4820302319	-3.5763723978	0.9624984234
17	1	H	-2.8438469859	-1.7673889069	1.9222660407
18	12	C	-2.6343885109	-3.9436013687	-1.2486855059
19	1	H	-1.4001948518	-2.383256589	-2.0479252999
20	6	C	-3.3987669242	-4.3729271533	-0.1717060214
21	1	H	-4.0781592306	-3.9017558531	1.8116756896
22	1	H	-2.5583297013	-4.5603165535	-2.1409166991
23	1	H	-3.9247306075	-5.3230321897	-0.2151742301
24	6	C	0.8304892074	-0.2547614584	0.0594132135
25	6	C	1.5310728847	-0.6426799064	1.2081377861
26	6	C	1.5989891675	0.1119082407	-1.0526898606
27	6	C	2.9193813347	-0.6717238317	1.2468219422
28	1	H	0.9641972725	-0.9204921321	2.0909383952
29	6	C	2.9880456918	0.1048366106	-1.0187515938
30	1	H	1.0854884892	0.3967517225	-1.9660464592
31	12	C	3.655560086	-0.2914862071	0.1323903189
32	1	H	3.4300560826	-0.9869792381	2.153565649
33	1	H	3.5532983451	0.4047809884	-1.897908745
34	1	H	4.7418908672	-0.3048844366	0.1607794057
35	9	F	-1.1603255322	-0.2620458001	1.7664456641
36	9	F	-1.0482395379	-0.1624882697	-1.7429856309

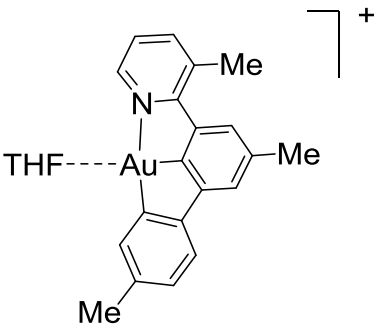

Standard orientation:

Center Number	Atomic Number	Atomic Type	Coordinates (Angstroms) X	Y	Z
1	6	C	-1.134019	0.997443	0.002979
2	6	C	-0.734438	2.328889	0.005817
3	6	C	-1.741609	3.286210	-0.001320
4	6	C	-3.083185	2.900201	-0.012305
5	6	C	-3.426538	1.549160	-0.013626
6	6	C	-2.447605	0.542277	-0.001984
7	1	H	-1.493421	4.345686	-0.002105
8	1	H	-4.479064	1.305990	-0.029814
9	6	C	0.718433	2.514781	0.013309
10	6	C	1.398553	3.723490	0.026541
11	6	C	1.471568	1.320430	0.010580
12	6	C	2.789397	3.742825	0.038591
13	1	H	0.847014	4.660402	0.028356

14	6	C	2.847582	1.343877	0.024495
15	6	C	3.532793	2.568721	0.039053
16	1	H	3.310019	4.696737	0.049106
17	1	H	3.420151	0.416890	0.026745
18	6	C	-2.636906	-0.926759	-0.006015
19	6	C	-3.851876	-1.629015	0.022911
20	6	C	-3.793026	-3.022075	-0.000477
21	6	C	-1.433478	-2.956420	-0.055700
22	6	C	-2.592966	-3.704306	-0.043138
23	1	H	-4.725988	-3.577885	0.018136
24	1	H	-0.447772	-3.413170	-0.083743
25	1	H	-2.551950	-4.785979	-0.061671
26	6	C	-5.200083	-0.984385	0.083936
27	1	H	-5.299243	-0.328537	0.953877
28	1	H	-5.408701	-0.390454	-0.811432
29	1	H	-5.974468	-1.749974	0.157742
30	6	C	5.028824	2.590983	0.056096
31	1	H	5.420911	2.086353	0.945849
32	1	H	5.441880	2.069996	-0.814416
33	1	H	5.413022	3.613788	0.051599
34	6	C	-4.152683	3.949315	-0.010025
35	1	H	-5.140971	3.518591	-0.186886
36	1	H	-4.182990	4.473051	0.951733

37	1	H	-3.966227	4.704214	-0.780039
38	7	N	-1.468445	-1.627636	-0.037025
39	79	Au	0.304817	-0.357545	-0.019297
40	6	C	2.673398	-2.274008	-1.199187
41	6	C	3.504732	-3.404195	0.707193
42	6	C	2.476827	-2.402864	1.178768
43	1	H	2.780528	-1.380775	-1.820171
44	1	H	2.135160	-3.044129	-1.762805
45	1	H	3.034559	-4.377837	0.530841
46	1	H	4.312080	-3.536755	1.429234
47	1	H	1.682432	-2.819121	1.804083
48	1	H	2.932038	-1.547542	1.694823
49	6	C	3.967633	-2.790508	-0.609806
50	1	H	4.662123	-1.963767	-0.421497
51	1	H	4.461140	-3.506010	-1.269529
52	8	O	1.866043	-1.926832	-0.044314

THF

Standard orientation:

Center	Atomic	Atomic	Coordinates (Angstroms)		
Number	Number	Type	X	Y	Z

1	6	C	1.174502	-0.458010	-0.000000
2	8	C	0.000011	-1.248147	-0.000001
3	6	C	-1.174493	-0.458027	-0.000000
4	6	C	-0.766999	1.016536	0.000001
5	6	C	0.766983	1.016544	0.000000
6	1	H	1.774604	-0.711366	0.883891
7	1	H	1.774604	-0.711366	-0.883892
8	1	H	-1.774598	-0.711399	-0.883886
9	1	H	-1.774599	-0.711400	0.883885
10	1	H	-1.163395	1.532104	-0.878059
11	1	H	-1.163395	1.532103	0.878062
12	1	H	1.163369	1.532121	-0.878060
13	1	H	1.163369	1.532120	0.878061

References

[1] Zhao, Y.; Truhlar, D. G.; *Theor. Chem. Acc.* **2008**, *120*, 215-241.

[2] Gaussian 09, Revision D.01; M. J. Frisch, G. W. Trucks, H. B. Schlegel, G. E. Scuseria, M. A. Robb, J. R. Cheeseman, G. Scalmani, V. Barone, B. Mennucci, G. A. Petersson, H. Nakatsuji, M. Caricato, X. Li, H. P. Hratchian, A. F. Izmaylov, J. Bloino, G. Zheng, J. L. Sonnenberg, M. Hada, M. Ehara, K. Toyota, R. Fukuda, J. Hasegawa, M. Ishida, T. Nakajima, Y. Honda, O. Kitao, H. Nakai, T. Vreven, J. A. Montgomery, Jr., J. E. Peralta, F. Ogliaro, M. Bearpark, J. J. Heyd, E. Brothers, K. N. Kudin, V. N. Staroverov, T. Keith, R. Kobayashi, J. Normand, K. Raghavachari, A. Rendell, J. C. Burant, S. S. Iyengar, J. Tomasi, M. Cossi, N. Rega, J. M. Millam, M. Klene, J. E. Knox, J. B. Cross, V. Bakken, C. Adamo, J. Jaramillo, R. Gomperts, R. E. Stratmann, O. Yazyev, A. J. Austin, R. Cammi, C. Pomelli, J. W. Ochterski, R. L. Martin, K. Morokuma, V. G. Zakrzewski, G. A. Voth, P. Salvador, J. J. Dannenberg, S. Dapprich, A.

D. Daniels, O. Farkas, J. B. Foresman, J. V. Ortiz, J. Cioslowski, and D. J. Fox, Gaussian, Inc., Wallingford CT, **2013**.

[3] Fuentealba, P.; Preuss, H.; Stoll, H.; Szentpály, L. v., *Chem. Phys. Lett.* **1982**, *89*, 418-422.

[4] (a) Cancès, E.; Mennucci, B.; Tomasi, J. *J. Chem. Phys*. **1997**, *107*, 3032–3047. (b) Cossi, M.; Barone, V.;Mennuci, B.; Tomasi, J. *Chem. Phys. Lett.* **1998**, *286*, 253–260. (c) Tomasi, J.; Mennucci, B.; Cancès, E. *J. Mol. Struct. (Theochem)*, **1999**, *464*, 211–226

[5] Gonzalez, C.; Schlegel, H. B. *J. Phys. Chem.* **1990**, *94*, 5523–5527.

CHAPTER 6

CONCLUSIONS AND OUTLOOK

CHAPTER 6

Conclusions and Outlook

Gold-catalyzed oxidative cross-couplings have bloomed in the past few years postulating gold(III) fluorides as productive intermediates. However, experimental support for these species is to-date scarce due to their labile nature, and thus the reactivity of Au^{III}-F bonds remains largely unexplored.

In this thesis, to address the above mentioned challenges, novel 3,5-disubstituted phenylpyridine based N^C^C ligands (**1a**) were designed. We envisioned that the simultaneous double Csp^2-H functionalization of the aromatic rings would give access to a new class of N^C^C pincer Au^{III} complexes, in which the central aromatic ring would exert a strong *trans* influence facilitating a direct anionic ligand exchange to produce (N^C^C)Au^{III}-F complexes (**3**) from the corresponding chlorido complexes (**2**). We have developed the synthesis of the first stable Csp^2-Au^{III}-fluorido complexes via a facile Cl/F ligand exchange and their structural characterization by X-Ray crystallography. Additionally, these complexes reacted with different terminal alkynes under mild reaction conditions resulting in the formation of corresponding gold(III)-alkynyl species **4**. These results showcase the strong basicity of the Au^{III}-F bond, comparable to that of Au^{III}-OH species previously described in the literature. Complexes **4** exhibit striking luminescent properties compared to their analogous (C^N^C)Au^{III} complexes (Scheme 1). In the future, the luminescent properties of these species will be improved by introducing electron donating groups in the anionic substituents and by extending the conjugation on the ancillary tridentate ligands.

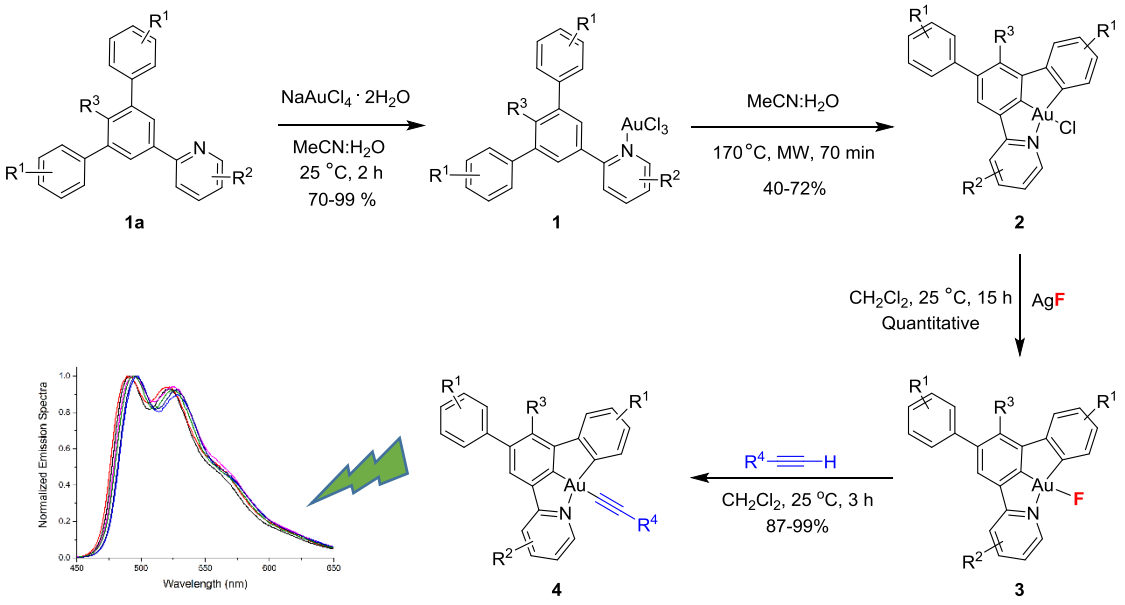

Scheme 1: Synthesis and reactivity of (N^C^C)Au^{III}-F (*Angew. Chem. Int. Ed.* **2015**, *54*, 14287-14290; *Angew. Chem. Int. Ed.* **2017**, *56*, 1994-2015).

Most gold catalyzed oxidative-cross couplings involving boronic acids as reaction partners employ Selectfluor as stoichiometric oxidant and thus Au^{III}-F species have been invoked as the key partners of boron species towards the formation of new C-C bonds. However, the nature of the interaction Au^{III}-F/B was not clear. In the third chapter of this thesis we report the synthesis and isolation of monocyclometalated (C^N)Au^{III}(R)F (R = F, alkyl, aryl) complexes **5** in monomeric form which were used to probe the interaction of Au^{III}-F with aryl boronic acids (Scheme 2). It was found that these compounds directly transmetalate with aryl boronic acids and the corresponding transmetalated complex undergo reductive elimination to produce the coupling products, thus ruling out a bimolecular reductive elimination pathway previously proposed in the literature.

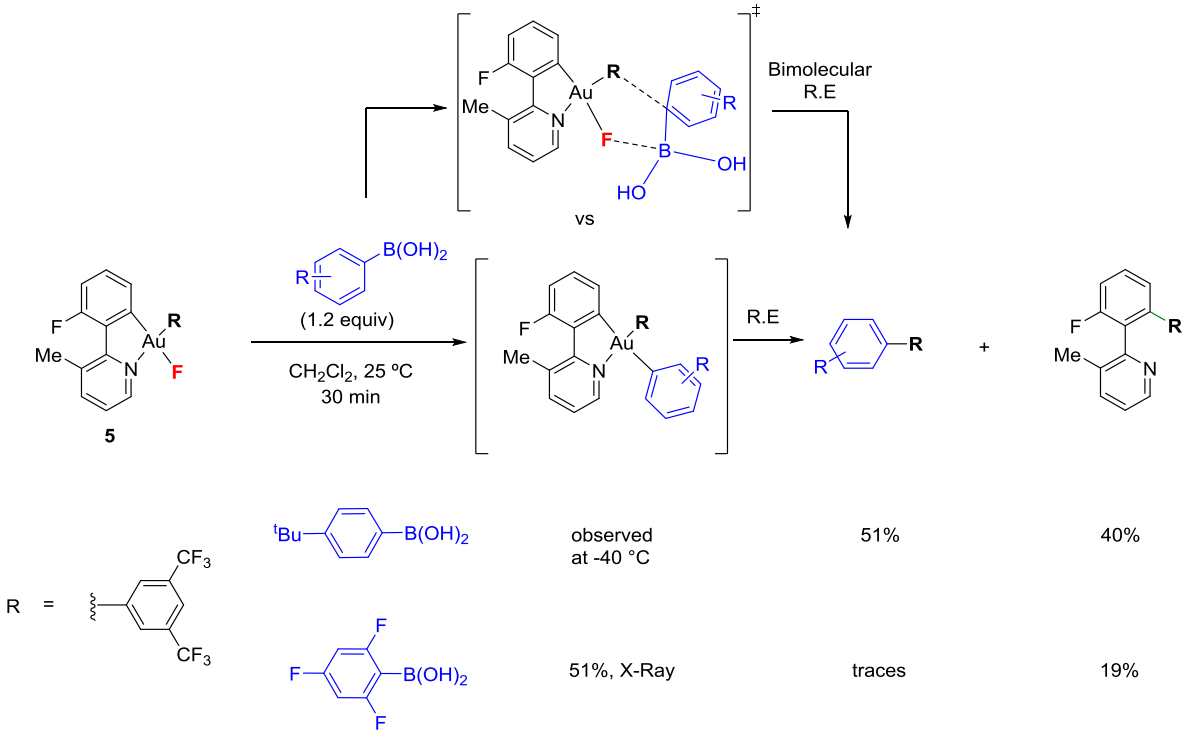

Scheme 2: Synthesis and reactivity of (C^N)Au^{III}(R)F complexes (*J. Am. Chem. Soc.* **2016,** *138,* 13790-13793).

Gold formates have been postulated as intermediates in the gold catalyzed heterogeneous dehydrogenation of formic acid (FA) but their synthesis and characterization was lacking. Utilizing the N^C^C ligand developed in house (Chapters 2 & 3), we have synthesized the first stable gold(III)-fomate and demonstrated its reactivity towards the homogeneous dehydrogenation of formic acid via a fomate-hydride catalytic cycle that was also supported by DFT calculations (Scheme 3). The efficiency of this catalytic system will be further improved by synthesizing water soluble derivatives.

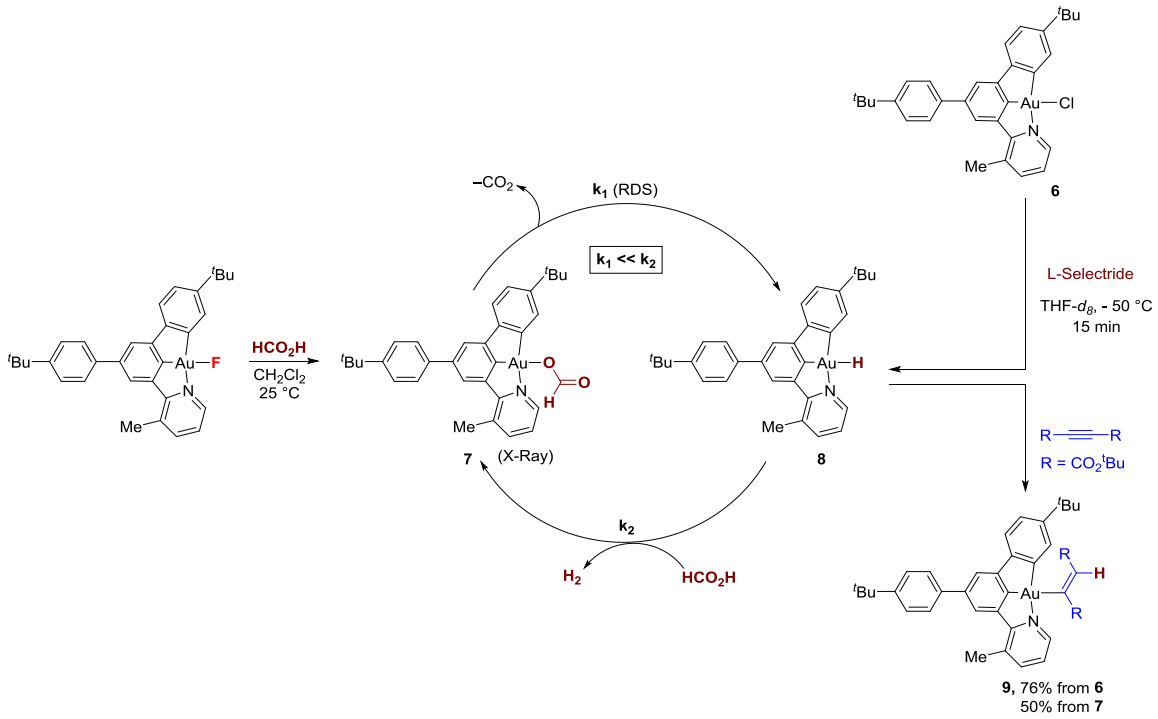

Scheme 3: Synthesis and reactivity of Au^{III} formate (*Angew. Chem. Int. Ed.* **2017**, *accepted*).

The gold(III) hydride invoked in the above-mentioned process could be accessed by an alternative route from (N^C^C)Au^{III}-Cl (**6**) upon reaction with L-selectride. The putative Au^{III}-H (**8**) can react with di-*tert*-butyl acetylenedicarboxylate to produce *trans*-vinyl gold(III) complex **9** (Scheme 3). Interestingly, the reaction of (N^C^C)Au^{III}-F with triphenylsilane in dichloromethane at room temperature furnished similar results. Taking advantage of deuterium labelling experiments and Cryo-MS spectroscopy, we have been able to characterize cationic gold(III) complexes that are likewise involved in this hydroauration process. This reactivity will be harnessed to develop gold(III) catalyzed hydrofunctionalization reactions.

Curriculum Vitae - Roopender Kumar

University of Zurich

Department of Chemistry

Winterthurestrasse 190

CH-8057, Zurich, Switzerland

Mobile: +41 788835450

Email: roopender.kumar@chem.uzh.ch

Personal details:

Date of Birth : 22nd June 1986

Nationality : Indian

Marital Status : Single

Language : Hindi, English, German (basic)

Education and Research Experience:

09.2012-09.2017 PhD at University of Zurich, Zurich, Switzerland (Supervisor: Prof. Dr. C. Nevado).

01.2010-12.2010 Master thesis at Free University of Berlin, Berlin, Germany (Supervisor: Prof. Dr. H.-U. Reissig).

06.2008-06.2011 Master of Technology (M.Tech) in Chemical Synthesis and Process Technologies (First class), University of Delhi, Delhi, India and Free University Berlin, Berlin, Germany.

06.2004-06.2007 Bachelor of Science (B.S.) in Chemistry, Zoology and Botany (First class), C.C.S. University, Meerut, Uttar Pradesh, India.

Professional Experience and Laboratory Skills:

- Organic synthesis, organometallic chemistry under inert atmosphere, heterocycle synthesis, multi-component reactions, gold catalysis and microwave assisted reactions.
- **Techniques:** NMR, MS, GC-MS, LC-MS, HPLC, IR, UV, Cyclic-voltammetry, Polarimeter, X-Ray analysis, Glovebox and Schlenk techniques.
- **Teaching** assistant for medicine bachelor students, laboratory course (three semesters, ≈ 600 hours).
- **Computer/Internet knowledge:** MS-Office, Origin, Photoshop, Chemdraw, Hyperchem, Scifinder.

Awards and Fellowships:

- ❖ COST action grant awarded by STSM to support a research stay November 28th – December 2nd, 2016 in the laboratory of Prof. Xavi Ribas at the University of Girona, Girona, Spain.
- ❖ Travel award by CMSZH graduate school for attending BOSS-2016 July 12-16, 2016 held in Antwerp, Belgium**.**
- ❖ Fellowship awarded by the Free University of Berlin for Master Thesis work.
- ❖ Fellowship awarded by the University of Delhi for master degree.
- ❖ Scholarship awarded by the C.C.S. University Meerut for bachelor degree.

Posters and Oral Presentations:

- ❖ Oral presentation in "Annual Retreat" organized by the Department of Chemistry, University of Zurich January 18-22, 2017 held in Evolène, Valais, Switzerland.
- ❖ Poster presentation in "ICOS-21" December 11-16, 2016 held in IIT Bomaby, Mumbai, India.
- ❖ Poster presentation in "Swiss Chemical Society Fall Meeting" on September 15th 2016 held in the Department of Chemistry, University of Zurich, Zurich, Switzerland.

- Poster presentation in "BOSS-2016" July 12-16, 2016 held in Antwerp, Belgium**.**
- Oral presentation in "13th Annual Doktorandentag" organized by the Department of Chemistry, University of Zurich June 8, 2016 held in Schloss Au, Zurich, Switzerland.
- Oral presentation in "The Zurich School of Crystallography" June 7-20, 2015 held in the Department of Chemistry, University of Zurich, Zurich, Switzerland.
- Poster presentation in annual "Dorothy Crowfoot Hodgkins Symposium" (2013-2016) held in the Department of Chemistry University of Zurich, Zurich, Switzerland.
- Poster presentation in Swiss Summer School on "Synthesis and Catalysis" August 12-16, 2013 held in Villars sur Ollon, Switzerland.

Publications:

1. First Gold(III)-Formate: Evidence for β-Hydride Elimination. Roopender Kumar, Jean-Philippe Krieger, Enrique Gómez-Bengoa, Tomas Fox, Anthony Linden, and Cristina Nevado. *Angew. Chem. Int. Ed.* **2017**, *accepted.*
2. Cyclometalated Au^{III} Complexes: Synthesis, Reactivity and Physicochemical Properties. Roopender Kumar, and Cristina Nevado. *Angew. Chem. Int. Ed.* **2017**, *56*, 1994-2015.
3. Gold-Catalyzed Direct Oxidative Arylation with Boron Coupling Partners. Manuel Hofer, Alexandre Genaux, Roopender Kumar, and Cristina Nevado. *Angew. Chem. Int. Ed.* **2016**, *56*, 1021-1025.
4. Evidence for Direct Transmetalation of Au^{III}-F with Boronic Acids. Roopender Kumar, Anthony Linden, and Cristina Nevado. *J. Am. Chem. Soc.* **2016**, *138*, 13790-13793.
5. Luminescent (N^C^C) Gold(III) Complexes: Stabilized Gold(III) Fluorides. Roopender Kumar, Anthony Linden, and Cristina Nevado. *Angew. Chem. Int. Ed.* **2015**, *54*, 14287-14290.
6. A Practical Two-Step Procedure for the Preparation of Enantiopure Pyridines: Multicomponent Reactions of Alkoxyallenes, Nitriles and Carboxylic Acids followed by a Cyclocondensation Reaction. Christian Eidamshaus, Roopender Kumar, Mrinal K. Bera, and Hans-Ulrich Reissig. *Beilstein J. Org. Chem.* **2011**, *7*, 962−975.


CMSZH
CHEMICAL MOLECULAR SCIENCES ZURICH
GRADUATE SCHOOL


UNIVERSITAS TURICENSIS
MDCCC XXXIII
University of
Zurich UZH